INSTYTUT
GENETYKI CZŁOWIEKA
POLSKIEJ AKADEMII NAUK

mgr Alicja Małgorzata Rabiasz

Analiza funkcjonalna wybranych genów zaangażowanych w patogenezę pierwotnej dyskinezy rzęsek przy użyciu organizmu modelowego *Schmidtea mediterranea*

Rozprawa doktorska przygotowana
w Instytucie Genetyki Człowieka Polskiej Akademii Nauk

Promotor: prof. dr hab. Ewa Ziętkiewicz

Poznań 2025

Serdecznie dziękuję

Prof. dr hab. Ewie Ziętkiewicz za opiekę naukową,
przekazaną wiedzę, wszelką pomoc i wsparcie oraz za ogromną życzliwość,

Byłym i obecnym Pracownikom Zakładu Genetyki Molekularnej i Klinicznej
za wspólne lata pracy, inspirujące rozmowy przy kawie oraz nieocenioną pomoc,

Moim Rodzicom za nieustanną wiarę we mnie oraz troskę,

Mojemu Narzeczonemu Tomkowi za ogrom wsparcia, wyrozumiałość
oraz obecność każdego dnia.

Rozprawa doktorska przygotowana na podstawie następujących publikacji:

1. **Alicja Rabiasz**, Ewa Ziętkiewicz
   „*Schmidtea mediterranea* as a Model Organism to Study the Molecular Background of Human Motile Ciliopathies"
   Int J Mol Sci. 2023 Feb 24;24(5):4472
   (praca przeglądowa)
   Impact Factor: 4.9
   Punkty MNiSW: 140

2. Ewa Ziętkiewicz, Zuzanna Bukowy-Bieryłło, **Alicja Rabiasz**, Patrycja Daca-Roszak, Alina Wojda, Katarzyna Voelkel, Ewa Rutkiewicz, Andrzej Pogorzelski, Margarida Rasteiro, Michał Witt
   „*CFAP300*: Mutations in Slavic Patients with Primary Ciliary Dyskinesia and a Role in Ciliary Dynein Arms Trafficking"
   Am J Respir Cell Mol Biol. 2019 Oct;61(4):440-449
   (praca oryginalna)
   Impact Factor: 5.373
   Punkty MNiSW: 100

3. **Alicja Rabiasz**, Zuzanna Bukowy-Bieryłło, Patrycja Kaźmierczak*, Hanna Przystałowska-Macioła*, Marcin Mikoś, Irena Wojsyk-Banaszak, Ewa Ziętkiewicz
   *równorzędny wkład
   „A novel pathogenic variant of *CFAP221* is a cause of a mild form of primary ciliary dyskinesia"
   Biochim Biophys Acta Mol Basis Dis. 2025 Apr 16;1871(6):167855
   (praca oryginalna)
   Impact Factor: 4.2
   Punkty MNiSW: 140

4. **Alicja Rabiasz,** Monika Drobna-Śledzińska, Patrycja Kaźmierczak, Michał Witt, Ewa Ziętkiewicz
   „The lack of homozygotes with a large deletion encompassing *SPAG1* and *POLR2K* in primary ciliary dyskinesia patients suggests the lethal effect of the loss of POLR2K protein"
   Genes & Diseases, https://doi.org/10.1016/j.gendis.2025.101535
   praca zaakceptowana, dostępna online, oczekuje na nadanie numeru tomu
   (praca oryginalna)
   Impact Factor: 6.9
   Punkty MNiSW: 140

Rozprawa doktorska realizowana w ramach projektów finansowanych przez:

NARODOWE CENTRUM NAUKI

OPUS 2018/31/B/NZ2/03248, Kierownik: prof. dr hab. Ewa Ziętkiewicz

OPUS 2014/13/B/NZ2/03858, Kierownik: prof. dr hab. Ewa Ziętkiewicz

PRELUDIUM 2018/29/N/NZ5/00810, Kierownik: mgr Alicja Rabiasz

INSTYTUT
GENETYKI CZŁOWIEKA
POLSKIEJ AKADEMII NAUK

Mingrant 2021/01, Kierownik: mgr Alicja Rabiasz

Pozostałe publikacje nie obejmujące prac stanowiących rozprawę doktorską:

1. Zuzanna Bukowy-Bieryłło, **Alicja Rabiasz**[*], Maciej Dąbrowski[*], Andrzej Pogorzelski, Alina Wojda, Hanna Dmeńska, Katarzyna Grzela, Jakub Sroczyński, Michał Witt, Ewa Ziętkiewicz
   „Truncating mutations in exons 20 and 21 of *OFD1* can cause primary ciliary dyskinesia without associated syndromic symptoms"
   J Med Genet. 2019 Nov;56(11):769-777.
   Impact Factor: 4.943
   Punkty MNiSW: 140

2. Małgorzata Grabowska[*], Konrad Kuczyński[*], Monika Piwecka, **Alicja Rabiasz**, Joanna Zemła, Paweł Głodowicz, Dariusz Wawrzyniak, Małgorzata Lekka, Katarzyna Rolle
   [*]równorzędny wkład
   „miR-218 affects the ECM composition and cell biomechanical properties of glioblastoma cells."
   J Cell Mol Med. 2022 Jul;26(14):3913-3930.
   Impact Factor: 5.3
   Punkty MNiSW: 100

Lista plakatów i wystąpień konferencyjnych zaprezentowanych w trakcie realizacji rozprawy doktorskiej:

13-15.10.2024	6th European Meeting on Planarian Biology, Platja d'Aro, Hiszpania **Plakat** „*Smed-spag1* is required for motile cilia function, while *Smed-polr2k* is essential for planarian regeneration and maintaining body homeostasis" **Alicja Rabiasz**[*], Ewa Ziętkiewicz
04-07.10.2022	5th European Cilia Conference, Kolonia, Niemcy **Plakat** „The genomic deletion encompassing important parts of *POLR2K* and *SPAG1*: detrimental effect of the loss of POLR2K function explains the lack of SPAG1-del homozygotes among primary ciliary dyskinesia patients" **Alicja Rabiasz**[*], Monika Drobna-Śledzińska, Ewa Ziętkiewicz
27-30.06.2022	VI Kongres Genetyki, Kraków, Polska **Plakat** „*POLR2K* as a passenger gene mutated together with *SPAG1*, the known primary ciliary dyskinesia (PCD) gene" **Alicja Rabiasz**[*], Monika Drobna-Śledzińska, Natalia Maćkowska-Maślak, Ewa Ziętkiewicz Nagroda „Helisa 2022" za najlepszy plakat **Plakat**„Using SPEF2 antibody to analyze potential pathogenicity of new *HYDIN* variants detected in the patient with primary ciliary dyskinesia" Hanna Przystałowska Macioła[*], Zuzanna Bukowy-Bieryłło, **Alicja Rabiasz**, Ewa Ziętkiewicz
25-25.02.2021	International Young Scientists Conference on Molecular and Cell Biology, Warszawa, Polska **Wystąpienie** „Searching for novel genes involved in the pathogenesis of primary ciliary dyskinesia (PCD)"

	Alicja Rabiasz[*], Patrycja Kaźmierczak, Michał Witt, Ewa Ziętkiewicz
27.04.2019	X Wykłady Otwarte z cyklu Spotkania Młodych z Nauką, Poznań, Polska **Wystąpienie** „Identyfikacja genów potencjalnie zaangażowanych w patogenezę pierwotnej dyskinezy rzęsek" **Alicja Rabiasz**[*], Michał Witt, Ewa Ziętkiewicz Nagroda za najlepsze wystąpienie
26-29.03.2019	4rd Beat-PCD Conference & 5th PCD Training School, Poznań, Polska **Plakat** „Short Scientific Mission in Lisbon: Analysis of the cilia-related phenotypes in *CFAP300*-knockdown zebrafish" **Alicja Rabiasz**[*], Margarida Rasteiro, Susana Lopes, Michał Witt, Ewa Ziętkiewicz
13-15.09.2018	IX Zjazd Polskiego Towarzystwa Genetyki Człowieka, Bydgoszcz, Polska **Plakat** „*Schmidtea mediterranea* as a model organism to study novel genes potentially involved in primary ciliary dyskinesia pathogenesis" **Alicja Rabiasz**[*], Michał Witt, Ewa Ziętkiewicz Nagroda „Helisa 2018" za najlepszy poster **Plakat** „Sequential culture of primary respiratory epithelium cells, although suitable for diagnosis of genetic cilia defects, is not a suitable model for respiratory epithelium differentiation studies" Zuzanna Bukowy-Bieryłło[*], Maciej Dąbrowski, Patrycja Daca-Roszak, Magdalena Pikulska, **Alicja Rabiasz**, Agnieszka Fedoruk-Wyszomirska, Eliza Wyszko, Michał Witt, Ewa Ziętkiewicz

[*]osoba prezentująca

Lista nagród i stypendiów otrzymanych w trakcie realizacji rozprawy doktorskiej

- Stypendium „EMBO Scientific Exchange Grant" na realizację projektu „The use of mRNA therapy to restore ciliary function in zebrafish with knockout of *CCDC39*, the known primary ciliary dyskinesia (PCD) gene" i odbycie trzymiesięcznego stażu w NOVA Medical School, Lizbona, Portugalia (realizacja stażu: 06.03-03.06.2023)
- Grant podróżny uzyskany w ramach programu COST (BM1407) na realizację krótkoterminowego stażu „Short Term Scientific Mission" w Chronic Diseases Research Center (CEDOC), NOVA Medical School, Lizbona, Portugalia (realizacja stażu: 10-24.11.2018)
- Grant podróżny uzyskany w ramach programu COST (BM1407) na udział w 3rd Beat-PCD Conference & 4th PCD Training School, Lizbona, Portugalia, 06-09.02.2018
- Nagroda „Helisa 2022" za najlepszy plakat podczas VI Kongres Genetyki, Kraków, Polska, 27-30.06.2022
- Nagroda za najlepsze wystąpienie ustne podczas X Wykładów Otwartych z cyklu Spotkania Młodych z Nauką, Poznań, Polska, 27.04.2019
- Nagroda „Helisa 2018" za najlepszy plakat podczas IX Zjazdu Polskiego Towarzystwa Genetyki Człowieka, Bydgoszcz, Polska, 13-15.09.2018

Spis treści

Wykaz skrótów

ALI	granica faz ciecz-powietrze (*air-liquid interface*)
ASCs	dorosłe komórki macierzyste (*adult stem cells*)
ATP	adenozyno-5′-trifosforan (*adenozyno-5′-trifosforan)*
CBF	częstotliwość bicia rzęsek (*ciliary beat frequency*)
cDNA	komplementarny RNA (*complementary RNA*)
dsRNA	dwuniciowy RNA (double-stranded RNA)
eGFP	białko wzmocnionej zielonej fluorescencji *(enhanced green fluorescent protein)*
FGF	czynnik wzrostu fibroblastów (*fibroblast growth factor)*
HAE	ludzki nabłonek oddechowy (*human airway epithelium*)
HSVM	mikroskopia szybkoklatkowa (*high-speed videomicroscopy*)
IDA	wewnętrzne ramiona dyneinowe (*inner dynein arm*)
IF	immunofluorescencja (*immunofluorescence*)
IFT	transport wewnątrzrzęskowy (*intraflagellar transport*)
N-DRC	regulatorowe kompleksy neksynowo-dyneinowe (*nexin-dynein regulatory complexes)*
NGS	sekwencjonowanie nowej generacji (*next-generation sequencing)*
NIH	Narodowe Instytuty Zdrowia (*National Institutes of Health*)
NMD	rozpad mRNA wywołany obecnością przedwczesnego kodonu nonsensownego (*nonsense mediated mRNA decay*)
mRNA	matrycowy RNA (*messenger RNA*)
ODA	zewnętrzne ramiona dyneinowe (*outer dynein arm*)
PCD	pierwotna dyskineza rzęsek (*primary ciliary dyskinesia*)
PCR	łańcuchowa reakcja polimerazy (*polymerase chain reaction*)

PDGFRα	czynnik wzrostu alfa uwalniany z płytek krwi (*platelet-derived growth factor receptor-alpha*)
qRT-PCR	ilościowa łańcuchowa reakcja polimerazy z odwrotną transkrypcją (*quantitative reverse transcription polymerase chain reaction*)
RNAi	interferencja RNA (*RNA interference*)
RS	szprychy promieniste (*radial spokes*)
RT-PCR	łańcuchowa reakcja polimerazy z odwrotną transkrypcją (*reverse transcription polymerase chain reaction*)
siRNA	mały interferujący RNA (*small interfering RNA*)
SSCP	polimorfizm konformacji jednoniciowych fragmentów (*single-strand conformation polymorphism*)
TEM	transmisyjny mikroskop elektronowy (*transmission electron microscope*)
WES	sekwencjonowanie całoeksomowe (*whole-exome sequencing*)
WHO	Światowa Organizacja Zdrowia (*World Health Organization)*

Wykaz nazw genów

C11orf70	*chromosome 11 open reading frame 70*
CCDC39	*coiled-coil domain containing 39*
CCDC40	*coiled-coil domain containing 40*
CCDC151	*coiled-coil domain containing 151*
CFAP45	*cilia and flagella associated protein 45*
CFAP52	*cilia and flagella associated protein 52*
CFAP221	*cilia and flagella associated protein 221*
CFAP298	*cilia and flagella associated protein 298*
CFAP300	*cilia and flagella associated protein 300*
CFAP45	*cilia and flagella associated protein 45*
CFAP52	*cilia and flagella associated protein 52*
DAW1	*dynein assembly factor with WD repeats 1*
DNAAF11	*dynein axonemal assembly factor 11*
DNAH5	*dynein axonemal heavy chain 5*
DNAI1	*dynein axonemal intermediate chain 1*
DNAI2	*dynein axonemal intermediate chain 1*
DNALI1	*dynein axonemal light intermediate chain 1*
DYX1C1	*dyslexia susceptibility 1 candidate gene 1*
FOXJ1	*forkhead box protein J1*
GAPDH	*glyceraldehyde-3-phosphate dehydrogenase*
GAS8	*growth arrest specific 8*
LRRC6	*leucine rich repeat containing 6*
PCDP1	*primary ciliary dyskinesia protein 1*

POLR2K	*RNA polymerase II, I and III subunit K*
RSPH4A	*radial spoke head component 4A*
SPAG1	*sperm-associated antigen 1*
SPEF2	*sperm flagellar 2*
STK36	*serine/threonine-protein kinase 36*
TTC25	*tetratricopeptide repeat protein 25*

Wstęp

Rzęski są ewolucyjnie zakonserwowanymi organellami, które tworzą wypustki na powierzchni wielu komórek eukariotycznych. Głównym elementem tych organelli jest wystająca ponad powierzchnię komórki aksonema, zakotwiczona w błonie komórkowej za pośrednictwem ciałka podstawnego[1]. Ze względu na różnice w budowie i funkcji, rzęski można tradycyjnie podzielić na dwa rodzaje: rzęski ruchowe (i dłuższe od nich wici) oraz pozbawione zdolności ruchu rzęski pierwotne (czuciowe); dokładna klasyfikacja rzęsek jest bardziej skomplikowana[2,3].

Rzęski ruchowe mogą występować na komórce w liczbie od jednej do kilkuset[4]. Na wczesnym etapie ewolucji, obecność tych organelli komórkowych zapewniała możliwość przemieszczania się organizmów jednokomórkowych w środowisku wodnym. U organizmów bardziej zaawansowanych ewolucyjnie (zwierząt wielokomórkowych) rzęski zostały zaadaptowane do pełnienia szeregu funkcji wymagających przemieszczania płynów zewnątrzkomórkowych[5]. Skoordynowany ruch licznych rzęsek obecnych na apikalnej powierzchni komórek nabłonka odpowiada za oczyszczanie górnych dróg oddechowych poprzez transport śluzowo-rzęskowy, a także za przepływ płynu mózgowo-rdzeniowego oraz transport oocytów w jajowodach[6]. Pojedyncze rzęski ruchowe komórek węzła zarodkowego ssaków (i podobnych struktur niektórych kręgowców) regulują kierunkowy przepływ morfogenów wymaganych do ustanowienia w zarodku wzorca symetrii osi ciała „lewo-prawo"; pojedyncza wić plemnika (witka) odpowiada za ruchliwość męskiej gamety[5,7]. Chociaż funkcja rzęsek ruchowych i wici jest głównie związana z ich zdolnością do ruchu, mogą też one pełnić funkcje sensoryczne[2,8,9].

Drugi rodzaj rzęsek to rzęski pierwotne, występujące pojedynczo na powierzchni większości komórek eukariotycznych. Ich główną rolą jest odbieranie i przekazywanie sygnałów biorących udział w regulacji procesów komórkowych w trakcie rozwoju oraz utrzymaniu homeostazy tkanek[10]. Rzęski pierwotne są zaangażowane w koordynację wielu ścieżek sygnalizacyjnych, np. regulowanych przez Hedgehog (Hh), wingless (WNT), czynnik wzrostu fibroblastów (*fibroblast growth factor,* FGF*),* czy czynnik wzrostu alfa uwalniany z płytek krwi *(platelet-derived growth factor receptor-alpha,* PDGFRα*);* ponadto odgrywają istotną rolę w regulacji wewnątrzkomórkowego poziomu wapnia[11].

Istotna rola rzęsek w wielu procesach biologicznych sprawia, że genetycznie uwarunkowane zmiany w ich strukturze lub funkcji prowadzą do rozwoju szeregu chorób

genetycznych zwanych ciliopatiami. Większość tych chorób wynika z dysfunkcji rzęsek pierwotnych[7,12]. Są to zwykle choroby syndromiczne, do których można zaliczyć: zespół Bardet-Biedla, zespół policystycznych nerek, zespół Jouberta i inne[13]. Zaburzenia dotyczące rzęsek ruchowych są podłożem heterogennej genetycznie choroby znanej jako pierwotna dyskineza rzęsek (*primary ciliary dyskinesia,* PCD)[7]. Należy podkreślić, że słowo „pierwotna" w nazwie choroby nie odnosi się do rzęsek pierwotnych. Określenie to podkreśla mechanizm patogenezy wynikający z genetycznie uwarunkowanej dysfunkcji rzęsek ruchowych, w odróżnieniu od przyczyn wtórnej dyskinezy rzęsek, która jest chorobą niedziedziczną i wynika z działania czynników środowiskowych.

Ze względu na tematykę rozprawy doktorskiej w dalszej części opisu skupiono się na rzęskach ruchowych oraz pierwotnej dyskinezie rzęsek.

Rzęski ruchowe

Aksonemę typowych rzęsek ruchowych charakteryzuje wysoce uporządkowana podstawowa struktura składająca się z dziewięciu peryferyjnie ułożonych dubletów mikrotubul typu A i B, które otaczają jedną parę centralną mikrotubul (wzór na przekroju rzęski 9x2 +2)[1,5] [Rycina 1]. W pracy przeglądowej (Artykuł 1) stanowiącej element niniejszej rozprawy doktorskiej przedstawiono odstępstwa w budowie rzęsek ruchowych różnych typów. Wielobiałkowe kompleksy, do których należą zewnętrzne i wewnętrzne ramiona dyneinowe (odpowiednio: *outer dynein arm*, ODA; *inner dynein arms,* IDA), kompleksy dokujące ODA, szprychy promieniste (*radial spokes,* RS) i regulatorowe kompleksy neksynowo-dyneinowe (*nexin-dynein regulatory complexes,* N-DRC), związane są z peryferyjnie ułożonymi mikrotubulami typu A i rozmieszczone na całej ich długości[1,5]. Ruch rzęsek możliwy jest dzięki aktywacji białek dyneinowych wchodzących w skład kompleksów ODA i IDA, które wykazują aktywność adenozynotrifosfatazy (ATPazy)[14,15]. Hydroliza adenozynotrifosforanu (*adenozyno-5'-trifosforan*, ATP) uwalnia energię niezbędną do wzajemnego ruchu mikrotubul względem siebie[16]. ODA i IDA poruszają się w sposób synchroniczny wzdłuż mikrotubuli B sąsiedniego dubletu, a powstałe w ten sposób wzajemne przesuwanie się dubletów jest ograniczone przez N-DRC łączące sąsiadujące dublety, co ostatecznie prowadzi do zgięcia rzęski[17]. Ponadto ruch rzęsek jest regulowany przez RSy, które tworzą strukturalne połączenie między centralną parą mikrotubul a mikrotubulami peryferyjnymi[14,18].

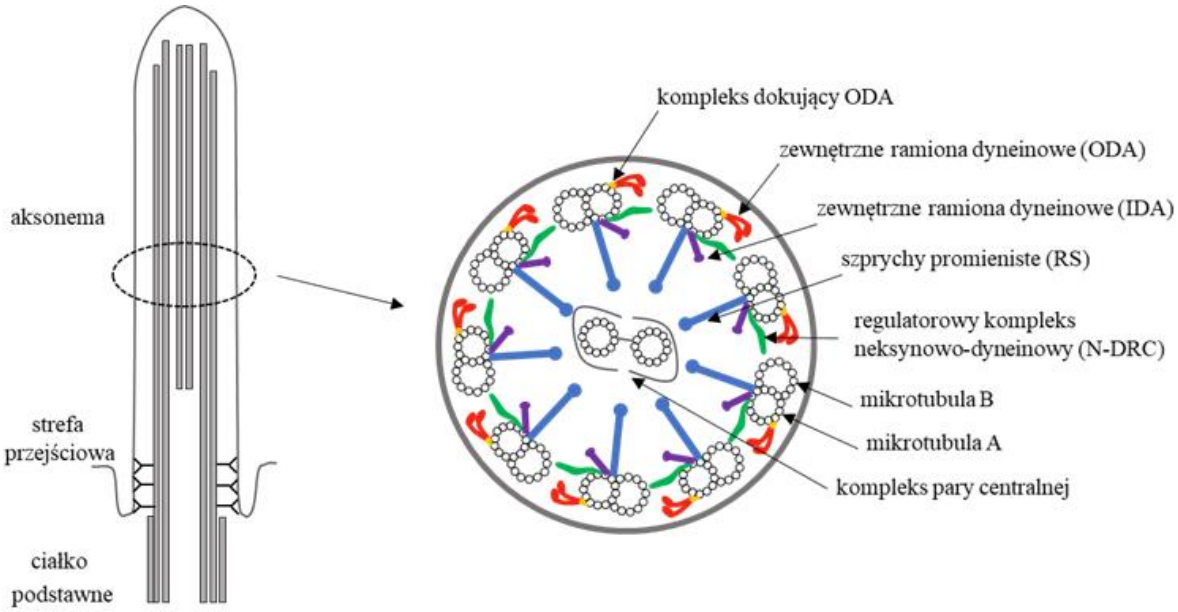

Rycina 1. Schemat przedstawiający przekrój podłużny przez typową rzęskę ruchową. Po prawej stronie: przekrój poprzeczny rzęski.

Składanie i wzrost rzęsek są możliwe dzięki obecności specjalnego dwukierunkowego systemu transportującego elementy składowe struktury rzęsek wzdłuż mikrotubul, zwanego transportem wewnątrzrzęskowym (*intraflagellar transport*, IFT). IFT jest niezbędny do wzrostu rzęsek poprzez transport białek strukturalnych lub ich kompleksów, z wnętrza komórki do apikalnej części rzęski; odpowiada również za transport w przeciwnym kierunku[19]. Transport do i z rzęski jest kontrolowany poprzez zlokalizowaną u podstawy aksonemy rzęski strefę przejściową, która tworzy selektywną barierę dla transportowanych elementów[20].

Badania proteomiczne z wykorzystaniem dwuwiciowego organizmu modelowego *Chlamydomonas reinhardtii*, wykazały, że istnieje około 360-650 białek strukturalnych rzęsek i wici[21]. Późniejsze badania z wykorzystaniem innych organizmów modelowych oraz komórek ludzkiego nabłonka oddechowego dowiodły, że genów kodujących białka strukturalne oraz białka cytoplazmatyczne zaangażowane w biogenezę rzęsek może być prawie tysiąc[22,23]. Patogenne warianty w części tych genów stanowią molekularne podłoże pierwotnej dyskinezy rzęsek.

Pierwotna dyskineza rzęsek (*primary ciliary dyskinesia*, PCD)

Pierwotna dyskineza rzęsek (OMIM244400) jest rzadką, genetycznie heterogenną chorobą należącą do grupy ciliopatii związanych z dysfunkcją rzęsek ruchowych. PCD jest chorobą dziedziczoną najczęściej autosomalnie w sposób recesywny, ale w rzadkich przypadkach może być przekazywana wraz z chromosomem X lub autosomalnie w sposób dominujący[24]. Częstość występowania PCD w populacji oceniana jest najczęściej jako 1:10 000-1:20 000 żywych urodzeń, jednak ze względu na heterogenność objawów klinicznych, złożoność diagnostyki oraz w zależności od analizowanej populacji, rzeczywista częstość występowania PCD może być wyższa[7,25].

Objawy PCD odzwierciedlają funkcje rzęsek ruchowych w organizmie człowieka. Dysfunkcja rzęsek komórek nabłonka oddechowego prowadzi do upośledzenia transportu śluzowo-rzęskowego, co zazwyczaj wiąże się z niewydolnością oddechową u noworodków, a następnie objawia się nawracającymi infekcjami dolnych i górnych dróg oddechowych, zapaleniem zatok przynosowych oraz wysiękowym zapaleniem ucha środkowego[26]. Konsekwencją częstych infekcji mogą być rozstrzenia oskrzeli oraz upośledzenie funkcji płuc, w najcięższych przypadkach wymagające wdrożenia tlenoterapii lub przeszczepu płuc[27]. Dysfunkcja rzęsek ruchowych w jajowodach może wpływać niekorzystnie na transport komórek jajowych, a defekty witek plemników na ich ruch, co może skutkować obniżeniem płodności u kobiet i mężczyzn. Dysfunkcja pojedynczych rzęsek w węźle zarodkowym na wczesnym etapie embriogenezy zaburza gradient morfogenów, co może powodować odwrócenie osi symetrii ciała, obserwowane u około 50% pacjentów z PCD (tzw. syndrom Kartagenera)[7,28]. Niezwykle rzadko obserwuje się też wodogłowie spowodowane dysfunkcją rzęsek ruchowych nabłonka wyścielającego komory mózgu, które odpowiadają za transport płynu mózgowo-rdzeniowego[7].

Ze względu na niespecyficzne objawy, trudności w rozpoznaniu choroby oraz brak specjalistycznych ośrodków w niektórych krajach, PCD jest często diagnozowana późno[7,29,30]. Wieloośrodkowa analiza dotycząca diagnostyki PCD w 18 krajach wykazała, że tylko u 17% spośród 3013 analizowanych pacjentów, PCD została zdiagnozowana w pierwszych latach życia (0-9 lat); najwięcej pacjentów (38%) otrzymało diagnozę w wieku 10-19 lat[31]. Intensywne badania naukowe oraz współpraca międzynarodowa w ciągu ostatnich lat pozwoliły na lepsze zrozumienie zarówno klasycznych, jak i nietypowych objawów PCD, zaobserwowanie korelacji między obserwowanym fenotypem a genotypem

oraz określenie regionalnych różnic w częstości występowania choroby[30,32]. Mimo opracowania nowych standardów diagnostycznych, PCD pozostaje trudna do zdiagnozowania ze względu na heterogenny obraz kliniczny choroby oraz złożoność podstaw molekularnych i genetycznych. PCD nie można potwierdzić ani wykluczyć za pomocą jednego testu diagnostycznego. Przykładowo, chociaż analiza struktury rzęsek przy użyciu transmisyjnego mikroskopu elektronowego (*transmission electron microscope*, TEM) od lat stanowi jeden ze standardów diagnostycznych PCD, nie zawsze pozwala ona na jednoznaczne potwierdzenie lub wykluczenie PCD; u około 30% pacjentów ultrastruktura rzęsek analizowana tą metodą jest bowiem prawidłowa, podczas gdy u zdrowych osób narażonych na czynniki środowiskowe lub po infekcji struktura rzęsek może ulec wtórnym, odwracalnym zmianom[33,34]. Doskonalenie diagnostyki wymaga dalszej współpracy między klinicystami, genetykami i biologami, połączonej z analizą funkcjonalną i strukturalną rzęsek oraz skutecznym wykrywaniem patogennych wariantów genetycznych[35].

Molekularne podstawy zaburzenia funkcjonowania rzęsek ruchowych u pacjentów z PCD

Ze względu na znaczny wzrost wiedzy na temat molekularnego i genetycznego podłoża PCD, coraz większe znaczenie w diagnostyce tej choroby zyskują testy genetyczne. Aktualnie znanych jest ponad 50 genów zaangażowanych w patogenezę PCD, których patogenne warianty pozwalają na wyjaśnienie podstawy zaburzeń struktury lub funkcji rzęsek ruchowych obserwowanych u pacjentów[32].

W większości przypadków upośledzenie ruchu rzęsek jest spowodowane zmianami w ultrastrukturze tych organelli, takimi jak: brak lub skrócenie ODA, IDA lub obu ramion dyneinowych (ODA+IDA), czy nieprawidłowości w liczbie oraz lokalizacji mikrotubul[1,7,36]. Zaburzenia ultrastruktury rzęsek mogą wynikać z obecności patogennych wariantów w genach kodujących białka strukturalne rzęsek, jak również genach kodujących białka cytoplazmatyczne zaangażowane w biogenezę rzęsek (tzw. ciliogenezę). Te drugie, mimo iż nie są fizycznie częścią rzęsek, odgrywają istotną rolę w montażu oraz transporcie elementów budujących aksonemę[37], a wynikające z ich braku lub dysfunkcji wady ultrastruktury rzęsek są często nie do odróżnienia od wad wywołanych przez zaburzenia lub brak białek strukturalnych[1,7]. Patogenne warianty innych genów (kodujących czynniki transkrypcyjne istotne w procesie ciliogenezy) nie powodują wprawdzie istotnych zmian w strukturze, ale poprzez redukcję liczby rzęsek w komórkach wielorzęskowych zaburzają

ich prawidłowe funkcjonowanie[38]. Z drugiej strony, patogenne warianty w niektórych genach kodujących białka strukturalne, nie prowadzą do łatwo obserwowalnych zmian liczby czy struktury rzęsek komórek nabłonka oddechowego, ale mogą powodować subtelne, a przez to trudno zauważalne zmiany we wzorze ich ruchu[39,40].

Mimo, iż zastosowanie technik sekwencjonowania nowej generacji (*next-generation sequencing,* NGS) pozwoliło na identyfikację wielu patogennych wariantów w genach PCD, u około 1/3 pacjentów genetyczne podłoże PCD pozostaje niewyjaśnione[34,41]. W celu lepszego zrozumienia tej heterogennej genetycznie choroby i zwiększenia efektywności diagnostyki PCD, konieczne jest poszukiwanie nowych patogennych wariantów w znanych genach PCD lub identyfikacja kolejnych genów potencjalnie zaangażowanych w patogenezę tej choroby (tzw. genów kandydatów). Udowodnienie wpływu nowo zidentyfikowanych genów kandydatów na funkcjonowanie rzęsek ruchowych wymaga przeprowadzenia analizy funkcjonalnej tych genów przy użyciu organizmów modelowych lub hodowli komórkowych *in vitro.*

Analiza funkcjonalna genów kandydatów potencjalnie zaangażowanych w patogenezę PCD

Dużym ograniczeniem badań mających na celu wyjaśnienie roli genów potencjalnie zaangażowanych w ciliopatie związane z dysfunkcją rzęsek ruchowych jest brak komercyjnie dostępnych linii komórkowych, które reprezentowałyby zróżnicowane komórki ludzkiego nabłonka oddechowego (*human airway epithelium,* HAE)[42]. Alternatywnym rozwiązaniem jest zastosowanie pierwotnych komórek nabłonka oddechowego dostępnych komercyjnie lub uzyskanych od pacjentów lub zdrowych dawców[43,44]. Hodowle komórek HAE są jednak stosunkowo drogie, czasochłonne, wykazują ograniczone zdolności proliferacyjne, a modyfikacje genetyczne tych komórek stanowią wyzwanie badawcze[42]. Dopiero stosunkowo niedawno opisano użycie zmodyfikowanych komórek HAE w celu wyjaśnienia roli nowo zidentyfikowanego genu w patogenezie PCD[45].

Znaczny wzrost wiedzy na temat biologii rzęsek oraz roli genów związanych z rzęskami w patogenezie chorób człowieka jest wynikiem badań z użyciem organizmów modelowych, możliwych dzięki wysokiemu poziomowi ewolucyjnego zakonserwowania tych organelli[21,46,47]. Identyfikacja pierwszego genu zaangażowanego w patogenezę PCD – *DNAI1* (*Dynein Axonemal Intermediate Chain 1*) – była poparta badaniami z wykorzystaniem jednokomórkowej dwuwiciowej zielonej algi, *Chlamydomonas*

reinhardtii[48]. Do badania rzęsek ruchowych wykorzystywane są również inne organizmy: jednokomórkowe np. *Paramecium tetraurelia*[49], *Trypanosoma brucei*[50]; bezkręgowe jak muszka owocowa (*Drosophila melanogaster*)[51], czy płaziniec z gatunku *Schmidtea mediterranea*[52]; oraz zaawansowane modele kręgowców, np. żaba (*Xenopus laevis*)[53], ryba – danio pręgowane (*Danio rerio*)[54], mysz (*Mus musculus)*[55], czy pies (*Canis lupus familiaris)*[56].

S. mediterranea jest wolnożyjącym, słodkowodnym płazińcem, który słynie z ogromnych zdolności regeneracyjnych związanych z obecnością licznej grupy dorosłych komórek macierzystych (*adult stem cells,* ASCs) zwanych neoblastami[57,58]. Pocięcie robaków na kilka fragmentów skutkuje odtworzeniem brakujących części ciała, co jest możliwe dzięki proliferacji neoblastów i wytworzeniu tzw. blastemy, w której mogą różnicować się brakujące tkanki[59,60]. Cecha ta sprawiła, że *S. mediterranea* jest chętnie wykorzystywana jako organizm modelowy do badania procesu regeneracji i komórek macierzystych. Znajomość sekwencji genomu i transkryptomu[61], dane z sekwencjonowania pojedynczych komórek[62], protokoły opisujące możliwości użycia różnych technik biologii molekularnej do badań z użyciem robaków[63], stosunkowo łatwa i niedroga hodowla[64], stwarzają warunki do wykorzystania planarii jako organizmu modelowego w wielu obszarach badawczych.

Pod kątem wykorzystania planarii do badania rzęsek ruchowych istotne jest, że ruch robaków zależy od pokrywającego brzuszną stronę ich ciała nabłonka składającego się z wielorzęskowych komórek, który w znacznym stopniu odzwierciedla złożoność nabłonka oddechowego u ludzi. Dodatkowo, wpływ wyciszenia genów rzęskowych na funkcjonowanie rzęsek ruchowych może być łatwo monitorowany poprzez analizę ruchu robaków[65]. Mimo to, dotychczas stosunkowo mało uwagi poświęcono możliwości wykorzystania *S. mediterranea* jako organizmu modelowego do badania genów związanych z patogenezą pierwotnej dyskinezy rzęsek. Aktualny stan wiedzy na temat możliwości wykorzystania *S. mediterranea* do badania rzęsek ruchowych i ciliopatii przedstawiono w pracy przeglądowej (Artykuł 1) stanowiącej element niniejszej rozprawy doktorskiej. Jak podkreślono w tej pracy, mimo wielu danych literaturowych na temat wykorzystania płazińca z gatunku *S. mediterranea* jako organizmu modelowego do badania niektórych aspektów związanych z rzęskami (np. ewolucji rzęsek, składania elementów rzęsek), niewiele jest doniesień naukowych opisujących użycie tego gatunku jako modelu *in vivo* do potwierdzenia roli badanych genów w patogenezie PCD.

Cel rozprawy doktorskiej

Uzyskanie pełnego obrazu genetycznego i molekularnego podłoża pierwotnej dyskinezy rzęsek wymaga poszukiwania nowych patogennych wariantów i identyfikacji kolejnych genów związanych z patogenezą PCD.

Pierwszą hipotezą badawczą było założenie, że potencjalnie patogenne warianty genów *CFAP300* i *CFAP221,* wykryte w badaniach przesiewowych u chorych na PCD, leżą u podłoża patogenezy PCD, natomiast delecja części genu *POLR2K* występująca razem z delecją części znanego genu PCD, *SPAG1,* nie jest bezpośrednią przyczyną choroby. **Druga hipoteza** postawiona w niniejszej rozprawie doktorskiej zakładała, że wykorzystanie prostego, taniego i łatwo dostępnego modelu planarii z gatunku *S. mediterranea* pozwala na efektywne potwierdzenie zaangażowania badanych genów w dysfunkcję rzęsek ruchowych leżącą u podłoża patogenezy PCD.

W związku z powyższym, **celem** niniejszej rozprawy doktorskiej było zoptymalizowanie i praktyczne zastosowanie *S. mediterranea* jako organizmu modelowego do potwierdzenia związku wybranych genów z zaburzeniami funkcji rzęsek ruchowych i patogenezą PCD.

Cel ten został zrealizowany poprzez realizację poszczególnych zadań badawczych:

1. Analiza danych literaturowych pod kątem wykorzystania *S. mediterranea* do badania genów leżących u podłoża ciliopatii związanych z dysfunkcją rzęsek ruchowych
2. Analiza *in silico* ewolucyjnego zakonserwowania wybranych genów z wykorzystaniem baz danych dedykowanych *S. mediterranea*
3. Optymalizacja użycia planarii jako organizmu modelowego do badania genów związanych z funkcjonowaniem rzęsek ruchowych
4. Analiza funkcjonalna wybranych genów zaangażowanych lub potencjalnie zaangażowanych w patogenezę PCD oraz ocena związku między wpływem ich wyciszenia na fenotyp planarii a wpływem patogennych wariantów na funkcję nabłonka oddechowego u pacjentów.

Omówienie publikacji wchodzących w skład cyklu prac stanowiących rozprawę doktorską

Artykuł 1

Schmidtea mediterranea as a Model Organism to Study the Molecular Background of Human Motile Ciliopathies

Alicja Rabiasz, Ewa Ziętkiewicz

Int J Mol Sci. 2023 Feb 24;24(5):4472.

Wykorzystanie organizmów modelowych do badania homologów genów rzęskowych przyczyniło się do lepszego zrozumienia molekularnych podstaw chorób związanych z dysfunkcją rzęsek ruchowych, a w szczególności pierwotnej dyskinezy rzęsek. Wyróżnić można dwa podejścia stosowane w badaniach z użyciem organizmów modelowych: (1) wykorzystanie opublikowanych już informacji na temat homologów genów rzęskowych zidentyfikowanych u organizmów modelowych w celu lepszego zrozumienia molekularnych i genetycznych podstaw chorób człowieka lub (2) wykorzystanie organizmów modelowych do przeprowadzenia analizy funkcjonalnej genów o nieznanej lub niepewnej roli w funkcjonowaniu rzęsek ruchowych oraz patogenezie ciliopatii związanej z dysfunkcją rzęsek ruchowych. Dzięki rozwojowi technik wysokoprzepustowych liczba patogennych wariantów znanych genów PCD oraz genów potencjalnie zaangażowanych w ciliopatie stale rośnie, a potwierdzenie ich statusu jako genów PCD stanowi wciąż aktualne wyzwanie badawcze.

W niniejszej publikacji przedstawiono aktualny stan wiedzy na temat genetycznych podstaw PCD, roli organizmów modelowych w zrozumieniu funkcji genów zaangażowanych w patogenezę tej choroby oraz skupiono się na możliwości wykorzystania *S. mediterranea* jako organizmu modelowego do badania genów zaangażowanych w tę chorobę. Ponadto w pracy uwzględniono przykłady genów o niepewnej roli w patogenezie PCD lub genów powodujących choroby ze spektrum PCD. W ramach omawianej pracy dokonano przeglądu 245 pozycji literaturowych, na podstawie których wyodrębniono trzy główne rozdziały. W rozdziale pierwszym, który stanowi wstęp do dalszej części pracy, opisano rzęski oraz ciliopatie, skupiając się głównie na rzęskach ruchowych, których

dotyczy omawiana praca. Następnie omówiono pierwotną dyskinezę rzęsek; w formie dwóch tabeli przedstawiono aktualny stan wiedzy na temat genów PCD, przykładów genów o niepewnej roli w patogenezie PCD oraz genów zaangażowanych w rozwój chorób ze spektrum PCD. Ze względu na tematykę rozprawy doktorskiej, w przedstawionych tabelach uwzględniono zarówno organizmy modelowe, które zostały użyte do potwierdzenia roli badanych genów w patogenezie PCD i innych ciliopatii związanych z dysfunkcją rzęsek ruchowych, jak i organizmy, które nie zostały użyte lub zacytowane w tych pracach, ale przyczyniły się do lepszego zrozumienia roli wymienionych genów w strukturze lub funkcji rzęsek ruchowych. Podkreślono także konieczność potwierdzenia udziału genów kandydatów w patogenezie PCD i chorób ze spektrum PCD przy użyciu organizmów modelowych.

Rozdział drugi został poświęcony opisowi płazińca z gatunku *Schmidtea mediterranea* – jego klasyfikacji systematycznej, ogromnym zdolnościom regeneracyjnym oraz budowie anatomicznej. Przedstawiono zalety planarii jako organizmu modelowego, m.in. poprzez zwrócenie uwagi na obecność wielu homologów genów ludzkich, łatwość hodowli tego organizmu oraz dostępność rożnych protokołów opisujących techniki biologii molekularnej, które można wykorzystać do badań z użyciem tego organizmu. Zaletą planarii jest możliwość wykonania wyciszenia badanych genów poprzez zastosowane metody interferencji RNA (*RNA interference,* RNAi) z wykorzystaniem dwuniciowych RNA (*double-stranded RNA,* dsRNA). Istnieją różne strategie wprowadzania dsRNA do organizmu planarii: poprzez mikroiniekcję, z pokarmem (w postaci bakterii zdolnych do ekspresji zaprojektowanego dsRNA lub jako wcześniej przygotowane dsRNA). Następnie omówiono model *S. mediterranea* w kontekście badania rzęsek (np. ewolucji rzęsek, roli rzęsek w ścieżkach sygnalizacyjnych), uwzględniając aktualny stan wiedzy na temat rzęsek ruchowych obecnych u planarii. Ruch planarii (tzw. *gliding movement*) zależy od synchronicznego ruchu rzęsek (występujących w liczbie około 80 rzęsek na komórkę) zlokalizowanych w nabłonku po brzusznej stronie ich ciała; w związku z tym, wyciszenie genów rzęskowych skutkuje zaburzeniem ruchu planarii, które objawia się jako spowolnienie i zmiana wzorca przemieszczania się robaków (tzw. *inchworming movement*). Ponadto w pracy omówiono metody badawcze, która można zastosować w celu analizy wpływu wyciszenia badanych genów na ruch robaków oraz rzęski ruchowe planarii. Używając stereoskopu z kamerą można w łatwy sposób dokumentować zmiany ruchu robaków, a następnie stosując darmowy, ogólnodostępny program ImageJ można

porównywać dystans jaki w określonej jednostce czasu pokonały robaki kontrolne i robaki z wyciszonym genem. Ponadto, podobnie jak przypadku ludzkich komórek nabłonka oddechowego, można dokonać analizy funkcji lub struktury rzęsek poprzez użycie: mikroskopii szybkoklatkowej (*high-speed videomicroscopy, HSVM),* immunofluorescencji (*immunofluorescenc*e, IF) lub transmisyjnego mikroskopu elektronowego.

Na końcu rozdziału drugiego przedstawiono opis modelu płazińca w kontekście badania PCD oraz innych ciliopatii przypominających PCD. Przegląd danych literaturowych wykazał, że chociaż płaziniec z gatunku *S. mediterranea* bywa wykorzystywany do wyjaśnienia roli różnych genów w funkcjonowaniu rzęsek ruchowych, to niewiele jest prac opisujących bezpośrednie zastosowanie tego organizmu w badaniach patogenezy ciliopatii. W przypadku prac opisujących patogenne warianty różnych genów, płaziniec ten był wykorzystany do badania roli dwóch genów związanych z patogenezą ciliopatii jak dotąd niezaklasyfikowanej jako PCD (*CFAP45* i *CFAP52*) oraz trzech genów o potwierdzonym związku z patogenezą PCD (*CFAP298, CCDC151* i *CFAP300*)*;* badanie genu *CFAP300* opisano w **Artykule 2** wchodzącym w skład niniejszej rozprawy doktorskiej. W pracy przeglądowej zwrócono również uwagę na geny, które w momencie badania z wykorzystaniem *S. mediterranea* nie były opisywane jako geny PCD (np. *FOXJ1, DAW1*), ale po znalezieniu patogennych wariantów tych genów u ludzi, w oparciu o dane kliniczne pacjentów oraz inne wyniki badań, zostały zaklasyfikowane jako geny zaangażowane w patogenezę tej choroby.

W rozdziale trzecim przedstawiono perspektywy dotyczące wykorzystania *S. mediterranea* jako organizmu modelowego. Ze względu na rosnącą liczbę naukowców zajmujących się badaniem planarii, wiedza na temat robaków, liczba danych genomowych, transkryptomicznych, fenotypowych, filogenetycznych, a w konsekwencji liczba narzędzi oraz baz danych dedykowanych *S. mediterranea* nieustannie rośnie, czyniąc ten organizm bardziej dostępnym i atrakcyjnym dla środowiska naukowego.

Podsumowanie:

Przedstawione w pracy przeglądowej dane dotyczące *S. mediterranea* jako modelu do badania genów związanych z funkcjonowaniem rzęsek ruchowych oraz genów zaangażowanych w PCD i inne ciliopatie rzęsek ruchowych, pozwoliły na wysunięcie wniosku, że organizm ten może być efektywnym i niedrogim modelem do przeprowadzenia wstępnej analizy funkcjonalnej genów związanych z rzęskami ruchowymi, w tym genów

potencjalnie zaangażowanych w PCD. Pokrywający brzuszną część ciała planarii nabłonek, którego komórki na swej apikalnej części posiadają liczne rzęski ruchowe, w zadowalającym stopniu odzwierciedla złożoność ludzkiego nabłonka oddechowego, czyniąc ten organizm bardziej atrakcyjnym od popularnych modeli jednokomorowych (np. *C. reinhardtii, P. tetraureli*). Równocześnie, ze względu na prostotę, niskie koszty, planarie są modelem łatwiej dostępnym niż bardziej zaawansowane modele kręgowców (np. ryby, myszy).

Mój wkład w powstanie publikacji:

- ustalenie koncepcji i planu pracy
- przegląd i wybór prac omówionych w publikacji
- pisanie oryginalnej wersji publikacji
- opracowanie rycin i tabel.

Publikacja jest dostępna pod następującym adresem internetowym:

https://doi.org/10.3390/ijms24054472

International Journal of
Molecular Sciences

MDPI

Review

Schmidtea mediterranea as a Model Organism to Study the Molecular Background of Human Motile Ciliopathies

Alicja Rabiasz and Ewa Ziętkiewicz *

Institute of Human Genetics Polish Academy of Sciences, 32 Strzeszyńska Street, 60-479 Poznań, Poland
* Correspondence: ewa.zietkiewicz@igcz.poznan.pl; Tel.: +48-61-65-79-203

Abstract: Cilia and flagella are evolutionarily conserved organelles that form protrusions on the surface of many growth-arrested or differentiated eukaryotic cells. Due to the structural and functional differences, cilia can be roughly classified as motile and non-motile (primary). Genetically determined dysfunction of motile cilia is the basis of primary ciliary dyskinesia (PCD), a heterogeneous ciliopathy affecting respiratory airways, fertility, and laterality. In the face of the still incomplete knowledge of PCD genetics and phenotype-genotype relations in PCD and the spectrum of PCD-like diseases, a continuous search for new causative genes is required. The use of model organisms has been a great part of the advances in understanding molecular mechanisms and the genetic basis of human diseases; the PCD spectrum is not different in this respect. The planarian model (*Schmidtea mediterranea*) has been intensely used to study regeneration processes, and—in the context of cilia—their evolution, assembly, and role in cell signaling. However, relatively little attention has been paid to the use of this simple and accessible model for studying the genetics of PCD and related diseases. The recent rapid development of the available planarian databases with detailed genomic and functional annotations prompted us to review the potential of the *S. mediterranea* model for studying human motile ciliopathies.

Keywords: candidate genes; flatworms; motile cilia; planarians; primary ciliary dyskinesia (PCD); RNA interference (RNAi)

Citation: Rabiasz, A.; Ziętkiewicz, E. *Schmidtea mediterranea* as a Model Organism to Study the Molecular Background of Human Motile Ciliopathies. *Int. J. Mol. Sci.* 2023, 24, 4472. https://doi.org/10.3390/ijms24054472

Academic Editor: Apostolos Zaravinos

Received: 1 February 2023
Revised: 21 February 2023
Accepted: 22 February 2023
Published: 24 February 2023

1. Introduction–Cilia and Ciliopathies

Cilia and flagella are evolutionarily conserved organelles that form protrusions on the surface of many growth-arrested or differentiated eukaryotic cells, from simple unicellular organisms such as *Chlamydomonas* to specialized cells in higher animals—fish and mammals [1–3]. The cilium is anchored at the cell membrane via the basal body, which extends into the axoneme, the main part of the cilium protruding outside the cell; the transition zone between the basal body and axoneme has a function of ciliary gating [4]. Due to structural and functional differences, cilia can be roughly classified as motile and non-motile (also called primary or sensory), although their detailed classification is much more complicated [5,6].

Motile cilia are ancient organelles that were already present in the Last Eukaryotic Common Ancestor, LECA [2]. Their main function is associated with their ability to move; they also perform some sensory functions [5,7,8]. In unicellular organisms, such as *Chlamydomonas*, *Paramecium*, or *Tetrahymena*, cilia or flagella (structurally related to motile cilia, but much longer) are responsible for the movement of cells. In higher organisms, motile cilia (5–10 um long) form a dense carpet (hundreds of organelles per cell) on the apical side of multiciliated cells (MCCs), and through their coordinated planar beating are responsible for the flow of fluids covering epithelium [9]. Single flagella are responsible for sperm motility [10], and single motile cilia in the mammalian embryonal node regulate the directional flow of signals required for the establishment of left-right patterning [11]. **Primary cilia** found as singular entities on the surface of almost every differentiated

metazoan cell type [1], are not in focus in this review, but it should be mentioned that they evolved from motile cilia. Due to the difference in their structure, they are immotile [12], but they play an important role in the reception and transmission of signals involved in the regulation of cellular processes essential for development and the maintenance of tissue homeostasis. The main signaling pathways coordinated by primary cilia include those regulated by Hedgehog (HH), G-protein-coupled receptors (GPCR), wingless (WNT), receptor-tyrosine kinases (RTKs), and TGFβ/BMP receptors [12–15].

In the axoneme of a typical motile cilium or flagellum (Figure 1), nine peripheral doublets of microtubules (A and B) surround two single central microtubules (C1 and C2). In the cross-section of the axoneme observed in the transmission electron microscope (TEM), this arrangement is known as the 9 × 2 + 2 pattern. Additional protein elements attached to the microtubules are distributed periodically along the axoneme length. Multiprotein complexes associated with the peripheral A microtubules form characteristic auxiliary structures: outer and inner dynein arms (ODA and IDA), ODA docking complexes, radial spokes (RS), and nexin-dynein regulatory complexes (N-DRC). Several detailed reviews describing the axonemal structure components have been published in recent years, e.g., [16–18].

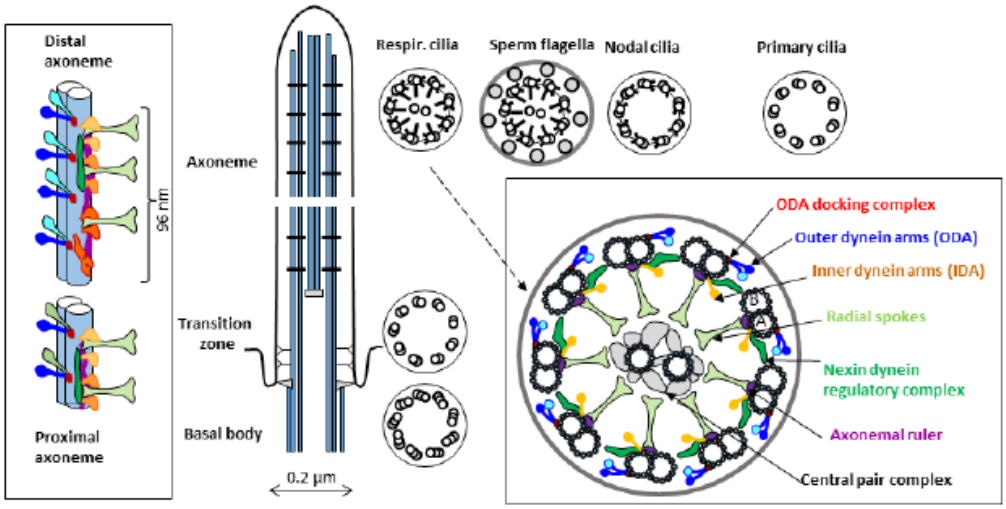

Figure 1. Simplified schematic representation of the ultrastructure of a motile cilium (longitudinal and cross sections detailing microtubule-associated elements). Cross-sections of the axoneme of different types of motile cilia (respiratory and nodal cilia, sperm flagellum) are compared with that of a primary cilium. The periodic longitudinal unit (organized in 96 nm repeats) consists of four ODAs (attached to A microtubules of the peripheral dublets through the ODA-docking complexes), three radial spokes, and a set of IDAs (consisting of different complexes identified using a cryoelectron tomography [16,19]). The length of this unit is determined by the molecular ruler proteins (in humans, CCDC39 and CCDC40, homologs of Chlamydomonas proteins FAP59 and FAP172 [20]). In mammalian motile cilia, ODAs differ in the proximal and distal parts of the axoneme (by the presence of DNAH11 and DNAH9 proteins, respectively); in sperm flagella, they are replaced by a single protein DNAH17 [21]. Several small elements attached to the A microtubule, not visible in classical TEM, have been identified in model organisms using cryoelectron tomography [22]; additional small proteins are docked at the luminal side of both A- and B-microtubules [23,24]. The central microtubules, connected by a multiprotein bridge, and surrounded by a set of projections, form the central pair complex [25].

Cilia movement is powered by ODAs and IDAs, which act as ATP-dependent molecular motors. They move in synchrony along the B microtubule of the adjacent doublet. The resulting mutual sliding of the peripheral doublets is restricted by the N-DRCs, which connect neighboring doublets; the net result is a bend of the cilium [26]. Radial spokes, attached to the peripheral A microtubules and transiently contacting the projections of the central microtubules, stabilize the structure and functionally connect the central apparatus to the dynein arms [27]. The cooperation of all these ultrastructural elements results in a coordinated planar beating of motile cilia, with a fast power stroke and a slower recovery stroke occurring in the same plane; for the review see, e.g., [18].

The ciliogenesis of motile cilia is a multi-step process, starting from the cell cycle exit and involving many signaling factors; it has been the subject of many excellent reviews, e.g., [28]. The inhibition of the NOTCH1 signal and activation of the MCIDAS-dependent pathway initiates the biogenesis process specific to MCCs [29]. In MCCs, the MCIDAS pathway orchestrates massive centriole amplification and their docking in the apical cell membrane (through the activation of cyclin O) [30]. The expression of the FOXJ1 transcription factor switches on the synthesis of proteins directly involved in the formation of motile cilia ultrastructure [31]. Cilia elongation and maintenance are possible thanks to the presence of a dedicated protein shuttle system, named intraflagellar transport (IFT), which involves the transport of molecules from the cell body through the basal body, transition zone to the tip of cilia and back [32,33]. Some of the multiprotein ciliary elements of motile cilia (e.g., dynein arms, ODA docking complexes) are preassembled in the cytoplasm in a process that requires the presence of proteins, which are physically not a part of the axonemal ultrastructure [34,35].

Genetically determined dysfunction of cilia is the cause of a large group of diseases, collectively referred to as ciliopathies. With the expanding knowledge of cilia biology and genetics, their number is now estimated as at least 35 [36]. The majority of ciliopathies are caused by the dysfunction of primary/sensory cilia [37]. Consistent with the presence of primary cilia on almost all cell types and their function in basic cellular pathways, their dysfunction affects multiple systems, including kidneys, brain, heart, skeleton, and eyes (e.g., polycystic kidney disease, PKD; nephronophthisis, NPHP; Bardet-Biedl syndrome, BBS; Joubert syndrome, JBTS; Meckel syndrome, MKS; Senior-Locken syndrome, SLSN; retinitis pigmentosa, RP); for the reviews see [36–38]. In this review, however, we focus on the diseases caused by the genetically determined defects of the structure and/or function of **motile** cilia.

1.1. Primary Ciliary Dyskinesia

Primary ciliary dyskinesia, PCD (OMIM244400; population frequency of 1:10,000 to 1:20,000), is the flagship ciliopathy resulting from the dysfuntion of motile cilia [34,35,39–43]. It has to be emphasized that the word "primary" in the name of the disease refers to the fact that PCD is a genetically-based condition, as opposed to a "secondary" ciliary dyskinesia, where the dysfunction of motile cilia is caused by environmental factors.

Typical clinical symptoms of PCD reflect the role of motile cilia in different parts of the human body. Defects of cilia on the apical surface of the epithelial cells lining the respiratory tract impair mucociliary clearance; as a result, PCD patients suffer from recurrent respiratory airway infections leading to chronic bronchopulmonary disease, recurrent sinusitis, rhinitis, otitis media, and bronchiectasis. The immotility of sperm flagella is a cause of male infertility, and the immotility of cilia on the epithelial cells lining fallopian tubes reduces fertility in females. Dysfunction of cilia present on the ependymal cells in the brain, which are responsible for cerebrospinal fluid flow, can lead to hydrocephalus. Finally, the defects of single motile cilia in the embryonic node impair the flow of morphogens and body patterning (situs), resulting in the randomization of body organ symmetry (*situs inversus totalis* in about 50% of PCD patients).

Due to the largely nonspecific clinical symptoms of PCD and insufficient diagnostic methods, PCD patients are often diagnosed late. The range and severity of PCD symptoms

depend on the mutated gene, reflecting different impacts of the dysfunctional protein on the ciliary structure and/or function [34,35,42–45].

Theoretically, the diagnostic problems can be overcome by applying genetic tests with high efficiency of mutation detection. However, the genetic basis of PCD is highly heterogeneous, reflecting a large number of proteins involved in the structure and function of motile cilia [46,47]. The inheritance of PCD in most families is autosomal recessive; the X-linked or autosomal dominant inheritance is rare. To date, ~50 genes have been reported to be involved in PCD pathogenesis (Table 1), and the involvement of more is still under investigation [34,35,39,40,42,44] (Table 2). The role of these genes in the axonemal structure, ciliary function, or in the biogenesis of motile cilia has been confirmed in animal models using a range of approaches, including analysis of mutant organisms, knockout of the gene in question by targeted mutation or gene knockdown using double-stranded RNA (dsRNA) or morpholinos.

Table 1. Genes involved in PCD pathogenesis.

Gene (Alias)	Role in Motile Cilia Biogenesis or Part of Axonemal Structure	Defects (Mode of Detection)	Confirmation from Selected Animal Models	Seminal References
Cytoplasmic proteins				
CCNO	Centriole amplification	Sparse cilia (light microscope, TEM, IF against AcAT)	Xenopus	[30]
MCIDAS	"		Xenopus	[29,30]
FOXJ1 [1]; *autos. dominant*	BB stabiliz./orientation	BB mislocalized and more (TEM–except for GAS2L2; IF against BB elements)	Xenopus, Drerio, mouse, Smed	[31,48–50]
RPGR; X-linked	BB docking		Drerio	[51–53]
OFD1; X-linked	BB docking		Paramecium, Smed, mouse	[54–58]
GAS2L2	BB stabilization		Mouse, Xenopus	[59]
DNAAF3 (c19orf51)	ODA/IDA preassembly	Absent/shortened DA (TEM; IF against ODA or IDA elements)	Chlamy, Drerio	[60]
CFAP300 (c11orf70)	"		Chlamy, Paramecium, Smed	[61–63]
SPAG1 (DNAAF13)	"		Drerio	[64]
DNAAF1 (LRRC50)	"		Chlamy, Tryp, Drerio, Smed	[65–68]
DNAAF5 (HEATR2)	"		Drosi, mouse	[69,70]
DNAAF6 (PIH1D3); X-linked	"		Drerio, Drosi, mouse	[71–74]
DNAAF7 (ZMYND10)	"		Drerio, Drosi, Xenopus, mouse	[75,76]
DNAAF11 (LRRC6)	"		Drosi, Drerio, mouse	[75,77–80]
CFAP298 (c21orf59)	"		Drerio, Chlamy, Smed	[81]
DNAAF2 (KTU)	Distal ODA preassembly		medaka, Chlamy, mouse	[82]
DNAAF4 (DYX1C1)	"		Drerio, mouse	[83]
DAW1 (WDR69,ODA16)	"		Drerio, Smed, mouse, Chlamy	[84–86]
TTC12	IDA assembly (in sperm IDA and ODA)	Some IDA types absent (TEM; IF against IDA elements, e.g., DNALI1)	Paramecium	[87]
Elements of axonemal ultrastructure				
DNAI1	ODA	Absent/shortened ODA (TEM–except for DNAH11; IF against ODA elements, e.g., DNAH5, DNAI2)	Chlamy	[88,89]
DNAI2	"		Chlamy, Smed	[90–92]
DNAH5 [2]	"		Chlamy	[93,94]
TXNDC3 (NME8; DNAI8)	"		Ciona	[95,96]
DNAL1	"		Chlamy, Smed, Tryp	[91,97–99]
DNAH11 [3]	Proximal ODA		Chlamy, mouse	[94,100,101]
DNAH9 [3]	Distal ODA		Chlamy, Paramecium, mouse	[94,102,103]
CCDC114 (ODAD1)	ODA targeting/docking	Absent/shortened ODA (TEM; IF against ODA elements)	Chlamy	[104,105]
ARMC4 (ODAD2)	"		Drerio, mouse	[106]
TTC25 (ODAD4)	"		Xenopus, mouse, Drerio	[107,108]
CCDC151 (ODAD3)	"		Chlamy, Smed, Drerio, mouse	[109–111]
CCDC103 [4]	Distal ODA		Chlamy, Drerio	[112,113]
LRRC56 (DNAAF12)	targeting/docking		Tryp	[114]
CFAP57(WDR65)	IDA assembly	No TEM defect (IF)	Chlamy	[115,116]
CCDC39 (CFAP59)	AR	Mislocalized MTs, absent IDA (TEM; IF against AR elements or GAS8)	Drerio, mouse, dog	[117]
CCDC40 (CFAP172)	"		Drerio, mouse	[118]
GAS8 (GAS11; DRC4)	NDR complex	MT mislocalized or no visible defect (IF against GAS8)	Chlamy, Tryp, Drerio, mouse	[119–122]
DRC1 (CCDC164)	"		Chlamy	[123]
CCDC65 (DRC2; CFAP250)	"		Chlamy, Drerio	[81,124,125]
RSPH1	RS head	Central pair and MTs mislocalized (TEM except for DNAJB13; IF against RS elements)	mouse	[126–128]
RSPH4A	"		mouse	[129,130]
RSPH9	"		Chlamy, Drerio, mouse	[129]
RSPH3	RS stalk		Chlamy	[131,132]
DNAJB13 (RSPH16A)	"		Chlamy, mouse	[133–135]
NME5 (RSPH23)	RS neck		Drerio, dog	[136,137]

Table 1. *Cont.*

Gene (Alias)	Role in Motile Cilia Biogenesis or Part of Axonemal Structure	Defects (Mode of Detection)	Confirmation from Selected Animal Models	Seminal References
HYDIN	CP complex	CP complex defects (no visible defect in TEM; IF against SPEF2, STK36; not for CFAP74)	Chlamy, mouse, Tryp	[138–142]
STK36 (FUSED)	"		Smed, Drerio, mouse	[143–145]
SPEF2	"		mouse	[139,146]
CFAP74	"		Chlamy	[147,148]
CFAP221 (PCDP1)	"	No TEM defect	mouse, Chlamy	[148–150]

[1] with hydrocephaly; [2] in sperm replaced by *DNAH8*; [3] in sperm replaced by *DNAH17*; [4] effect is variant-dependent. Abbreviations: AcaT—acetylated alpha-tubulin marker of microtubules; AR—axonemal ruler; BB—basal body; CP—central pair; IDA—inner dynein arm; IF—immunofluorescence; NDR—nexin-dynein regulatory; ODA—outer dynein arm; RS—radial spokes; TEM—transmission electron microscope; Xenopus—*Xenopus laevis*, Drerio—*Danio rerio*, Smed—*Schmidtea mediterranea*, Drosi—*Drosophila melanogaster*, Chlamy—*Chlamydomonas reinhardtii*, Ciona—*Ciona intestinalis*, Paramecium—*Paramecium tetraurelia*, Tryp—*Trypanosoma brucei*.

Table 2. Examples of genes with an uncertain role in PCD or involved in PCD-like diseases.

Gene (Alias)	Role in Motile Cilia Biogenesis or Part of Axonemal Structure	Relevance for PCD	Confirmation from Selected Animal Models	Seminal References
CCDC19 (CFAP45)	Inner lumen protein	Only mild respiratory symptoms	*Ch. reinhardtii*, *S. mediterranea*, mouse	[24,151]
WDR16 (CFAP52)	Inner lumen protein	Only mild respiratory symptoms	*Ch. reinhardtii*, *S. mediterranea*	[24,151,152]
TP73; lissencephaly	Ciliogenesis	Strong PCD candidate	mouse	[153,154]
NEK10	Centrosome; kinase	PCD candidate	medaka	[155,156]
CCDC113 (CCDC96)	NDR complex	PCD candidate	*T. thermophila*	[22]
TEKT1	Centrosome, BB, axoneme	PCD candidate	*D. rerio*	[157]
CEP164	Centriole; BB docking	PCD candidate	mouse	[158,159]
CFAP206	BB and axoneme	PCD candidate	*T. thermophila*, *Ch. reinhardtii*, *X. laevis*, mouse	[160–162]
MNS1	ODA docking	Laterality defect, male infertility	mouse	[163,164]
BRWD1	Axoneme	Male infertility	-	[165]
CFAP43	Axoneme	Male infertility	*X. laevis*, mouse	[166]
CCDC11 (CFAP53)	Ciliogenesis	Laterality defects	*X. laevis*	[167,168]

Abbreviations: BB, ODA, NDR are as in Table 1.

Pathogenic variants in many of the PCD genes result in obvious ultrastructural and/or functional defects of cilia, which can be readily visualized using transmission electron microscopy (TEM) or analysis of the ciliary beat [45,169,170]. The most frequent ultrastructural defects include the absence or shortening of ODA or both ODA and IDA, disorganization of microtubule arrangement, scarcity, or a complete lack of cilia. The defects of the ciliary beat can manifest as immotility, flickering, slow beating, or disturbed pattern of beating [169,170]. On the other hand, mutations identified in some of the genes, e.g., encoding central pair complex proteins, N-DRC proteins, or some of the dynein arm elements, have no clear effect on the axonemal structure or on the cilia beat frequency [102,119,123,139,147,171].

Importantly, even the use of high-throughput genome sequencing fails to detect mutations in known PCD genes in ~1/3 of the patients [34,35]. This may be due to the presence of unknown pathogenic variants, lying outside the most commonly studied coding sequences or impossible to detect with copy number insensitive techniques, as well as the presence of pathogenic mutations in yet-unidentified PCD genes. Moreover, the association of some candidate genes with PCD pathogenesis remains a matter of debate, especially when mutations have been described in single families. In addition, there is an expanding list of genes from the so-called PCD spectrum [172], in which mutations in cilia-related genes are associated with an atypical clinical picture of the disease, with a syndromic presen-

tation [51,52,54,55,173] or without (or very mild) respiratory symptoms [10,102,174–176]. Classification and curation of gene-disease relationships involving PCD and related motile cilia disorders are currently the focus of the Motile Ciliopathy Gene Curation Expert Panel, a part of the ClinicalGenome consortium [https://www.clinicalgenome.org/ (accessed on 20 February 2023)] [177].

The overall result of the heterogeneity of heritable motile ciliopathies is that—to better characterize the molecular/genetic basis of the unsolved cases of PCD and to differentiate them from the PCD-like spectrum diseases—the search for new candidate genes potentially involved in the pathogenesis is still needed.

1.2. The Validation of New Genes Underlying PCD and PCD-like Ciliopathies—The Role of Model Organisms

The easy access to NGS-based genetic screening of PCD patients increases the chances to reveal new candidate genes. Validation of their impact on motile cilia structure and function requires functional studies. The use of primary cell cultures in such studies requires obtaining respiratory epithelial biopsies from patients with pathogenic variants in candidate genes; the amount of the biological material obtained this way is limited, and often insufficient for detailed biochemical and molecular analyses. Another approach, silencing candidate genes in the in vitro culture of healthy human respiratory epithelium (HRE), is not in a routine laboratory method (reviewed in [178]). Primary HRE cells have limited ability to proliferate in culture. While the recent development of conditionally reprogrammed HRE cell cultures increased the proliferative lifespan of these cells and their ability to differentiate, this model is very demanding and still not sufficiently robust and replicable [178]. This is especially important in functional studies, where genome modification is required to overexpress or silence specific candidate genes.

Thanks to the high level of evolutionary conservation of motile cilia [3], a variety of model organisms have been successfully used for studying cilia biology. The same approach, which has allowed explaining the molecular basis of cilia assembly, structure, and function across Eukaryotic species, is widely used as a tool in the functional analysis of candidate genes underlying the pathogenesis of PCD and other cilia-related diseases.

For almost half of the causative genes identified during over twenty years of PCD research, their involvement in motile cilia function has been revealed by earlier (non-PCD) forward genetics studies in model organisms, performed to study cilia biology–the identity of proteins, their ultrastructural localization, interactions, and function. The loss-of-function variants in these genes, when found among patients, have been directly associated with PCD pathogenesis. For another half of PCD genes, with deleterious variants identified during the genetic screening of patients, their involvement in motile cilia dysfunction has been confirmed by follow-up reverse genetics studies, involving candidate gene silencing in model organisms.

The majority of all these studies had been based on a model of double-flagella unicellular alga, *Chlamydomonas reinhardtii*. *DNAI1*, the first gene identified as involved in the pathogenesis of PCD, has been earlier associated with the flagellar dysfunction caused by the mutation of *IC78*, *DNAI1* homolog in a double-flagella unicellular alga, *Ch. reinhardtii* [88]. Other models, which had supported the role of then-candidate PCD genes in motile cilia dysfunction, include unicellular organisms (*P. reinhardtii*, *Trypanosoma* brucei, *Tetrahymena thermophila*), invertebrates (*Drosophila melanogaster*, *Schmidtea mediterranea*) or vertebrates (frog *Xenopus leavis*, fish *Danio rerio*/zebrafish, mouse, dog); reviewed in [179,180]. Among these model organisms considered in the context of PCD, relatively little attention has been put to the use of *S. mediterranea*.

2. *Schmidtea mediterranea*

S. mediterranea is a representative of freshwater planarians, free-living invertebrates from the phylum Platyhelminthes (flatworms). These animals belong to the group of organisms that have three germ layers (endoderm, mesoderm, and ectoderm), bilateral

symmetry, and tissues with separate organs. The manner of reproduction of the freshwater planarians varies across the species and can be exclusively asexual (by transverse fission), seasonally sexual, and exclusively sexual (by the cross-fertilization of hermaphrodites) [181]. Planarians achieved popularity due to their great ability to regenerate after amputation or injury. In some cases, a full organism can be rebuilt after several days from 1/279 piece of a single worm, although the regenerative abilities of planarians are different across the species [182–185]. This regenerative potential makes planarians practically immortal and enables researchers to use them as efficient model organisms in a variety of studies.

There are several hundred species of planarians, but their use as animal models in molecular and genetic studies has been mostly limited to the Dugesiidae family (e.g., genera Dugesia, Girardia, Schmidtea), with the majority of research conducted using two species, *S. mediterranea* and *Dugesia japonica* [186]. *D. japonica* is favored for behavioral studies and toxicology screening, while *S. mediterranea* is popular and attractive for molecular experiments [187]. Two distinct strains of *S. mediterranea* exist in nature: a sexual strain (2 cm long) and an asexual strain (slightly shorter). Both are diploid, with four pairs of chromosomes (2n = 8); the asexual form results from a chromosome translocation between the sexual strain chromosomes 1 and 3 [181,188].

A planarian organism has a complex anatomy. The nervous system of flatworms is comprised of a bilobed 'brain' with different types of neurons and glia, and two longitudinal nerve cords connected by many transverse nerves [181,185]. Photo-, chemo- and rheoreceptors located at the front of the planarian's body send signals to the brain, where they are processed, leading to behavioral responses [181,184]. Paired 'eyes' located on the planarian head allow the detection of light and shadow, and consist of two types of cells: pigmented optic cup cells, and photoreceptor neurons [189,190]. Due to the lack of respiratory and circulatory systems in planarians, oxygen is obtained and transported by diffusion. A centrally located pharynx is in charge of food intake and removal and is connected to a highly branched intestine, which circulates nutrients within the body. The excretory system (protonephridia) is responsible for the removal of waste products and osmoregulation [181]. Internal organs are surrounded by a mesenchymal tissue, parenchyma, consisting of adult pluripotent stem cells (neoblasts), which are essential for worms' regeneration ability and comprise ~30% of the cells in the adult animal [185,191]. Planarians possess a set of muscle fibers, organized in longitudinal, diagonal, and circular orientations. The planarians body is covered with an epidermis; the ventral epidermis consists of a single layer of multiciliated cells (MCCs), and gland cells involved in the production and secretion of mucus, which is used by flatworms for protection, locomotion, catching food, and adhesion to substrates [181].

2.1. Advantages of the S. mediterranea as a Model Organism

Although planarians do not fully reflect the complexity of the human organism, many of the annotated *S. mediterranea's* genes have known orthologs (or at least homologs) in the human genome, and researchers increasingly use *S. mediterranea* in studies aiming to better understand aspects related to human development and function involving certain cell types or tissues.

The maintenance of planarians is relatively easy and cheap, and does not require specialized equipment; only habitat conditions, such as temperature, darkness, feeding, and water culture, have to be provided, and many methodological guidelines have been published [e.g., [188,192,193]]. An important feature of using planarians as a model organism is the easy way to perform simple modifications of their gene expression. This can be achieved by knockdown/silencing genes of interest through RNA interference (RNAi) using double-stranded RNA (dsRNA). DsRNA can be administered to the worms by microinjection, by feeding them with dsRNA-containing bacteria, or with food mixed with free dsRNA [194–196]. The efficacy of gene silencing on the mRNA level can be evaluated using reverse transcription polymerase chain reaction (RT-PCR) or quantitative reverse transcription PCR (RT-qPCR), while the gene expression pattern of a silenced gene can

be determined using whole-mount fluorescent in situ hybridization (FISH) and whole-mount in situ hybridization (WMISH). The phenotypic effect/s of gene silencing is typically observed within a week or two after implementing the RNAi procedure [188].

The genome of *S. mediterranea* has been well annotated, which makes this species more attractive than other planarians. The advances in single-cell RNA sequencing increased molecular knowledge about planarian stem cell differentiation, and have allowed for determining the transcriptomes for each cell type in *S. mediterranea*, and tracking the transcriptomic changes during the regeneration process [197–200]. The genomic and transcriptomic data are deposited in specialized databases and freely available to the research community [197,201–204].

2.2. *S. mediterranea* Model in the Context of Studying Cilia Biology

The potential of using *S. mediterranea* as a model organism to study evolutionarily conserved motile cilia was first described in 2009, and its value has been confirmed in later publications [188,192,205,206].

Motile cilia are present in many planarian cell types (Figure 2). Multiple motile cilia (9 × 2 + 2) covering the apical side of MCCs (~80 per cell) in the planarian body epidermis beat in a synchronized way and are responsible for worms' locomotion [188,207]. MCCs are also present in the epithelium that covers the feeding organ (pharynx) [188,207,208]. Specialized ciliated cells at the proximal end of protonephridia (so-called flame cells) play role in fluid ultrafiltration and circulation. Cilia with the same ultrastructure as motile ones are also found in the sensory neurons in planarians, although their ability to move is not clear [188,207]. Finally, sperm cells with flagella are present in the sexual strains of planarians [209,210]. In planarians, basal bodies are assembled de novo during terminal differentiation of ciliated cells from neoblast progenies, and never have the function of a centrosome [1,58,207]. While it is currently unclear how the flatworms generate multiple centrioles in cells that are initially centriole-free, RNAi experiments show that the known key factors of centriole duplication are crucial for their amplification [208].

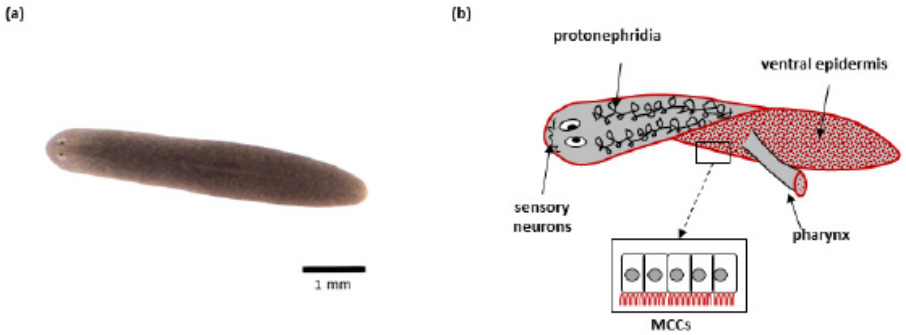

Figure 2. *Schmidtea mediterranea*: (a) Representative *S. mediterranea* individual–top view; (b) Schematic representation of a planarian. Tissues with cells featuring motile cilia are indicated. The red color indicates tissues/organs with multiciliated cells (MCCs).

Both ventral and pharyngeal epidermis are easily accessible and form cilia at high density and in known orientation [188]. The great advantage of using *S. mediterranea* as a model in motile cilia studies is that the effect of gene silencing on cilia function can be readily analyzed by recording the change in the speed of planarian locomotion. Importantly, defects that compromise the function and structure of the cilia are not detrimental to planarians, making them an ideal system for loss-of-function studies concerning cilia-related genes [192]. Under normal conditions, planarians move by the use of ciliated epithelium covering the ventral side of worms' body (so-called gliding movement), while cilia-related

gene silencing manifests in a so-called "inch-worming" movement that engages the muscles (waves of whole-body contraction and extension) [188,207]. This phenotype (inch-worming) is easily visible to even unaided human eyes; a stereoscope (with camera) makes it more precise and allows to record movies showing the movement of planarians, which can then be used to measure the distance traveled by worms (using ImageJ software) [192]. The motility impairment may be associated with edema, which results from the dysfunction of cilia in protonephridia [211]. The beating of cilia covering the lateral part of worms can be recorded using high-speed video camera microscopy (HSVM), and the cilia beating frequency, pattern, and synchrony can be analyzed in slow motion under a microscope. The number and length of cilia can be inspected using a fluorescence microscope after immunofluorescence staining (IF) with cilia-specific antibodies (acetylated alpha-tubulin, a marker of the axoneme). After RNAi, changes in the gene expression pattern of epidermal markers can be tracked using WMISH. In addition, the possibility to stimulate cell differentiation through worms' fragmentation (cutting) that triggers the regeneration process allows for tracing changes in the gene expression during the differentiation of the neoblasts into ciliated cells. The effect of gene silencing on the ultrastructure of planarian cilia can be also examined using a transmission electron microscope (TEM). In addition, the flatworms bloat due to the inhibition of ciliary function in flame cells, which leads to defective osmoregulation and edema formation [207].

Planarians have been widely used as a model for studying signaling networks implicated in the maintenance of tissue homeostasis, regeneration, and polarity. A large number of studies were devoted to essential cellular pathways, including Wnt and Hedgehog signaling in establishing polarity [212], Akt signaling in tissue maintenance and regeneration [213], EGFR signaling in the regulation of excretory system [211]. Like in most bilaterally symmetric animals, canonical Wnt signal is transduced through frizzled receptor and with the help of disheveled stabilizes beta-catenin, which activates expression cascade controlling anterior/posterior axis during regeneration [212,214]. Wnt signals transduced through frizzled receptors to various non-canonical pathways (disheveled-dependent or Ca^{2+}-dependent) control cell movement and planar cell polarity (apical positioning of the basal bodies of epithelial cells). Hedgehog signaling modulates Wnt/beta-catenin's role in establishing the anterior/posterior axis; when Wnt signaling is low, heads develop, and when it is high, tails are formed [145,215]. The majority of these signaling networks have the ciliary context, linking various aspects of Hedgehog signaling, regeneration, and the biogenesis of cilia, e.g., [145,213,216,217].

2.3. *S. mediterranea* Model in the Context of Studying PCD and PCD-like Ciliopathies

RNAi-mediated silencing of a variety of genes in *S. mediterranea* has been used to explain/confirm the connection between the homologous genes, defects of the ciliary ultrastructure, and cilia dysfunction in other organisms. The explicit use of *S. mediterranea* as an animal model to elucidate the pathogenesis of motile ciliopathies (and in particular, the role of candidate PCD genes) includes relatively few studies, where the effect of gene silencing on motile cilia function has been examined using dsRNA-mediated knockdown of the planarian homologs of human candidate genes not previously linked to PCD. In many more *S. mediterranea* studies, the demonstrated phenotypic effects of motile cilia-related genes' silencing strongly resemble those seen when PCD genes are mutated, but their involvement in the pathogenesis remains to be confirmed by finding deleterious variants in PCD patients.

Deleterious variants of ***CFAP298 (C21orf59)*** [81], ***CCDC151*** [109], and ***CFAP300 (C11orf70)*** [63] have been found in PCD patients. Knockdown of the planarian homologs of these genes has revealed the impaired locomotion phenotype in worms. The details of this phenotype have been explained using further assays. HSVM analysis of planarians with silenced *CFAP300 (C11orf70)* demonstrated changes in cilia motility pattern and lowered beat frequency, while TEM analysis of cilia in planarians with *CFAP298 (C21orf59)* and *CCDC151* knockdown revealed ODA assembly defects of dynein arms and loss of ODA,

respectively. The effects of these three genes' silencing are consistent with the observations in other animal models. *Ch. reinhardtii* and zebrafish mutants lacking *CCDC151* orthologues featured a loss of ODAs [111,218]; silencing of *CCDC151* in zebrafish and mice was shown to alter ODA assembly [109]. Knockdown of *CCDC298* in zebrafish and *Ch. reinhardtii*, and of *CFAP300* in *P. tetraurelia* and *Ch. reinhardtii* resulted in a complete lack of ODA and IDA [61,81]. All three genes are presently considered PCD genes, involved in the assembly of dynein arms (*CFAP298*, *CFAP300*), and proper functioning of the ODA docking complex (*CCD151*).

The role of FOXJ1 as the key transcription factor controlling motile cilia biogenesis has been reported in various FOXJ1-deficient model organisms, including mice [49], *X. laevis*, and zebrafish [50]. The *S. mediterranea* model has been used to demonstrate the conserved role of vertebrate *FOXJ1*. Among four ***FOXJ1*** homologs found in planarians, silencing of *FOXJ1-4* caused the absence of motile cilia, resulting in a characteristic inch-worming locomotion and edema formation [48]. The *FOXJ1* involvement in PCD pathogenesis in humans has been demonstrated several years later, when dominant pathogenic variants in *FOXJ1* were found in PCD patients with mild respiratory symptoms and hydrocephalus, caused by the severely reduced number of cilia per MCC due to defect in the apical docking of basal bodies [31].

Proteins essential to basal body assembly in *S. mediterranea* include orthologs of many conserved genes required for centriole assembly or function in humans. In planarians, depleting the ortholog of *OFD1* (among other proteins) results in the decreased locomotion of knocked-down animals, apparently due to the inhibition of basal body docking [58]. A similar ciliary phenotype has been recently demonstrated in PCD patients with the disease caused by nonsense mutations in the few last exons of the ***OFD1*** gene [55]. In humans, the truncation of the C-terminus of the protein causes PCD without severe neurological, skeletal, or renal symptoms characteristic for other *OFD1*-related syndromes associated with the loss of a larger part of the OFD1 protein cause syndromic diseases (e.g., oral-facial-digital syndrome type 1 or Joubert syndrome type 10). While the effect of the gene knockdown in planarians does not explain truncation size-dependent differences in human clinical phenotype, it corroborates the proposed mechanism for the ciliary phenotype in PCD patients, showing that apical docking of basal bodies in planarians and in humans employ, at least in part, the same molecular components.

DAW1 (WDR69/ODA16) encodes a WD repeat protein, whose role as a dynein assembly factor has been shown in many model organisms. Depletion of DAW1 protein homologs results in ultrastructural defect characterized by the reduced number of ODAs in *Ch. reinhardtii* [219], zebrafish [220], and mouse [221]; *Ch. reinhardtii* studies have shown that DAW1 is involved in ODA transport through interaction with IFT46 protein [86,222,223]. The knockdown of *DAW1* homolog in *S. mediterranea* results in shortened epidermal cilia and decreased abundance of ciliated protonephridia [85]. The recent finding of deleterious *DAW1* variants in patients with disturbed laterality and respiratory symptoms has confirmed the predicted involvement of this gene in PCD pathogenesis, although only in patients whose cilia are characterized by subtle beating abnormalities [84].

Deleterious variants in two other genes, ***CFAP45/CCDC19/NESG1***, and ***CFAP52/WDR16***, have been found in human individuals whose clinical presentation, with situs inversus and asthenozoospermia, but only mild respiratory symptoms, did not allow for classifying them as classical PCD cases [151]. Earlier studies in *Ch. reinhardtii* have localized these two proteins in the lumen of the B microtubule of the peripheral doublet [24]. The knockdown of the planarian homologs resulted in significant impairment of planarian locomotion in viscous but not in a normal medium; TEM of the silenced worms has shown normal ciliary ultrastructure, consistent with TEM cross-sections of *CFAP45*- and *CFAP52*-deficient respiratory cilia from CRISPR-Cas9 generated mice or from humans with mutated genes [151]. Therefore, planarian results confirm the uncertain status of *CFAP45* and *CFAP52* as PCD genes.

IC2 and *LC1* are *S. mediterranea* homologs of human *DNAI2* and *DNAL1* genes, respectively, encoding integral components of ODA. Mutations in *DNAI2(IC2)* cause defects in ODA resulting in the reduction in ciliary beat frequency in *Ch. reinhardtii*, and are known to cause PCD in humans [90]. Mutations in ***DNAL1(LC1)*** disturb the proper function of ODA in *Ch. reinhardtii* [224], but the data supporting this gene's role in human PCD are scarce [97,225]. The knockdown of either of these two genes in *S. mediterranea* severely decreases worms' motility, due to the reduction in the ciliary beat frequency and coordination (metachronal synchrony). However, while TEM and IF reveal the loss of ODA in *IC2*-silenced planarians, no ODA defects are visible *in LC1*-silenced worms [91]. This is consistent with the still uncertain role of *DNAL1* in PCD pathogenesis in humans.

The ODA-docking complex is a microtubule-associated structure that targets ODA to its binding site on the axonemal microtubule [226]. In *Ch. reinhardtii* it contains three proteins, referred to as DC1, DC2, and DC3, of which DC1 and DC2 can assemble ODA in the absence of DC3 [227]. *Ch. reinhardtii* mutants with the loss of DC2 (a major subunit of the ODA-docking complex) have two flagella of normal length but show slow jerky swimming [228]. Two *DC2* homologs, *CCDC63* and *CCDC114*, function in ODA docking in vertebrates. Respiratory cilia in PCD patients with deleterious variants in ***CCDC114*** have normal length, but lack ODAs due to the defects in ODA docking to microtubules [229]. In mice, in which ***CCDC63*** (the testis-specific *DC2* homolog) is knocked out, spermatozoa flagella are shortened, but ODAs remain unaffected, probably due to the compensation by overexpression of *CCDC114* [230]. The knockdown of *DC2* orthologue in *S. mediterranea* impairs worms' locomotion due to the low-frequency, uncoordinated ciliary beating caused by the inefficient ODA docking; in addition, cilia density and length are decreased [231]. The importance of these findings for PCD pathogenesis remains to be explored.

WDR92 is a highly conserved WD-repeat protein. Silencing of the planarian homolog of ***WDR92*** results in a phenotype similar to those observed when acknowledged PCD genes are knocked down. Peristaltic contractions instead of smooth gliding of the worms reduced and uncoordinated the ciliary beat; in TEM analysis, partial loss of dynein arms, incomplete closure of the B-microtubule, and lack of normal central pair complex are observed [232]. *WDR92* is required for the assembly of ODAs and IDAs in *D. melanogaster* and *Ch. reinhardtii* [233–235]. Based on these observations, *WDR92* has been proposed to act as a part of a cytoplasmic chaperone required for the proper folding and stability of key axonemal components. So far, no pathogenic variants have been found in human PCD patients.

IFT88 (Tg737) encodes a component of the IFT complex; its mutations in *Ch. reinhardtii* results in a lack of flagella, while in mice they cause shortening of primary cilia, as well as kidney and liver defects [236]. The importance of *IFT88* in motile cilia biogenesis has been confirmed in the *S. mediterranea* model, where silencing of *IFT88* significantly reduced planarians motility and caused the complete absence of cilia on the ventral surface of knocked-down animals [91]. Defects in IFT are likely to affect motile cilia in humans. Defects in the *Tg737* gene in mice are very similar to those seen in humans with autosomal recessive polycystic kidney disease [237], but so far no pathogenic *IFT88* variants have been reported in PCD patients.

Ch. reinhardtii protein FAP163 is an intermediate dynein chain closely related to the FAP133 intermediate dynein chain that powers retrograde IFT required for the assembly of cilia. The functional role of FAP163 has been examined by the knockdown of the orthologous gene ***WD60 (FAP163)*** in *S. mediterranea* [238]. The silenced animals exhibited severely impaired movement (reduced velocity and inch-worming), resulting from a dramatic reduction in both the number and length of cilia. Cilia and ciliary stubs examined by TEM contained doublet microtubules and associated structures but had an enlarged diameter due to the presence of large quantities of amorphous electron-dense material located between the axonemal doublet microtubules and the ciliary membrane. These observations suggest that *WD60(FAP163)* is required for ciliary assembly. So far, no pathogenic variants have been found in human PCD patients.

An interesting application of RNAi-mediated gene silencing in *S. mediterranea* concerns the analysis of planarian protonephridia as a model of pathological features of human cystic kidney diseases (CKDs), in which fluid-filled cysts develop from nephric tubules due to defective flow sensing, cell proliferation, and differentiation. In contrast to mammalian kidneys that contain only immotile sensory cilia, the excretory system of planarians is equipped with motile cilia that drive fluid flow into and through the tubules [239,240]. Interestingly, structure and function comparisons revealed that the combination of ultrafiltration and flow-associated filtrate modification is remarkably conserved between the planarian excretory system (flame cells) and the vertebrate nephrons (podocytes) [67]. The genome of *S. mediterranea* contains many genes that cause cysts when their equivalents are mutated in humans. Silencing of planarian homologs of human ***DNAH1*** and ***LRRC50*** genes resulted in abnormal worms locomotion due to the loss of cilia beating; animals also developed edema and formed protonephridial cysts [67]. These results suggest that cilia-driven fluid flow is crucial for maintaining cell homeostasis in planarian protonephridia and establish planarians as a novel and experimentally accessible invertebrate model for the study of human kidney pathologies.

In the majority of the aforementioned studies, *S. mediterranea* was not the only organism used in the functional assessment of cilia-related genes, which are or can be considered candidate PCD genes. While the application of the planarian model in these studies may seem redundant, it can be seen that abundant work using *S. mediterranea* genes silencing has been performed to analyze the role of various proteins in the assembly, maintenance, and function of motile cilia, without immediate referring to PCD pathogenesis. These results are often used later, whenever deleterious variants in candidate PCD genes are found in human patients (see, e.g., the cases of *FOXJ1* or *DAW1*). On the other hand, when a new candidate PCD gene comes into focus based on genetic screening in humans, using the planarian model is perhaps the most efficient way to perform preliminary functional studies. When compared to the most popular single-cell organisms (*Ch. reinhardtii*, *P. tetraurelia*, *T. brucei*, *T. thermophila*), *S. mediterranea* offers an advantage of studying the epidermis that closely resembles human epithelium with MCCs, and compared to fish or mammals allows a much faster, easier and more affordable alternative modeling.

3. Perspectives

For many years, the use of the planarian model in the analysis of human candidate genes has been hampered by the lack of information on human-planarian orthologues. Recently, the rapid and extensive growth of the genomic, transcriptomic, phenotypic, and phylogenetic data generated by the planarian research community has alleviated this problem.

In this review, the human gene names or aliases are used to facilitate comparison with the part of the text describing human cilia and ciliopathies. However, it should be emphasized that to establish a uniform method for naming genes and proteins and for describing RNAi experiments in *S. mediterranea*, nomenclature guidelines have been developed [241], where the main rule is that the name of the gene is preceded by a 'Smed' prefix. In addition, to enhance cross-platform and cross-species searchability, the Planarian Anatomy Ontology (PLANA), an extendable relational framework of defined *S. mediterranea* anatomical terms has been recently developed [242].

The rapid growth of the amount of genomic and functional data on *S. mediterranea* prompted the development of integration tools that would enable the collection and use of these data by the scientific community. In response to these needs, the SmedGD database has been developed by the Sánchez Alvarado team [201,202]. The data deposited in SmedGD refer to the *S. mediterranea* genome and include predicted and annotated genes, protein homologies, gene expression patterns, and RNAi phenotypes, among others. SmedGD has been a stand-alone web resource for 15 years. Recently, the *S. mediterranea* genome assembly from SmedGD has been transferred to SIMRbase at the Stowers Institute for Medical Research (https://simrbase.stowers.org/ (accessed on 20 February 2023)).

Another high-quality *S. mediterranea* genome assembly can be found in the Planmine database (https://planmine.mpinat.mpg.de/planmine/begin.do (accessed on 20 February 2023)), developed in 2016 by the Rink team [199,203,243]. Originally, Planmine was based on the independently assembled transcriptomes from the Rink team and contributors from the planarian community. The updated database provides also genomic information, including a gene prediction set that assigns existing transcripts to defined genomic coordinates. In addition, Planmine uses recent datasets from the single-cell RNA-seq (e.g., from Digiworm resource and Planaria Single Cell Atlas), allowing for the expansion of the available gene expression information [197,198]. Both Digiworm and Planaria Single Cell Atlas refer to transcriptomes published by the Rink team, which makes these resources compatible with data in the Planmine database. Moreover, in contrast to other planarian databases, Planmine is also a resource of transcriptomes from other flatworm species. Planmine can be used to search for the planarian homologs of interesting transcripts and corresponding predicted genes. Planmine provides information about functional annotations (gene ontology), the best BLAST hits, expression patterns of homologs in planarian cell types, as well as phenotypes after RNAi of specified genes, among others.

Planosphere (https://planosphere.stowers.org/ (accessed on 20 February 2023)) is a new website dedicated to *S. mediterranea*, which contains a collection of data and tools from the Sánchez Alvarado laboratory [242]. One of the Planosphere tools is "gene search", which can be used to search homologs in *S. mediterranea*, and to define experimentally determined cell/tissue-specific gene expression patterns. In addition to transcriptomic and genomic data, Planosphere provides information about predicted protein sequences. This website is linked to the data deposited in the Planmine database and refers to data (e.g., from RNAseq) published by other teams.

For researchers studying cilia or cilia-related diseases, it is important that RNAseq, together with other techniques, has allowed to characterize and reconstruct epidermal cell lineages, including the stages between neoblasts and fully differentiated epidermal cells [197,198,244–246]. Using Digiworm, researchers can check at which stage of epidermal lineage the gene of interest is expressed (it is possible for all cell/tissue types, e.g., protonephridia).

The available web resources, especially Planmine, Planosphere, and Digiworm, provide researchers with a powerful tool to design experiments using *S. mediterranea* as a model organism. They can be used to simply explore their contents to better understand planarian biology. Importantly, they allow the cross-searching of databases devoted to other organisms, using gene names, sequences, annotation terms, etc. (the details of such searches differ among planarian websites). This facilitates using the growing planarian knowledge in applications related to studies of human ciliopathies.

Author Contributions: The authors (A.R. and E.Z.) wrote the original draft; reviewing and editing, E.Z.; drawings and tables, A.R. All authors have read and agreed to the published version of the manuscript.

Funding: This work was supported by the grants funded by the National Science Centre, Poland: 2018/29/N/NZ5/00810 to A.R. and 2018/31/B/NZ2/03248 to E.Z.

Institutional Review Board Statement: Not applicable.

Informed Consent Statement: Not applicable.

Data Availability Statement: Not applicable.

Conflicts of Interest: The authors declare no conflict of interest.

References

1. Carvalho-Santos, Z.; Azimzadeh, J.; Pereira-Leal, J.B.; Bettencourt-Dias, M. Evolution: Tracing the origins of centrioles, cilia, and flagella. *J. Cell Biol.* **2011**, *194*, 165–175. [CrossRef] [PubMed]
2. Mitchell, D.R. Evolution of cilia. *Cold Spring Harb. Perspect. Biol.* **2017**, *9*, a028290. [CrossRef] [PubMed]

3. Khan, S.; Scholey, J.M. Assembly, functions and evolution of archaella, flagella and cilia. *Curr. Biol.* **2018**, *28*, R278–R292. [CrossRef] [PubMed]
4. Garcia-Gonzalo, F.R.; Reiter, J.F. Open sesame: How transition fibers and the transition zone control ciliary composition. *Cold Spring Harb. Perspect. Biol.* **2017**, *9*, a028134. [CrossRef]
5. Takeda, S.; Narita, K. Structure and function of vertebrate cilia, towards a new taxonomy. *Differentiation* **2012**, *83*, S4–S11. [CrossRef]
6. Kempeneers, C.; Chilvers, M.A. To beat, or not to beat, that is question! The spectrum of ciliopathies. *Pediatr. Pulmonol.* **2018**, *53*, 1122–1129. [CrossRef]
7. Shah, A.S.; Ben-Shahar, Y.; Moninger, T.O.; Kline, J.N.; Welsh, M.J. Motile cilia of human airway epithelia are chemosensory. *Science* **2009**, *325*, 1131–1134. [CrossRef]
8. Jain, R.; Javidan-Nejad, C.; Alexander-Brett, J.; Horani, A.; Cabellon, M.C.; Walter, M.J.; Brody, S.L. Sensory functions of motile cilia and implication for bronchiectasis. *Front. Biosci.* **2012**, *4*, 1088–1098. [CrossRef]
9. Brooks, E.R.; Wallingford, J.B. Multiciliated cells. *Curr. Biol.* **2014**, *24*, R973–R982. [CrossRef]
10. Sironen, A.; Shoemark, A.; Patel, M.; Loebinger, M.R.; Mitchison, H.M. Sperm defects in primary ciliary dyskinesia and related causes of male infertility. *Cell. Mol. Life Sci.* **2020**, *77*, 2029–2048. [CrossRef]
11. Shinohara, K.; Hamada, H. Cilia in left-right symmetry breaking. *Cold Spring Harb. Perspect. Biol.* **2017**, *9*, a028282. [CrossRef] [PubMed]
12. Anvarian, Z.; Mykytyn, K.; Mukhopadhyay, S.; Pedersen, L.B.; Christensen, S.T. Cellular signalling by primary cilia in development, organ function and disease. *Nat. Rev. Nephrol.* **2019**, *15*, 199–219. [CrossRef] [PubMed]
13. Goetz, S.C.; Anderson, K.V. The primary cilium: A signalling centre during vertebrate development. *Nat. Rev. Genet.* **2010**, *11*, 331–344. [CrossRef]
14. Nishimura, Y.; Kasahara, K.; Shiromizu, T.; Watanabe, M.; Inagaki, M. Primary cilia as signaling hubs in health and disease. *Adv. Sci.* **2019**, *6*, 1801138. [CrossRef] [PubMed]
15. Nachury, M.V.; Mick, D.U. Establishing and regulating the composition of cilia for signal transduction. *Nat. Rev. Mol. Cell Biol.* **2019**, *20*, 389–405. [CrossRef] [PubMed]
16. Samsel, Z.; Sekretarska, J.; Osinka, A.; Wloga, D.; Joachimiak, E. Central apparatus, the molecular kickstarter of ciliary and flagellar nanomachines. *Int. J. Mol. Sci.* **2021**, *22*, 3013. [CrossRef]
17. Kurkowiak, M.; Ziętkiewicz, E.; Witt, M. Recent advances in primary ciliary dyskinesia genetics. *J. Med. Genet.* **2015**, *52*, 1–9. [CrossRef]
18. Osinka, A.; Poprzeczko, M.; Zielinska, M.M.; Fabczak, H.; Joachimiak, E.; Wloga, D. Ciliary proteins: Filling the gaps. Recent advances in deciphering the protein composition of motile ciliary complexes. *Cells* **2019**, *8*, 730. [CrossRef]
19. Nicastro, D.; Schwartz, C.; Pierson, J.; Gaudette, R.; Porter, M.E.; McIntosh, J.R. The molecular architecture of axonemes revealed by cryoelectron tomography. *Science* **2006**, *313*, 944–948. [CrossRef]
20. Oda, T.; Yanagisawa, H.; Kamiya, R.; Kikkawa, M. A molecular ruler determines the repeat length in eukaryotic cilia and flagella. *Science* **2014**, *346*, 857–860. [CrossRef]
21. Whitfield, M.; Thomas, L.; Bequignon, E.; Schmitt, A.; Stouvenel, L.; Montantin, G.; Tissier, S.; Duquesnoy, P.; Copin, B.; Chantot, S.; et al. Mutations in DNAH17, encoding a sperm-specific axonemal outer dynein arm heavy chain, cause isolated male infertility due to asthenozoospermia. *Am. J. Hum. Genet.* **2019**, *105*, 198–212. [CrossRef] [PubMed]
22. Bazan, R.; Schröfel, A.; Joachimiak, E.; Poprzeczko, M.; Pigino, G.; Wloga, D. Ccdc113/Ccdc96 complex, a novel regulator of ciliary beating that connects radial spoke 3 to dynein g and the nexin link. *PLoS Genet.* **2021**, *17*, e1009388. [CrossRef] [PubMed]
23. Ma, M.; Stoyanova, M.; Rademacher, G.; Dutcher, S.K.; Brown, A.; Zhang, R. Structure of the decorated ciliary doublet microtubule. *Cell* **2019**, *179*, 909–922.e12. [CrossRef]
24. Owa, M.; Uchihashi, T.; Yanagisawa, H.-A.; Yamano, T.; Iguchi, H.; Fukuzawa, H.; Wakabayashi, K.-I.; Ando, T.; Kikkawa, M. Inner lumen proteins stabilize doublet microtubules in cilia and flagella. *Nat. Commun.* **2019**, *10*, 1143. [CrossRef] [PubMed]
25. Joachimiak, E.; Osinka, A.; Farahat, H.; Świderska, B.; Sitkiewicz, E.; Poprzeczko, M.; Fabczak, H.; Wloga, D. Composition and function of the C1b/C1f region in the ciliary central apparatus. *Sci. Rep.* **2021**, *11*, 11760. [CrossRef]
26. Satir, P.; Heuser, T.; Sale, W.S. A structural basis for how motile cilia beat. *Bioscience* **2014**, *64*, 1073–1083. [CrossRef]
27. Pigino, G.; Ishikawa, T. Axonemal radial spokes: 3D structure, function and assembly. *Bioarchitecture* **2012**, *2*, 50–58. [CrossRef]
28. Choksi, S.P.; Lauter, G.; Swoboda, P.; Roy, S. Switching on cilia: Transcriptional networks regulating ciliogenesis. *Development* **2014**, *141*, 1427–1441. [CrossRef]
29. Boon, M.; Wallmeier, J.; Ma, L.; Loges, N.T.; Jaspers, M.; Olbrich, H.; Dougherty, G.W.; Raidt, J.; Werner, C.; Amirav, I.; et al. MCIDAS mutations result in a mucociliary clearance disorder with reduced generation of multiple motile cilia. *Nat. Commun.* **2014**, *5*, 4418. [CrossRef]
30. Wallmeier, J.; Al-Mutairi, D.A.; Chen, C.-T.; Loges, N.T.; Pennekamp, P.; Menchen, T.; Ma, L.; Shamseldin, H.E.; Olbrich, H.; Dougherty, G.W.; et al. Mutations in CCNO result in congenital mucociliary clearance disorder with reduced generation of multiple motile cilia. *Nat. Genet.* **2014**, *46*, 646–651. [CrossRef]
31. Wallmeier, J.; Frank, D.; Shoemark, A.; Nöthe-Menchen, T.; Cindric, S.; Olbrich, H.; Loges, N.T.; Aprea, I.; Dougherty, G.W.; Pennekamp, P.; et al. De novo mutations in FOXJ1 result in a motile ciliopathy with hydrocephalus and randomization of left/right body asymmetry. *Am. J. Hum. Genet.* **2019**, *105*, 1030–1039. [CrossRef]

32. Lechtreck, K.F. IFT-Cargo interactions and protein transport in cilia. *Trends Biochem. Sci.* **2015**, *40*, 765–778. [CrossRef]
33. Ishikawa, H.; Marshall, W.F. Intraflagellar transport and ciliary dynamics. *Cold Spring Harb. Perspect. Biol.* **2017**, *9*, a021998. [CrossRef] [PubMed]
34. Wallmeier, J.; Nielsen, K.G.; Kuehni, C.E.; Lucas, J.S.; Leigh, M.W.; Zariwala, M.A.; Omran, H. Motile ciliopathies. *Nat. Rev. Dis. Prim.* **2020**, *6*, 77. [CrossRef] [PubMed]
35. Legendre, M.; Zaragosi, L.-E.; Mitchison, H.M. Motile cilia and airway disease. *Semin. Cell Dev. Biol.* **2021**, *110*, 19–33. [CrossRef] [PubMed]
36. Reiter, J.F.; Leroux, M.R. Genes and molecular pathways underpinning ciliopathies. *Nat. Rev. Mol. Cell Biol.* **2017**, *18*, 533–547. [CrossRef] [PubMed]
37. Focșa, I.O.; Budișteanu, M.; Bălgrădean, M. Clinical and genetic heterogeneity of primary ciliopathies (review). *Int. J. Mol. Med.* **2021**, *48*, 176. [CrossRef] [PubMed]
38. Tobin, J.L.; Beales, P.L. The nonmotile ciliopathies. *Genet. Med.* **2009**, *11*, 386–402. [CrossRef]
39. Horani, A.; Ferkol, T.W.; Dutcher, S.K.; Brody, S.L. Genetics and biology of primary ciliary dyskinesia. *Paediatr. Respir. Rev.* **2016**, *18*, 18–24. [CrossRef]
40. Mirra, V.; Werner, C.; Santamaria, F. Primary ciliary dyskinesia: An update on clinical aspects, genetics, diagnosis, and future treatment strategies. *Front. Pediatr.* **2017**, *5*, 135. [CrossRef]
41. Damseh, N.; Quercia, N.; Rumman, N.; Dell, S.D.; Kim, R.H. Primary ciliary dyskinesia: Mechanisms and management. *Appl. Clin. Genet.* **2017**, *10*, 67–74. [CrossRef]
42. Lucas, J.S.; Davis, S.D.; Omran, H.; Shoemark, A. Primary ciliary dyskinesia in the genomics age. *Lancet Respir. Med.* **2020**, *8*, 202–216. [CrossRef]
43. Horani, A.; Ferkol, T.W. Understanding primary ciliary dyskinesia and other ciliopathies. *J. Pediatr.* **2021**, *230*, 15–22. [CrossRef]
44. Wheway, G.; Thomas, N.S.; Carroll, M.; Coles, J.; Doherty, R.; Genomics England Research Consortium; Goggin, P.; Green, B.; Harris, A.; Hunt, D.; et al. Whole genome sequencing in the diagnosis of primary ciliary dyskinesia. *BMC Med. Genom.* **2021**, *14*, 234. [CrossRef] [PubMed]
45. Brennan, S.K.; Ferkol, T.W.; Davis, S.D. Emerging genotype-phenotype relationships in primary ciliary dyskinesia. *Int. J. Mol. Sci.* **2021**, *22*, 8272. [CrossRef] [PubMed]
46. van Dam, T.J.; Wheway, G.; Slaats, G.G.; SYSCILIA Study Group; Huynen, M.A.; Giles, R.H. The SYSCILIA gold standard (SCGSv1) of known ciliary components and its applications within a systems biology consortium. *Cilia* **2013**, *2*, 7. [CrossRef]
47. Vasquez, S.S.V.; van Dam, J.; Wheway, G. An updated SYSCILIA gold standard (SCGSv2) of known ciliary genes, revealing the vast progress that has been made in the cilia research field. *Mol. Biol. Cell* **2021**, *32*, br13. [CrossRef]
48. Vij, S.; Rink, J.C.; Ho, H.K.; Babu, D.; Eitel, M.; Narasimhan, V.; Tiku, V.; Westbrook, J.; Schierwater, B.; Roy, S. Evolutionarily ancient association of the FoxJ1 transcription factor with the motile ciliogenic program. *PLoS Genet.* **2012**, *8*, e1003019. [CrossRef] [PubMed]
49. Brody, S.L.; Yan, X.H.; Wuerffel, M.K.; Song, S.K.; Shapiro, S.D. Ciliogenesis and left-right axis defects in forkhead factor HFH-4-Null mice. *Am. J. Respir. Cell. Mol. Biol.* **2000**, *23*, 45–51. [CrossRef]
50. Stubbs, J.L.; Oishi, I.; Izpisúa Belmonte, J.C.; Kintner, C. The forkhead protein Foxj1 specifies node-like cilia in xenopus and zebrafish embryos. *Nat. Genet.* **2008**, *40*, 1454–1460. [CrossRef]
51. Moore, A.; Escudier, E.; Roger, G.; Tamalet, A.; Pelosse, B.; Marlin, S.; Clément, A.; Geremek, M.; Delaisi, B.; Bridoux, A.-M.; et al. RPGR Is mutated in patients with a complex X linked phenotype combining primary ciliary dyskinesia and retinitis pigmentosa. *J. Med. Genet.* **2006**, *43*, 326–333. [CrossRef]
52. Bukowy-Bieryłło, Z.; Ziętkiewicz, E.; Loges, N.T.; Wittmer, M.; Geremek, M.; Olbrich, H.; Fliegauf, M.; Voelkel, K.; Rutkiewicz, E.; Rutland, J.; et al. RPGR mutations might cause reduced orientation of respiratory cilia. *Pediatr. Pulmonol.* **2013**, *48*, 352–363. [CrossRef] [PubMed]
53. Ghosh, A.K.; Murga-Zamalloa, C.A.; Chan, L.; Hitchcock, P.F.; Swaroop, A.; Khanna, H. Human retinopathy-associated ciliary protein retinitis pigmentosa GTPase regulator mediates cilia-dependent vertebrate development. *Hum. Mol. Genet.* **2010**, *19*, 90–98. [CrossRef] [PubMed]
54. Hannah, W.B.; DeBrosse, S.; Kinghorn, B.; Strausbaugh, S.; Aitken, M.L.; Rosenfeld, M.; Wolf, W.E.; Knowles, M.R.; Zariwala, M.A. The expanding phenotype of OFD1-related disorders: Hemizygous loss-of-function variants in three patients with primary ciliary dyskinesia. *Mol. Genet. Genom. Med.* **2019**, *7*, e911. [CrossRef] [PubMed]
55. Bukowy-Bieryllo, Z.; Rabiasz, A.; Dabrowski, M.; Pogorzelski, A.; Wojda, A.; Dmenska, H.; Grzela, K.; Sroczynski, J.; Witt, M.; Zietkiewicz, E. Truncating mutations in exons 20 and 21 of OFD1 can cause primary ciliary dyskinesia without associated syndromic symptoms. *J. Med. Genet.* **2019**, *56*, 769–777. [CrossRef] [PubMed]
56. Bengueddach, H.; Lemullois, M.; Aubusson-Fleury, A.; Koll, F. Basal body positioning and anchoring in the multiciliated cell paramecium tetraurelia: Roles of OFD1 and VFL3. *Cilia* **2017**, *6*, 6. [CrossRef]
57. Ferrante, M.I.; Zullo, A.; Barra, A.; Bimonte, S.; Messaddeq, N.; Studer, M.; Dollé, P.; Franco, B. Oral-facial-digital type I protein is required for primary cilia formation and left-right axis specification. *Nat. Genet.* **2006**, *38*, 112–117. [CrossRef]
58. Azimzadeh, J.; Wong, M.L.; Downhour, D.M.; Sánchez Alvarado, A.; Marshall, W.F. Centrosome loss in the evolution of planarians. *Science* **2012**, *335*, 461–463. [CrossRef]

59. Bustamante-Marin, X.M.; Yin, W.-N.; Sears, P.R.; Werner, M.E.; Brotslaw, E.J.; Mitchell, B.J.; Jania, C.M.; Zeman, K.L.; Rogers, T.D.; Herring, L.E.; et al. Lack of GAS2L2 causes PCD by impairing cilia orientation and mucociliary clearance. *Am. J. Hum. Genet.* **2019**, *104*, 229–245. [CrossRef]
60. Mitchison, H.M.; Schmidts, M.; Loges, N.T.; Freshour, J.; Dritsoula, A.; Hirst, R.A.; O'Callaghan, C.; Blau, H.; Al Dabbagh, M.; Olbrich, H.; et al. Mutations in axonemal dynein assembly factor DNAAF3 cause primary ciliary dyskinesia. *Nat. Genet.* **2012**, *44*, 381–389, S1-2. [CrossRef]
61. Fassad, M.R.; Shoemark, A.; le Borgne, P.; Koll, F.; Patel, M.; Dixon, M.; Hayward, J.; Richardson, C.; Frost, E.; Jenkins, L.; et al. C11orf70 mutations disrupting the intraflagellar transport-dependent assembly of multiple axonemal dyneins cause primary ciliary dyskinesia. *Am. J. Hum. Genet.* **2018**, *102*, 956–972. [CrossRef]
62. Höben, I.M.; Hjeij, R.; Olbrich, H.; Dougherty, G.W.; Nöthe-Menchen, T.; Aprea, I.; Frank, D.; Pennekamp, P.; Dworniczak, B.; Wallmeier, J.; et al. Mutations in C11orf70 cause primary ciliary dyskinesia with randomization of left/right body asymmetry due to defects of outer and inner dynein arms. *Am. J. Hum. Genet.* **2018**, *102*, 973–984. [CrossRef]
63. Zietkiewicz, E.; Bukowy-Bieryllo, Z.; Rabiasz, A.; Daca-Roszak, P.; Wojda, A.; Voelkel, K.; Rutkiewicz, E.; Pogorzelski, A.; Rasteiro, M.; Witt, M. CFAP300: Mutations in slavic patients with primary ciliary dyskinesia and a role in ciliary dynein arms trafficking. *Am. J. Respir. Cell Mol. Biol.* **2019**, *61*, 440–449. [CrossRef] [PubMed]
64. Knowles, M.R.; Ostrowski, L.E.; Loges, N.T.; Hurd, T.; Leigh, M.W.; Huang, L.; Wolf, W.E.; Carson, J.L.; Hazucha, M.J.; Yin, W.; et al. Mutations in SPAG1 cause primary ciliary dyskinesia associated with defective outer and inner dynein arms. *Am. J. Hum. Genet.* **2013**, *93*, 711–720. [CrossRef]
65. Loges, N.T.; Olbrich, H.; Becker-Heck, A.; Häffner, K.; Heer, A.; Reinhard, C.; Schmidts, M.; Kispert, A.; Zariwala, M.A.; Leigh, M.W.; et al. Deletions and point mutations of LRRC50 cause primary ciliary dyskinesia due to dynein arm defects. *Am. J. Hum. Genet.* **2009**, *85*, 883–889. [CrossRef] [PubMed]
66. Duquesnoy, P.; Escudier, E.; Vincensini, L.; Freshour, J.; Bridoux, A.-M.; Coste, A.; Deschildre, A.; de Blic, J.; Legendre, M.; Montantin, G.; et al. Loss-of-function mutations in the human ortholog of Chlamydomonas reinhardtii ODA7 disrupt dynein arm assembly and cause primary ciliary dyskinesia. *Am. J. Hum. Genet.* **2009**, *85*, 890–896. [CrossRef]
67. Thi-Kim Vu, H.; Rink, J.C.; McKinney, S.A.; McClain, M.; Lakshmanaperumal, N.; Alexander, R.; Sánchez Alvarado, A. Stem cells and fluid flow drive cyst formation in an invertebrate excretory organ. *eLife* **2015**, *4*, e07405. [CrossRef]
68. Van Rooijen, E.; Giles, R.H.; Voest, E.E.; van Rooijen, C.; Schulte-Merker, S.; van Eeden, F.J. LRRC50, a conserved ciliary protein implicated in polycystic kidney disease. *J. Am. Soc. Nephrol.* **2008**, *19*, 1128–1138. [CrossRef] [PubMed]
69. Horani, A.; Druley, T.E.; Zariwala, M.A.; Patel, A.C.; Levinson, B.T.; Van Arendonk, L.G.; Thornton, K.C.; Giacalone, J.C.; Albee, A.J.; Wilson, K.S.; et al. Whole-exome capture and sequencing identifies HEATR2 mutation as a cause of primary ciliary dyskinesia. *Am. J. Hum. Genet.* **2012**, *91*, 685–693. [CrossRef]
70. Diggle, C.P.; Moore, D.J.; Mali, G.; zur Lage, P.; Ait-Lounis, A.; Schmidts, M.; Shoemark, A.; Munoz, A.G.; Halachev, M.R.; Gautier, P.; et al. HEATR2 plays a conserved role in assembly of the ciliary motile apparatus. *PLoS Genet.* **2014**, *10*, e1004577. [CrossRef]
71. Paff, T.; Daniels, J.M.A.; Weersink, E.J.; Lutter, R.; Vonk Noordegraaf, A.; Haarman, E.G. A randomised controlled trial on the effect of inhaled hypertonic saline on quality of life in primary ciliary dyskinesia. *Eur. Respir. J.* **2017**, *49*, 1601770. [CrossRef] [PubMed]
72. Olcese, C.; Patel, M.P.; Shoemark, A.; Kiviluoto, S.; Legendre, M.; Williams, H.J.; Vaughan, C.K.; Hayward, J.; Goldenberg, A.; Emes, R.D.; et al. X-linked primary ciliary dyskinesia due to mutations in the cytoplasmic axonemal dynein assembly factor PIH1D3. *Nat. Commun.* **2017**, *8*, 14279. [CrossRef]
73. Lennon, J.; zur Lage, P.; von Kriegsheim, A.; Jarman, A.P. Strongly truncated Dnaaf4 plays a conserved role in drosophila ciliary dynein assembly as part of an R2TP-Like co-chaperone complex with Dnaaf6. *Front. Genet.* **2022**, *13*, 943197. [CrossRef] [PubMed]
74. Dong, F.; Shinohara, K.; Botilde, Y.; Nabeshima, R.; Asai, Y.; Fukumoto, A.; Hasegawa, T.; Matsuo, M.; Takeda, H.; Shiratori, H.; et al. Pih1d3 is required for cytoplasmic preassembly of axonemal dynein in mouse sperm. *J. Cell Biol.* **2014**, *204*, 203–213. [CrossRef] [PubMed]
75. Zariwala, M.A.; Gee, H.Y.; Kurkowiak, M.; Al-Mutairi, D.A.; Leigh, M.W.; Hurd, T.W.; Hjeij, R.; Dell, S.D.; Chaki, M.; Dougherty, G.W.; et al. ZMYND10 is mutated in primary ciliary dyskinesia and interacts with LRRC6. *Am. J. Hum. Genet.* **2013**, *93*, 336–345. [CrossRef]
76. Moore, D.J.; Onoufriadis, A.; Shoemark, A.; Simpson, M.A.; zur Lage, P.I.; de Castro, S.C.; Bartoloni, L.; Gallone, G.; Petridi, S.; Woollard, W.J.; et al. Mutations in ZMYND10, a gene essential for proper axonemal assembly of inner and outer dynein arms in humans and flies, cause primary ciliary dyskinesia. *Am. J. Hum. Genet.* **2013**, *93*, 346–356. [CrossRef]
77. Kott, E.; Duquesnoy, P.; Copin, B.; Legendre, M.; Dastot-Le Moal, F.; Montantin, G.; Jeanson, L.; Tamalet, A.; Papon, J.-F.; Siffroi, J.-P.; et al. Loss-of-function mutations in LRRC6, a gene essential for proper axonemal assembly of inner and outer dynein arms, cause primary ciliary dyskinesia. *Am. J. Hum. Genet.* **2012**, *91*, 958–964. [CrossRef] [PubMed]
78. Kavlie, R.G.; Kernan, M.J.; Eberl, D.F. Hearing in drosophila requires TilB, a conserved protein associated with ciliary motility. *Genetics* **2010**, *185*, 177–188. [CrossRef]
79. Kishimoto, N.; Cao, Y.; Park, A.; Sun, Z. Cystic kidney gene seahorse regulates cilia-mediated processes and wnt pathways. *Dev. Cell* **2008**, *14*, 954–961. [CrossRef]

80. Xue, J.C.; Goldberg, E. Identification of a novel testis-specific leucine-rich protein in humans and mice. *Biol. Reprod.* **2000**, *62*, 1278–1284. [CrossRef]
81. Austin-Tse, C.; Halbritter, J.; Zariwala, M.A.; Gilberti, R.M.; Gee, H.Y.; Hellman, N.; Pathak, N.; Liu, Y.; Panizzi, J.R.; Patel-King, R.S.; et al. Zebrafish ciliopathy screen plus human mutational analysis identifies C21orf59 and CCDC65 defects as causing primary ciliary dyskinesia. *Am. J. Hum. Genet.* **2013**, *93*, 672–686. [CrossRef]
82. Omran, H.; Kobayashi, D.; Olbrich, H.; Tsukahara, T.; Loges, N.T.; Hagiwara, H.; Zhang, Q.; Leblond, G.; O'Toole, E.; Hara, C.; et al. Ktu/PF13 is required for cytoplasmic pre-assembly of axonemal dyneins. *Nature* **2008**, *456*, 611–616. [CrossRef]
83. Tarkar, A.; Loges, N.T.; Slagle, C.E.; Francis, R.; Dougherty, G.W.; Tamayo, J.V.; Shook, B.; Cantino, M.; Schwartz, D.; Jahnke, C.; et al. DYX1C1 is required for axonemal dynein assembly and ciliary motility. *Nat. Genet.* **2013**, *45*, 995–1003. [CrossRef] [PubMed]
84. Leslie, J.S.; Hjeij, R.; Vivante, A.; Bearce, E.A.; Dyer, L.; Wang, J.; Rawlins, L.; Kennedy, J.; Ubeyratna, N.; Fasham, J.; et al. Biallelic DAW1 variants cause a motile ciliopathy characterized by laterality defects and subtle ciliary beating abnormalities. *Genet. Med.* **2022**, *24*, 2249–2261. [CrossRef]
85. Lesko, S.L.; Rouhana, L. Dynein assembly factor with WD repeat domains 1 (DAW1) is required for the function of motile cilia in the planarian schmidtea mediterranea. *Dev. Growth Differ.* **2020**, *62*, 423–437. [CrossRef] [PubMed]
86. Ahmed, N.T.; Gao, C.; Lucker, B.F.; Cole, D.G.; Mitchell, D.R. ODA16 aids axonemal outer row dynein assembly through an interaction with the intraflagellar transport machinery. *J. Cell Biol.* **2008**, *183*, 313–322. [CrossRef] [PubMed]
87. Thomas, L.; Bouhouche, K.; Whitfield, M.; Thouvenin, G.; Coste, A.; Louis, B.; Szymanski, C.; Bequignon, E.; Papon, J.-F.; Castelli, M.; et al. TTC12 loss-of-function mutations cause primary ciliary dyskinesia and unveil distinct dynein assembly mechanisms in motile cilia versus flagella. *Am. J. Hum. Genet.* **2020**, *106*, 153–169. [CrossRef] [PubMed]
88. Pennarun, G.; Escudier, E.; Chapelin, C.; Bridoux, A.M.; Cacheux, V.; Roger, G.; Clément, A.; Goossens, M.; Amselem, S.; Duriez, B. Loss-of-function mutations in a human gene related to Chlamydomonas reinhardtii dynein IC78 result in primary ciliary dyskinesia. *Am. J. Hum. Genet.* **1999**, *65*, 1508–1519. [CrossRef]
89. Guichard, C.; Harricane, M.C.; Lafitte, J.J.; Godard, P.; Zaegel, M.; Tack, V.; Lalau, G.; Bouvagnet, P. Axonemal dynein intermediate-chain gene (DNAI1) mutations result in situs inversus and primary ciliary dyskinesia (kartagener syndrome). *Am. J. Hum. Genet.* **2001**, *68*, 1030–1035. [CrossRef]
90. Loges, N.T.; Olbrich, H.; Fenske, L.; Mussaffi, H.; Horvath, J.; Fliegauf, M.; Kuhl, H.; Baktai, G.; Peterffy, E.; Chodhari, R.; et al. DNAI2 mutations cause primary ciliary dyskinesia with defects in the outer dynein arm. *Am. J. Hum. Genet.* **2008**, *83*, 547–558. [CrossRef]
91. Rompolas, P.; Patel-King, R.S.; King, S.M. An outer arm dynein conformational switch is required for metachronal synchrony of motile cilia in planaria. *Mol. Biol. Cell* **2010**, *21*, 3669–3679. [CrossRef]
92. Pennarun, G.; Chapelin, C.; Escudier, E.; Bridoux, A.M.; Dastot, F.; Cacheux, V.; Goossens, M.; Amselem, S.; Duriez, B. The human dynein intermediate chain 2 gene (DNAI2): Cloning, mapping, expression pattern, and evaluation as a candidate for primary ciliary dyskinesia. *Hum. Genet.* **2000**, *107*, 642–649. [CrossRef]
93. Olbrich, H.; Häffner, K.; Kispert, A.; Völkel, A.; Volz, A.; Sasmaz, G.; Reinhardt, R.; Hennig, S.; Lehrach, H.; Konietzko, N.; et al. Mutations in DNAH5 cause primary ciliary dyskinesia and randomization of left-right asymmetry. *Nat. Genet.* **2002**, *30*, 143–144. [CrossRef]
94. DiBella, L.M.; King, S.M. Dynein motors of the Chlamydomonas flagellum. *Int. Rev. Cytol.* **2001**, *210*, 227–268. [CrossRef]
95. Duriez, B.; Duquesnoy, P.; Escudier, E.; Bridoux, A.-M.; Escalier, D.; Rayet, I.; Marcos, E.; Vojtek, A.-M.; Bercher, J.-F.; Amselem, S. A common variant in combination with a nonsense mutation in a member of the thioredoxin family causes primary ciliary dyskinesia. *Proc. Natl. Acad. Sci. USA* **2007**, *104*, 3336–3341. [CrossRef] [PubMed]
96. Padma, P.; Hozumi, A.; Ogawa, K.; Inaba, K. Molecular cloning and characterization of a thioredoxin/nucleoside diphosphate kinase related dynein intermediate chain from the ascidian, ciona intestinalis. *Gene* **2001**, *275*, 177–183. [CrossRef] [PubMed]
97. Mazor, M.; Alkrinawi, S.; Chalifa-Caspi, V.; Manor, E.; Sheffield, V.C.; Aviram, M.; Parvari, R. Primary ciliary dyskinesia caused by homozygous mutation in DNAL1, encoding dynein light chain 1. *Am. J. Hum. Genet.* **2011**, *88*, 599–607. [CrossRef]
98. Piperno, G.; Huang, B.; Luck, D.J. Two-dimensional analysis of flagellar proteins from wild-type and paralyzed mutants of Chlamydomonas reinhardtii. *Proc. Natl. Acad. Sci. USA* **1977**, *74*, 1600–1604. [CrossRef]
99. Baron, D.M.; Kabututu, Z.P.; Hill, K.L. Stuck in reverse: Loss of LC1 in trypanosoma brucei disrupts outer dynein arms and leads to reverse flagellar beat and backward movement. *J. Cell Sci.* **2007**, *120*, 1513–1520. [CrossRef]
100. Schwabe, G.C.; Hoffmann, K.; Loges, N.T.; Birker, D.; Rossier, C.; de Santi, M.M.; Olbrich, H.; Fliegauf, M.; Failly, M.; Liebers, U.; et al. Primary ciliary dyskinesia associated with normal axoneme ultrastructure is caused by DNAH11 mutations. *Hum. Mutat.* **2008**, *29*, 289–298. [CrossRef] [PubMed]
101. Dougherty, G.W.; Loges, N.T.; Klinkenbusch, J.A.; Olbrich, H.; Pennekamp, P.; Menchen, T.; Raidt, J.; Wallmeier, J.; Werner, C.; Westermann, C.; et al. DNAH11 localization in the proximal region of respiratory cilia defines distinct outer dynein arm complexes. *Am. J. Respir. Cell. Mol. Biol.* **2016**, *55*, 213–224. [CrossRef] [PubMed]
102. Loges, N.T.; Antony, D.; Maver, A.; Deardorff, M.A.; Güleç, E.Y.; Gezdirici, A.; Nöthe-Menchen, T.; Höben, I.M.; Jelten, L.; Frank, D.; et al. Recessive DNAH9 loss-of-function mutations cause laterality defects and subtle respiratory ciliary-beating defects. *Am. J. Hum. Genet.* **2018**, *103*, 995–1008. [CrossRef] [PubMed]

103. Fassad, M.R.; Shoemark, A.; Legendre, M.; Hirst, R.A.; Koll, F.; le Borgne, P.; Louis, B.; Daudvohra, F.; Patel, M.P.; Thomas, L.; et al. Mutations in outer dynein arm heavy chain DNAH9 cause motile cilia defects and situs inversus. *Am. J. Hum. Genet.* **2018**, *103*, 984–994. [CrossRef] [PubMed]
104. Knowles, M.R.; Leigh, M.W.; Ostrowski, L.E.; Huang, L.; Carson, J.L.; Hazucha, M.J.; Yin, W.; Berg, J.S.; Davis, S.D.; Dell, S.D.; et al. Exome sequencing identifies mutations in CCDC114 as a cause of primary ciliary dyskinesia. *Am. J. Hum. Genet.* **2013**, *92*, 99–106. [CrossRef] [PubMed]
105. Onoufriadis, A.; Paff, T.; Antony, D.; Shoemark, A.; Micha, D.; Kuyt, B.; Schmidts, M.; Petridi, S.; Dankert-Roelse, J.E.; Haarman, E.G.; et al. Splice-site mutations in the axonemal outer dynein arm docking complex gene CCDC114 cause primary ciliary dyskinesia. *Am. J. Hum. Genet.* **2013**, *92*, 88–98. [CrossRef]
106. Hjeij, R.; Lindstrand, A.; Francis, R.; Zariwala, M.A.; Liu, X.; Li, Y.; Damerla, R.; Dougherty, G.W.; Abouhamed, M.; Olbrich, H.; et al. ARMC4 mutations cause primary ciliary dyskinesia with randomization of left/right body asymmetry. *Am. J. Hum. Genet.* **2013**, *93*, 357–367. [CrossRef]
107. Wallmeier, J.; Shiratori, H.; Dougherty, G.W.; Edelbusch, C.; Hjeij, R.; Loges, N.T.; Menchen, T.; Olbrich, H.; Pennekamp, P.; Raidt, J.; et al. TTC25 Deficiency results in defects of the outer dynein arm docking machinery and primary ciliary dyskinesia with left-right body asymmetry randomization. *Am. J. Hum. Genet.* **2016**, *99*, 460–469. [CrossRef]
108. Xu, Y.; Cao, J.; Huang, S.; Feng, D.; Zhang, W.; Zhu, X.; Yan, X. Characterization of tetratricopeptide repeat-containing proteins critical for cilia formation and function. *PLoS ONE* **2015**, *10*, e0124378. [CrossRef]
109. Hjeij, R.; Onoufriadis, A.; Watson, C.M.; Slagle, C.E.; Klena, N.T.; Dougherty, G.W.; Kurkowiak, M.; Loges, N.T.; Diggle, C.P.; Morante, N.F.C.; et al. CCDC151 mutations cause primary ciliary dyskinesia by disruption of the outer dynein arm docking complex formation. *Am. J. Hum. Genet.* **2014**, *95*, 257–274. [CrossRef]
110. Alsaadi, M.M.; Erzurumluoglu, A.M.; Rodriguez, S.; Guthrie, P.A.I.; Gaunt, T.R.; Omar, H.Z.; Mubarak, M.; Alharbi, K.K.; Al-Rikabi, A.C.; Day, I.N.M. Nonsense mutation in coiled-coil domain containing 151 gene (CCDC151) causes primary ciliary dyskinesia. *Hum. Mutat.* **2014**, *35*, 1446–1448. [CrossRef]
111. Dean, A.B.; Mitchell, D.R. Chlamydomonas ODA10 is a conserved axonemal protein that plays a unique role in outer dynein arm assembly. *Mol. Biol. Cell* **2013**, *24*, 3689–3696. [CrossRef] [PubMed]
112. Panizzi, J.R.; Becker-Heck, A.; Castleman, V.H.; Al-Mutairi, D.A.; Liu, Y.; Loges, N.T.; Pathak, N.; Austin-Tse, C.; Sheridan, E.; Schmidts, M.; et al. CCDC103 mutations cause primary ciliary dyskinesia by disrupting assembly of ciliary dynein arms. *Nat. Genet.* **2012**, *44*, 714–719. [CrossRef] [PubMed]
113. King, S.M.; Patel-King, R.S. The oligomeric outer dynein arm assembly factor CCDC103 is tightly integrated within the ciliary axoneme and exhibits periodic binding to microtubules. *J. Biol. Chem.* **2015**, *290*, 7388–7401. [CrossRef] [PubMed]
114. Bonnefoy, S.; Watson, C.M.; Kernohan, K.D.; Lemos, M.; Hutchinson, S.; Poulter, J.A.; Crinnion, L.A.; Berry, I.; Simmonds, J.; Vasudevan, P.; et al. Biallelic mutations in LRRC56, encoding a protein associated with intraflagellar transport, cause mucociliary clearance and laterality defects. *Am. J. Hum. Genet.* **2018**, *103*, 727–739. [CrossRef]
115. Bustamante-Marin, X.M.; Horani, A.; Stoyanova, M.; Charng, W.-L.; Bottier, M.; Sears, P.R.; Yin, W.-N.; Daniels, L.A.; Bowen, H.; Conrad, D.F.; et al. Mutation of CFAP57, a protein required for the asymmetric targeting of a subset of inner dynein arms in Chlamydomonas, causes primary ciliary dyskinesia. *PLoS Genet.* **2020**, *16*, e1008691. [CrossRef]
116. Lin, J.; Le, T.V.; Augspurger, K.; Tritschler, D.; Bower, R.; Fu, G.; Perrone, C.; O'Toole, E.T.; Mills, K.V.; Dymek, E.; et al. FAP57/WDR65 targets assembly of a subset of inner arm dyneins and connects to regulatory hubs in cilia. *Mol. Biol. Cell* **2019**, *30*, 2659–2680. [CrossRef]
117. Merveille, A.-C.; Davis, E.E.; Becker-Heck, A.; Legendre, M.; Amirav, I.; Bataille, G.; Belmont, J.; Beydon, N.; Billen, F.; Clément, A.; et al. CCDC39 is required for assembly of inner dynein arms and the dynein regulatory complex and for normal ciliary motility in humans and dogs. *Nat. Genet.* **2011**, *43*, 72–78. [CrossRef]
118. Becker-Heck, A.; Zohn, I.E.; Okabe, N.; Pollock, A.; Lenhart, K.B.; Sullivan-Brown, J.; McSheene, J.; Loges, N.T.; Olbrich, H.; Haeffner, K.; et al. The coiled-coil domain containing protein CCDC40 is essential for motile cilia function and left-right axis formation. *Nat. Genet.* **2011**, *43*, 79–84. [CrossRef]
119. Olbrich, H.; Cremers, C.; Loges, N.T.; Werner, C.; Nielsen, K.G.; Marthin, J.K.; Philipsen, M.; Wallmeier, J.; Pennekamp, P.; Menchen, T.; et al. Loss-of-function GAS8 mutations cause primary ciliary dyskinesia and disrupt the nexin-dynein regulatory complex. *Am. J. Hum. Genet.* **2015**, *97*, 546–554. [CrossRef]
120. Rupp, G.; Porter, M.E. A subunit of the dynein regulatory complex in chlamydomonas is a homologue of a growth arrest-specific gene product. *J. Cell Biol.* **2003**, *162*, 47–57. [CrossRef]
121. Hutchings, N.R.; Donelson, J.E.; Hill, K.L. Trypanin is a cytoskeletal linker protein and is required for cell motility in African trypanosomes. *J. Cell Biol.* **2002**, *156*, 867–877. [CrossRef]
122. Colantonio, J.R.; Vermot, J.; Wu, D.; Langenbacher, A.D.; Fraser, S.; Chen, J.-N.; Hill, K.L. The dynein regulatory complex is required for ciliary motility and otolith biogenesis in the inner ear. *Nature* **2009**, *457*, 10. [CrossRef] [PubMed]
123. Wirschell, M.; Olbrich, H.; Werner, C.; Tritschler, D.; Bower, R.; Sale, W.S.; Loges, N.T.; Pennekamp, P.; Lindberg, S.; Stenram, U.; et al. The nexin-dynein regulatory complex subunit DRC1 is essential for motile cilia function in algae and humans. *Nat. Genet.* **2013**, *45*, 262–268. [CrossRef]

124. Horani, A.; Brody, S.L.; Ferkol, T.W.; Shoseyov, D.; Wasserman, M.G.; Ta-shma, A.; Wilson, K.S.; Bayly, P.V.; Amirav, I.; Cohen-Cymberknoh, M.; et al. CCDC65 mutation causes primary ciliary dyskinesia with normal ultrastructure and hyperkinetic cilia. *PLoS ONE* **2013**, *8*, e72299. [CrossRef] [PubMed]
125. Bower, R.; Tritschler, D.; VanderWaal, K.; Perrone, C.A.; Mueller, J.; Fox, L.; Sale, W.S.; Porter, M.E. The N-DRC forms a conserved biochemical complex that maintains outer doublet alignment and limits microtubule sliding in motile axonemes. *Mol. Biol. Cell* **2013**, *24*, 1134–1152. [CrossRef]
126. Kott, E.; Legendre, M.; Copin, B.; Papon, J.-F.; Dastot-Le Moal, F.; Montantin, G.; Duquesnoy, P.; Piterboth, W.; Amram, D.; Bassinet, L.; et al. Loss-of-function mutations in RSPH1 cause primary ciliary dyskinesia with central-complex and radial-spoke defects. *Am. J. Hum. Genet.* **2013**, *93*, 561–570. [CrossRef] [PubMed]
127. Knowles, M.R.; Ostrowski, L.E.; Leigh, M.W.; Sears, P.R.; Davis, S.D.; Wolf, W.E.; Hazucha, M.J.; Carson, J.L.; Olivier, K.N.; Sagel, S.D.; et al. Mutations in RSPH1 cause primary ciliary dyskinesia with a unique clinical and ciliary phenotype. *Am. J. Respir. Crit. Care Med.* **2014**, *189*, 707–717. [CrossRef]
128. Yin, W.; Livraghi-Butrico, A.; Sears, P.R.; Rogers, T.D.; Burns, K.A.; Grubb, B.R.; Ostrowski, L.E. Mice with a deletion of Rsph1 exhibit a low level of mucociliary clearance and develop a primary ciliary dyskinesia phenotype. *Am. J. Respir. Cell Mol. Biol.* **2019**, *61*, 312–321. [CrossRef]
129. Castleman, V.H.; Romio, L.; Chodhari, R.; Hirst, R.A.; de Castro, S.C.P.; Parker, K.A.; Ybot-Gonzalez, P.; Emes, R.D.; Wilson, S.W.; Wallis, C.; et al. Mutations in radial spoke head protein genes RSPH9 and RSPH4A cause primary ciliary dyskinesia with central-microtubular-pair abnormalities. *Am. J. Hum. Genet.* **2009**, *84*, 197–209. [CrossRef]
130. Yoke, H.; Ueno, H.; Narita, A.; Sakai, T.; Horiuchi, K.; Shingyoji, C.; Hamada, H.; Shinohara, K. Rsph4a is essential for the triplet radial spoke head assembly of the mouse motile cilia. *PLoS Genet.* **2020**, *16*, e1008664. [CrossRef]
131. Jeanson, L.; Copin, B.; Papon, J.-F.; Dastot-Le Moal, F.; Duquesnoy, P.; Montantin, G.; Cadranel, J.; Corvol, H.; Coste, A.; Désir, J.; et al. RSPH3 mutations cause primary ciliary dyskinesia with central-complex defects and a near absence of radial spokes. *Am. J. Hum. Genet.* **2015**, *97*, 153–162. [CrossRef] [PubMed]
132. Gaillard, A.R.; Diener, D.R.; Rosenbaum, J.L.; Sale, W.S. Flagellar radial spoke protein 3 is an a-kinase anchoring protein (Akap). *J. Cell Biol.* **2001**, *153*, 443–448. [CrossRef] [PubMed]
133. El Khouri, E.; Thomas, L.; Jeanson, L.; Bequignon, E.; Vallette, B.; Duquesnoy, P.; Montantin, G.; Copin, B.; Dastot-Le Moal, F.; Blanchon, S.; et al. Mutations in DNAJB13, encoding an HSP40 family member, cause primary ciliary dyskinesia and male infertility. *Am. J. Hum. Genet.* **2016**, *99*, 489–500. [CrossRef] [PubMed]
134. Guan, J.; Yuan, L. A heat-shock protein 40, DNAJB13, is an axoneme-associated component in mouse spermatozoa. *Mol. Reprod. Dev.* **2008**, *75*, 1379–1386. [CrossRef] [PubMed]
135. Yang, C.; Owen, H.A.; Yang, P. Dimeric heat shock protein 40 binds radial spokes for generating coupled power strokes and recovery strokes of 9 + 2 flagella. *J. Cell Biol.* **2008**, *180*, 403–415. [CrossRef] [PubMed]
136. Cho, E.H.; Huh, H.J.; Jeong, I.; Lee, N.Y.; Koh, W.-J.; Park, H.-C.; Ki, C.-S. A nonsense variant in NME5 causes human primary ciliary dyskinesia with radial spoke defects. *Clin. Genet.* **2020**, *98*, 64–68. [CrossRef]
137. Anderegg, L.; Im Hof Gut, M.; Hetzel, U.; Howerth, E.W.; Leuthard, F.; Kyöstilä, K.; Lohi, H.; Pettitt, L.; Mellersh, C.; Minor, K.M.; et al. NME5 frameshift variant in alaskan malamutes with primary ciliary dyskinesia. *PLoS Genet.* **2019**, *15*, e1008378. [CrossRef]
138. Olbrich, H.; Schmidts, M.; Werner, C.; Onoufriadis, A.; Loges, N.T.; Raidt, J.; Banki, N.F.; Shoemark, A.; Burgoyne, T.; Al Turki, S.; et al. Recessive HYDIN mutations cause primary ciliary dyskinesia without randomization of left-right body asymmetry. *Am. J. Hum. Genet.* **2012**, *91*, 672–684. [CrossRef]
139. Cindrić, S.; Dougherty, G.W.; Olbrich, H.; Hjeij, R.; Loges, N.T.; Amirav, I.; Philipsen, M.C.; Marthin, J.K.; Nielsen, K.G.; Sutharsan, S.; et al. SPEF2- and HYDIN-mutant cilia lack the central pair-associated protein SPEF2, aiding primary ciliary dyskinesia diagnostics. *Am. J. Respir. Cell Mol. Biol.* **2020**, *62*, 382–396. [CrossRef]
140. Broadhead, R.; Dawe, H.R.; Farr, H.; Griffiths, S.; Hart, S.R.; Portman, N.; Shaw, M.K.; Ginger, M.L.; Gaskell, S.J.; McKean, P.G.; et al. Flagellar motility is required for the viability of the bloodstream trypanosome. *Nature* **2006**, *440*, 224–227. [CrossRef]
141. Lechtreck, K.-F.; Delmotte, P.; Robinson, M.L.; Sanderson, M.J.; Witman, G.B. Mutations in hydin impair ciliary motility in mice. *J. Cell Biol.* **2008**, *180*, 633–643. [CrossRef] [PubMed]
142. Lechtreck, K.-F.; Witman, G.B. Chlamydomonas reinhardtii hydin is a central pair protein required for flagellar motility. *J. Cell Biol.* **2007**, *176*, 473–482. [CrossRef] [PubMed]
143. Edelbusch, C.; Cindrić, S.; Dougherty, G.W.; Loges, N.T.; Olbrich, H.; Rivlin, J.; Wallmeier, J.; Pennekamp, P.; Amirav, I.; Omran, H. Mutation of serine/threonine protein kinase 36 (STK36) causes primary ciliary dyskinesia with a central pair defect. *Hum. Mutat.* **2017**, *38*, 964–969. [CrossRef] [PubMed]
144. Wilson, C.W.; Nguyen, C.T.; Chen, M.-H.; Yang, J.-H.; Gacayan, R.; Huang, J.; Chen, J.-N.; Chuang, P.-T. Fused has evolved divergent roles in vertebrate hedgehog signaling and motile ciliogenesis. *Nature* **2009**, *459*, 98–102. [CrossRef]
145. Rink, J.C.; Gurley, K.A.; Elliott, S.A.; Sánchez Alvarado, A. Planarian Hh signaling regulates regeneration polarity and links Hh pathway evolution to cilia. *Science* **2009**, *326*, 1406–1410. [CrossRef]
146. Sironen, A.; Kotaja, N.; Mulhern, H.; Wyatt, T.A.; Sisson, J.H.; Pavlik, J.A.; Miiluniemi, M.; Fleming, M.D.; Lee, L. Loss of SPEF2 function in mice results in spermatogenesis defects and primary ciliary dyskinesia. *Biol. Reprod.* **2011**, *85*, 690–701. [CrossRef]

147. Biebach, L.; Cindrić, S.; Koenig, J.; Aprea, I.; Dougherty, G.W.; Raidt, J.; Bracht, D.; Ruppel, R.; Schreiber, J.; Hjeij, R.; et al. Recessive mutations in CFAP74 cause primary ciliary dyskinesia with normal ciliary ultrastructure. *Am. J. Respir. Cell Mol. Biol.* **2022**, *67*, 409–413. [CrossRef]
148. DiPetrillo, C.G.; Smith, E.F. Pcdp1 is a central apparatus protein that binds Ca2+-calmodulin and regulates ciliary motility. *J. Cell Biol.* **2010**, *189*, 601–612. [CrossRef]
149. Bustamante-Marin, X.M.; Shapiro, A.; Sears, P.R.; Charng, W.-L.; Conrad, D.F.; Leigh, M.W.; Knowles, M.R.; Ostrowski, L.E.; Zariwala, M.A. Identification of genetic variants in CFAP221 as a cause of primary ciliary dyskinesia. *J. Hum. Genet.* **2020**, *65*, 175–180. [CrossRef]
150. Lee, L.; Campagna, D.R.; Pinkus, J.L.; Mulhern, H.; Wyatt, T.A.; Sisson, J.H.; Pavlik, J.A.; Pinkus, G.S.; Fleming, M.D. Primary ciliary dyskinesia in mice lacking the novel ciliary protein Pcdp1. *Mol. Cell Biol.* **2008**, *28*, 949–957. [CrossRef]
151. Dougherty, G.W.; Mizuno, K.; Nöthe-Menchen, T.; Ikawa, Y.; Boldt, K.; Ta-Shma, A.; Aprea, I.; Minegishi, K.; Pang, Y.-P.; Pennekamp, P.; et al. CFAP45 deficiency causes situs abnormalities and asthenospermia by disrupting an axonemal adenine nucleotide homeostasis module. *Nat. Commun.* **2020**, *11*, 5520. [CrossRef] [PubMed]
152. Ta-Shma, A.; Perles, Z.; Yaacov, B.; Werner, M.; Frumkin, A.; Rein, A.J.J.T.; Elpeleg, O. A human laterality disorder associated with a homozygous WDR16 deletion. *Eur. J. Hum. Genet.* **2015**, *23*, 1262–1265. [CrossRef] [PubMed]
153. Wallmeier, J.; Bracht, D.; Alsaif, H.S.; Dougherty, G.W.; Olbrich, H.; Cindric, S.; Dzietko, M.; Heyer, C.; Teig, N.; Thiels, C.; et al. Mutations in TP73 cause impaired mucociliary clearance and lissencephaly. *Am. J. Hum. Genet.* **2021**, *108*, 1318–1329. [CrossRef] [PubMed]
154. Nemajerova, A.; Kramer, D.; Siller, S.S.; Herr, C.; Shomroni, O.; Pena, T.; Gallinas Suazo, C.; Glaser, K.; Wildung, M.; Steffen, H.; et al. TAp73 is a central transcriptional regulator of airway multiciliogenesis. *Genes. Dev.* **2016**, *30*, 1300–1312. [CrossRef]
155. Al Mutairi, F.; Alkhalaf, R.; Alkhorayyef, A.; Alroqi, F.; Yusra, A.; Umair, M.; Nouf, F.; Khan, A.; Meshael, A.; Hamad, A.; et al. Homozygous truncating NEK10 mutation, associated with primary ciliary dyskinesia: A case report. *BMC Pulm. Med.* **2020**, *20*, 141. [CrossRef]
156. Porpora, M.; Sauchella, S.; Rinaldi, L.; Delle Donne, R.; Sepe, M.; Torres-Quesada, O.; Intartaglia, D.; Garbi, C.; Insabato, L.; Santoriello, M.; et al. Counterregulation of CAMP-directed kinase activities controls ciliogenesis. *Nat. Commun.* **2018**, *9*, 1224. [CrossRef]
157. Ryan, R.; Failler, M.; Reilly, M.L.; Garfa-Traore, M.; Delous, M.; Filhol, E.; Reboul, T.; Bole-Feysot, C.; Nitschké, P.; Baudouin, V.; et al. Functional characterization of tektin-1 in motile cilia and evidence for TEKT1 as a new candidate gene for motile ciliopathies. *Hum. Mol. Genet.* **2018**, *27*, 266–282. [CrossRef]
158. Devlin, L.A.; Coles, J.; Jackson, C.L.; Barroso-Gil, M.; Green, B.; Walker, W.T.; Thomas, N.S.; Thompson, J.; Rock, S.A.; Neatu, R.; et al. Biallelic variants in CEP164 cause a motile ciliopathy-like syndrome. *Clin. Genet.* **2022**, *103*, 330–334. [CrossRef]
159. Reed, M.; Takemaru, K.-I.; Ying, G.; Frederick, J.M.; Baehr, W. Deletion of CEP164 in mouse photoreceptors post-ciliogenesis interrupts ciliary intraflagellar transport (IFT). *PLoS Genet.* **2022**, *18*, e1010154. [CrossRef]
160. Beckers, A.; Adis, C.; Schuster-Gossler, K.; Tveriakhina, L.; Ott, T.; Fuhl, F.; Hegermann, J.; Boldt, K.; Serth, K.; Rachev, E.; et al. The FOXJ1 target Cfap206 is required for sperm motility, mucociliary clearance of the airways and brain development. *Development* **2020**, *147*, dev188052. [CrossRef]
161. Vasudevan, K.K.; Song, K.; Alford, L.M.; Sale, W.S.; Dymek, E.E.; Smith, E.F.; Hennessey, T.; Joachimiak, E.; Urbanska, P.; Wloga, D.; et al. FAP206 is a microtubule-docking adapter for ciliary radial spoke 2 and dynein c. *Mol. Biol. Cell* **2015**, *26*, 696–710. [CrossRef] [PubMed]
162. Lin, J.; Tritschler, D.; Song, K.; Barber, C.F.; Cobb, J.S.; Porter, M.E.; Nicastro, D. Building blocks of the nexin-dynein regulatory complex in Chlamydomonas flagella. *J. Biol. Chem.* **2011**, *286*, 29175–29191. [CrossRef] [PubMed]
163. Ta-Shma, A.; Hjeij, R.; Perles, Z.; Dougherty, G.W.; Abu Zahira, I.; Letteboer, S.J.F.; Antony, D.; Darwish, A.; Mans, D.A.; Spittler, S.; et al. Homozygous loss-of-function mutations in MNS1 cause laterality defects and likely male infertility. *PLoS Genet.* **2018**, *14*, e1007602. [CrossRef] [PubMed]
164. Zhou, J.; Yang, F.; Leu, N.A.; Wang, P.J. MNS1 is essential for spermiogenesis and motile ciliary functions in mice. *PLoS Genet.* **2012**, *8*, e1002516. [CrossRef] [PubMed]
165. Guo, T.; Tu, C.-F.; Yang, D.-H.; Ding, S.-Z.; Lei, C.; Wang, R.-C.; Liu, L.; Kang, X.; Shen, X.-Q.; Yang, Y.-F.; et al. Bi-Allelic BRWD1 variants cause male infertility with asthenoteratozoospermia and likely primary ciliary dyskinesia. *Hum. Genet.* **2021**, *140*, 761–773. [CrossRef]
166. Rachev, E.; Schuster-Gossler, K.; Fuhl, F.; Ott, T.; Tveriakhina, L.; Beckers, A.; Hegermann, J.; Boldt, K.; Mai, M.; Kremmer, E.; et al. CFAP43 modulates ciliary beating in mouse and xenopus. *Dev. Biol.* **2020**, *459*, 109–125. [CrossRef]
167. Narasimhan, V.; Hjeij, R.; Vij, S.; Loges, N.T.; Wallmeier, J.; Koerner-Rettberg, C.; Werner, C.; Thamilselvam, S.K.; Boey, A.; Choksi, S.P.; et al. Mutations in CCDC11, which encodes a coiled-coil containing ciliary protein, causes situs inversus due to dysmotility of monocilia in the left-right organizer. *Hum. Mutat.* **2015**, *36*, 307–318. [CrossRef]
168. Silva, E.; Betleja, E.; John, E.; Spear, P.; Moresco, J.J.; Zhang, S.; Yates, J.R.; Mitchell, B.J.; Mahjoub, M.R. Ccdc11 is a novel centriolar satellite protein essential for ciliogenesis and establishment of left–right asymmetry. *Mol. Biol. Cell* **2016**, *27*, 48–63. [CrossRef]

169. Shapiro, A.J.; Leigh, M.W. Value of transmission electron microscopy for primary ciliary dyskinesia diagnosis in the era of molecular medicine: Genetic defects with normal and non-diagnostic ciliary ultrastructure. *Ultrastruct. Pathol.* **2017**, *41*, 373–385. [CrossRef]
170. Amirav, I.; Mussaffi, H.; Roth, Y.; Schmidts, M.; Omran, H.; Werner, C. Israeli PCD consortium investigators a reach-out system for video microscopy analysis of ciliary motions aiding PCD diagnosis. *BMC Res. Notes* **2015**, *8*, 71. [CrossRef]
171. Knowles, M.R.; Leigh, M.W.; Carson, J.L.; Davis, S.D.; Dell, S.D.; Ferkol, T.W.; Olivier, K.N.; Sagel, S.D.; Rosenfeld, M.; Burns, K.A.; et al. Mutations of DNAH11 in patients with primary ciliary dyskinesia with normal ciliary ultrastructure. *Thorax* **2012**, *67*, 433–441. [CrossRef] [PubMed]
172. Bhatt, R.; Hogg, C. Primary ciliary dyskinesia: A major player in a bigger game. *Breathe* **2020**, *16*, 200047. [CrossRef] [PubMed]
173. Budny, B.; Chen, W.; Omran, H.; Fliegauf, M.; Tzschach, A.; Wisniewska, M.; Jensen, L.R.; Raynaud, M.; Shoichet, S.A.; Badura, M.; et al. A novel x-linked recessive mental retardation syndrome comprising macrocephaly and ciliary dysfunction is allelic to oral-facial-digital type I syndrome. *Hum. Genet.* **2006**, *120*, 171–178. [CrossRef] [PubMed]
174. Yiallouros, P.K.; Kouis, P.; Pirpa, P.; Michailidou, K.; Loizidou, M.A.; Potamiti, L.; Kalyva, M.; Koutras, G.; Kyriacou, K.; Hadjisavvas, A. Wide phenotypic variability in RSPH9-associated primary ciliary dyskinesia: Review of a case-series from cyprus. *J. Thorac. Dis.* **2019**, *11*, 2067–2075. [CrossRef] [PubMed]
175. Liu, W.; Sha, Y.; Li, Y.; Mei, L.; Lin, S.; Huang, X.; Lu, J.; Ding, L.; Kong, S.; Lu, Z. Loss-of-function mutations in SPEF2 cause multiple morphological abnormalities of the sperm flagella (MMAF). *J. Med. Genet.* **2019**, *56*, 678–684. [CrossRef]
176. Ostrowski, L.E.; Yin, W.; Smith, A.J.; Sears, P.R.; Bustamante-Marin, X.M.; Dang, H.; Hildebrandt, F.; Daniels, L.A.; Capps, N.A.; Sullivan, K.M.; et al. Expression of a truncated form of ODAD1 associated with an unusually mild primary ciliary dyskinesia phenotype. *Int. J. Mol. Sci.* **2022**, *23*, 1753. [CrossRef]
177. Preston, C.G.; Wright, M.W.; Madhavrao, R.; Harrison, S.M.; Goldstein, J.L.; Luo, X.; Wand, H.; Wulf, B.; Cheung, G.; Mandell, M.E.; et al. ClinGen variant curation interface: A variant classification platform for the application of evidence criteria from ACMG/AMP guidelines. *Genome Med.* **2022**, *14*, 6. [CrossRef]
178. Bukowy-Bieryłło, Z. Long-term differentiating primary human airway epithelial cell cultures: How far are we? *Cell Commun. Signal* **2021**, *19*, 63. [CrossRef]
179. Poprzeczko, M.; Bicka, M.; Farahat, H.; Bazan, R.; Osinka, A.; Fabczak, H.; Joachimiak, E.; Wloga, D. Rare human diseases: Model organisms in deciphering the molecular basis of primary ciliary dyskinesia. *Cells* **2019**, *8*, 1614. [CrossRef]
180. Niziolek, M.; Bicka, M.; Osinka, A.; Samsel, Z.; Sekretarska, J.; Poprzeczko, M.; Bazan, R.; Fabczak, H.; Joachimiak, E.; Wloga, D. PCD genes-from patients to model organisms and back to humans. *Int. J. Mol. Sci.* **2022**, *23*, 1749. [CrossRef]
181. Newmark, P.A.; Sánchez Alvarado, A. Not your father's planarian: A classic model enters the era of functional genomics. *Nat. Rev. Genet.* **2002**, *3*, 210–219. [CrossRef] [PubMed]
182. Morgan, T.H. Experimental studies of the regeneration of planaria maculata. *Arch. Entwickelungsmechanik Org.* **1898**, *7*, 364–397. [CrossRef]
183. Vila-Farré, M.; C Rink, J. The ecology of freshwater planarians. *Methods Mol. Biol.* **2018**, *1774*, 173–205. [CrossRef]
184. Reddien, P.W.; Sánchez Alvarado, A. Fundamentals of planarian regeneration. *Annu. Rev. Cell Dev. Biol.* **2004**, *20*, 725–757. [CrossRef] [PubMed]
185. Reddien, P.W. The cellular and molecular basis for planarian regeneration. *Cell* **2018**, *175*, 327–345. [CrossRef] [PubMed]
186. Oviedo, N.J.; Nicolas, C.L.; Adams, D.S.; Levin, M. Planarians: A versatile and powerful model system for molecular studies of regeneration, adult stem cell regulation, aging, and behavior. *CSH Protoc.* **2008**, *2008*, pdb.emo101. [CrossRef]
187. Deochand, N.; Costello, M.S.; Deochand, M.E. Behavioral research with planaria. *Perspect. Behav. Sci.* **2018**, *41*, 447–464. [CrossRef] [PubMed]
188. Basquin, C.; Orfila, A.-M.; Azimzadeh, J. The planarian Schmidtea mediterranea as a model for studying motile cilia and multiciliated cells. *Methods Cell Biol.* **2015**, *127*, 243–262. [CrossRef]
189. Saló, E.; Pineda, D.; Marsal, M.; Gonzalez, J.; Gremigni, V.; Batistoni, R. Genetic network of the eye in Platyhelminthes: Expression and functional analysis of some players during planarian regeneration. *Gene* **2002**, *287*, 67–74. [CrossRef]
190. LoCascio, S.A.; Lapan, S.W.; Reddien, P.W. Eye absence does not regulate planarian stem cells during eye regeneration. *Dev. Cell* **2017**, *40*, 381–391.e3. [CrossRef]
191. Önal, P.; Grün, D.; Adamidi, C.; Rybak, A.; Solana, J.; Mastrobuoni, G.; Wang, Y.; Rahn, H.-P.; Chen, W.; Kempa, S.; et al. Gene expression of pluripotency determinants is conserved between mammalian and planarian stem cells. *EMBO J.* **2012**, *31*, 2755–2769. [CrossRef] [PubMed]
192. Rompolas, P.; Azimzadeh, J.; Marshall, W.F.; King, S.M. Analysis of ciliary assembly and function in planaria. *Methods Enzym.* **2013**, *525*, 245–264. [CrossRef]
193. Merryman, M.S.; Alvarado, A.S.; Jenkin, J.C. Culturing planarians in the laboratory. *Methods Mol. Biol.* **2018**, *1774*, 241–258. [CrossRef] [PubMed]
194. Sánchez Alvarado, A.; Newmark, P.A. Double-stranded RNA specifically disrupts gene expression during planarian regeneration. *Proc. Natl. Acad. Sci. USA* **1999**, *96*, 5049–5054. [CrossRef]
195. Reddien, P.W.; Bermange, A.L.; Murfitt, K.J.; Jennings, J.R.; Sánchez Alvarado, A. Identification of genes needed for regeneration, stem cell function, and tissue homeostasis by systematic gene perturbation in planaria. *Dev. Cell* **2005**, *8*, 635–649. [CrossRef] [PubMed]

196. Rouhana, L.; Weiss, J.A.; Forsthoefel, D.J.; Lee, H.; King, R.S.; Inoue, T.; Shibata, N.; Agata, K.; Newmark, P.A. RNA interference by feeding in vitro-synthesized double-stranded rna to planarians: Methodology and dynamics. *Dev. Dyn.* **2013**, *242*, 718–730. [CrossRef]
197. Fincher, C.T.; Wurtzel, O.; de Hoog, T.; Kravarik, K.M.; Reddien, P.W. Cell Type transcriptome atlas for the planarian Schmidtea mediterranea. *Science* **2018**, *360*, eaaq1736. [CrossRef]
198. Plass, M.; Solana, J.; Wolf, F.A.; Ayoub, S.; Misios, A.; Glažar, P.; Obermayer, B.; Theis, F.J.; Kocks, C.; Rajewsky, N. Cell type atlas and lineage tree of a whole complex animal by single-cell transcriptomics. *Science* **2018**, *360*, eaaq1723. [CrossRef]
199. Grohme, M.A.; Schloissnig, S.; Rozanski, A.; Pippel, M.; Young, G.R.; Winkler, S.; Brandl, H.; Henry, I.; Dahl, A.; Powell, S.; et al. The genome of Schmidtea mediterranea and the evolution of core cellular mechanisms. *Nature* **2018**, *554*, 56–61. [CrossRef]
200. Benham-Pyle, B.W.; Brewster, C.E.; Kent, A.M.; Mann, F.G.; Chen, S.; Scott, A.R.; Box, A.C.; Sánchez Alvarado, A. Identification of rare post-mitotic cell states induced by injury and required for whole-body regeneration in Schmidtea mediterranea. *Nat. Cell Biol.* **2021**, *23*, 939–952. [CrossRef]
201. Robb, S.M.C.; Ross, E.; Sánchez Alvarado, A. SmedGD: The Schmidtea mediterranea genome database. *Nucleic Acids Res.* **2008**, *36*, D599–D606. [CrossRef]
202. Robb, S.M.C.; Gotting, K.; Ross, E.; Sánchez Alvarado, A. SmedGD 2.0: The Schmidtea mediterranea genome database. *Genesis* **2015**, *53*, 535–546. [CrossRef] [PubMed]
203. Rozanski, A.; Moon, H.; Brandl, H.; Martín-Durán, J.M.; Grohme, M.A.; Hüttner, K.; Bartscherer, K.; Henry, I.; Rink, J.C. PlanMine 3.0-improvements to a mineable resource of flatworm biology and biodiversity. *Nucleic Acids Res.* **2019**, *47*, D812–D820. [CrossRef] [PubMed]
204. Castillo-Lara, S.; Abril, J.F. PlanNET: Homology-based predicted interactome for multiple planarian transcriptomes. *Bioinformatics* **2018**, *34*, 1016–1023. [CrossRef] [PubMed]
205. Rompolas, P.; Patel-King, R.S.; King, S.M. Schmidtea mediterranea: A model system for analysis of motile cilia. *Methods Cell Biol.* **2009**, *93*, 81–98. [CrossRef] [PubMed]
206. King, S.M.; Patel-King, R.S. Planaria as a model system for the analysis of ciliary assembly and motility. *Methods Mol. Biol.* **2016**, *1454*, 245–254. [CrossRef]
207. Azimzadeh, J.; Basquin, C. Basal bodies across eukaryotes series: Basal bodies in the freshwater planarian Schmidtea mediterranea. *Cilia* **2016**, *5*, 15. [CrossRef]
208. Li, Y.; Guo, F.; Jing, Q.; Zhu, X.; Yan, X. Characterisation of centriole biogenesis during multiciliation in planarians. *Biol. Cell* **2020**, *112*, 398–408. [CrossRef]
209. Harrath, A.H.; Gammoudi, M.; Mansour, L.; Ahmed, M.; Sirotkin, A.V.; Al Omar, S.Y.; Ibrahim, K.E.; Alwasel, S.H. Investigation of the ultrastructure of dendrocoelum constrictum (*Platyhelminthes, Tricladida*) spermatogenesis and mature spermatozoa. *C. R. Biol.* **2014**, *337*, 513–520. [CrossRef]
210. Christman, D.A.; Curry, H.N.; Rouhana, L. Heterotrimeric kinesin II is required for flagellar assembly and elongation of nuclear morphology during spermiogenesis in Schmidtea mediterranea. *Dev. Biol.* **2021**, *477*, 191–204. [CrossRef]
211. Rink, J.C.; Vu, H.T.-K.; Sánchez Alvarado, A. The maintenance and regeneration of the planarian excretory system are regulated by EGFR signaling. *Development* **2011**, *138*, 3769–3780. [CrossRef]
212. Katoh, M.; Katoh, M. WNT signaling pathway and stem cell signaling network. *Clin. Cancer Res.* **2007**, *13*, 4042–4045. [CrossRef]
213. Peiris, T.H.; Ramirez, D.; Barghouth, P.G.; Oviedo, N.J. The akt signaling pathway is required for tissue maintenance and regeneration in planarians. *BMC Dev. Biol.* **2016**, *16*, 7. [CrossRef]
214. Petersen, C.P.; Reddien, P.W. Polarized notum activation at wounds inhibits wnt function to promote planarian head regeneration. *Science* **2011**, *332*, 852–855. [CrossRef] [PubMed]
215. De Robertis, E.M. Wnt signaling in axial patterning and regeneration: Lessons from planaria. *Sci. Signal.* **2010**, *3*, pe21. [CrossRef] [PubMed]
216. Glazer, A.M.; Wilkinson, A.W.; Backer, C.B.; Lapan, S.W.; Gutzman, J.H.; Cheeseman, I.M.; Reddien, P.W. The Zn finger protein iguana impacts hedgehog signaling by promoting ciliogenesis. *Dev. Biol.* **2010**, *337*, 148–156. [CrossRef] [PubMed]
217. Currie, K.W.; Pearson, B.J. Transcription factors Lhx1/5-1 and Pitx are required for the maintenance and regeneration of serotonergic neurons in planarians. *Development* **2013**, *140*, 3577–3588. [CrossRef]
218. Jerber, J.; Baas, D.; Soulavie, F.; Chhin, B.; Cortier, E.; Vesque, C.; Thomas, J.; Durand, B. The coiled-coil domain containing protein CCDC151 is required for the function of IFT-dependent motile cilia in animals. *Hum. Mol. Genet.* **2014**, *23*, 563–577. [CrossRef]
219. Ahmed, N.T.; Mitchell, D.R. ODA16p, a Chlamydomonas flagellar protein needed for dynein assembly. *Mol. Biol. Cell* **2005**, *16*, 5004–5012. [CrossRef]
220. Gao, C.; Wang, G.; Amack, J.D.; Mitchell, D.R. Oda16/Wdr69 is essential for axonemal dynein assembly and ciliary motility during zebrafish embryogenesis. *Dev. Dyn.* **2010**, *239*, 2190–2197. [CrossRef]
221. Solomon, G.M.; Francis, R.; Chu, K.K.; Birket, S.E.; Gabriel, G.; Trombley, J.E.; Lemke, K.L.; Klena, N.; Turner, B.; Tearney, G.J.; et al. Assessment of ciliary phenotype in primary ciliary dyskinesia by micro-optical coherence tomography. *JCI Insight* **2017**, *2*, e91702. [CrossRef] [PubMed]
222. Taschner, M.; Mourão, A.; Awasthi, M.; Basquin, J.; Lorentzen, E. Structural basis of outer dynein arm intraflagellar transport by the transport adaptor protein ODA16 and the intraflagellar transport protein IFT46. *J. Biol. Chem.* **2017**, *292*, 7462–7473. [CrossRef] [PubMed]

223. Hou, Y.; Witman, G.B. The N-terminus of IFT46 mediates intraflagellar transport of outer arm dynein and its cargo-adaptor ODA16. *Mol. Biol. Cell* **2017**, *28*, 2420–2433. [CrossRef] [PubMed]
224. Patel-King, R.S.; King, S.M. An outer arm dynein light chain acts in a conformational switch for flagellar motility. *J. Cell Biol.* **2009**, *186*, 283–295. [CrossRef] [PubMed]
225. Horváth, J.; Fliegauf, M.; Olbrich, H.; Kispert, A.; King, S.M.; Mitchison, H.; Zariwala, M.A.; Knowles, M.R.; Sudbrak, R.; Fekete, G.; et al. Identification and analysis of axonemal dynein light chain 1 in primary ciliary dyskinesia patients. *Am. J. Respir. Cell Mol. Biol.* **2005**, *33*, 41–47. [CrossRef]
226. Takada, S.; Wilkerson, C.G.; Wakabayashi, K.; Kamiya, R.; Witman, G.B. The outer dynein arm-docking complex: Composition and characterization of a subunit (Oda1) necessary for outer arm assembly. *Mol. Biol. Cell* **2002**, *13*, 1015–1029. [CrossRef] [PubMed]
227. Casey, D.M.; Inaba, K.; Pazour, G.J.; Takada, S.; Wakabayashi, K.; Wilkerson, C.G.; Kamiya, R.; Witman, G.B. DC3, the 21-KDa subunit of the outer dynein arm-docking complex (ODA-DC), is a novel EF-hand protein important for assembly of both the outer arm and the ODA-DC. *Mol. Biol. Cell* **2003**, *14*, 3650–3663. [CrossRef]
228. Takada, S.; Kamiya, R. Functional reconstitution of chlamydomonas outer dynein arms from alpha-beta and gamma subunits: Requirement of a third factor. *J. Cell Biol.* **1994**, *126*, 737–745. [CrossRef]
229. Onoufriadis, A.; Shoemark, A.; Munye, M.M.; James, C.T.; Schmidts, M.; Patel, M.; Rosser, E.M.; Bacchelli, C.; Beales, P.L.; Scambler, P.J.; et al. Combined exome and whole-genome sequencing identifies mutations in ARMC4 as a cause of primary ciliary dyskinesia with defects in the outer dynein arm. *J. Med. Genet.* **2014**, *51*, 61–67. [CrossRef]
230. Young, S.A.M.; Miyata, H.; Satouh, Y.; Kato, H.; Nozawa, K.; Isotani, A.; Aitken, R.J.; Baker, M.A.; Ikawa, M. CRISPR/Cas9-mediated rapid generation of multiple mouse lines identified Ccdc63 as essential for spermiogenesis. *Int. J. Mol. Sci.* **2015**, *16*, 24732–24750. [CrossRef]
231. Kyuji, A.; Patel-King, R.S.; Hisabori, T.; King, S.M.; Wakabayashi, K.-I. Cilia loss and dynein assembly defects in planaria lacking an outer dynein arm-docking complex subunit. *Zoolog. Sci.* **2020**, *37*, 7–13. [CrossRef] [PubMed]
232. Patel-King, R.S.; King, S.M. A prefoldin-associated WD-repeat protein (WDR92) is required for the correct architectural assembly of motile cilia. *Mol. Biol. Cell* **2016**, *27*, 1204–1209. [CrossRef] [PubMed]
233. Zur Lage, P.; Stefanopoulou, P.; Styczynska-Soczka, K.; Quinn, N.; Mali, G.; von Kriegsheim, A.; Mill, P.; Jarman, A.P. Ciliary dynein motor preassembly is regulated by Wdr92 in association with HSP90 co-chaperone, R2TP. *J. Cell Biol.* **2018**, *217*, 2583–2598. [CrossRef] [PubMed]
234. Liu, G.; Wang, L.; Pan, J. Chlamydomonas WDR92 in association with R2TP-like complex and multiple DNAAFs to regulate ciliary dynein preassembly. *J. Mol. Cell Biol.* **2019**, *11*, 770–780. [CrossRef]
235. Patel-King, R.S.; Sakato-Antoku, M.; Yankova, M.; King, S.M. WDR92 Is required for axonemal dynein heavy chain stability in cytoplasm. *Mol. Biol. Cell* **2019**, *30*, 1834–1845. [CrossRef]
236. Pazour, G.J.; Dickert, B.L.; Vucica, Y.; Seeley, E.S.; Rosenbaum, J.L.; Witman, G.B.; Cole, D.G. Chlamydomonas IFT88 and its mouse homologue, polycystic kidney disease gene Tg737, are required for assembly of cilia and flagella. *J. Cell Biol.* **2000**, *151*, 709–718. [CrossRef]
237. Moyer, J.H.; Lee-Tischler, M.J.; Kwon, H.Y.; Schrick, J.J.; Avner, E.D.; Sweeney, W.E.; Godfrey, V.L.; Cacheiro, N.L.; Wilkinson, J.E.; Woychik, R.P. Candidate gene associated with a mutation causing recessive polycystic kidney disease in mice. *Science* **1994**, *264*, 1329–1333. [CrossRef]
238. Patel-King, R.S.; Gilberti, R.M.; Hom, E.F.Y.; King, S.M. WD60/FAP163 Is a dynein intermediate chain required for retrograde intraflagellar transport in cilia. *Mol. Biol. Cell* **2013**, *24*, 2668–2677. [CrossRef]
239. Scimone, M.L.; Srivastava, M.; Bell, G.W.; Reddien, P.W. A regulatory program for excretory system regeneration in planarians. *Development* **2011**, *138*, 4387–4398. [CrossRef]
240. Marra, A.N.; Li, Y.; Wingert, R.A. Antennas of organ morphogenesis: The roles of cilia in vertebrate kidney development. *Genesis* **2016**, *54*, 457–469. [CrossRef]
241. Reddien, P.W.; Newmark, P.A.; Sánchez Alvarado, A. Gene nomenclature guidelines for the planarian Schmidtea mediterranea. *Dev. Dyn.* **2008**, *237*, 3099–3101. [CrossRef] [PubMed]
242. Nowotarski, S.H.; Davies, E.L.; Robb, S.M.C.; Ross, E.J.; Matentzoglu, N.; Doddihal, V.; Mir, M.; McClain, M.; Sánchez Alvarado, A. Planarian anatomy ontology: A resource to connect data within and across experimental platforms. *Development* **2021**, *148*, dev196097. [CrossRef] [PubMed]
243. Brandl, H.; Moon, H.; Vila-Farré, M.; Liu, S.-Y.; Henry, I.; Rink, J.C. PlanMine–a mineable resource of planarian biology and biodiversity. *Nucleic Acids Res.* **2016**, *44*, D764–D773. [CrossRef] [PubMed]
244. van Wolfswinkel, J.C.; Wagner, D.E.; Reddien, P.W. Single-cell analysis reveals functionally distinct classes within the planarian stem cell compartment. *Cell Stem Cell* **2014**, *15*, 326–339. [CrossRef] [PubMed]

245. Tu, K.C.; Cheng, L.-C.; TK Vu, H.; Lange, J.J.; McKinney, S.A.; Seidel, C.W.; Sánchez Alvarado, A. Egr-5 is a post-mitotic regulator of planarian epidermal differentiation. *eLife* **2015**, *4*, e10501. [CrossRef]
246. Wurtzel, O.; Oderberg, I.M.; Reddien, P.W. Planarian epidermal stem cells respond to positional cues to promote cell type diversity. *Dev. Cell* **2017**, *40*, 491–504.e5. [CrossRef]

Artykuł 2

***CFAP300*: Mutations in Slavic Patients with Primary Ciliary Dyskinesia and a Role in Ciliary Dynein Arms Trafficking**

Ewa Ziętkiewicz, Zuzanna Bukowy-Bieryłło, Alicja Rabiasz, Patrycja Daca-Roszak, Alina Wojda, Katarzyna Voelkel, Ewa Rutkiewicz, Andrzej Pogorzelski, Margarida Rasteiro, Michał Witt

Am J Respir Cell Mol Biol. 2019 Oct;61(4):440-449.

Wieloletnie badania prowadzone w Zakładzie Genetyki Molekularnej i Klinicznej IGC pozwoliły na wyjaśnienie genetycznego podłoża PCD u około 50% rodzin pochodzenia słowiańskiego (grupa badawcza: 398 Polaków i 16 Słowaków). W celu lepszego zrozumienia podłoża PCD, przeprowadzono sekwencjonowanie całoeksomowe (*whole-exome sequencing*, WES) u 120 polskich pacjentów z PCD o niezidentyfikowanym dotąd podłożu tej choroby. Analiza WES pozwoliła na identyfikację nowych patogennych wariantów w znanych genach PCD, jak również genów kandydatów, potencjalnie zaangażowanych w patogenezę tej ciliopatii. Jednym z takich genów był zlokalizowany w chromosomie 11 *CFAP300* (*cilia and flagella associated protein 300*; alias *C11orf70*), w którym u siedmiu niespokrewnionych pacjentów (homozygot) zidentyfikowano potencjalnie patogenny wariant c.[198_200 delTTTinsCC] (p.Phe67ProfsTer10) w eksonie 3.

W momencie projektowania, jak i realizacji badań do publikacji nie było danych na temat związku genu *CFAP300* z patogenezą PCD, w związku z czym został on zaklasyfikowany jako gen kandydat potencjalnie zaangażowany w PCD. Celem omawianej pracy było potwierdzenie roli *CFAP300* w patogenezie PCD i określenie wpływu badanego genu na strukturę i funkcję rzęsek ruchowych**.**

Przy użyciu sekwencjonowania Sangera w rodzinach pacjentów potwierdzono recesywny sposób dziedziczenia wariantu c.[198_200 delTTTinsCC]. Dodatkowa analiza materiału od pozostałych (około 80) pacjentów, oparta o metodę polimorfizmu konformacji jednoniciowych fragmentów (*single-strand conformation polymorphism,* SSCP) i sekwencjonowanie Sangera, pozwoliła na identyfikację tego wariantu u kolejnych dziesięciu niespokrewnionych chorych: siedmiu homozygot, dwóch złożonych heterozygot

(u jednego pacjenta drugi patogenny wariant w eksonie 4 c.353A>G (p.Asp188Gly); u drugiego w intronie 6: c.675+3_delAAGT) i jednego nosiciela, u którego w toku dalszych badań zidentyfikowano homozygotyczny patogenny wariant w innym genie PCD, *TTC25.* Analiza *in silico* wykazała potencjalnie patogenny charakter wariantu c.[198_200 delTTTinsCC], którego obecność może prowadzić do wprowadzenia przedwczesnego kodonu STOP i tym samym powstania skróconego białka CFAP300. Dostępność materiału (cDNA uzyskanego z RNA wyizolowanego z komórek nabłonka oddechowego pacjenta) umożliwiła sprawdzenie wpływu obecności homozygotycznego wariantu c.[198_200 delTTTinsCC] na poziom ekspresji mRNA *CFAP300* poniżej (3') i powyżej (5') patogennego wariantu w odniesieniu do kontroli (zdrowego dawcy). Analiza RT-PCR wykazała brak fragmentu transkryptu *CFAP300* poniżej (3') eksonu 3 u pacjenta, przy jednocześnie niezmienionym poziomie ekspresji równolegle analizowanych genów (genów kodujących białka strukturalne rzęsek: *DNAH5, RSPH4A* oraz genu referencyjnego: *GAPDH*). Poziom ekspresji fragmentu transkryptu powyżej (5') eksonu 3 był znacznie obniżony (do około 10% w odniesieniu do kontroli). Obserwacje te sugerują degradację nieprawidłowego mRNA *CFAP300* na drodze NMD (*nonsense mediated mRNA decay*), który polega na wykryciu i eliminacji cząsteczek mRNA zawierających przedwczesny kodon STOP. Analiza *in silico* pozostałych wariantów *CFAP300* (c.353A>G oraz c.675+3_6delAAGT) wskazała na ich potencjalny udział w składaniu (splicingu) transkryptu kodowanego przez *CFAP300*, co również może mieć charakter patogenny. Ze względu na brak materiału od pacjentów, nie zostało to potwierdzone eksperymentalnie.

Analiza danych klinicznych pacjentów z patogennymi wariantami w genie *CFAP300* wykazała, że wszyscy pacjenci mieli typowe objawy PCD; odwrócenie narządów (*situs inversus totalis*) było obserwowane u dziewięciu (na 19) pacjentów, zaś dane dostępne dla pięciu pacjentów wykazały, że zmiany w badanym genie prowadzą do znacznego obniżenia poziomu tlenku azotu w odniesieniu do wartości referencyjnej. Dostępne dla pięciu pacjentów filmy z HSVM wykazały całkowity brak ruchu rzęsek komórek nabłonka oddechowego, zaś analiza archiwalnych zdjęć przekroju rzęsek komórek nabłonka oddechowego (dla dwóch pacjentów) wskazała na zaburzenia w strukturze rzęsek: brak ODA i IDA, przy jednoczesnym zachowaniu wzorca układu mikrotubul aksonemy (9x2 + 2). W celu lepszego zrozumienia wpływu c.[198_200 delTTTinsCC] na ultrastrukturę rzęsek, przeprowadzono analizę immunofluorescencyjną komórek nabłonka oddechowego pacjenta w odniesieniu do kontroli z użyciem przeciwciał skierowanych na różne elementy

strukturalne rzęsek. Podczas gdy GAS8, CCDC39 i RSPH4A wykazywały prawidłową lokalizację w aksonemie (wskazanej przez markerowe przeciwciało, acetylowaną alfa-tubulinę), stwierdzono brak obecnych w kontroli markerów ODA (DNAH5 i DNAI2) oraz IDA (DNALI1), co potwierdziło obserwacje z TEM. Chociaż białka te nie występowały w aksonemie rzęsek, w większości komórek zaobserwowano ich obecność w apikalnej części cytoplazmy. Co ciekawe, sygnał DNALI1 zlokalizowany był bardziej dystalnie niż marker ciałek podstawnych (centryna), podczas gdy sygnał DNAH5 nie przechodził z cytoplazmy poza ciałko podstawne.

W celu lepszego zrozumienia profilu ekspresji *CFAP300* względem wybranych genów reprezentujących różne elementy rzęsek ruchowych (*FOXJ1, DNAH5, DNAI1, CCDC40, RSPH4A, DYX1C1*), przeprowadzono kompleksową analizę względnej ekspresji badanych genów w trakcie różnicowania hodowli komórek nabłonka oddechowego pochodzących z polipów zdrowych dawców. Profil ekspresji *CFAP300* (wzrost ekspresji między dniem 3 a 11 ciliogenezy, następnie stopniowe efekt plateau lub delikatny spadek ekspresji) był podobny do profilu ekspresji innych genów rzęskowych: *DYX1C1*, który jest zaangażowany w składanie ramion dyneinowych, genów kodujących białka strukturalne ramion dyneinowych (*DNAH5, DNAI1*) oraz genu kodującego białko kompleksu N-DRC (*CCDC40*).

Kolejnym etapem była analiza ewolucyjnego zakonserwowania *CFAP300* między człowiekiem a organizmami modelowymi, *Danio rerio* oraz *S. mediterranea.* Analiza *in silico* struktury genu wykazała, że gen ryby, podobnie jak człowieka, składa się z siedmiu eksonów, podczas gdy gen *S. mediterranea* z pięciu. Porównanie sekwencji białkowej CFAP300 pozwoliło na stwierdzenie, że najwyższy stopień zakonserwowania (>43% identyczności) we wszystkich trzech organizmach dotyczy sekwencji białkowej opowiadającej eksonowi drugiemu oraz piątemu genu człowieka.

Ostatnim etapem badań było potwierdzenie ewolucyjnego zakonserwowania roli genu *CFAP300* w funkcjonowaniu rzęsek ruchowych przy użyciu metody interferencji RNA (*RNA interference,* RNAi) z wykorzystaniem dwuniciowych RNA (*double-stranded RNA,* dsRNA) podawanych w pożywieniu organizmowi modelowemu, *S. mediterranea.* Efektywność wyciszenia potwierdzono na poziomie mRNA *S. mediterranea.* Dzień po ostatnim karmieniu robaki cięto w celu stymulacji procesu regeneracji, w tym tworzenia nowych komórek nabłonka i procesu ciliogenezy. Po upływie 6-7 dni od cięcia robaków

obserwowano wpływ wyciszenia homologa *CFAP300* (*Smed-cfap300*) na lokomocję robaków (wzór i prędkość ruchu). Robaki z wyciszonym *Smed-cfap300* poruszały się w charakterystyczny sposób spowodowany zaburzeniem funkcji rzęsek ruchowych, wykazując ruch typowy dla funkcji aparatu mięśniowego (tzw. *inchworming movement*). Przemieszczanie się robaków było około 5 razy wolniejsze w porównaniu do robaków kontrolnych karmionych wątróbką z dsRNA skierowanym przeciwko białku zielonej fluorescencji (*enhanced Green Fluorescent Protein*, eGFP) (robaki z wyciszonym *Smed-cfap300*: 0.29 ± 0.04 mm/s; robaki kontrolne: 1.47 ± 0.21 mm/s). Analiza ruchu rzęsek planarii przy użyciu HSVM potwierdziła wpływ wyciszenia na funkcję rzęsek ruchowych robaków; w odróżnieniu od robaków kontrolnych, rzęski robaków z wyciszonym *Smed-cfap300* poruszały się bez zachowania koordynacji ruchowej.

Omówiona praca pozwoliła na potwierdzenie roli *CFAP300* w patogenezie PCD. Ze względu na stosunkowo dużą częstość obecności patogennego wariantu *CFAP300:*c.[198_200 delTTTinsCC] w analizowanej grupie pacjentów pochodzenia słowiańskiego, stwierdzono, że testy diagnostyczne w polskiej populacji powinny zostać rozszerzone o analizę tego genu. Analiza materiału od pacjentów wykazała, że patogenne warianty genu *CFAP300* mają związek z zaburzeniem ruchu rzęsek (całkowity brak ruchu) oraz zaburzeniami ultrastruktury rzęsek (brak zewnętrznych i wewnętrznych ramion dyneinowych). Uzyskane wyniki z IF i analiza profilu ekspresji mRNA C*FAP300* oraz innych genów rzęskowych, wraz z analizą dostępnych danych literaturowych (Dyskusja pracy) wskazują na rolę CFAP300 w cytoplazmatycznym składaniu ramion dyneinowych oraz ich transporcie. Ponadto potwierdzono ewolucyjnie zakonserwowaną rolę *CFAP300* w funkcjonowaniu rzęsek ruchowych; wyciszenie *Smed-cfap300* spowodowało zaburzenie funkcji rzęsek ruchowych w organizmie modelowym, *S. mediterranea.*

Wykorzystanie *S. mediterranea* jako organizmu modelowego w omawianej pracy było poprzedzone optymalizacją użycia tego organizmu do badania genów związanych z funkcjonowaniem rzęsek ruchowych. Organizm ten nie był wcześniej wykorzystywany w Zakładzie, ani Instytucie, w którym realizowana była rozprawa doktorska; jego wprowadzenie i optymalizacja użycia stanowiły istotny element przedłożonej rozprawy doktorskiej.

Mój wkład w powstanie publikacji:

- udział w ustaleniu koncepcji i metodologii badań
- analiza wpływu obecności patogennego wariantu na poziom ekspresji wybranych genów (RT-PCR na archiwalnym materiale pacjenta)
- udział w hodowli komórek nabłonka oddechowego
- analiza *in silico* ewolucyjnego zakonserwowania *CFAP300* między organizmami
- zaprojektowanie, wykonanie i interpretacja doświadczeń z wykorzystaniem *S. mediterranea*: wyciszenie homologa genu *CFAP300* (w tym zaprojektowanie i synteza dsRNA przy użyciu transkrypcji *in vitro*), potwierdzenie efektywności wyciszenia na poziomie mRNA (izolacja RNA, synteza cDNA, qRT-PCR), analiza wpływu wyciszenia na funkcjonowanie rzęsek ruchowych planarii (analiza lokomocji robaków i ruchu rzęsek)
- udział w przygotowaniu rycin i tabel
- udział w pisaniu oryginalnej wersji manuskryptu i krytyczny przegląd ostatecznej wersji manuskryptu.

Publikacja oraz informacje dodatkowe (załączniki) są dostępne pod następującym adresem internetowym:
https://doi.org/10.1165/rcmb.2018-0260OC

ORIGINAL RESEARCH

CFAP300: Mutations in Slavic Patients with Primary Ciliary Dyskinesia and a Role in Ciliary Dynein Arms Trafficking

Ewa Zietkiewicz[1], Zuzanna Bukowy-Bieryllo[1], Alicja Rabiasz[1], Patrycja Daca-Roszak[1], Alina Wojda[1], Katarzyna Voelkel[1], Ewa Rutkiewicz[1], Andrzej Pogorzelski[2], Margarida Rasteiro[3], and Michal Witt[1]

[1]Institute of Human Genetics, Polish Academy of Sciences, Poznan, Poland; [2]Department of Pneumology and Cystic Fibrosis, Institute of Tuberculosis and Lung Diseases, Rabka, Poland; and [3]Chronic Diseases Research Centre (CEDOC), NOVA Medical School–Faculdade de Ciências Médicas, Lisbon, Portugal

ORCID IDs: 0000-0003-2437-5088 (E.Z.); 0000-0002-6945-1059 (Z.B.-B.); 0000-0003-3365-4812 (A.R.); 0000-0003-1094-1333 (P.D.-R.); 0000-0003-1729-4159 (M.W.).

Abstract

Primary ciliary dyskinesia (PCD) is a rare, genetically heterogeneous hereditary disease from a class of ciliopathies. In spite of the recent progress, the genetic basis of PCD in one-third of patients remains unknown. In search for new genes and/or mutations, whole-exome sequencing was performed in 120 unrelated Polish patients with PCD, in whom no genetic cause of PCD was earlier identified. Among a number of pathogenic variants in PCD genes, mutations in *CFAP300* (alias *C11orf70*) were detected. Extended screening in the whole Polish PCD cohort revealed the relatively high frequency (3.6%) of otherwise rare c.[198_200 del_insCC] variant, indicating that it should be included in population-specific genetic tests for PCD in Slavic populations. Immunofluorescence analysis of the respiratory epithelial cells from patients with *CFAP300* mutations revealed the absence or aberrant localization of outer and inner dynein arm markers, consistent with transmission electron microscope images indicating the lack of both dynein arms. Interestingly, the disparate localization of DNAH5 and DNALI1 proteins in patients with *CFAP300* mutations suggested differential mechanisms for the trafficking of preassembled outer and inner dynein arms to the axoneme. The profile of *CFAP300* expression during ciliogenesis in suspension culture was consistent with its role in cilia assembly. Gene silencing experiments, performed in a model organism, *Schmidtea mediterranea* (flatworm), pointed to the conserved role of *CFAP300* in ciliary function.

Keywords: population; founder effect; cilia assembly; gene silencing; planaria

Primary ciliary dyskinesia (PCD; OMIM244400) is a rare systemic disorder with an average incidence of 1:10,000–1:20,000 live births (1–3). The estimates of PCD prevalence range from 1 per 2,200 to 40,000 (4, 5), depending on the population and diagnostic schemes; the average value of 1 per 10,000 is often suggested (6). PCD is caused by the genetically determined dysfunction of motile cilia, evolutionary conserved organelles present on the surface of many cell types; the impairment of cilia motility is usually mirrored by changes in their ultrastructure. Dysfunction of multiple cilia on the apical surface of the epithelial cells lining the respiratory tract impairs mucociliary clearance; in effect, patients with PCD suffer from recurrent respiratory airways infections leading to chronic bronchopulmonary disease, recurrent sinusitis, rhinitis, otitis media, and bronchiectasis. The immotility of sperm flagella is the cause of male infertility, whereas immotility of cilia present on epithelial cells lining the fallopian tubes lowers fertility in female patients. The defects of primary cilia in the embryonic node cause randomization of the body plan symmetry, resulting in the reversal of visceral organ

(Received in original form August 11, 2018; accepted in final form February 15, 2019)

Supported by the Polish National Science Centre, granted based on decision numbers 2014/13/B/NZ2/03858 (E.Z.), 2013/09/D/NZ4/01692 (Z.B.-B.), and 2018/29/N/NZ5/00810 (A.R.).

Author Contributions: Conception and design—E.Z., Z.B.-B., A.R., and M.W.; analysis and interpretation—E.Z., Z.B.-B., A.R., P.D.-R., A.W., K.V., E.R., A.P., and M.R.; drafting or critically revising the manuscript for important intellectual content—E.Z., Z.B.-B., A.R., P.D.-R., A.P., and M.W.

Correspondence and requests for reprints should be addressed to Ewa Zietkiewicz, Ph.D., Institute of Human Genetics, Polish Academy of Sciences, Strzeszyńska 32, 60-479 Poznań, Poland. E-mail: ewa.zietkiewicz@igcz.poznan.pl.

This article has a data supplement, which is accessible from this issue's table of contents at www.atsjournals.org.

Am J Respir Cell Mol Biol Vol 61, Iss 4, pp 440–449, Oct 2019

Originally Published in Press as DOI: 10.1165/rcmb.2018-0260OC on March 27, 2019
Internet address: www.atsjournals.org

symmetry (*situs inversus*) in approximately approximately 50% of patients with PCD (Kartagener syndrome; for a review, *see*, e.g., Reference 7).

PCD is inherited in an autosomal recessive or, less frequently, X-linked manner. To date, over 40 genes have been described, mutations in which cause PCD (reviewed in References 2, 8–11; *see* also References 12–21). The number of reported mutations in the PCD genes is on a constant rise. In spite of the recent progress, the genetic basis of PCD can be presently explained in approximately 70% of the cases worldwide (11). In addition, the frequency of pathogenic variants is not uniform among populations, indicating the need to investigate population-specific profiles of mutation frequency in the PCD genes. *CFAP300* gene (cilia- and flagella-associated protein 300, ENSG00000137691; previously reported as *C11orf70*) is among the most recent additions to the growing list of genes reported to be involved in PCD pathogenesis. Located on chromosome 11q22.1, it encompasses approximately 37.12 kb of the genomic DNA. Its main transcript (CFAP300-201, ENST00000434758.7; 2,193 bp) comprises 7 exons and encodes a protein of 267 amino acids. The role of the CFAP300 in cilia assembly has been demonstrated, but the protein cellular localization and function remains ambiguous (17–18).

Our previous screening efforts performed in a large group of approximately 390 unrelated patients with PCD of Slavic (mostly Polish) origin, resulted in mutation detection in approximately 50% of the examined families (22–25, and E. Zietkiewicz and colleagues, unpublished results). In the search for further genes and mutations, whole-exome sequencing (WES) was performed in 120 of approximately 200 unrelated individuals with PCD, in whom no mutations were previously identified. Among a number of pathogenic variants in known PCD genes and in several candidate genes (E. Zietkiewicz and colleagues, unpublished results), a truncating mutation in exon 3 of *CFAP300* was detected in several individuals. To characterize the frequency of pathogenic variants in *CFAP300* in a Slavic population, the coding sequence of the gene was screened for pathogenic variants in the remaining part of the PCD cohort. To better understand the role of CFAP300 protein in motile cilia assembly, the effect of CFAP300 depletion on the cilia structure was examined in epithelial cells from patients with *CFAP300* mutations. The temporal expression of *CFAP300* during ciliogenesis was compared with the expression of other ciliary genes in a sequential, two-phase culture of epithelial cells from a control subject without PCD. The evolutionary conservation of the role of *CFAP300* orthologs in cilia biology was examined by gene silencing in an animal model—a flatworm from the genus *Planaria* (*Schmidtea mediterranea*), which uses multiple cilia covering its ventral side for locomotion.

Methods

Biological Material from Patients

Patients were classified as having PCD in accordance with European guidelines on PCD (14) (*see* Text E1 in the data supplement for the details on inclusion criteria and sample collection).

WES

Total genomic DNA was extracted from the peripheral blood samples obtained from patients with PCD. Library preparation and pair-ends sequencing were performed by a commercial provider (BGI and Macrogen Inc.) using SureSelect^{XT} V5 PostCap exome library preparation system (Agilent Technologies) and Illumina HiSeq4000 platform (Illumina, Inc.). *See* Text E2 for details.

Genetic Screening in Polish Patients with PCD

To confirm mutations segregation and to estimate the frequency of *CFAP300* pathogenic variants in Polish PCD population, the gene's coding sequence was analyzed using single strand conformation polymorphism analysis and/or dideoxy sequencing in the families of patients with *CFAP300*, and in the remaining patients with PCD (~80 unrelated individuals; *see* Text E3 and Table E1). The predicted deleterious effects of new variants were examined *in silico* using online tools (Text E3).

Analysis the Effect of *CFAP300* Mutation at the Transcription Level

Qualitative gene expression analysis was performed using Enhanced Avian RT First Strand Synthesis Kit (Sigma-Aldrich) (25). Primers used for cDNA analysis from the total RNA were designed to amplify trans-exonic sequences (Table E1). Amplification products were separated in 10% polyacrylamide gel (29:1) and silver stained.

Analysis of the Effect of CFAP300 Protein Depletion

High-speed video microscopy (HSVM) was used to visualize the effect of CFAP300 depletion on the ciliary beating pattern (Text E4). To examine the impact of mutation on the ciliary structure, respiratory epithelial cells were analyzed by high-resolution immunofluorescence (IF), using antibodies against markers of the selected elements of ciliary ultrastructure (Text E4). The HSVM and IF results were compared with the archival transmission electron microscopy (TEM) data (Text E4).

Analysis of Selected Cilia-related Transcripts in Non-PCD Cell Culture

Primary respiratory epithelial cells from non-PCD nasal polyps collected in RPMI medium were cultured *in vitro* toward ciliogenesis (Text E5). Relative quantitation of gene expression was performed using custom-made 384-well TLDA cards (Thermo Fisher Scientific), containing primers and TaqMan probes targeting genes involved in cilia biology, and two housekeeping genes (Table E2). Gene expression was analyzed using the comparative Ct method (ΔΔct) (26).

CFAP300 Orthologs in Model Organisms

The nucleotide and protein sequences of human *CFAP300* were compared with its orthologs in planarian *S. mediterranea* and in zebrafish (*Danio rerio*) (Text E6).

Analysis of the Role of CFAP300 in the Planarian Model (*S. mediterranea*) Using RNA Interference

To examine the effect of CFAP300 protein depletion in *S. mediterranea*, RNA interference was performed; the effects on worm locomotion and cilia motility were examined (Text E7).

Results

CFAP300 Mutations in Polish Patients with PCD

WES analysis was performed in a group of 120 clinically diagnosed patients with PCD

with no previously detected pathogenic variants in PCD genes. The presence of a homozygous frame-shifting mutation, c.[198_200 delTTTinsCC], in exon 3 of the *CFAP300* gene was revealed in seven unrelated individuals. An autosomal-recessive inheritance pattern of the variant was confirmed by dideoxy sequencing in the available relatives of the patients (Figure E1). The c.[198_200 delTTTinsCC], corresponding to two linked polymorphims reported in the SNP database as two separate entries (rs745839898 and rs758492644), introduces a premature stop codon (p.F67Pfs*10), which results in the severe truncation of the predicted protein.

To better estimate the involvement of *CFAP300* in PCD pathogenesis, the remaining part of our Slavic PCD cohort (consisting of ~80 patients with no mutations identified in other known PCD genes, and not analyzed by WES) was screened, using single strand conformation polymorphism and dideoxy sequencing techniques, for mutations in the *CFAP300* coding sequence (Text E3). The c.[198_200 delTTTinsCC] variant was found in 10 more unrelated patients: 7 were homozygotes (in addition to 7 identified by WES), and 3 carried this variant on one allele (Figure E1).

One of the heterozygotes (#1106, family 520) turned out to be a carrier, as two deleterious variants were later found in another PCD gene, *TTC25* (E. Zietkiewicz and colleagues, unpublished results). In two remaining c.[198_200 delTTTinsCC] heterozygotes, two novel *CFAP300* variants were identified (Figure E1). In one of these patients (#34, family 146), the c.[198_200 delTTTinsCC] variant was accompanied *in trans* by a mutation in exon 4, c.353A > G, resulting in a p.D118G substitution. This change was deemed neutral by a protein variation effect analyzer (PROVEAN), and prediction of the functional effects of SNPs using the Polyphen software; however, the scores calculated using Human Splicing Finder tool predicted c.353A > G to activate a cryptic exonic donor site. In another patient (#1075, family 504), the c.[198_200 delTTTinsCC] was accompanied (presumably *in trans*) by a 4-bp deletion in intron 6, c.675 + 3_6 delAAGT. According to the Human Splicing Finder tool, this mutation may affect the donor splice site in intron 6. Due to the lack of epithelial cells from the patients, the pathogenic character of mutations in exon 4 and intron 6 was not confirmed by transcript analysis, but the possibility of their deleterious character was provisionally assumed. The overall frequency of pathogenic *CFAP300* variants, calculated for the whole PCD cohort of 412 individuals (398 Polish and 16 Slovak), was 3.6%.

To shed light on the origin of c.[198_200 delTTTinsCC], the predominant pathogenic variant in *CFAP300*, the background haplotype, composed of three neutral SNPs localized in *CFAP300* introns 1, 2, and 3, was examined in the patients with the mutation, and in 120 unrelated chromosomes not carrying any of the deleterious *CFAP300* variants, considered here as representative of the general Polish population. In all cases, c.[198_200 delTTTinsCC] was found on the identical haplotype background 1-1-2 (Table 1). This haplotype was present in only 15% (18/120) of the nonaffected chromosomes.

Impact of Deleterious Variants in *CFAP300* on the Clinical and Ciliary Phenotype

All individuals with the deleterious variant in *CFAP300* presented with classical clinical PCD symptoms, such as chronic lower respiratory tract infections, sinusitis, otitis media, bronchiectasis, and neonatal respiratory distress syndrome. In five affected individuals, for whom data was available, the nasal nitric oxide production rate was much lower than the PCD diagnostic thresholds recommended in North America or Europe (*see* Table 2 and Text E4) (14, 27–29). In 9 out of 16 families with pathogenic *CFAP300* variants, the affected individuals had *situs inversus totalis*. HSVM analysis of the ciliary motility in nasal respiratory epithelial cells from five of the patients revealed complete lack of cilia motility (Text E4 and Video E1).

Archival pictures of the respiratory cilia cross-sections analyzed by TEM in the material from three individuals with the homozygous c.[198_200 delTTTinsCC] variant displayed loss of both outer dynein arms (ODAs) and inner dynein arms (IDAs), with the undisturbed 9 + 2 pattern of axonemal microtubules (Text E4 and Figure E2); loss of ODA and IDA occurred in 75–100% of the analyzed ciliary cross-sections (61–85 cross-sections per patient).

To assess the mutation's impact on *CFAP300* expression, transcripts from a control subjects without PCD and from a patient with the homozygous c.[198_200 delTTTinsCC] variant (#914, family 417)

Table 1. Distribution of the *CFAP300* Haplotype Variants among Analyzed Slavic Chromosomes

	Neutral SNPs in *CFAP300* Introns			
	Intron 1: c.110 + 16A > G rs12804542	Intron 2: c.192G + 59A > C rs7934495	Intron 3: c.268 + 214T > C rs 10750626	Chromosome Count
Chromosomes with the pathogenic c.[198_200delTTTinsCC] variant	1	1	2	31
Chromosomes without pathogenic variants in *CFAP300**	1	1	1	13
	1	2	1	83
	1	1	2	18
	2	1	1	6

1 denotes ancestral alleles (found in the orthologous sequence in chimpanzee); 2 denotes derived alleles.
*Unrelated chromosomes, including parental chromosomes not transferred to the patients.

Table 2. Slavic Patients with *CFAP300* Mutations

Patient ID	Family ID	Sex/Age [y.o.]	S.I.	Respiratory Symptoms	nNO [ppb] (Production [nl/min])	TEM	Cilia Motility (HSVM)	Mutation Detection*	IF Results	Mutation's Location	Allele 1 (Nucleotide, Protein)	Allele 2 (Nucleotide, Protein)	Remarks
904	409	m/34	Yes	Recurrent infections of upper and lower respiratory tract, mucus plugging	n.a.	n.a.	n.a.	WES	n.a.	exon 3/exon 3	c.198-200TTT > CC, p.F67Pfs*7	c.198-200TTT > CC, p.F67Pfs*7	—
566	255	m/17	Yes	Sinusitis, lower respiratory tract infections, bronchiectasis	n.a.	n.a.	n.a.	WES	n.a.	exon 3/exon 3	c.198-200TTT > CC, p.F67Pfs*7	c.198-200TTT > CC, p.F67Pfs*7	—
989	452	m/8	No	Respiratory tract infections	91 (31.9); 63 (22.1); 16 (5.6); 45 (15.8)	n.a.	No motility	WES	Yes	exon 3/exon 3	c.198-200TTT > CC, p.F67Pfs*7	c.198-200TTT > CC, p.F67Pfs*7	—
993	455	m/62	No	Respiratory tract infections	n.a.	n.a.	n.a.	WES	Yes	exon 3/exon 3	c.198-200TTT > CC, p.F67Pfs*7	c.198-200TTT > CC, p.F67Pfs*7	—
360	217	f/28	No	Sinusitis, lower respiratory tract infections, neonatal respiratory distress	13 (4.6)	75% lack ODA/IDA, 25% lack IDA	n.a.	SSCP	n.a.	exon 3/exon 3	c.198-200TTT > CC, p.F67Pfs*7	c.198-200TTT > CC, p.F67Pfs*7	—
361	217	m/20	No	Sinusitis, otitis media, lower respiratory tract infections, neonatal respiratory distress	64 (22.4)	n.a.	n.a.	WES	n.a.	exon 3/exon 3	c.198-200TTT > CC, p.F67Pfs*7	c.198-200TTT > CC, p.F67Pfs*7	—
363	217	m/adult	No	n.a.	n.a.	n.a.	n.a.	SSCP	n.a.	exon 3/exon 3	c.198-200TTT > CC, p.F67Pfs*7	c.198-200TTT > CC, p.F67Pfs*7	PCD detected through genetics
633	184	m/23	Yes	Sinusitis, lower respiratory tract infections, bronchiectasis, neonatal respiratory distress	n.a.	100% lack ODA/IDA	n.a.	WES	n.a.	exon 3/exon 3	c.198-200TTT > CC, p.F67Pfs*7	c.198-200TTT > CC, p.F67Pfs*7	—
102	157†	m/adult	Yes	Respiratory tract infections	n.a.	100% lack ODA/IDA	n.a.	WES (in parents)	n.a.	exon 3/exon 3	c.198-200TTT > CC, p.F67Pfs*7	c.198-200TTT > CC, p.F67Pfs*7	—
432	111	f/40	No	Sinusitis, otitis media, lower respiratory tract infections, bronchiectasis	n.a.	100% lack ODA/IDA	n.a.	SSCP	n.a.	exon 3/exon 3	c.198-200TTT > CC, p.F67Pfs*7	c.198-200TTT > CC, p.F67Pfs*7	—
914	417	m/8	No	Otitis media, chronic bronchitis, bronchiectasis, rhinitis	n.a.	n.a.	No motility	SSCP	Yes	exon 3/exon 3	c.198-200TTT > CC, p.F67Pfs*7	c.198-200TTT > CC, p.F67Pfs*7	—
1074	503	m/8	No	Sinusitis, otitis media, lower respiratory tract infections, neonatal respiratory distress	24 (8.4)	100% lack ODA/IDA	No motility	SSCP	Yes	exon 3/exon 3	c.198-200TTT > CC, p.F67Pfs*7	c.198-200TTT > CC, p.F67Pfs*7	—
1061	496	m/11	Yes	Sinusitis, lower respiratory tract infections, bronchiectasis, neonatal respiratory distress	61 (21.4); 33 (11.6); 44 (15.4); 16 (5.6)	n.a.	No motility	SSCP	n.a.	exon 3/exon 3	c.198-200TTT > CC, p.F67Pfs*7	c.198-200TTT > CC, p.F67Pfs*7	—
1138	543	m/1	Yes	Neonatal respiratory distress, neonatal respiratory tract infections, rhinitis	n.a.	n.a.	No motility	Sanger sequencing	n.a.	exon 3/exon 3	c.198-200TTT > CC, p.F67Pfs*7	c.198-200TTT > CC, p.F67Pfs*7	—
1144	546	f/6	Yes	Sinusitis, lower respiratory tract infections, bronchiectasis, neonatal respiratory distress, tract infections	51 (17.9)	n.a.	No motility	Sanger sequencing	Yes	exon 3/exon 3	c.198-200TTT > CC, p.F67Pfs*7	c.198-200TTT > CC, p.F67Pfs*7	—
1166	565	f/7	No	Recurrent respiratory tract infections, neonatal respiratory distress, rhinitis	8 (2.8)	n.a.	n.a.	Sanger sequencing	n.a.	exon 3/exon 3	c.198-200TTT > CC, p.F67Pfs*7	c.198-200TTT > CC, p.F67Pfs*7	—
34	146	m/30	Yes	Sinusitis, lower respiratory tract infections, bronchiectasis, neonatal respiratory distress	n.a.	n.a.	n.a.	SSCP	n.a.	exon 3/exon 4	c.198-200TTT > CC, p.F67Pfs*7	c.353A > G, p.D118G	Compound heterozygote
1075	504	f/1	Yes‡	Sinusitis, lower respiratory tract infections, neonatal respiratory distress	n.a.	n.a.	No motility	SSCP	n.a.	exon 3/intron 6	c.198-200TTT > CC, p.F67Pfs*7	c.675 + 3-6del, SpliceDonor	Compound heterozygote
1106	520	m/3	No	Respiratory tract infections	n.a.	n.a.	n.a.	SSCP	n.a.	exon 3/=	c.198-200TTT > CC, p.F67Pfs*7	None	Carrier§

Definition of abbreviations: f = female; HSVM = high-speed video microscopy; IDA = inner dynein arm; IF = immunofluorescence; m = male; n.a. = not available; ODA = outer dynein arm; PCD = primary ciliary dyskinesia; S.I. = situs inversus; SSCP = single strand conformation polymorphism; TEM = transmission electron microscopy; WES = whole-exome sequencing; y.o. = years old.

Notes: sampling flow rate of 350 ml/min were used for calculation of NO production rate (nl/min). Otitis media, if not reported in the table, were not found. No data about infertility in any of the adult patients were available.

*In all cases, the detected pathogenic variants were confirmed by dideoxy sequencing.

†Slovak family.

‡Isomerism of the pulmonary artery branch (hyperarterial bronchi), suggesting presence of bi-lobed lungs, midline liver, intestinal malrotation, interruption of inferior vena cava, polysplenia.

§Two mutations in another PCD gene (*CCDC39*).

were compared. cDNA was amplified using two different sets of primers, one targeting *CFAP300* transcript downstream and another upstream of the mutation site (Figure 1). Expression of other ciliary genes (*RSPH4A*, *DNAH5*) and a housekeeping gene (*GAPDH*) was assessed in parallel. The levels of *RSPH4A* and *DNAH5* transcripts in the patient remained unaffected, but no amplification product was obtained using primers targeting the *CFAP300* transcript sequence downstream of the premature STOP codon in exon 3. At the same time, only a very low amount of the product (10% compared with the control subject without PCD) was amplified using primers located upstream of the mutation site,

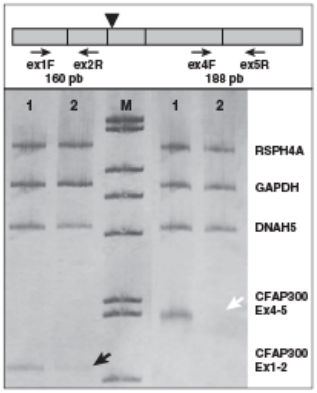

Figure 1. Multiplex PCR amplification was performed using cDNA from (1) a non-PCD control individual, and from (2) the PCD patient #914 with the homozygous c.[198_200delTTTinsCC] variant. *GAPDH* product (exons 4-8; 382 bp) was used to normalize the PCR efficiency; *RSPH4A* (exons 1-2; 436 bp), and *DNAH5* (exons 24-25; 308bp) represented expression of other ciliary genes. Two fragments of *CFAP300* were amplified: downstream and upstream from the mutation site (see inset for primers' localization; c.[198_200delTTTinsCC] mutation site is indicated by an arrowhead). M – size marker (1 kd DNA Ladder, Invitrogen). No *CFAP300* product was observed in the patient's cDNA amplified using the downstream set of primers (white arrow). The densitometrically determined intensity of the product amplified using primers located upstream from the mutation (black arrow) was approximately ten times lower than in the non-PCD control. PCD = primary ciliary dyskinesia.

suggesting that the majority of the truncated transcript was removed by nonsense-mediated decay.

To better characterize the impact of CFAP300 protein depletion on the ciliary ultrastructure, high-resolution IF analysis using antibodies against selected protein markers was performed in epithelial cell samples from four homozygous c.[198_200 delTTTinsCC] patients (Figure 2). The correct axonemal localization of GAS8, CCDC39, and RSPH4A indicated that the CFAP300 protein depletion had no effect on nexin links, nexin-dynein regulatory complexes (N-DRC), or radial spokes (RS), respectively. The absence of DNAH5 and DNAI2 (markers of ODA) and DNALI1 (marker of IDA) in the axoneme was consistent with the lack of both dynein arms, indicated by the TEM data and by the lack of ciliary motility in HSVM analysis. Interestingly, although in some of the cells the dynein arm proteins were totally missing, in the majority of cells the signals of DNAH5, DNAI2, and DNALI1 were present, but aberrantly localized in the apical part of the cytoplasm (Figure 2).

To more closely examine the localization of dynein arm markers in the CFAP300-depleted cells, IF analysis was performed using anti-CENTRIN (marker of basal bodies) with either anti-DNALI1 or anti-DNAH5 (Figure 2, two last rows). Interestingly, in the patients, DNALI1 localized more distally than CENTRIN, as opposed to DNAH5, which did not cross the basal body position marked by CENTRIN. Additional double staining analysis using anti-CENTRIN and anti-DNALI1 or anti-DNAH5 antibodies was performed in the cells from patients with PCD with mutations in *SPAG1*, another gene affecting dynein arm assembly. DNALI1 in individuals with these mutations did not enter the axoneme, but was also localized distally to CENTRIN, whereas DNAH5 remained in the cytoplasm (data not shown).

CFAP300 Expression during Ciliogenesis in Cultured Human Epithelial Cells

To assess the expression of *CFAP300* in relation to other genes involved in cilia biology, the level of selected transcripts was analyzed quantitatively during ciliogenesis in the primary adherent-sequential epithelial cell culture from non-PCD nasal polyps (Text E5). The transcripts analyzed using TLDA cards represented: motile ciliogenesis regulator (*FOXJ1*); elements of the ciliary structure—ODA (*DNAH5*), IDA (*DNAI1*), nexin-dynein regulatory complex (*CCDC40*), and RS (*RSPH4A*); and dynein arm assembly proteins—*DYX1C1* and *CFAP300* (Figure 3).

A strong upregulation of *FOXJ1* expression was observed at the very beginning of the suspension culture. The increase in the expression of all the remaining genes was delayed by approximately 2 days. The temporal profile of the fold change in *CFAP300* expression (increase from Day 3 to 11, then a plateau or a slight decrease) was very similar to that of *DYX1C1* involved in dynein arm assembly, and to those of structural dynein arm proteins (*DNAH5* and *DNAI1*) or N-DRC proteins (*CCDC40*). The increase in the expression of *RSPH4A*, which encodes a protein component of RS, was more rapid, and the level of transcript was approximately three times higher than that of other ciliary genes.

CFAP300 Orthologs in Model Organisms

Evolutionary conservation of *CFAP300* was analyzed in two model organisms, *D. rerio* (zebrafish) and *S. mediterranea* (asexual strain) (Text E6 and Figure E3). The zebrafish *CFAP300* ortholog, *si:rp17-1p14.7*, occupies approximately 4.3 kbp of the genomic sequence on chromosome 21 and consists of 7 exons. Its single transcript, 201, encodes protein of 272 aa. The ortholog of *CFAP300* in *S. mediterranea* (asexual strain) occupies approximately 2.4 kbp of the genomic sequence; transcript Smed_v6_12801_0_1 (annotated in the PlanMine database) encodes a protein of 249 aa. The comparison of the orthologous gene structures revealed that the planarian gene consists of 5 exons: exon 3 corresponds to human/zebrafish exons 3–4; and exon 4 corresponds to human/zebrafish exons 5–6. The highest conservation of the protein in the three species (>43%) was seen in human exons 2 and 5, encompassing DUF4498, the single domain in the protein structure.

Gene Silencing of the Planarian Ortholog of *CFAP300*

To confirm the conserved role of *CFAP300* in the ciliary function, the effect of

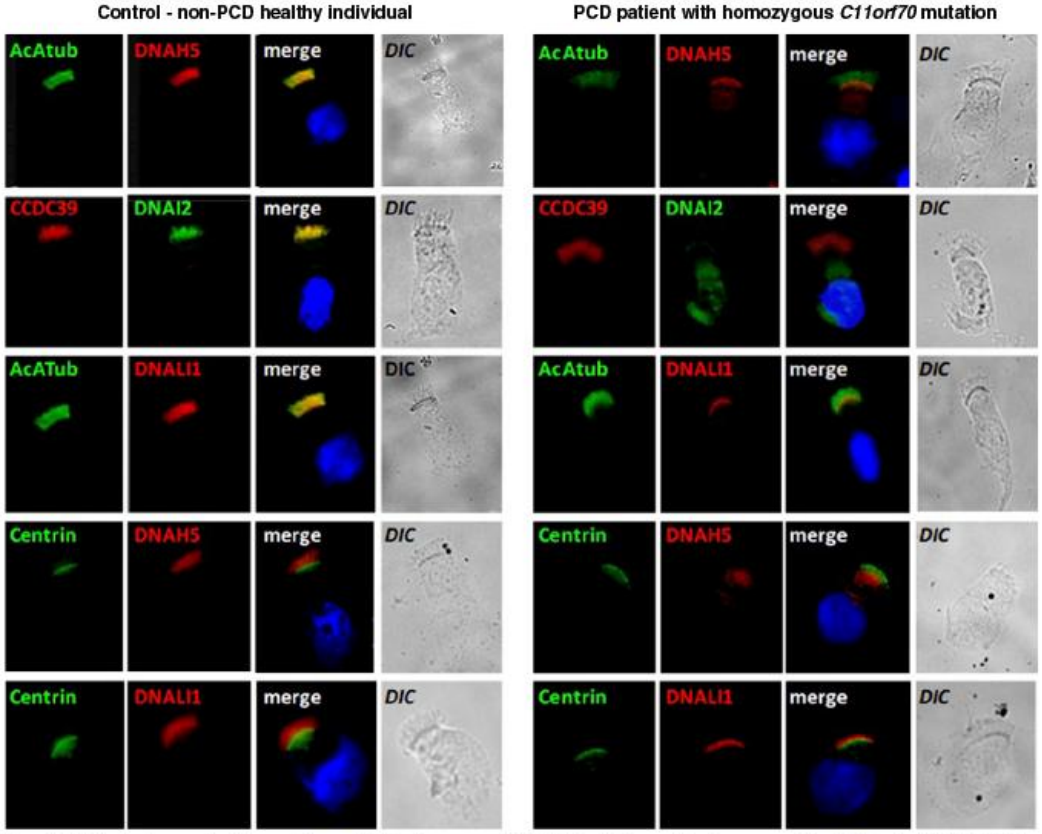

Figure 2. Ciliated cells were from the respiratory epithelium from a non-PCD individual (left panels) and a representative PCD patient (#989) with the homozygous exon 3 mutation in *CFAP300* (right panels). Cells were double-labeled with antibodies directed against elements of ciliary ultrastructure, from the top to the bottom: AcAtub (green) and DNAH5 (red); CCDC39 (red) and DNAI2 (green); AcAtub (green) and DNALI1 (red); CENTRIN (green) and DNAH5 (red); CENTRIN (green) and DNALI1 (red). Nuclei were stained with DAPI (blue). The signal of DNAH5 and DNAI2 (ODA) and DNALI1 (IDA) in the patients was missing from the axonemes and either totally absent from the cells or aberrantly localized in the apical part of the cytoplasm, indicating that the depletion of CFAP300 results in the failure to assemble/properly localize both dynein arms. Aberrant localization of DNALI1 (cytoplasmic, apical to CENTRIN) differed from that of DNAH5 (cytoplasmic, proximal to CENTRIN). Staining of GAS8, CCDC39, RSPH4A, and CENTRIN in the patients was not affected. AcAtub = acetylated α-tubulin; CCDC39 = coiled-coiled domain containing 39; DIC = differential interference contrast; DNAH5 = dynein axonemal heavy chain 5; DNALI1 = dynein axonemal light intermediate chain 1; GAS8 = growth arrest specific 8; IDA = inner dynein arm; ODA = outer dynein arm; RSPH4A = radial spoke head component 4A.

RNA interference of its ortholog in *S. mediterranea* was examined. dsRNA corresponding to the 402-bp segment in the 5′ part of the Smed_v6_12801_0_1 transcript was administered to the worms by repetitive feeding (*see* Text E8 and Table E1 for details). Ciliogenesis was stimulated by cutting worms and allowing regeneration from pluripotential stem cells (neoblasts). Symptoms of the impairment of the cilia-mediated locomotion of planaria were seen 6–7 days after worms' fragmentation, and manifested as a slow crawling aided by body contraction (so called "inchworming" movement) instead of cilia-mediated gliding (Video E2). A five- to sixfold reduction in the average speed of locomotion in *CFAP300*-silenced worms (0.29 ± 0.04 mm/s) compared with controls fed with eGFP dsRNA (1.47 ± 0.21 mm/s) was observed (Figure 4). HSVM analysis showed the severe reduction of cilia motility in planaria fed with *CFAP300* dsRNA (Video E3). Examination at 1/8 speed revealed the lack of coordination in cilia beating and heterogeneity of their motility. The silencing effect lasted for 1–2 days; after that time, the cilia motility and worm locomotion returned to normal.

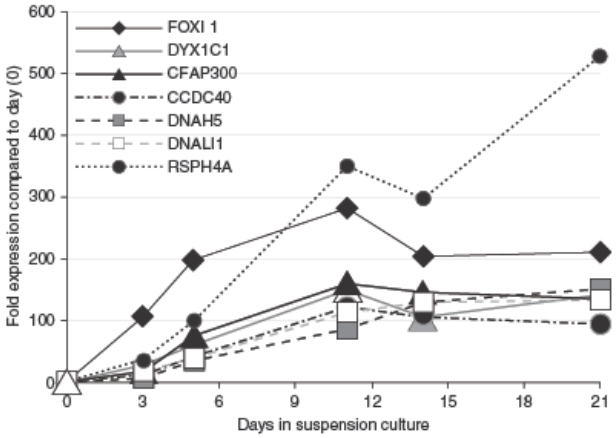

Figure 3. Expression profiles of seven cilia-related genes were analyzed at days 0, 3, 5, 11, 14, and 21 of the suspension phase in the culture of primary epithelial cells from non-PCD nasal polyps; expression on day 0 was used as a calibrator. The genes represented different stages of ciliogenesis: *FOXJ1* – motile ciliogenesis induction (thin solid line with diamonds); *DNAAF4/DYX1C1* and *CFAP300* – cilia assembly (thick solid lines with triangles); *CCDC40* – structural elements of the axoneme (dashed and dotted line with circles); *DNAH5*, *DNALI1* – dynein arms (dashed lines with squares), *RSPH4A* – radial spokes (dashed line with small circles); two stable housekeeping genes (*18S* and *TBP*) were used for data normalization.

Discussion

The c.[198_200 delTTTinsCC] mutation in *CFAP300* (alias *C11orf70*) was found to be causative in 16 of 412 analyzed Slavic PCD families; two other presumably pathogenic variants (c.353A > G in exon 4 and c.675 + 3–6del in intron 6) were private; four previously reported rare pathogenic variants (17, 18) were not identified in any of the analyzed patients (Figure 5).

The relatively high frequency of c.[198_200 delTTTinsCC] in exon 3 of *CFAP300* (30/824 chromosomes in the whole cohort) may be indicative of a Slavic founder effect, especially given that this pathogenic variant has not been found in the targeted WES analysis of 161 PCD individuals of non-Slavic origin (18). On the other hand, c.[198_200 delTTTinsCC] has been reported in 2 of 15 PCD families analyzed in another targeted WES study (17); however, with no information on the ethnic affiliation of these patients and a small preselected group analyzed in that study, it neither supports nor contradicts the possibility of the mutation's Slavic origin. Our study has shown that c.[198_200 delTTTinsCC] resides on the same background haplotype, otherwise found in only 15% of the nonaffected Polish chromosomes; this is consistent with the common ancestry of c.[198_200 delTTTinsCC]. However, inferences about the age of the mutation and the possible Slavic founder effect would require analyzing more markers, localized at much longer genomic distances. Nevertheless, the high frequency of c.[198_200 delTTTinsCC] among Slavic patients with PCD places this variant among mutations, which should be considered in designing population-specific panels for genetic tests.

The impact of *CFAP300* mutations on the ciliary structure, as demonstrated by TEM- and IF-based analyses, confirmed earlier observations (17, 18), that the depletion of CFAP300 results in the defects of both ODAs and IDAs, but does not affect other structures, like RS, N-DRC, or basal bodies. This pattern of IF staining in the respiratory epithelia cells from patients with biallelic *CFAP300* mutations resembled the one observed earlier in patients with mutations in the genes encoding proteins involved in different stages of cilia assembly. The profile of *CFAP300* expression during ciliogenesis, examined in the suspension phase of the two-phase culture of epithelial cells from non-PCD nasal polyps, paralleled that of DNAAF4/DYX1C1 protein, and was therefore consistent with the proposed role of CFAP300 in cilia assembly (17, 18).

However, the cilia assembly is not a single-step process. The first group of proteins involved in the cilia assembly combines cytoplasmic proteins acting as cochaperons: DNAAF1/LRRC50 (30, 31); DNAAF2/KTU (32); DNAAF3 (33); DNAAF4/DYX1C1 (34); DNAAF5/HEATR2 (35, 36); LRRC6 (37, 38); CCDC103 (39, 40); and SPAG1 (41). The second group plays a role in the cytoplasmic assembly of dynein arms and/or their transport to the proper axonemal location: C21orf59 (42) and ZMYND10 (43, 44). Other proteins required for proper trafficking of the preassembled dynein arms, revealed by studies in *Chlamydomonas* and zebrafish, but not found to cause PCD in humans, include ODA8 (human LRRC56) and ODA16 (human WDR69), shown to interact with IFT46, a component of the intraflagellar retrograde transport, IFT (45–47).

The cytoplasmic protein, DNAAF2, together with SPAG1 and DNAAF5, have been shown to be involved in the early stages of dynein arm assembly (48). The late preassembly proteins, PIH1D3 and DNAAF4, have also been shown to bind DNAAF2 (16, 34). Therefore, the function of DNAAF2 as a link between early and late preassembly complexes has been suggested (48). The direct interaction of CFAP300 with DNAAF2 has been reported (17), suggesting its cytoplasmic localization and the role in the assembly of dynein arms. Western blots performed in *Chlamydomonas* and *Paramecium* confirmed the predominant presence of CFAP300 ortholog in the cytoplasm, but revealed that a small amount was also in cilia; the localization of CFAP300 in the detergent-soluble fraction of cilia indicated its localization in the matrix and membrane, as opposed

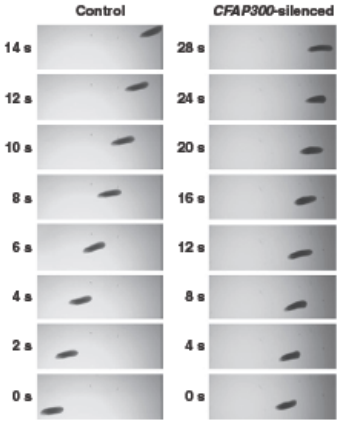

Figure 4. The impact of RNAi on planarias' locomotion was observed seven days after the fragmentation of worms fed with dsRNA (*eGFP* - left panel or *CFAP300* - right panel). The picture shows worms with regenerated tails. *CFAP300*-silenced worms moved by body contractions only, as opposed to control worms, which moved by cilia-mediated gliding. The distance covered by the control and silenced worms during 14 and 28 s, respectively, are shown as snapshots taken every 2 or 4 s. The average speed of *CFAP300*-silenced worms (calculated in 20 animals) was 5-6 times slower than in the controls. dsRNA = double-strand RNA; RNAi = RNA interference.

to the insoluble axonemal fraction (18). This cytoplasmic and ciliary matrix localization of CFAP300, similar to that proposed for C21orf59 (42) and ZMYND10 (43, 44), may suggest its role in dynein arm transport within the axoneme. The exact role of CFAP300 remains to be elucidated.

In this context, it is interesting that, in our hands, IF staining in cells from patients with two truncating mutations in *CFAP300* often indicated that dynein arm components (DNAH5, DNAI2, and DNALI1), although absent from the cilia, were in the apical part of the cytoplasm, close to the base of the axoneme (Figure 2). Similar IF staining has been observed previously (17), but not discussed. It is tempting to speculate that the apical localization of the preassembled dynein arms observed in individuals with *CFAP300* mutations reflects their arrest in place, from which they should have been further trafficked into the axonemal compartment with the aid of CFAP300. This scenario appears consistent with the large-scale comparative analysis of the *Chlamydomonas* genome, where *FBB5*, the *CFAP300* ortholog, has been identified as a member of a group of flagellar basal body genes (49).

Both DNALI1 and DNAH5 were absent from ciliary axonemes in the cells with mutations in *CFAP300*. Interestingly, double IF staining with anti-CENTRIN and either anti-DNALI1 or anti-DNAH5 antibodies (Figure 2) revealed that the position of ODA and IDA markers with respect to the basal body marker was different, with DNAH5 localized proximally and DNALI1 distally to CENTRIN. This may suggest different mechanisms for the trafficking of preassembled IDA and ODA elements to the axoneme. This phenomenon appears not to be restricted to the cells with mutations in *CFAP300*, because a similar difference in the localization of DNAH5 and DNALI1 was also observed in cells from patients with mutations in other assembly-related genes (e.g., *SPAG1*; data not shown).

To shed more light upon the evolutionary conservation of the role of *CFAP300* in cilia biology, we examined the effect of silencing the gene ortholog in a model organism, the *S. mediterranea* flatworm. The worms' locomotion defect observed in the knockdown experiments demonstrated that the role of the protein in ciliary function is highly conserved in evolution, consistent with similar observations in *Chlamydomonas* and *Paramecium* (18). The evolutionary conservation of the CFAP300 function is striking, especially in light of the relatively low level of amino acid identity among its orthologs (Figure 3). On the other hand, the much higher level of sequence conservation observed in the protein segment encompassing human exons 2 and 5 indicates that these fragments may have a particularly important role in CFAP300 protein functioning, and thus in cilia biology. This information could be useful for further studies on the molecular function of DUF4498, the large eukaryotic domain of unknown function. The domain encompasses the major part of CFAP300 protein and is disrupted by all the mutations in this gene reported so far in patients with PCD. ■

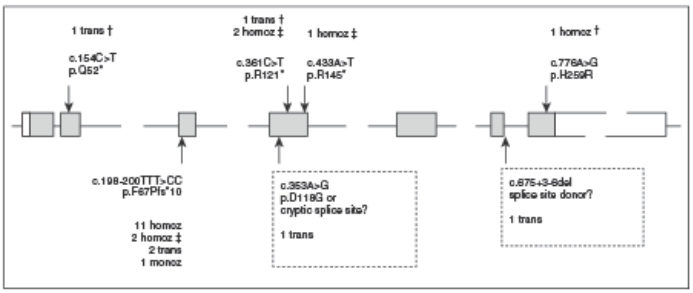

Figure 5. Schematic representation of the *CFAP300* gene. Exons are represented by filled boxes are driven up to scale. Summary of pathogenic variants reported in this study and in two previous reports is provided; (18) † and (17) ‡. The number of families carrying *CFAP300* mutations is shown (homoz - in homozygosity, trans - in trans with another mutation; monoz – with mutation on one allele only). Mutations of uncertain pathogenicity are framed.

Author disclosures are available with the text of this article at www.atsjournals.org.

Acknowledgment: The authors gratefully acknowledge all primary ciliary dyskinesia families for contributing biological material for this study, Dr. Roman Jaksik (Technical University, Gliwice, Poland) for the help in whole-exome sequencing data annotation, Dr. Maciej Dabrowski (Institute of Human Genetics, Polish Academy of Sciences, Poznan, Poland) for help in tissue culture maintenance, and Dr. Patrick Perrigue (Institute of Bioorganic Chemistry, Polish Academy of Sciences, Poznan, Poland) for help in developing planaria facility. They are indebted to the anonymous reviewers for thoughtful remarks and to Dr. Susana Lopes (CEDOC, Chronic Diseases Research Centre, NOVA Medical School–Faculdade de Ciencias Medicas, Lisbon, Portugal) for helpful consultations.

References

1. Pifferi M, Di Cicco M, Piras M, Cangiotti AM, Saggese G. Up to date on primary ciliary dyskinesia in children. *Early Hum Dev* 2013;89: S45–S48.
2. Knowles MR, Daniels LA, Davis SD, Zariwala MA, Leigh MW. Primary ciliary dyskinesia: recent advances in diagnostics, genetics, and characterization of clinical disease. *Am J Respir Crit Care Med* 2013; 188:913–922.
3. Knowles MR, Zariwala M, Leigh M. Primary ciliary dyskinesia. *Clin Chest Med* 2016;37:449–461.
4. Kuehni CE, Frischer T, Strippoli MP, Maurer E, Bush A, Nielsen KG, *et al.*; ERS Task Force on Primary Ciliary Dyskinesia in Children. Factors influencing age at diagnosis of primary ciliary dyskinesia in European children. *Eur Respir J* 2010;36:1248–1258.
5. Lucas JS, Burgess A, Mitchison HM, Moya E, Williamson M, Hogg C; National PCD Service, UK. Diagnosis and management of primary ciliary dyskinesia. *Arch Dis Child* 2014;99:850–856.
6. Kuehni CE, Lucas JS. Diagnosis of primary ciliary dyskinesia: summary of the ERS task force report. *Breathe (Sheff)* 2017;13: 166–178.
7. Marshall WF. The cell biological basis of ciliary disease. *J Cell Biol* 2008; 180:17–21.
8. Collins SA, Walker WT, Lucas JS. Genetic testing in the diagnosis of primary ciliary dyskinesia: state-of-the-art and future perspectives. *J Clin Med* 2014;3:491–503.
9. Kurkowiak M, Ziętkiewicz E, Witt M. Recent advances in primary ciliary dyskinesia genetics. *J Med Genet* 2015;52:1–9.
10. Shapiro AJ, Zariwala MA, Ferkol T, Davis SD, Sagel SD, Dell SD, *et al.*; Genetic Disorders of Mucociliary Clearance Consortium. Diagnosis, monitoring, and treatment of primary ciliary dyskinesia: PCD foundation consensus recommendations based on state of the art review. *Pediatr Pulmonol* 2016;51:115–132.
11. Mirra V, Werner C, Santamaria F. Primary ciliary dyskinesia: an update on clinical aspects, genetics, diagnosis, and future treatment strategies. *Front Pediatr* 2017;5:135–147.
12. Olbrich H, Cremers C, Loges NT, Werner C, Nielsen KG, Marthin JK, *et al.* Loss-of-function GAS8 mutations cause primary ciliary dyskinesia and disrupt the nexin-dynein regulatory complex. *Am J Hum Genet* 2015;97:546–554.
13. Horani A, Ferkol TW, Dutcher SK, Brody SL. Genetics and biology of primary ciliary dyskinesia. *Paediatr Respir Rev* 2016;18: 18–24.
14. Lucas JS, Barbato A, Collins SA, Goutaki M, Behan L, Caudri D, *et al.* European Respiratory Society guidelines for the diagnosis of primary ciliary dyskinesia. *Eur Respir J* 2017;49:1601090.
15. Edelbusch C, Cindrić S, Dougherty GW, Loges NT, Olbrich H, Rivlin J, *et al.* Mutation of serine/threonine protein kinase 36 (STK36) causes primary ciliary dyskinesia with a central pair defect. *Hum Mutat* 2017; 38:964–969.
16. Paff T, Loges NT, Aprea I, Wu K, Bakey Z, Haarman EG, *et al.* Mutations in PIH1D3 cause X-linked primary ciliary dyskinesia with outer and inner dynein arm defects. *Am J Hum Genet* 2017;100:160–168.
17. Höben IM, Hjeij R, Olbrich H, Dougherty GW, Nöthe-Menchen T, Aprea I, *et al.* Mutations in *C11ORF70* cause primary ciliary dyskinesia with randomization of left/right body asymmetry due to defects of outer and inner dynein arms. *Am J Hum Genet* 2018;102: 973–984.
18. Fassad MR, Shoemark A, le Borgne P, Koll F, Patel M, Dixon M, *et al.* C11orf70 mutations disrupting the intraflagellar transport-dependent assembly of multiple axonemal dyneins cause primary ciliary dyskinesia. *Am J Hum Genet* 2018;102:956–972.
19. Fassad MR, Shoemark A, Legendre M, Hirst RA, Koll F, le Borgne P, *et al.* Mutations in outer dynein arm heavy chain DNAH9 cause motile cilia defects and situs inversus. *Am J Hum Genet* 2018;103: 984–994.
20. Loges NT, Antony D, Maver A, Deardorff MA, Güleç EY, Gezdirici A, *et al.* Recessive DNAH9 loss-of-function mutations cause laterality defects and subtle respiratory ciliary-beating defects. *Am J Hum Genet* 2018;103:995–1008.
21. Bonnefoy S, Watson CM, Kernohan KD, Lemos M, Hutchinson S, Poulter JA, *et al.*; Care4Rare Canada Consortium. Biallelic mutations in LRRC56, encoding a protein associated with intraflagellar transport, cause mucociliary clearance and laterality defects. *Am J Hum Genet* 2018;103:727–739.
22. Ziętkiewicz E, Nitka B, Voelkel K, Skrzypczak U, Bukowy Z, Rutkiewicz E, *et al.* Population specificity of the DNAI1 gene mutation spectrum in primary ciliary dyskinesia (PCD). *Respir Res* 2010;11:174.
23. Ziętkiewicz E, Bukowy-Bieryłło Z, Voelkel K, Klimek B, Dmeńska H, Pogorzelski A, *et al.* Mutations in radial spoke head genes and ultrastructural cilia defects in East-European cohort of primary ciliary dyskinesia patients. *PLoS One* 2012;7:e33667.
24. Bukowy-Bieryllo Z, Ziętkiewicz E, Loges NT, Wittmer M, Geremek M, Olbrich H, *et al.* RPGR mutations might cause reduced orientation of respiratory cilia. *Pediatr Pulmonol* 2013;48:352–363.
25. Kurkowiak M, Ziętkiewicz E, Greber A, Voelkel K, Wojda A, Pogorzelski A, *et al.* ZMYND10—mutation analysis in Slavic patients with primary ciliary dyskinesia. *PLoS One* 2016;11:e0148067.
26. Pfaffl MW. A new mathematical model for relative quantification in real-time RT-PCR. *Nucleic Acids Res* 2001;29:e45.
27. Leigh MW, Hazucha MJ, Chawla KK, Baker BR, Shapiro AJ, Brown DE, *et al.* Standardizing nasal nitric oxide measurement as a test for primary ciliary dyskinesia. *Ann Am Thorac Soc* 2013;10:574–581.
28. Boon M, Smits A, Cuppens H, Jaspers M, Proesmans M, Dupont LJ, *et al.* Primary ciliary dyskinesia: critical evaluation of clinical symptoms and diagnosis in patients with normal and abnormal ultrastructure. *Orphanet J Rare Dis* 2014;9:11.
29. Shapiro AJ, Josephson M, Rosenfeld M, Yilmaz O, Davis SD, Polineni D, *et al.* Accuracy of nasal nitric oxide measurement as a diagnostic test for primary ciliary dyskinesia: a systematic review and meta-analysis. *Ann Am Thorac Soc* 2017;14:1184–1196.
30. Duquesnoy P, Escudier E, Vincensini L, Freshour J, Bridoux AM, Coste A, *et al.* Loss-of-function mutations in the human ortholog of *Chlamydomonas* reinhardtii ODA7 disrupt dynein arm assembly and cause primary ciliary dyskinesia. *Am J Hum Genet* 2009;85: 890–896.
31. Loges NT, Olbrich H, Becker-Heck A, Häffner K, Heer A, Reinhard C, *et al.* Deletions and point mutations of LRRC50 cause primary ciliary dyskinesia due to dynein arm defects. *Am J Hum Genet* 2009;85: 883–889.
32. Omran H, Kobayashi D, Olbrich H, Tsukahara T, Loges NT, Hagiwara H, *et al.* Ktu/PF13 is required for cytoplasmic pre-assembly of axonemal dyneins. *Nature* 2008;456:611–616.
33. Mitchison HM, Schmidts M, Loges NT, Freshour J, Dritsoula A, Hirst RA, *et al.* Mutations in axonemal dynein assembly factor DNAAF3 cause primary ciliary dyskinesia. *Nat Genet* 2012;44:381–389, S1–S2.
34. Tarkar A, Loges NT, Slagle CE, Francis R, Dougherty GW, Tamayo JV, *et al.*; UK10K. DYX1C1 is required for axonemal dynein assembly and ciliary motility. *Nat Genet* 2013;45:995–1003.
35. Horani A, Druley TE, Zariwala MA, Patel AC, Levinson BT, Van Arendonk LG, *et al.* Whole-exome capture and sequencing identifies HEATR2 mutation as a cause of primary ciliary dyskinesia. *Am J Hum Genet* 2012;91:685–693.
36. Diggle CP, Moore DJ, Mali G, zur Lage P, Ait-Lounis A, Schmidts M, *et al.* HEATR2 plays a conserved role in assembly of the ciliary motile apparatus. *PLoS Genet* 2014;10:e1004577.
37. Kott E, Duquesnoy P, Copin B, Legendre M, Dastot-Le Moal F, Montantin G, *et al.* Loss-of-function mutations in LRRC6, a gene essential for proper axonemal assembly of inner and outer dynein arms, cause primary ciliary dyskinesia. *Am J Hum Genet* 2012;91:958–964.
38. Horani A, Ferkol TW, Shoseyov D, Wasserman MG, Oren YS, Kerem B, *et al.* LRRC6 mutation causes primary ciliary dyskinesia with dynein arm defects. *PLoS One* 2013;8:e59436.
39. Panizzi JR, Becker-Heck A, Castleman VH, Al-Mutairi DA, Liu Y, Loges NT, *et al.* CCDC103 mutations cause primary ciliary dyskinesia by disrupting assembly of ciliary dynein arms. *Nat Genet* 2012;44: 714–719.
40. King SM, Patel-King RS. The oligomeric outer dynein arm assembly factor CCDC103 is tightly integrated within the ciliary axoneme and exhibits periodic binding to microtubules. *J Biol Chem* 2015;290: 7388–7401.

41. Knowles MR, Ostrowski LE, Loges NT, Hurd T, Leigh MW, Huang L, *et al*. Mutations in SPAG1 cause primary ciliary dyskinesia associated with defective outer and inner dynein arms. *Am J Hum Genet* 2013;93:711–720.
42. Austin-Tse C, Halbritter J, Zariwala MA, Gilberti RM, Gee HY, Hellman N, *et al*. Zebrafish ciliopathy screen plus human mutational analysis identifies C21orf59 and CCDC65 defects as causing primary ciliary dyskinesia. *Am J Hum Genet* 2013;93:672–686.
43. Moore DJ, Onoufriadis A, Shoemark A, Simpson MA, zur Lage PI, de Castro SC, *et al*. Mutations in ZMYND10, a gene essential for proper axonemal assembly of inner and outer dynein arms in humans and flies, cause primary ciliary dyskinesia. *Am J Hum Genet* 2013;93:346–356.
44. Zariwala MA, Gee HY, Kurkowiak M, Al-Mutairi DA, Leigh MW, Hurd TW, *et al*. ZMYND10 is mutated in primary ciliary dyskinesia and interacts with LRRC6. *Am J Hum Genet* 2013;93:336–345.
45. Ahmed NT, Gao C, Lucker BF, Cole DG, Mitchell DR. ODA16 aids axonemal outer row dynein assembly through an interaction with the intraflagellar transport machinery. *J Cell Biol* 2008;183:313–322.
46. Gao C, Wang G, Amack JD, Mitchell DR. Oda16/Wdr69 is essential for axonemal dynein assembly and ciliary motility during zebrafish embryogenesis. *Dev Dyn* 2010;239:2190–2197.
47. Desai PB, Freshour JR, Mitchell DR. *Chlamydomonas* axonemal dynein assembly locus ODA8 encodes a conserved flagellar protein needed for cytoplasmic maturation of outer dynein arm complexes. *Cytoskeleton (Hoboken)* 2015;72:16–28.
48. Horani A, Ustione A, Huang T, Firth AL, Pan J, Gunsten SP, *et al*. Establishment of the early cilia preassembly protein complex during motile ciliogenesis. *Proc Natl Acad Sci U S A* 2018;115:E1221–E1228.
49. Merchant SS, Prochnik SE, Vallon O, Harris EH, Karpowicz SJ, Witman GB, *et al*. The *Chlamydomonas* genome reveals the evolution of key animal and plant functions. *Science* 2007;318:245–250.

SUPPLEMENTARY FILE

Ewa Zietkiewicz, Zuzanna Bukowy-Bieryllo, Alicja Rabiasz, Patrycja Daca-Roszak, Alina Wojda, Katarzyna Voelkel, Ewa Rutkiewicz, Andrzej Pogorzelski, Margarida Rasteiro, Michal Witt

CFAP300 (alias *C11orf70*): mutations in Slavic primary ciliary dyskinesia patients and protein role in cilia function

CONTENTS:

SUPPLEMENTARY TEXT

Text E1.

Biological material from patients

Classical clinical symptoms included neonatal respiratory distress, recurrent upper and lower respiratory tract infections, sinusitis, bronchiectasis, otitis media, in some – abnormalities in left-right body asymmetry, mainly *situs inversus*. These were supported by any of the following criteria: i) low nasal nitric oxide (NO) production, i.e. <200ppb calculated using sampling flow rate of 350 ml/min (Table 2), measured either by using a hand-held Niox Mino (Aerocrine) or EcoMedics CLD88 (Duernten); ii) abnormal ciliary motion in high-speed videomicroscopy (HSVM); iii) ciliary ultrastructure defects in transmission electron microscopy (TEM); iv) defective staining using any of the two antibodies, anti-GAS8 or anti-DNAI2. Of note, NO level of 220 ppb, calculated using sampling flow rate 350 ml/min) for Ecomedics analyzer, corresponds to the threshold of 77 nL/min recommended by PCD organizations in the North America (27); the PCD threshold of <300 ppb is recommended in Europe (28); see also (29); there is currently no consensus over what threshold constitutes a positive or negative cut-off for nNO (14).

The institutional review board for human studies (the Ethics Review Board at the Medical University in Poznan) approved the protocols (permission # 435/13) and informed written consent was obtained from the subjects or their surrogates whenever required by the institutional review board.

A group of 120 unrelated Polish PCD patients, in whom no mutations were found in the previous screening efforts based on SSCP/heteroduplex analysis, ASO-genotyping or direct dideoxy sequencing (22-25; and our unpublished data), were analyzed using new generation sequencing of the whole exome. The total number of PCD families available for the genetic screening (and used for the calculation of *CFAP300* mutations frequency in Slavic PCD population) was 412 (398 families of Polish and 16 of Slovak origin).

Peripheral blood samples were collected during routine check-ups of the patients and used to isolate genomic DNA. **Human respiratory epithelial cells** from bronchial biopsies obtained during a routine check-up of the patients, used to isolate total RNA, were collected and stored at -80°C in RNALater solution (Qiagen). Samples used to prepare cells for immunofluorescence (IF) analysis (collected in RPMI, spread on glass slides and stored at -80°C) were obtained by nasal brush biopsies from patients and from consenting healthy volunteers. Epithelial cells used for *in vitro* ciliogenesis were obtained from routinely resected nasal polyps originating from non-PCD donors.

Nucleic acids isolation procedures

DNA was extracted using standard salting-out method. **RNA** from frozen samples of epithelial cells in RNALater was **extracted** using RNeasy®Plus Micro Kit (QIAGEN), according to manufacturer's protocol (*Total RNA containing small RNAs*). RNA quality was assessed using the Bioanalyzer (Pall Biosciences).

Text E2.

Whole exome sequencing (WES)

SureSelect^{XT} V5 PostCap system (Agilent Technologies, CA, USA) was used for the exome library preparation. Amplified libraries that passed quality control (DNA 1000 Bioanalyzer assay) were sequenced on HiSeq4000 platform (Illumina, Inc., CA, USA), as paired-end reads (2 x 100 bp; 5 Gbp of raw data). Each of the analyzed samples was sequenced in a separate flow cell. The aimed sequencing coverage at the raw data level was 100X.

Quality control was conducted using FastQC and FastQ Screen. Sequencing reads were aligned to the GRCh37 reference genome, using BWA-MEM (E1). On average, 83-fold mean coverage of the targeted exome was achieved (SureSelectXT V5 regions, covering 50.4 megabases [Mb]), with 91% positions covered at 20x or higher. Aligned reads were processed using MarkDuplicates algorithm from the Picard tool set and BaseRecalibrator which is a part of the Genome Analysis Toolkit (GATK v3.6) (E2). Germline SNVs and indels were identified using GATK's HaplotypeCaller in GVCF mode (v3.6). All of the identified variants were annotated using Variant Effect Predictor (v85) (E4).The annotation data (VCF files) were converted to an Excel file; this allowed direct comparison of all the samples analyzed, and manual variant filtration and prioritization. Consistent with the rare occurrence of PCD, variants from the dbSNP build 141 and/or the 1000 Genomes Project databases characterized by the minor allele frequency >0.01 in the general, European or European American population (whichever was higher), were excluded from the analysis. The data were filtered according to a recessive (or X-linked) disease model: the samples with biallelic (or monoallelic X-linked) deleterious mutations (nonsynonymous mutations in the coding sequence, splice-site substitutions or indels) found in any of the known PCD genes were considered solved. The remaining samples (including those with only monoallelic mutations found in autosomal PCD genes), were subjected to the search for candidate genes. Genes with novel deleterious variants (not reported in any public database) or with the minor allele frequency lower than 0.01, were selected for further studies, especially if the variants were present in more than one of the PCD patients, with no mutations in the known PCD genes identified.

Text E3

Genotyping *CFAP300* families and other PCD patients

CFAP300 exons containing deleterious variants found by WES were PCR-amplified and analyzed by dideoxy sequencing to confirm the presence of the variant allele. Whenever parents or siblings of the patient were available, segregation of the PCD-causing variants in a family was examined (**Fig. E1**). Evaluation of the sequencing results was performed using Chromas and Fasta Sequence Comparison tool [http://fasta.bioch.virginia.edu/fasta_www2].

The coding sequence of *CFAP300* was analyzed in the remaining PCD patients, who were not subjected to WES and for whom no biallelic mutation in any of the PCD genes was found (~80 unrelated individuals). The search for new rare variants was performed using SSCP analysis, as earlier described (23). PCR primers for *CFAP300* analysis (**Table E1**), designed with the use of Primer3, flanked whole exons and exon/intron junctions; the amplicon size for SSCP and sequencing was 250-300 bp; the details on *CFAP300* PCR and SSCP conditions are available from the authors upon request.

The predicted deleterious effects of new variants were examined *in silico* using online tools: Polyphen-2 [genetics.bwh.harvard.edu/pph2/] and Provean [provean.jcvi.org] for nonsynonymous mutations and Human Splicing Finder for the splice site mutation [www.umd.be/HSF/]. Sequence variants were described according to the recommendations [www.hgvs.org/mutnomen/checklist.html]; the cDNA numbering was according to the main Ensembl transcript CFAP300-201 (ENST00000434758.6, RefSeq: NM_032930).

Text E4

High-speed video microscopy (HSVM), immunofluorescence (IF) and transmission electron microscope (TEM) analysis

Cilia motility was assessed at room temperature in clusters of freshly collected nasal respiratory epithelium cells, suspended in RPMI medium. Cilia motility was evaluated using inverted Opta-Tech microscope at 400x magnification and recorded using a high-speed video Basler camera (120 fps). Ciliary beat pattern was assessed by analyzing slow-motion playbacks of the recordings in SAVA software (Sisson-Ammons Video Analysis software, Ammons Engineering, USA (E5); (**Video E1 A and B**).

Immunofluorescence (IF) analysis was performed as described (25), using the following primary antibodies: acetylated α-tubulin (mouse monoclonal T6793, SIGMA; used at 1: 15,000); DNAH5 (mouse polyclonal HPA037470, SIGMA; 1: 800); DNAI2 (mouse monoclonal H00064446-M01, ABNOVA; 1:550); DNALI1 (rabbit polyclonal ARP53611, AVIVA; 1:1200); GAS8 (rabbit polyclonal HPA041311, SIGMA; 1:500);

CCDC39 (rabbit polyclonal HPA035364, SIGMA; 1:500); RSPH4A (rabbit polyclonal HPA035364, SIGMA; 1:200); CENTRIN (mouse polyclonal 04-1624, MILIPORE; 1:2000); highly cross-adsorbed secondary antibodies (goat anti-rabbit IgG-546 and goat anti-mouse IgG-488, Molecular Probes MERCK; both 1:3000).

Ultrastructural defects in the patients were confirmed by reanalysis of available archival images from TEM analysis, prepared as described earlier (23). TEM was performed with a Philips CM10 at 16,000- to 50,000-fold magnification (**Fig. E2**).

Text E5

Ciliogenesis in culture

Primary respiratory epithelial cells from nasal polyps collected in RPMI medium were cultured *in vitro* toward ciliogenesis, using a sequential 2-phase method (E6), whereby cells proliferate in the adherent (ADH) phase, followed by cell differentiation during the suspension (SUSP) phase. Cultures were initiated using epithelial cells from nasal polyps; the culture conditions were as described before (E7). Epithelial cells were collected at the day preceding the SUSP culture (pre-SUSP, day 0) and days 3, 5, 11, 14,21 of the SUSP culture, suspended in RNA Later Plus buffer (Qiagen), frozen at -80°C and used for RNA isolation within 3 weeks.

Text E6

***CFAP300* orthologues in zebrafish and planaria**

CFAP300 orthologue transcript in *S. mediterranea* (asexual strain) was identified in the PlanMine database (http://planmine.mpi-cbg.de/planmine/begin.do) (E8). The genomic structure of the planarian gene was assessed by comparing transcript with the genomic DNA sequence from the SmedGD browser (*S. mediterranea* Genome Database (http://smedgdkc03.stowers.org/cgi-bin/gb2/gbrowse/SmedUnigenes). The nucleotide and protein sequences of human *CFAP300*, and its orthologues in zebrafish and *Schmidtea mediterranea* were compared in MultAlin software, using Blosum62-12-2 and DNA-5-0 score tables for DNA and protein comparisons, respectively [http://multalin.toulouse.inra.fr/multalin] (**Fig. E3**).

Text E7

Transient RNAi silencing of the C*FAP300* orthologue in planarian model

An asexual strain of *S. mediterranea* was maintained at 20 °C, as described (S9), and fed chicken liver once/twice per week. Animals measuring 3-5 mm in length were starved for at least one week before experiments.

DsRNA was designed using the coding sequence of *CFAP300* orthologue in *S. mediterranea* asexual strain, Smed_v6_12801_0_1 as a reference. Total RNA was isolated according to ThermoFisher Scientific protocol, using TRIzol and DNA-free kit. Total RNA was reverse transcribed using oligo(dT) primer and RevertAid H Minus First Strand cDNA Synthesis kit (ThermoFisher Scientific). The 402 bp long fragment encompassing planarian exons 1 (part), 2, 3 and exon 4 (part), corresponding to positions 180-601 in Smed_v6_12801_0_1, was amplified using primers tagged with T7 RNA polymerase promotor (**Table E1, Fig. E3**). The amplicon was used as a template for dsRNA preparation according to the manufacturer's protocol (MEGAscript™ T7 Transcription Kit, Thermo Fisher Scientific).

RNA interference was performed using the feeding protocol (E10). DsRNA was administered to the worms by repetitive feeding (five times, every second day) with a homogenized chicken liver mixed with *CFAP300* dsRNA (10 µg dsRNA mixed with 50 µl of liver paste per 10 worms); dsRNA prepared from the plasmid containing eGFP (enhanced green fluorescence protein) was fed to the control group. The efficiency of *CFAP300* silencing was confirmed by the analysis of cDNA isolated from the worms (data not shown). Next day after the last feeding, the worms were cut to stimulate the process of regeneration (planarias are known for their high regeneration capacity). The phenotypic effects of the knockdown were examined 6-9 days after worms fragmentation. The velocity of planarias' locomotion was recorded for 20-60 sec using a stereoscope (Opta-Tech, SK series) at 10x magnification, and OptaView IS software version 4.1.3 (**Video E2 A and B**). ImageJ software was used for image analysis and measurements (E11). The average distance traveled by ten knockdown worms in a time unit (10 or 20 sec) was compared with the corresponding measure for ten control animals (fed with the eGFP dsRNA). The effect of RNAi on cilia motility was assessed using HSVM and SAVA software, as described in ST4 section, at 400 x magnification (**Video E3 A and B**).

SUPPLEMENTARY REFERENCES:

E1. Li H. Aligning sequence reads, clone sequences and assembly contigs with BWA-MEM. *ArXiv E-Prints* 2013; 1303.3997 [q-bio.GN].

E2. DePristo MA, Banks E, Poplin R, Garimella KV, Maguire JR, Hartl C, Philippakis AA, del Angel G, Rivas MA, Hanna M, McKenna A, Fennell TJ, Kernytsky AM, Sivachenko AY, Cibulskis K, Gabriel SB, Altshuler D,

Daly MJ. A framework for variation discovery and genotyping using next-generation DNA sequencing data. *Nature Genetics* 2011; 43:491–98.

E3. Cibulskis K, Lawrence MS, Carter SL, Sivachenko A, Jaffe D, Sougnez C, Gabriel S, Meyerson M, Lander ES, and Getz G. Sensitive detection of somatic point mutations in impure and heterogeneous cancer samples. *Nature Biotechnology* 2013; 31: 213-19.

E4. McLaren W, Gil L, Hunt SE, Riat HS, Ritchie GRS, Thormann A, Flicek P, and Cunningham F. The Ensembl Variant Effect Predictor. *Genome Biology* 2016; 17:122.

E5. Sisson JH, Stoner JA, Ammons BA, Wyatt TA. All-digital image capture and whole-field analysis of ciliary beat frequency. *J Microsc* 2003; 211:103-111.

E6. Jorissen M, Van der Schueren B, Tyberghein J, Van der Berghe H, Cassiman JJ. Ciliogenesis and coordinated ciliary beating in human nasal epithelial cells cultured in vitro. *Acta Otorhinolaryngol Belg* 1989; 43:67-73.

E7. Bukowy-Bieryllo Z, Dabrowski M, Witt M, Zietkiewicz E. Aminoglycoside-stimulated readthrough of premature termination codons in selected genes involved in primary ciliary dyskinesia. *RNA Biol* 2016; 13:1041-1050.

E8. Brandl H, Moon H, Vila-Farre M, Liu SY, Henry I, Rink JC. PlanMine – a mineable resource of planarian biology and biodiversity. *Nucleic Acids Res* 2016; 44:64-73.

E9. Cebria F and Newmark PA. Planarian homologs of netrin and netrin receptor are required for proper regeneration of the central nervous system and the maintenance of nervous system architecture. *Development* 2005, 132:3691-3703.

E10. Rouhana L, Weiss JA, Forsthoefel DJ, Lee H, King RS, Inoue T, Shibata N, Agata K, Newmark PA. RNA interference by feeding in vitro-synthesized double-stranded RNA to planarians: methodology and dynamics. *Dev Dyn* 2013; 242:718-730.

E11. Rompolas P, Azimzadeh J, Marshall WF, King SM. Analysis of ciliary assembly and function in planaria. *Methods Enzymol* 2103; 525:245-264.

SUPPLEMENTARY TABLES

Table E1. Sequences of primers and oligonucleotides used in the study

Primers used in the analysis of human *CFAP300*	
PCR primers* (5'-3') for exon screening by SSCP and dideoxy sequencing:	
C11orf70-1_F	CATCCACCCAGCCGAGAG
C11orf70-1_R	gaagaccaagggcctcttct
C11orf70-2_F	gtgggtgggatcggttatc
C11orf70-2_R	agagacccagggaactctcc
C11orf70-3_F	aaaatatctaacttattcccctcaaat
C11orf70-3_R	tgaaaattcctgaggcaaaa
C11orf70-4_F	gcgatttattttggaaatagttga
C11orf70-4_R	ttcctgaaataaaattccactgc
C11orf70-5_F	tcaagattggttcttaaaataggtgt
C11orf70-5_R	agatttacatattgtgatctagcaaca
C11orf70-6_F	ttacttaaatgtatatgccaatgcct
C11orf70-6_R	tcctaggcataacattgtcctga
C11orf70-7_F	gcgacggagcaagactct
C11orf70-7_R	TCTTCTGCTCTAAGTAGGCTCCT
PCR primers† for cDNA analysis (5'-3'):	
C11orf70-e1_F	GGGGACTTGGGTGGCTACTA
C11orf70-e2_R	CCTTCCGATAGGACTGAAAGG
C11orf70-e3_F	TGAAGATATTGTACGAGACAGTGGA
C11orf70-e4_R	CTCCACCAAGGCAAAGATGT
GAPDH_e4 F	ACGGGAAGCTTGTCATCAAT
GAPDH_e8 R	GGGCCATCCACAGTCTTCT
RSPH4A_e1 F	CAGTCTCAGCAACCCAAACC
RSPH4A_e2 R	CCAAATGTCCCTGGAGAAAA
DNAH5_e24 F	ACCGGAGTGAGATGGAAAAC
DNAH5_e25 R	CTGGGCTGCAGTGAGACTAA

Primers used in the analysis of S. mediterranea orthologue of c11orf70 (*dd_Smed_v6_12801_0_1*)	
Primers used to prepare dsRNA for RNAi (5'-3'); sequence in brackets: T7 polymerase promotor:	
Smed_c11orf70_ds_e1_F	[TAATACGACTCACTATAGGG]GTTCTTTTATACCCTTGCCCG
Smed_c11orf70_ds_e4_R	[TAATACGACTCACTATAGGG]TCTGCGACTCTCTTCCGAAT
eGFP ds_R	[TAATACGACTCACTATAGGG]TGTTCTGCTGGTAGTGGTCG
eGFP_ds_F	[TAATACGACTCACTATAGGG]GACGTAAACGGCCACAAGTT

* Primers located in exons in introns are shown in uppercase and lowercase, respectively.

† Primers used for cDNA analysis were designed to amplify trans-exonic sequences.

Table E2. List of mRNA transcripts and TLDA probes

mRNA transcript name	TLDA probe name	Type of probe	Role in cilia biology
FOXJ1	Hs00230964_m1	Target	Induction of motile ciliogenesis
CFAP300	Hs00988407_m1	Target	Cilia assembly
DNAAF4/DYX1C1	Hs00984202_m1	Target	Cilia assembly
DNAH5	Hs00292485_m1	Target	ODA structure
DNALI1	Hs00185750_m1	Target	ODA structure
CCDC40	Hs00215769_m1	Target	N-DRC structure
RSPH4A	Hs00402529_m1	Target	Radial spoke structure
18S	Hs99999901_s1	Normalizing	Housekeeping gene
TBP	Hs99999910_m1	Normalizing	Housekeeping gene

ONLINE RESOURCES

Chromas and Fasta Sequence Comparison tool http://fasta.bioch.virginia.edu/fasta_www2

Multalin multiple sequence comparison http://multalin.toulouse.inra.fr/multalin

Gene Cards: http://genecards.org

DAVID software: https://david.ncifcrf.gov/home.jsp

Human Splicing Finder: http://www.umd.be/HSF/

Variant Effect Predictor: https://www.ensembl.org/info/docs/tools/vep/index.html

PlanMine database http://planmine.mpi-cbg.de/planmine/begin.do

S. mediterranea Genome Database http://smedgdkc03.stowers.org/cgi-bin/gb2/gbrowse/SmedUnigenes

E10

LEGENDS FOR SUPPLEMENTARY FIGURES

Figure E1. CFAP300 mutations found in Slavic PCD patients

Pedigrees of the families, in which *CFAP300* mutations were found by WES or follow-up screening. All families are Polish, except for family 157 (Slovak). Patients are filled in black; #363 in family 217 (light grey) was found to have PCD through genetic testing; carriers are indicated by the dot inside the symbol (black dot, if confirmed by dideoxy sequencing). Individuals included in the WES cohort are underlined; in family 157, both parents were WES-sequenced instead of the patient. #1106 in family 520, later found to be a homozygote for the consensus splicing site mutation in another PCD gene (c.397+1G>A/c.397+1G>A in *TTC25*), was only a carrier of *CFAP300* mutation in exon 3 (white asterisk inside the individuals symbol; parental origin of the mutation is unknown). Only representative chromatograms from dideoxy sequencing of the c.198-200TTT>CC mutation are shown.

The c.353A>G resulting in p.D118G substitution (fam. 146) was deemed neutral by Provean and benign by PolyPhen. However, the scores calculated using Human Splicing Finder tool predicted c.353A>G to activate a cryptic exonic donor site (HSF matrix score: 75.99 for the mutant and 49.16 and the wild type; variation 54.58%; MaxEnt score: 7.76 for the mutant and -0.41 and the wild type; variation 1992.68%). Activation of the donor site in exon 4 would result in shortening this exon by 93 bp, resulting in an in-frame deletion of 31 amino acids. The c.675+3delAAGT in exon 6 (fam. 504), according to the Human Splicing Finder tool, may affect the donor splice site in intron 6 (HSF matrix score: 61.96 for the mutant and 84.4 for the wild type; variation -26.59%; MaxEnt score: -5.27 for the mutant and 6.69 for the wild type; variation -178.77%).

Figure E2. TEM analysis of the representative cross-sections of cilia from the respiratory epithelium

Left panel – a non-PCD control with clearly discernible outer and inner dynein arms (black and white arrows, respectively). Right panel – three patients homozygous for the deleterious variant c.[198_200delTTTinsCC] in exon 3 of *CFAP300*; the lack of detectable dynein arms is indicated by arrowheads. Patients # 633 and #1074: 85 and 61 cross-sections analyzed, respectively; in 100% lack of ODA and IDA; patient #360 – 65 cross sections analyzed, in 75% lack of ODA and IDA, 25% – lack of IDA.

Figure E3. The evolutionary conservation of the CFAP300 gene structure and protein sequence

Upper panel: Schematic localization of exons in human *CFAP300* (upper panel) and its two orthologues: *Danio rerio* (middle) and *Schmidtea mediterranea* (bottom). Only exons are drawn to scale; the exact size of exons and introns is shown in bp. Approximate position of the primers used to obtain dsRNA for RNAi in planaria is indicated by black arrows.

Lower panel: Comparison of CFAP300 protein sequence in the three species: human (Hsap), zebrafish (Drer), and planaria (Smed). High consensus level (>90%) is indicated in red. Thick black lines above the alignment indicate position of exons in human and zebrafish; lines below the alignment delineate exons in planaria. The overall proportion of high consensus positions in the whole coding sequence is 27%; the pairwise sequence comparisons are expectedly higher (49% human-zebrafish and 36% human-planaria). The numbers above the alignment show relevant proportions calculated for each of the human exons, indicating the highest conservation (>43%) in exons 2 and 5. The grey bar below the alignment corresponds to the position of the DUF4498 domain.

LEGENDS FOR SUPPLEMENTARY VIDEOS

Video E1: A: Respiratory epithelium cells from healthy individual with normal ciliary function. **B-D:** Respiratory epithelium cells in three *CFAP300* patients (#914, #993, #1074) revealed the total lack of ciliary beating. Microscope: 400 x magnification.

Video E2: A: Normal locomotion of control planaria fed with GFP dsRNA. **B:** Disturbed locomotion (speed and pattern) of *CFAp300*-silenced planaria. Animals 7 days after fragmentation, with the regenerated tails. Stereoscope: 10 x magnification

Video E3: A: Cilia motility in control planaria fed with GFP dsRNA. **B:** Reduced speed and nonsynchronized cilia motility in *CFAP300*-silenced planaria. Microscope: 400 x magnification.

Figure E1

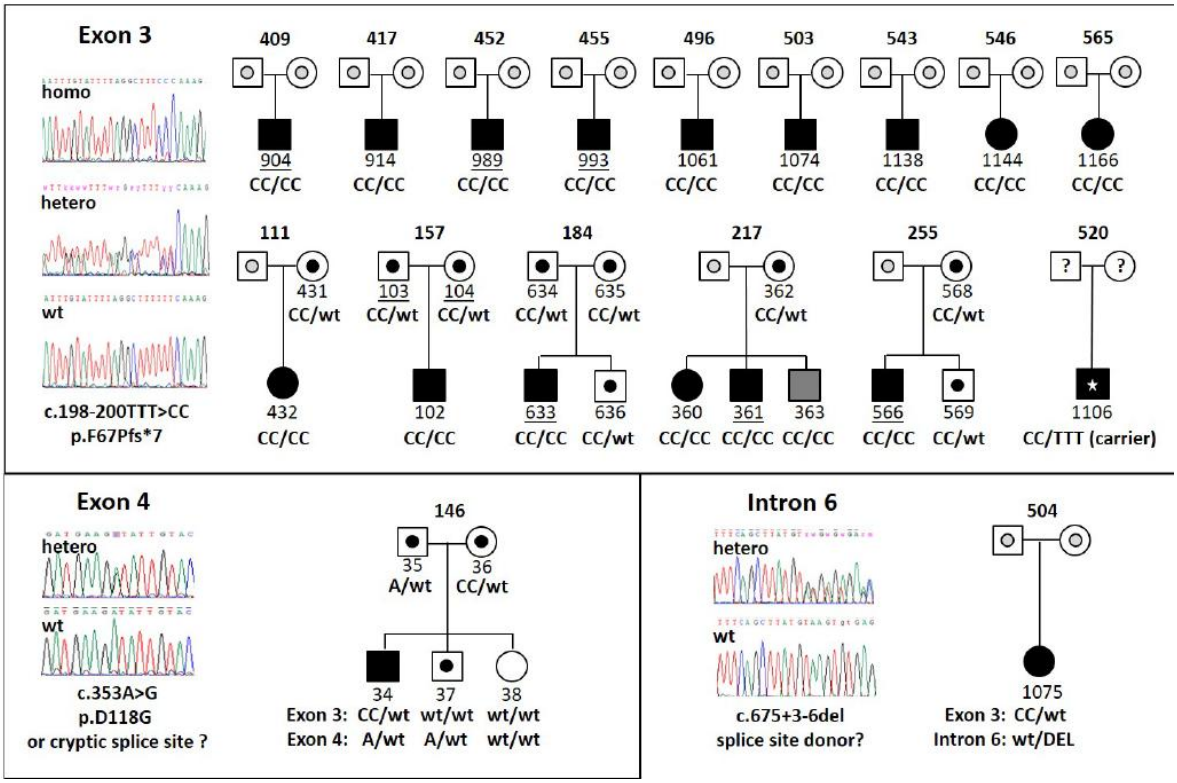

Figure E2

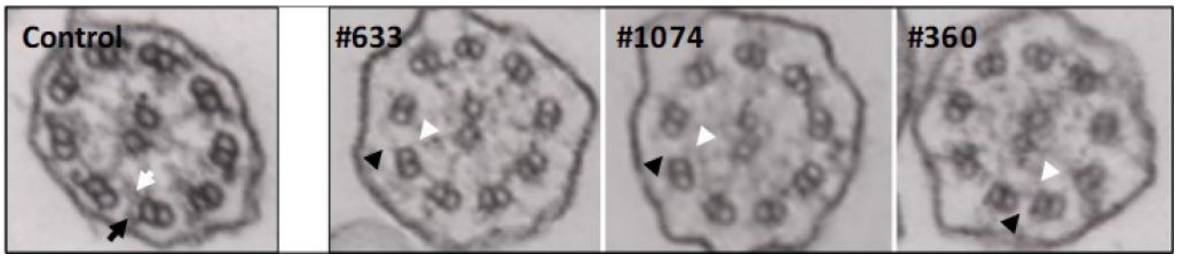

Figure E3

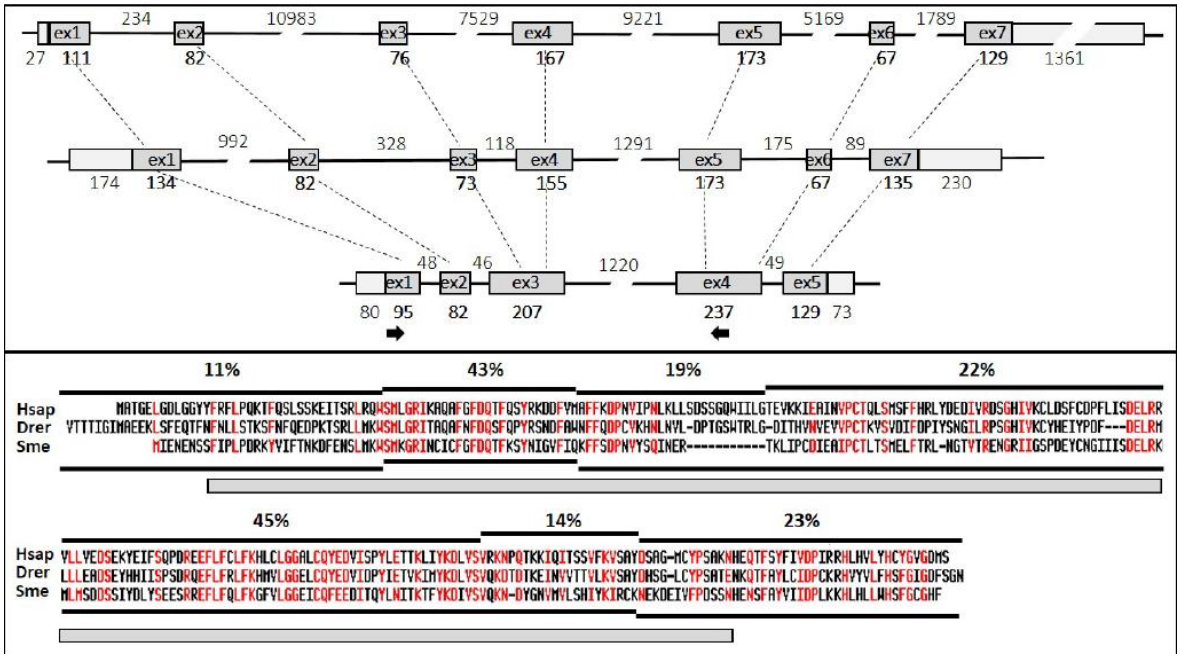
ex1
ex2
ex3
ex4
ex5
ex6
ex7
234
10983
7529
9221
5169
1789
27
111
82
76
167
173
67
129
1361
992
328
118
1291
175
89
174
134
82
73
155
173
67
135
230
48
46
1220
49
80
95
82
207
237
129
73
11%
43%
19%
22%
Hsap
Drer
Sme
45%
14%
23%

Artykuł 3

A novel pathogenic variant of *CFAP221* is a cause of a mild form of primary ciliary dyskinesia

Alicja Rabiasz, Zuzanna Bukowy-Bieryłło, Patrycja Kaźmierczak, Hanna Przystałowska-Macioła, Marcin Mikoś, Irena Wojsyk-Banaszak, Ewa Ziętkiewicz

Biochim Biophys Acta Mol Basis Dis. 2025 Apr 16;1871(6):167855.

W odpowiedzi na stale rosnącą liczbę genów raportowanych jako nowe geny zaangażowane w różne jednostki chorobowe powstała baza danych ClinGen (*Clinical Genome Resourse*) działająca przy Narodowych Instytutach Zdrowia (*National Institutes of Health*, NIH), która służy jako narzędzie do zdefiniowania znaczenia raportowanych patogennych wariantów i genów w różnych chorobach człowieka. Zgodnie z zasadami tej bazy, aby gen otrzymał status genu definitywnie zaangażowanego w patogenezę danej choroby, jego związek z określoną chorobą powinien zostać zgłoszony kilka razy. *CFAP221* (c*ilia and flagella associated protein 221*; alias *PCDP1*) zlokalizowany w chromosomie 2, jest jednym z genów PCD, który zdaniem grupy ekspertów ClinGen wymaga pilnego potwierdzenia poprzez opublikowanie dodatkowych przypadków pacjentów z patogennymi w wariantami w tym genie, co pozwoli na określenie spektrum wariantów powodujących chorobę oraz cech klinicznych związanych z tym genem a chorobą. Celem omawianej pracy było potwierdzenie roli genu *CFAP221* w patogenezie pierwotnej dyskinezy rzęsek.

Analiza genetyczna DNA pacjenta o lżejszym przebiegu PCD z dominującymi objawami laryngologicznymi, brakiem rozstrzeni oskrzeli, prawidłową funkcją płuc w wieku 18 lat, brakiem odwrócenia narządów, wadą serca w wywiadzie oraz obniżonym poziomem tlenku azotu, wykazała obecność patogennego wariantu (NM_012472.6:c.436G>C (p.Asp146His)) w znanym genie PCD, *LRRC6* (*leucine rich repeat containing 6;* alias *DNAAF11*). Ze względu na niezidentyfikowanie patogennego wariantu na drugim allelu, przeprowadzono analizę WES. Analiza ta również nie wykazała zmian na drugim allelu genu *LRRC6* u pacjenta, natomiast pozwoliła na identyfikację nowego patogennego wariantu, NM_001271049.2_c.1641dup (p.Asn548GlnfsTer6) w eksonie 16 genu *CFAP221* na obu allelach. Sekwencjonowanie Sangera u pacjenta i rodziców potwierdziło recesywny sposób dziedziczenia tego wariantu. Podczas gdy patogenny wariant *LRRC6*:c.436G>C był obecny tylko u pacjenta oraz jego matki,

nosicielstwo *CFAP221*:c.1641dup stwierdzono u obojga rodziców oraz u zdrowego brata pacjenta. Analiza in *silico* wskazała na potencjalnie silny patogenny wpływ zidentyfikowanego wariantu, którego pojawienie się może prowadzić do wprowadzenia przedwczesnego kodonu STOP. W celu określenia wpływu patogennego wariantu na poziom ekspresji *CFAP221* przeprowadzono analizę poziomu transkryptu oraz białka w odniesieniu do genu referencyjnego, *GAPDH*. Analiza RT-PCR dla eksonów zlokalizowanych powyżej (5'), pomiędzy oraz poniżej (3') miejsca występowania wariantu (odpowiednio, eksony 3-4, 8-9, 14-15, eksony 15-17 oraz eksony 18-19, 23-24), w odniesieniu do genu referencyjnego, wykazała całkowity brak produktu PCR w porównaniu do kontroli (zdrowego dawcy); obserwacja ta została potwierdzona na poziomie białkowym. Uzyskane wyniki sugerują degradację nieprawidłowego mRNA *CFAP221* na skutek szlaku NMD.

W celu scharakteryzowania wpływu patogennego wariantu *CFAP221*:c.1641dup (powodującego brak białka CFAP221) na funkcjonowanie rzęsek ruchowych przeprowadzono analizę struktury i funkcji rzęsek komórek nabłonka oddechowego u pacjenta w porównaniu do kontroli. Analiza IF z użyciem przeciwciał skierowanych przeciwko białkom DNAI1, RSPH4A, GAS8, acetylowanej alfa-tubulinie wskazała na brak wpływu patogennego wariantu *CFAP221* na główne elementy ultrastruktury aksonemy (ODA, RS, N-DRC); sygnał IF z użyciem przeciwciał dla białek pary centralnej (STK36 i SPEF2) był natomiast nieznacznie zmieniony. U kontroli oba przeciwciała specyficznie barwiły rzęski; u pacjenta sygnał anti-SPEF2, chociaż obecny w rzęskach, dominował w cytoplazmie, natomiast sygnał anti-STK36 w części komórek (31%) występował w rzęskach, a w pozostałych (69%) zarówno w rzęskach jak i w cytoplazmie. Kolejna analiza, badanie ruchu rzęsek przy użyciu HSVM, wykazała, że rzęski pacjenta poruszały się niesynchronicznie, w sposób okrężny. Aby wykluczyć wpływ czynników środowiskowych na ruch rzęsek, wyprowadzono hodowlę komórek pierwotnych nabłonka oddechowego pacjenta oraz kontroli, które następnie były różnicowane w hodowli na granicy faz ciecz-powietrze (*air-liquid interface,* ALI) w kierunku ciliogenezy. Ruch rzęsek pacjenta po ciliogenezie pozostał niesynchroniczny i okrężny; średnia częstotliwość bicia rzęsek (*ciliary beat frequency*, CBF) komórek pacjenta wynosiła 6.91 ± 0.91, a u kontroli 8.14 ± 1.36 Hz ($p<0.001$). W celu określenia wpływu okrężnego ruchu rzęsek na transport śluzowo-rzęskowy przeprowadzono eksperyment z użyciem kulek fluorescencyjnych (sferyczne/kuliste cząstki o średnicy 0.5 μm). Prędkość transportu kuleczek przez w pełni

zróżnicowane komórki nabłonka oddechowego była ponad 5 razy niższa u pacjenta w porównaniu do zdrowej kontroli (13.63 ±5.95 i 69.95 ±5.74 μm/s, odpowiednio; $p<0.001$). Uzyskanie materiału (próbka nasienia) od pacjenta umożliwiło analizę wpływu badanego wariantu na funkcję witek plemników. Znaczna większość plemników miała normalną witkę, a analiza ruchu oraz morfologii plemników nie odbiegała od norm przyjętych przez Światową Organizację Zdrowia (*World Health Organization,* WHO).

Ostatnim etapem badań było potwierdzenie roli *CFAP221* w funkcjonowaniu rzęsek ruchowych przy użyciu organizmu modelowego *S. mediterranea*. W celu wyciszenia badanego genu robakom podawano dsRNA skierowane przeciwko homologowi ludzkiego *CFAP221* – *Smed-cfap221* (jako kontrolę użyto robaki traktowane dsRNA przeciwko *eGFP*)*;* efektywność wyciszenia potwierdzono przy użyciu qRT-PCR. Wpływ wyciszenia badanego genu na fenotyp *S. mediterranea* obserwowano na całych, nieciętych robakach. RNAi *Smed-cfap221* nie wpłynęło na zmianę wzoru ruchu, ale spowodowało istotne statystycznie spowolnienie lokomocji planarii o 34% w porównaniu do kontroli (0.954 ± 0.303 i 1.451 ± 0.355 mm/s, odpowiednio; $p<0.001$). Analiza ruchu rzęsek zlokalizowanych w okolicy głowy robaków wykazała wpływ wyciszenia na ruch rzęsek: rzęski poruszały się wolniej i w sposób niesynchroniczny. Średnia częstotliwość bicia rzęsek u robaków z wyciszonym *Smed-cfap221* była o około 15% wolniejsza w porównaniu do robaków kontrolnych (17.44 ± 0.95 and 20.35 ± 0.58 Hz, odpowiednio; $p<0.001$).

Podsumowując, omówiona praca pozwoliła na potwierdzenie roli wariantu *CFAP221*:c.1641dup w patogenezie pierwotnej dyskinezy rzęsek o lżejszym przebiegu klinicznym. Analiza rzęsek nabłonka oddechowego pacjenta wykazała wpływ braku białka CFAP221 na zaburzenie elementów pary centralnej, przy jednoczesnym braku wpływu na inne struktury aksonemy rzęsek. Ruch rzęsek był niesynchroniczny i okrężny, co w konsekwencji prowadziło do istotnego spowolnienia transportu śluzowo-rzęskowego. Badanie nasienia pacjenta nie wykazało wpływu braku CFAP221 na standardowe parametry nasienia, w tym na morfologię plemników czy ich ruchliwość. Ponadto stwierdzono ewolucyjnie zakonserwowaną rolę badanego genu w funkcjonowaniu rzęsek ruchowych w organizmie modelowym, *S. mediterranea*. Co istotne, lżejszy przebieg choroby u pacjenta był spójny z fenotypem obserwowanym u planarii po wyciszeniu homologa genu *CFAP221* (*Smed-cfap221).*

Mój wkład w powstanie publikacji:

- udział w ustaleniu koncepcji; przygotowanie planu badań
- zabezpieczenie środków finansowych
- analiza wpływu obecności patogennego wariantu na poziom ekspresji mRNA i białka u pacjenta (w tym izolacja białka i RNA, synteza cDNA, qRT-PCR, Western-Blot)
- udział w analizie nasienia pacjenta
- zaprojektowanie, wykonanie i interpretacja doświadczeń z wykorzystaniem S. mediterranea: analiza *in silico*, wyciszenie homologa genu *CFAP221* (w tym zaprojektowanie i synteza dsRNA przy użyciu transkrypcji *in vitro*), potwierdzenie efektywności wyciszenia na poziomie mRNA (izolacja RNA, synteza cDNA, qRT-PCR), analiza wpływu wyciszenia na funkcjonowanie rzęsek ruchowych planarii (analiza lokomocji robaków i ruchu rzęsek)
- pisanie oryginalnej wersji manuskryptu, przygotowanie tabel i większości rycin
- przygotowanie ostatecznej wersji manuskryptu
- obowiązki autora korespondencyjnego.

Publikacja oraz informacje dodatkowe (załączniki) są dostępne pod następującym adresem internetowym:
https://doi.org/10.1016/j.bbadis.2025.167855

BBA - Molecular Basis of Disease 1871 (2025) 167855

Contents lists available at ScienceDirect

BBA - Molecular Basis of Disease

journal homepage: www.elsevier.com/locate/bbadis

A novel pathogenic variant of *CFAP221* is a cause of a mild form of primary ciliary dyskinesia

Alicja Rabiasz [a,*], Zuzanna Bukowy-Bieryłło [a], Patrycja Kaźmierczak [a,1], Hanna Przystałowska-Macioła [a,1], Marcin Mikoś [b,c], Irena Wojsyk-Banaszak [b], Ewa Ziętkiewicz [a,*]

[a] Institute of Human Genetics, Polish Academy of Sciences, Poznań, Poland
[b] Department of Pneumonology, Paediatric Allergy and Clinical Immunology, Poznan University of Medical Sciences, Poznań, Poland
[c] Vilda Clinic, Poznań, Poland

ARTICLE INFO

Keywords:
Ciliopathy
Motile cilia
PCD
Respiratory epithelial cells
Schmidtea mediterranea

ABSTRACT

Primary ciliary dyskinesia (PCD) is a heritable disease caused by the dysfunction of motile cilia, with a highly heterogeneous genetic background. *CFAP221* (Cilia and Flagella Associated Protein 221) is one of the genes, whose role in the PCD pathogenesis requires further evidence.

Using whole-exome sequencing we found a novel, homozygous protein-truncating variant in *CFAP221* in a Polish PCD patient. To better understand the effect of the identified pathogenic variant on motile cilia structure and function, the proband's nasal epithelium was examined using immunofluorescence, high-speed video-microscopy, and mucociliary transport assay. Subtle abnormalities in the protein composition of the ciliary central apparatus were consistent with the asynchronous, circular motion of cilia and reduced ciliary beat frequency in the proband; importantly, the motility of proband's sperm cells was within the normal range. To independently confirm the role of *CFAP221*, the impact of RNA interference (RNAi)-mediated knockdown of *CFAP221* homolog on motile cilia function in a ciliated flatworm, *Schmidtea mediterranea*, was analyzed. Knockdown of *CFAP221* homolog impaired motile cilia function and led to a visible change in the speed of worms' locomotion.

Taken together, our study provided an independent confirmation of the involvement of *CFAP221* in the PCD pathogenesis. The subtle effect of *Smed-cfap221* knockdown in worms was consistent with the mild course of PCD in the proband.

1. Introduction

Primary ciliary dyskinesia (PCD, OMIM244400) is a rare genetic disease caused by hereditary dysfunction of motile cilia, evolutionarily conserved organelles present on the surface of eukaryotic cells. PCD is typically inherited as autosomal recessive or, less frequently, X-linked recessive disorder. The most cited prevalence of PCD is 1:10,000–1:20,000 [1], but values vary depending on the population and diagnostic [2–4].

Clinical manifestation of PCD reflects dysfunction of motile cilia in different tissues and includes lower and upper respiratory tract distress, hearing impairment, infertility in men or lower fertility in women, and randomization of the body plan symmetry in 50 % of patients [5]. Diagnosis of PCD is often delayed, due to largely non-specific symptoms and insufficient access to specialized diagnostic procedures, such as measurement of nasal nitric oxide level and analysis of ciliary beating and/or ultrastructure defects [5,6]. Identification of underlying genetic pathogenic variants is therefore a crucial element of modern PCD diagnostics [5–9].

Genetically heterogeneous, PCD is caused by pathogenic variants in genes encoding ciliary proteins or cytoplasmic proteins involved in cilia biogenesis and assembly [7,9,10]. Among hundreds of cilia-related genes [11], over 50 have been found to harbor pathogenic variants; their involvement in PCD pathogenesis is either proven or under investigation [7,9]. Despite the improved efficiency of the human genome analysis, the genetic basis of PCD remains unexplained in 25–30 % of tested families [7–9].

A number of candidate genes have been reported in the last few

* Corresponding authors.
E-mail addresses: alicja.rabiasz@igcz.poznan.pl (A. Rabiasz), ewa.zietkiewicz@igcz.poznan.pl (E. Ziętkiewicz).
[1] Equal Contribution.

https://doi.org/10.1016/j.bbadis.2025.167855
Received 29 October 2024; Received in revised form 31 March 2025; Accepted 14 April 2025
Available online 16 April 2025

years, mostly owing to the development of high-throughput sequencing technologies. According to the rules set by the National Institutes of Health (NIH) ClinGen collaborative effort aiming to define the clinical relevance of genes and variants in various diseases [12], repeated reports of the gene-disease association are required for the gene to achieve the status of "definitively involved" [https://clinicalgenome.org/curation-activities/gene-disease-validity]. *CFAP221* (Cilia and Flagella Associated Protein 221; alias PCDP1), first reported as a candidate PCD gene in 2020 [13], is among the genes, which lack independent studies demonstrating its association with PCD in human patients.

Here we describe a Polish PCD family, in which the whole exome sequencing of the affected subject revealed a novel homozygous pathogenic variant in *CFAP221*. The family segregation and effect of the variant on motile cilia in the patient's nasal airway epithelium were analyzed; furthermore, the impact of the *CFAP221* deficiency on motile cilia function was examined using a model organism, *Schmidtea mediteranea*.

2. Materials and methods

2.1. Human subjects

Peripheral blood samples were collected from the proband and his family; in addition, samples of nasal epithelium (NE) brushing and sperm cells were collected from the proband. NE brushings from control healthy individuals were collected from consenting volunteers. None of the donors had acute airway inflammation for at least 6 weeks before material collection.

2.2. Nasal NO measurements

Nasal NO (nNO) level in the proband (at the age of 18 years old, yo) was measured using tidal breathing protocol and calculated as the mean of five measurements (flow rate 250 mL/min; FeNO+PFS Medisoft).

2.3. Genetic analysis

Identification of pathogenic variants in DNA from peripheral blood was performed as a part of the long-term PCD genes screening in a large cohort of over 630 PCD individuals. The screening was performed using single-strand conformation polymorphism (SSCP) analysis, multiplex ligation-dependent probe amplification (MLPA) analysis and targeted exon sequencing, or by whole exome sequencing (WES), as previously described [14]. The variants identified in the proband and his family were confirmed by Sanger sequencing (using primers listed in Supplementary Table 1). The variants were described using VariantValidator tool [15], and classified as pathogenic according to the recommendation of the American College of Medical Genetics and Genomics (ACMG) and the Association for Molecular Pathology (AMP) [16]. The frequencies in the general population were taken from the Genome Aggregation Database (gnomAD) v4.1.0 [gnomad.broadinstitute.org] [17].

2.4. Ciliary beat frequency (CBF) and pattern analysis

Ciliated NE cells from the proband and a non-PCD donor were either analyzed directly after brushing or cultured at the air-liquid interphase (ALI) as previously described [14,18]. Briefly, NE cells were expanded in adherent submerged culture using Pneumacult Ex-Plus medium (Stemcell) supplied with pen-strep and nystatin. At passage 2, cells were seeded into 12-well Transwell filters at the density of 2.2×10^5 cells/filter, with Pneumacult Ex-Plus medium added both to the apical and basolateral filter compartments. Upon reaching filter confluence (typically within 48 h), medium in the basolateral filter compartment was exchanged to Pneumacult ALI Medium, the apical filter compartment was exposed to atmospheric air, and the cells were differentiated for at least 28 days.

To evaluate the ciliary beat frequency and pattern, high resolution videos of the ciliated cells were analyzed as previously described [14,19]. Briefly, the NE cells suspension (from NE brushings or from ALI-cultured cells) was transferred to a microscopic slide and observed using Zeiss Zen Axio Observer A1, with 40× objective. Ciliary beating in epithelial cell aggregates was recorded using a Basler scA640-120 fm high-speed camera (120fps) and SAVA software (Ammons Engineering); the beat pattern was analyzed in the slow-motion. For CBF analysis, the mean CBF for each recorded field of view (movie) was automatically calculated in SAVA; CBF for at least 25 movies was averaged.

2.5. Mucociliary transport assay

Mucociliary transport assay was performed as previously described [20]. A suspension of beads (Thermo Fisher Scientific, diluted 1:2000 in RPMI medium with 20 mM HEPES; bead diameter 0.5 μm) was added to the apical side of the insert with fully differentiated ALI cultures. Bead transport was observed using Zeiss Axio Observer Z1 microscope, 10× objective, GFP filter and a monochromatic AxioCam mRm camera. Transport of beads was recorded in 1 s intervals, for at least 30s, in at least 6 randomly chosen filter localizations. Recorded movies were processed using ImageJ software with rolling disc background correction (100pix, no smoothening) and the Phansalkar automatic local threshold plugin. Beads were manually tracked in ImageJ using MTrackJ plugin; per each movie recorded, minimum 13 beads were tracked for at least 3 frames.

2.6. Immunofluorescence (IF) analysis

Ciliary ultrastructure elements in NE cells were analyzed by high resolution IF as previously described [14]. Several cilia-specific antibodies were used, targeting: axonemes (anti-acetylated α-tubulin); outer dynein arms (anti-DNAI2); nexin-dynein regulatory complex (anti-GAS8); radial spokes (anti-RSPH9); central apparatus (anti-SPEF2; anti-STK36); highly cross-adsorbed secondary antibodies were used (goat anti-rabbit IgG-594 and goat anti-mouse IgG-488). For details see Supplementary Table 2.

2.7. Reverse transcription polymerase chain reaction (RT-PCR)

Total RNA was isolated from NE brushings using TRI Reagent (Invitrogen), and purified from DNA contaminants with TURBO DNA-free Kit (Ambion) according to the manufacturers' protocols. 500 ng of RNA was reverse transcribed according to the manufacturer's protocols, using the RevertAid H Minus First Strand cDNA Synthesis Kit (ThermoScientific) and oligo(dT) primer. The resulting cDNA was used as a template in semi-quantitative RT-PCR, with primers designed to amplify trans-exonic sequences (listed in Supplementary Table 3).

2.8. Protein analysis

ALI-cultured NE cells were lysed using RIPA buffer with protease inhibitor cocktail and EDTA (ThermoScientific). Protein concentration was determined using Pierce BCA Protein Assay Kit (ThermoScientific). Proteins were denatured, separated on 4–20 % Mini-PROTEAN TGX Stain-free Gel (Bio Rad), and transferred onto 0.45 μm PVDF Low Fluorescence membrane (Bio Rad). Membranes were blocked with 5 % non-fat milk and incubated with anti-CFAP221 or anti-GAPDH antibody. After washing, membranes were incubated with anti-rabbit secondary antibody. For the antibodies details, see Supplementary Table 2. Immunoreactive protein bands were detected with Clarity Western ECL Substrate on ChemiDoc Imaging System (Bio Rad). The abundance of CFAP221 was assessed in reference to GAPDH or to the total protein on a blot in Stain-Free technology using Image Lab 6.0.1 software (Bio Rad). Western Blot was conducted in three technical replicates. Whole uncropped membranes are shown in Supplementary Fig. 1.

2.9. Semen analysis

Semen sample was collected by masturbation after 4 days of sexual abstinence. After liquefaction at room temperature, semen was evaluated within one hour of collection using a bright-light microscopy (DM 2000, Leica). Standard semen parameters (e.g. sperm count, motility, viability, morphology) was assessed according to the guidelines of the World Health Organization (WHO) [21].

2.10. RNAi-mediated knockdown in Schmidtea mediterranea

Gene knockdown in an asexual strain of *S. mediterranea* planarian was performed using double-stranded RNA (dsRNA)-feeding method as previously described [22]. Briefly, dsRNA was designed based on the transcriptomic and genomic data deposited in Planmine database [23], using the e-RNAi webservice [24], which provides information on the possible off-target effect at the dsRNA design stage. DsRNA of *Smed-cfap221* (dd_Smed_v6_12752_0_1) was synthetized using MEGAscript™ T7 Transcription Kit (Invitrogen). Transcript for dsRNA synthesis was amplified from *S. mediterranea* cDNA, using primers tagged with T7 RNA polymerase promotor [see Supplementary Table 3]. DsRNA used in the control group was prepared from the pEGFP-C1 plasmid containing eGFP (enhanced green fluorescence protein). Before experiments, planarians 3–5 mm in length were starved for at least 7 days. DsRNA was mixed with a homogenized chicken liver and administered to the worms by repetitive feeding (two times per week for 2 weeks); 10 μg dsRNA mixed with 50 μL of liver paste per 10 worms were used.

The phenotypic effects of the knockdown were examined 2 days after the last administration of dsRNA. The speed of the worms locomotion was recorded using a stereoscope (Opta-Tech, SK series) with camera and measured using ImageJ [25] (ten worms for each group). Worms' locomotion speed was calculated by dividing the actual distance traveled by the worm (distance traveled minus the length of a worm) by the duration of the movie. Ciliary beating of epithelial cells in the worms' head region was recorded using a Basler scA640-120 fm high-speed camera (120fps) and SAVA software; beat pattern was analyzed in slow-motion (three worms for each group); mean CBF for each analyzed movie was automatically calculated using the SAVA software (nine movies for each group).

2.11. Real-time quantitative reverse transcription PCR, qRT-PCR

The efficiency of the knockdown in *S. mediterranea* was confirmed using qRT-PCR. One day after the last feeding, RNA isolation and cDNA synthesis were performed as described above. The resulting cDNA was used as a template in qRT-PCR, with HOT FIREPol® EvaGreen® qPCR Mix Plus (Solis BioDyne) and primers designed to target specific mRNAs [see Supplementary Table 3]. The level of house-keeping transcript (*Smed-gapdh*) was used as an endogenous control. The relative quantification of the studied gene expression level was performed using a comparative CT (ΔΔ CT) method. All qRT-PCR reactions were performed in three technical replicates for each biological replicates (five worms for each group).

2.12. Statistical analysis

In the analyses, where two independent means were compared (the relative gene expression level, the mean bead velocity, CBF in ALI cultures and planarians, or the worms' locomotion speed), data were first analyzed for the normality with Shapiro–Wilk test, and statistical significance of the difference was calculated using two-tailed unpaired *t*-test. The statistical significance of the results was evaluated and visualized using the GraphPad Prism version 9 (GraphPad Software).

3. Results

3.1. Clinical description of the proband

The proband (DNA id:1174/1195), a Polish male, had a clinical diagnosis of PCD (since the age of 7 yo) confirmed by standard diagnostic criteria. Clinical evaluation using PICADAR prediction tool [26] returned the score of 10 points (neonatal respiratory distress, admission to neonatal unit, congenital heart defect, chronic cough, otitis media, and sinusitis, glue ear, conductive hearing loss; no *situs* abnormality), indicating PCD probability of 93 %. Follow up studies at 18 years of age ruled out bronchiectasis on chest CT-scan and showed preserved, normal lung function, which suggests clinically mild manifestation of PCD, with predominant ENT (Ear-Nose-Throat) symptoms and non-severe congenital heart defect: interatrial septum (IAS) aneurysm and two micro trial septal defects (ASD II) (see Supplementary Data for more details). Nasal NO (nNO) concentration (tidal breathing maneuver, TB) at the age of 18 years was 174 ppb (43.5 nL/min), with the value in a control non-PCD male (40 yo) of 957 ppb (239 nL/min).

3.2. Characterisation of a novel pathogenic CFAP221 variant

In the first round of genetic analyses, a single, presumably pathogenic variant NM_012472.6:c.436G > C (p.Asp146His), was found in exon 5 of the known PCD gene, *LRRC6* (Leucine Rich Repeat Containing 6; alias *DNAAF11*). Since the follow-up analysis of the *LRRC6* coding sequence and canonical splice sites did not reveal the complementary variant on the second allele, the whole exome sequencing was performed. WES revealed a homozygous frameshift variant in exon 16 of *CFAP221* (*PCDP1*) [Supplementary Fig. 2]: NM_001271049.2_c.1641dup, expected to result in the premature stop codon (p.Asn548GlnfsTer6). Both variants are pathogenic using ACMG/AMP criteria (with the evidence for *LRRC6*:c.436G > C strong and for *CFAP221*:c.1641dup very strong); for more details see Supplementary Table 4.

Segregation analysis in the proband's family [Fig. 1] revealed that the *LRRC6*:c.436G > C variant was inherited from the carrier father, and was absent in the unaffected brother. On the other hand, both parents and the unaffected brother were carriers of the *CFAP221*:c.1641dup variant. According to the information from the proband's mother, the parents were not related (families originating from different regions of Poland). No carriers of the *CFAP221*:c.1641dup variant were found among over 630 Polish individuals examined in our laboratory. The variant has been reported in the gnomAD database (v4.1.0) at the frequency of 0.0001441 in the European non-Finish population; so far, no homozygotes have been reported.

RT-PCR analysis of several fragments distributed along the whole *CFAP221* mRNA (primers spanning exons 3–4, 8–9, 14–15, 15–17, 18–19, 23–24) revealed the lack of products in the proband's cDNA, in contrast to the healthy control cDNA (Fig. 2A). The lack of products indicated that the whole *CFAP221* mRNA was missing, presumably due to the nonsense-mediated decay (NMD) of the aberrant transcript. Western blot (WB) analysis of the protein extract from fully differentiated NE cells from ALI culture showed complete absence of CFAP221 protein in the proband, in contrast to the healthy control [Fig. 2B].

3.3. Effect of pathogenic CFAP221 variant on motile cilia structure and function

To examine the impact of the lack of CFAP221 on the ciliary structure, IF staining of the proband's AE cells was performed with antibodies targeting various elements of the motile cilium (commercial anti-CFAP221 antibody was not specific in IF). The IF staining pattern for the antibodies targeting dynein arms, radial spokes and N-DRC was similar to that in the control cells (Supplementary Fig. 3). In contrast, the disturbed staining pattern was observed for anti-STK36 and anti-

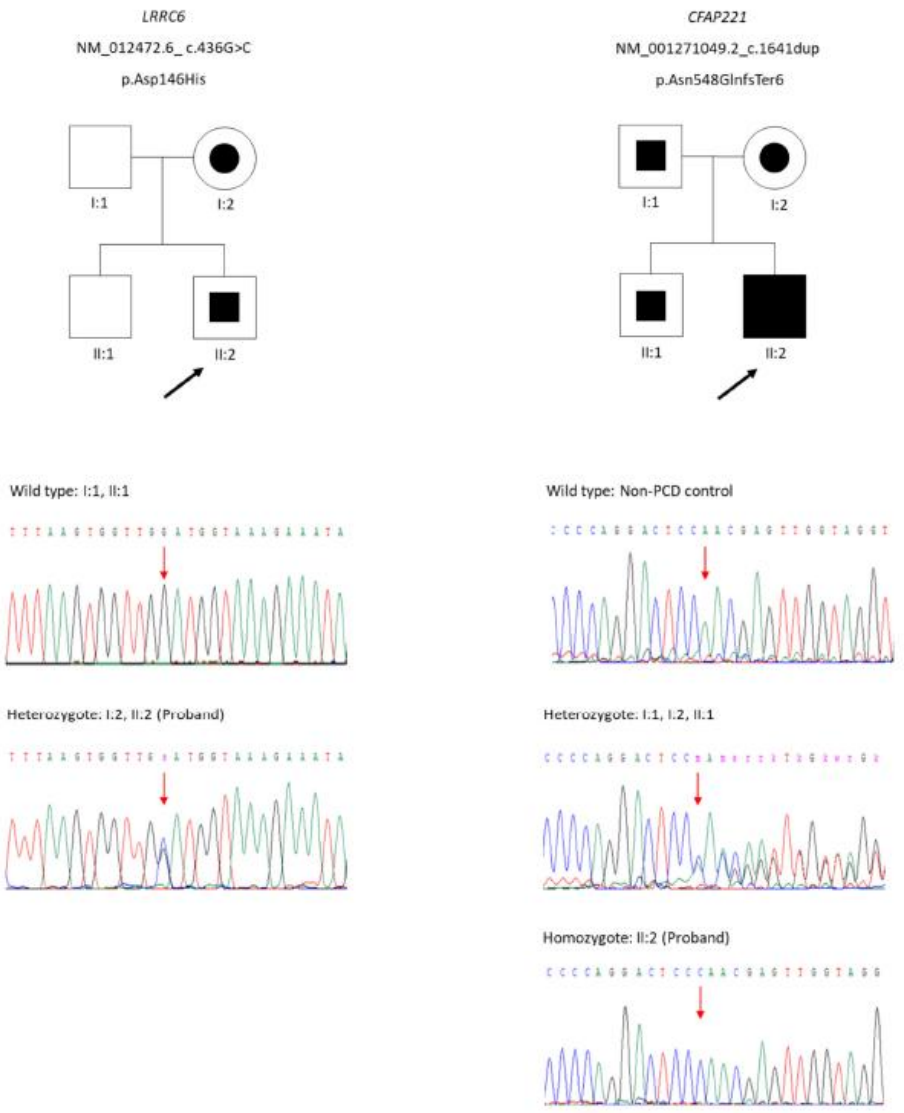

Fig. 1. Genetic analysis in the analyzed family.
Pedigrees and representative chromatograms for each genotype of *LRRC6* (left panel) and *CFAP221* (right panel). Proband is indicated by black arrows; described variants are marked with red arrows.

SPEF2 antibodies, targeting the central apparatus of the cilium (Fig. 3). In a non-PCD control, both antibodies stained only cilia. In the proband, anti-SPEF2 signal was predominant in the cytoplasm but also present in cilia of all the examined cells (30 ciliated cells per each staining). Anti-STK36 signal was observed in both cilia and cytoplasm in some (31 %) and only in cilia in other cells (69 %).

The impact of homozygous lack of functional CFAP221 on cilia motility was examined in primary NE cells from the proband using high-speed videomicroscopy (HSVM). An asynchronous, circular movement of cilia was observed. In order to eliminate the possibility of environmental distress, the NE cells were subjected to ALI culture. The ciliary motion after ciliogenesis was still asynchronous and circular, with the mean CBF for the proband culture being approx. 85 % of that for healthy individual 6.91 ± 0.91 and 8.14 ± 1.36 Hz, respectively; $p < 0.001$) [Supplementary Movies 1 and 2].

In order to analyze the influence of the circular ciliary movement on

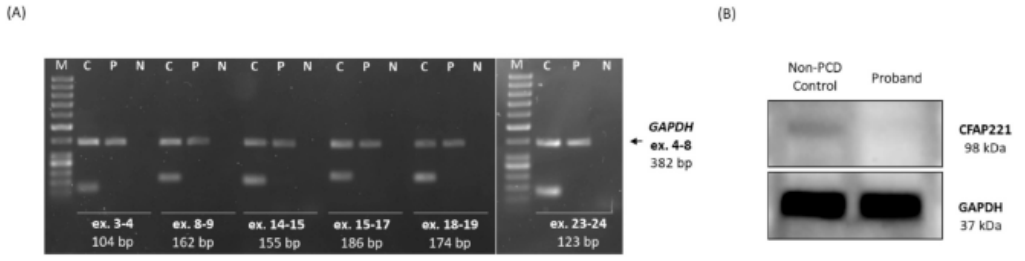

Fig. 2. The impact of the *CFAP221*: c.1641dup variant.
(A) At the mRNA level. Lower bands represent studied exons in *CFAP221*, higher bands correspond to housekeeping gene, *GAPDH*. M - DNA Molecular Weight Marker (50 bp Ladder, ThermoFisher Scientific), C - non-PCD control, P - proband, N - negative control (water). (B) At the protein level.

the mucociliary transport, we analyzed the ALI cultures from the proband using fluorescent beads. Analysis of the bead velocity (Fig. 4) revealed that mucociliary transport in the differentiated epithelial cells of the proband was almost 5 times slower than in non-PCD control (13.63 ± 5.95 μm/s and 69.95 ± 5.74 μm/s, respectively; $p < 0.001$).

The sperm sample collected from the *CFAP221* patient was examined to shed light on the importance of *CFAP221* for the sperm flagella morphology and function. Motile flagella were present in the majority of spermatozoa, and the percentage of sperm cells with overall normal morphology (of tail and head) was in the normal range [Supplementary Table 5, Supplementary Fig. 4, Supplementary Movie 3].

3.4. Effect of silencing of CFAP221 homolog in S. mediterranea

In order to confirm the impact of *CFAP221* deficiency on the ciliary function in a model organism, *CFAP221* homolog was silenced by RNAi in *S. mediterranea*. Administration of *Smed-cfap221* dsRNA led to the decrease in Smed-*cfap221* mRNA level (12 % compared to control worms fed with *eGFP* dsRNA) [Fig. 5A] and caused a statistically significant decrease of the worms' locomotion speed (~34 % slower compared to control; 0.954 ± 0.303 mm/s 1.451 ± 0.355 mm\s in *Smed-cfap221*-silenced and control worms, respectively) [Fig. 5B, Supplementary Movies 4 and 5]. Analysis of cilia motility in the epithelial cells in the worms' head region (videos at 1/5 speed) indicated asynchronous and slower ciliary beating in *Smed-cfap221*-silenced worms compared to control (the mean CBF was 17.44 ± 0.95 and 20.35 ± 0.58 Hz for *Smed-cfap221*-silenced and control worms, respectively; $p < 0.001$) [Supplementary Movies 6 and 7].

4. Discussion

Our study provides an independent confirmation of *CFAP221* being the gene directly involved in PCD pathogenesis. Unlike in the French Canadian PCD family reported earlier [13], where affected siblings were compound heterozygotes of two pathogenic variants (in exon 22 and intron 22), the Polish proband was a homozygote for another pathogenic variant (c.16412_13insC in exon 16). With the gnomAD frequency of *CFAP221*:c.1641dup, the probability of two, allegedly non-related, individuals (proband's parents) carrying this variant is very low. The possibility of a recurrent pathogenic variant versus common origin will require further analysis of the variant's haplotype background.

The clinical presentation of the Polish proband was largely concordant with the spectrum observed in the previously reported patients. The only noteworthy difference was level of the nNO, which in the Polish proband was just below the threshold considered as indicative of PCD for patients >2 years old (44 nL/min for TB maneuver) [27]. This contradicted the earlier observations [13], where the levels of nNO in the patients were far above the cut-off of 77 nL/min for the velum closure maneuver [28]. This discrepancy may reflect the differential impact of the various *CFAP221* variants. The homozygous frameshift variant in our proband caused NMD and the complete absence of *CFAP221* mRNA and protein. In the French Canadian patients, a frameshift deletion in exon 22, resulting in NMD, was accompanied by the in-frame deletion of exon 22; the possibility that the shorter isoform expressed the shortened protein has not been experimentally excluded [13]. Another possible, albeit unproven explanation for the clinical differences, could be that the missense variant *LRRC6*:c.436G > C, of which the Polish proband was a carrier, exerted additional effect on the phenotype. On the other hand, the frequency of *LRRC6*:c.436G > C in European population (0.0001863; gnomAD) does not exclude a fortuitous presence of this allele not related to the PCD status of its carrier.

A 15 % reduction in the CBF in our proband compared to the non-PCD control was statistically significant, in contrast to the previously reported slight reduction in the beat frequency, which has not been statistically significant ($p = 0.16$) [13]. On the other hand, rotational pattern of cilia movement in the NE cells from our proband confirmed the earlier observation [13], where highly significant maximum deviation from a linear beat was reported ($p < 0.0015$) [13]. The aberrant CBF in our study was confirmed by the significantly lower speed of the bead transport ($p < 0.001$).

Three affected siblings reported earlier have had normal ciliary structure in TEM analysis. While TEM results were not available for our proband, IF analyses confirmed the absence of defects in the major ciliary structure components (dynein arms, radial spokes and N-DRC). On the other hand, IF with antibodies against the elements of central pair or contacting central pair revealed subtle abnormalities. The localization of CFAP221 in the central apparatus of cilia is consistent with both the circular pattern of the ciliary beat, and the lack of *situs* abnormalities in *CFAP221* patients (reported before and observed in our proband). Based on the mouse and *Chlamydomonas* models, the orthologue of *CFAP221* (*FAP221*) is a component of the central pair (CP) projection C1d, while SPEF2 together with CFAP54 form the C1b projection [29,30]; see Fig. 6. Furthermore, the absence of the C1d complex in *Chlamydomonas* flagella results in a significant impairment of mobility, including a reduced beat frequency and altered waveform. Based on this information and observations in our study, we hypothesize that the complete absence of CFAP221 in human motile cilia may affect assembly/function of both the C1d and C1b projections. This may in turn disturb regular recruitment of STK36, which normally localizes between radial spokes and central apparatus [31]; however, STK36 interaction with other CP projections should not be affected. In any case, these defects are subtle and may not be visible in TEM, consistent with the earlier study [13].

Our experiments with RNAi knockdown of the *CFAP221* homolog in *S. mediterranea* confirmed the evolutionary conservation of the involvement of this gene in motile cilia function. While the statistically significant slow-down was observed in *Smed-cfap221* silenced worms, the effect was not as spectacular as for example in *Smed-cfap300* [14],

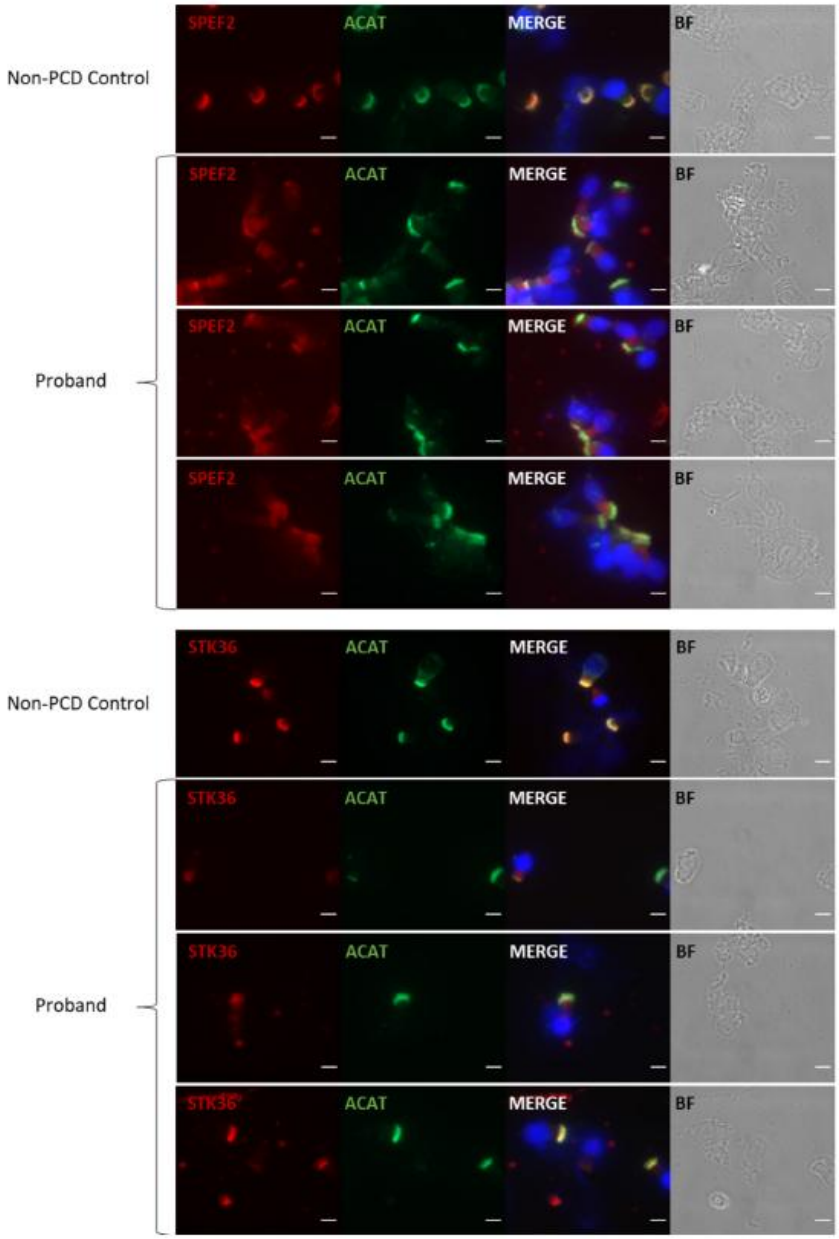

Fig. 8. IF staining of NE cells using antibodies targeting the central apparatus of motile cilia. (Upper panels – SPEF2, lower panels – STK36). Scale bar 10 μm; BF- Bright Field; ACAT- Acetylated-α-tubulin.

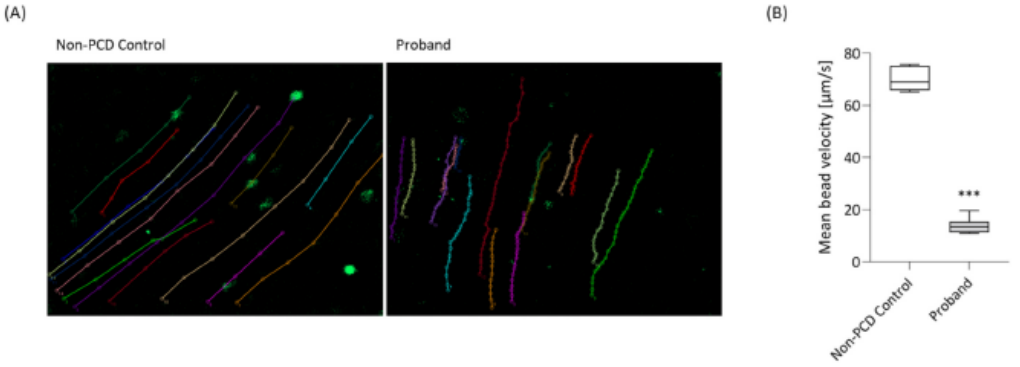

Fig. 4. The bead velocity analysis in ALI cultures of NE cells.
(A) Representative pictures of beads tracking for mucociliary transport assay (colors represent separate beads' tracks, dots indicate position at various frames). (B) Plots show the mean value of technical replicates (six movies for non-PCD control and seven for proband); significance assessed by two-tailed unpaired *t*-test; error bars indicate standard deviation; ***$p < 0.001$.

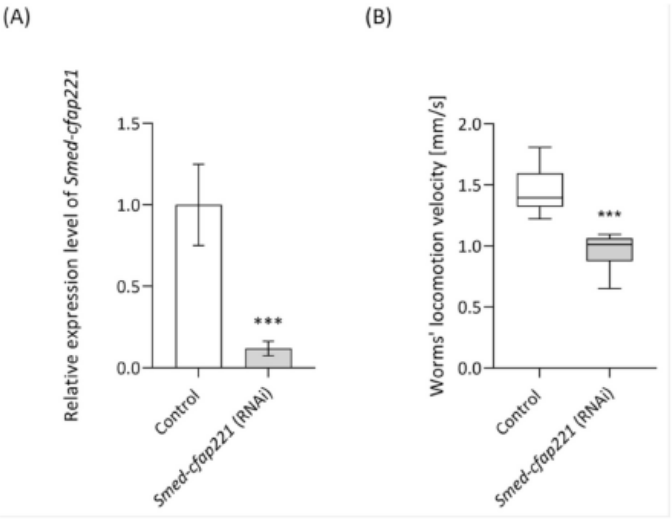

Fig. 5. Analysis of the effect of *Smed-cfap221* knockdown on *S. mediterranea* movement.
(A) Confirmation of the effectiveness of the daRNA-mediated knockdown of *Smed-cfap221*. Plots show the mean value of biological replicates (five worms); significance assessed by two-tailed unpaired *t*-test; error bars indicate standard deviation; ***$p < 0.001$. (B) The speed of planarian locomotion: plots show mean values of biological replicates (ten worms); significance assessed by two-tailed unpaired t-test; error bars indicate standard deviation; ***$p < 0.001$.

where characteristic inch-worming has been observed, typical for worms with a severe dysfunction of motile cilia. Nevertheless, CBF analysis confirmed the role of *Smed-cfap221* in the functioning of motile cilia.

In a mouse model, the *nm1054* mutant with a long deletion encompassing *CFAP221* ortholog has also been reported to cause symptoms of PCD with the normal ciliary ultrastructure and 25 % reduction of CBF in tracheal cilia [32]. Interestingly, the symptoms in *nm1054* mutant mice (on certain genetic background) included male infertility with the absence of flagellated sperm. Supported by rescue experiments, the authors suggested that loss of cfap221 could cause flagella instability during late spermiogenesis, resulting in the absence of mature sperm tails [32]. Of note, due to the young age of the male patients, no sperm examination has been performed in the original *CFAP221* study [13].

In an effort to shed light on whether the lack of CFAP221 would similarly affect human sperm flagella, we succeeded to obtain a sample of sperm from the proband. We found that the sperm cells were within the normal range, they had flagella, and they were motile. Our results suggest that the missing flagella previously reported in the mouse mutant [32] have reflected other abnormalities in the genetic composition of the mice strain or that different mechanisms underlie the role of *CFAP221* in human and mouse spermiogenesis.

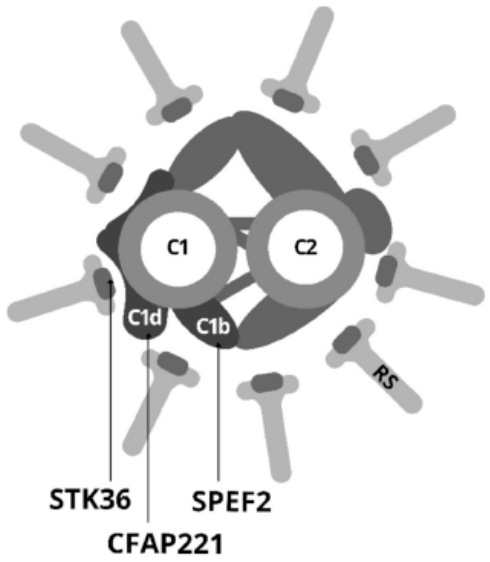

Fig. 6. Schematic localization of CFAP221 in relation to STK36 and SPEF2. C1, C2 – central pair of microtubules; C1d and C1b – two of seven central pair projections; RS – radial spokes; the localization of CFAP221, SPEF2 and STK26 is indicated by arrows. Modified from the mouse model [30].

While this paper was under revision, two other papers have been published concerning pathogenic variants in *CFAP221*. One of them has reported an adult Japanese male with obstructive azoospermia, respiratory symptoms with a persistent cough since the age of 37 years, and a history of lower airway symptoms exacerbations; no situs inversus was present [33]. As opposed to our proband, the level of nNO was normal, resembling the observation reported in the original *CFAP221* paper [13]. The patient was originally diagnosed to have Young's syndrome (OMIM phenotype %279,000 of unknown genetic background, characterized by infertility due to obstructive azoospermia associated with chronic sinobronchial infections). Upon finding a frameshift deletion in exon 15 and a large deletion encompassing exons 15–21 of *CFAP221*, possibility of the patient suffering from PCD has been raised. Unfortunately, neither WES analysis nor HSVM analysis demonstrating potential effect of CFAP221 deficiency on the ciliary motility have not been performed. For these reasons, the differentiating diagnosis between PCD and Young syndrome phenotype remains uncertain.

In another paper [34] (the full version access kindly provided by the authors), the effect of pathogenic *CFAP221* variant (along with other genes encoding proteins components of the Cd1 projection) has been described. The adult German female from the consanguineous union was a homozygote of a *CFAP221*:c.1641dup, p.Asn548GlnfsTer6 variant. Similar to our proband, the patient had chronic cough, sinusitis, otitis media, and no situs inversus. Unlike in our proband, bronchitis and bronchiectasis have been reported. The PICADAR score of 4 indicated PCD probability of <5 % (compared to 99 % in our proband), consistent with the lack of neonatal respiratory distress, admission to neonatal unit or congenital heart defect (observed in our proband). Contrary to the French Canadian family patients [13], the nNO production rate (28.9 nL/min) was below the cutoff value [27], resembling that observed in our proband. Normal ciliary ultrastructure by TEM and IF were in accord with the presence of the ciliary protein markers seen by IF in our proband, however in our proband, we observed a subtle abnormalities in central apparatus. Consistent with our findings, the in-vitro ciliary transport assays in the German patient indicated insufficient ciliary clearance. However, HSVM analysis of the ciliary beating were reported as subtle and not different from healthy controls, unlike in our proband where the significant decrease in the ciliary beat frequency and pattern was found. The effect of the pathogenic *CFAP221* variant of sperm motility could not be assessed (a female patient).

In summary, our study provides evidence that *CFAP221* is a causative PCD gene in human patients. The mild course of PCD in the proband, consistent with the subtle effect of *Smed-cfap221* gene silencing on worms' movement, confirms that *CFAP221* belongs to the subgroup of PCD genes, which do not exhibit unequivocal clinical symptoms nor easy-to-detect effects on the ciliary composition and function. As a result, PCD patients with pathogenic variants in *CFAP221* can largely benefit from early implementation of the genetic diagnostics.

Supplementary data to this article can be found online at https://doi.org/10.1016/j.bbadis.2025.167855.

Ethics declaration

The study was conducted according to the guidelines of the Declaration of Helsinki, and approved by the Ethics Committee of Poznan University of Medical Sciences (435/13 and 381/22). A written informed consent was obtained from all participants.

Funding

This research was funded by the National Science Centre, Poland: Grant no. 2018/29/N/NZ5/00810 to A.R. and Grant no. 2018/31/B/NZ2/03248 to E.Z.

CRediT authorship contribution statement

Alicja Rabiasz: Conceptualization, Data curation, Formal analysis, Funding acquisition, Investigation, Methodology, Validation, Visualization, Writing – original draft, Writing – review & editing. **Zuzanna Bukowy-Bieryłło:** Formal analysis, Investigation, Methodology, Validation, Writing – original draft, Writing – review & editing. **Patrycja Kaźmierczak:** Formal analysis, Investigation, Visualization, Writing – review & editing. **Hanna Przystałowska-Macioła:** Formal analysis, Investigation, Validation, Visualization, Writing – review & editing. **Marcin Mikoś:** Resources, Writing – review & editing. **Irena Wojsyk-Banaszak:** Writing – review & editing. **Ewa Ziętkiewicz:** Conceptualization, Data curation, Formal analysis, Funding acquisition, Supervision, Writing – original draft, Writing – review & editing.

Declaration of competing interest

The authors declare that they have no known competing financial interests or personal relationships that could have appeared to influence the work reported in this paper.

Acknowledgements

The authors gratefully acknowledge the primary ciliary dyskinesia family for contributing biological material for this study. The authors are very grateful: Dr. Marzena Kamieniczna for help in analyzing sperm sample; Dr. Magdalena Prauzińska for help in contacting the proband's family; Prof. Michał Witt for collecting biological material from the proband. The authors thank Dr. Patrick Perrigue (NanoBioMedical Centre, Adam Mickiewicz University) for providing *S. mediterranea* and help in developing the planarian facility and Dr. Marcin Śmiałek (Institute of Human Genetics, Polish Academy of Sciences) for providing pEGFP-C1 plasmid.

Data availability

Data will be made available on request.

References

[1] W.B. Wee, D. Gatt, E. Seidl, G. Santyr, T. To, S.D. Dell, Estimates of primary ciliary dyskinesia prevalence: a scoping review, ERJ Open Res. 10 (2024) 00989–02023, https://doi.org/10.1183/23120541.00989-2023.

[2] C.E. Kuehni, T. Frischer, M.-P.F. Strippoli, E. Maurer, A. Bush, K.G. Nielsen, A. Escribano, J.S.A. Lucas, P. Yiallouros, H. Omran, E. Eber, C. O'Callaghan, D. Snijders, A. Barbato, ERS Task Force on Primary Ciliary Dyskinesia in Children, Factors influencing age at diagnosis of primary ciliary dyskinesia in European children, Eur. Respir. J. 36 (2010) 1248–1258, https://doi.org/10.1183/09031936.00001010.

[3] C. Ardura-Garcia, M. Goutaki, S.B. Carr, S. Crowley, F.S. Halbeisen, K.G. Nielsen, P. Pennekamp, J. Raidt, G. Thouvenin, P.K. Yiallouros, H. Omran, C.E. Kuehni, Registries and collaborative studies for primary ciliary dyskinesia in Europe, ERJ Open Res. 6 (2020) 00005–02020, https://doi.org/10.1183/23120541.00005-2020.

[4] W.B. Hannah, B.A. Seifert, R. Truty, M.A. Zariwala, K. Ameel, Y. Zhao, K. Nykamp, B. Gaston, The global prevalence and ethnic heterogeneity of primary ciliary dyskinesia gene variants: a genetic database analysis, Lancet Respir. Med. 10 (2022) 459–468, https://doi.org/10.1016/S2213-2600(21)00453-7.

[5] J.S. Lucas, A. Barbato, S.A. Collins, M. Goutaki, L. Behan, D. Caudri, S. Dell, E. Eber, E. Escudier, R.A. Hirst, C. Hogg, M. Jorissen, P. Latzin, M. Legendre, M. W. Leigh, P. Midulla, K.G. Nielsen, H. Omran, J.-F. Papon, P. Pohunek, B. Redfern, D. Rigau, B. Rindlisbacher, F. Santamaria, A. Shoemark, D. Snijders, T. Tonia, A. Titieni, W.T. Walker, C. Werner, A. Bush, C.E. Kuehni, European Respiratory Society guidelines for the diagnosis of primary ciliary dyskinesia, Eur. Respir. J. 49 (2017) 1601090, https://doi.org/10.1183/13993003.01090-2016.

[6] A.J. Shapiro, S.D. Davis, D. Polineni, M. Manion, M. Rosenfeld, S.D. Dell, M. A. Chilvers, T.W. Ferkol, M.A. Zariwala, S.D. Sagel, M. Josephson, L. Morgan, O. Yilmaz, K.N. Olivier, C. Milla, J.E. Pittman, M.L.A. Daniels, M.H. Jones, I. A. Janahi, S.M. Ware, S.J. Daniel, M.L. Cooper, L.M. Nogee, B. Anton, T. Eastvold, L. Ehrne, E. Guadagno, M.R. Knowles, M.W. Leigh, Diagnosis of primary ciliary dyskinesia, An Official American Thoracic Society Clinical Practice Guideline, American Journal of Respiratory and Critical Care Medicine 197 (2018) e24, https://doi.org/10.1164/rccm.201805-0819ST.

[7] J. Wallmeier, K.G. Nielsen, C.E. Kuehni, J.S. Lucas, M.W. Leigh, M.A. Zariwala, H. Omran, Motile ciliopathies, Nat. Rev. Dis. Primers 6 (2020) 77, https://doi.org/10.1038/s41572-020-0209-6.

[8] R. Bhatt, C. Hogg, Primary ciliary dyskinesia: a major player in a bigger game, Breathe (Sheff.) 16 (2020) 200047, https://doi.org/10.1183/20734735.0047-2020.

[9] M. Legendre, L.-E. Zaragosi, H.M. Mitchison, Motile cilia and airway disease, Semin. Cell Dev. Biol. 110 (2021) 19–33, https://doi.org/10.1016/j.semcdb.2020.11.007.

[10] M. Goutaki, A. Shoemark, Diagnosis of primary ciliary dyskinesia, Clin. Chest Med. 43 (2022) 127–140, https://doi.org/10.1016/j.ccm.2021.11.008.

[11] G.J. Pazour, N. Agrin, J. Leszyk, G.B. Witman, Proteomic analysis of a eukaryotic cilium, J. Cell Biol. 170 (2005) 103–113, https://doi.org/10.1083/jcb.200504008.

[12] H.L. Rehm, J.S. Berg, L.D. Brooks, C.D. Bustamante, J.P. Evans, M.J. Landrum, D. H. Ledbetter, D.R. Maglott, C.L. Martin, R.L. Nussbaum, S.E. Plon, E.M. Ramos, S. T. Sherry, M.S. Watson, ClinGen, ClinGen—the clinical genome resource, N. Engl. J. Med. 372 (2015) 2235–2242, https://doi.org/10.1056/NEJMsr1406261.

[13] X.M. Bustamante-Marin, A. Shapiro, P.R. Sears, W.-L. Charng, D.P. Conrad, M. W. Leigh, M.R. Knowles, L.E. Ostrowski, M.A. Zariwala, Identification of genetic variants in CFAP221 as a cause of primary ciliary dyskinesia, J. Hum. Genet. 65 (2020) 175–180, https://doi.org/10.1038/s10038-019-0686-1.

[14] E. Zietkiewicz, Z. Bukowy-Bieryllo, A. Rabiasz, P. Daca-Roszak, A. Wojda, K. Voelkel, E. Rutkiewicz, A. Pogorzelski, M. Rasteiro, M. Witt, CFAP300: mutations in Slavic patients with primary ciliary dyskinesia and a role in ciliary dynein arms trafficking, Am. J. Respir. Cell Mol. Biol. 61 (2019) 440–449, https://doi.org/10.1165/rcmb.2018-0260OC.

[15] P.J. Freeman, R.K. Hart, L.J. Gretton, A.J. Brookes, R. Dalgleish, VariantValidator: accurate validation, mapping, and formatting of sequence variation descriptions, Hum. Mutat. 39 (2018) 61–68, https://doi.org/10.1002/humu.23348.

[16] S. Richards, N. Aziz, S. Bale, D. Bick, S. Das, J. Gastier-Foster, W.W. Grody, M. Hegde, E. Lyon, E. Spector, K. Voelkerding, H.L. Rehm, ACMG Laboratory Quality Assurance Committee, Standards and guidelines for the interpretation of sequence variants: a joint consensus recommendation of the American College of Medical Genetics and Genomics and the Association for Molecular Pathology, Genet. Med. 17 (2015) 405–424, https://doi.org/10.1038/gim.2015.30.

[17] S. Chen, L.C. Francioli, J.K. Goodrich, R.L. Collins, M. Kanai, Q. Wang, J. Alföldi, N. A. Watts, C. Vittal, L.D. Gauthier, T. Poterba, M.W. Wilson, Y. Tarasova, W. Phu, R. Grant, M.T. Yohannes, Z. Koenig, Y. Farjoun, E. Banks, S. Donnelly, S. Gabriel, N. Gupta, S. Ferriera, C. Tolonen, S. Novod, L. Bergelson, D. Roazen, V. Ruano-Rubio, M. Covarrubias, C. Llanwarne, N. Petrillo, G. Wade, T. Jeandet, R. Munshi, K. Tibbetts, Genome Aggregation Database Consortium, A. O'Donnell-Luria, M. Solomonson, C. Seed, A.R. Martin, M.E. Talkowski, H.L. Rehm, M.J. Daly, G. Tiao, B.M. Neale, D.G. MacArthur, K.J. Karczewski, A genomic mutational constraint map using variation in 76,156 human genomes, Nature 625 (2024) 92–100, https://doi.org/10.1038/s41586-023-06045-0.

[18] Z. Bukowy-Bieryłło, Long-term differentiating primary human airway epithelial cell cultures: how far are we? Cell Commun. Signal 19 (2021) 63, https://doi.org/10.1186/s12964-021-00740-z.

[19] Z. Bukowy-Bieryllo, A. Rabiasz, M. Dabrowski, A. Pogorzelski, A. Wojda, H. Dmenska, K. Grzela, J. Sroczynski, M. Witt, E. Zietkiewicz, Truncating mutations in exons 20 and 21 of OFD1 can cause primary ciliary dyskinesia without associated syndromic symptoms, J. Med. Genet. 56 (2019) 769–777, https://doi.org/10.1136/jmedgenet-2018-105918.

[20] C. Sakolish, A. Georgescu, D.D. Huh, I. Rusyn, A model of human small airway on a Chip for studies of subacute effects of inhalation toxicants, Toxicol. Sci. 187 (2022) 267–278, https://doi.org/10.1093/toxsci/kfac036.

[21] W.H. Organization, WHO Laboratory Manual for the Examination and Processing of Human Semen, World Health Organization, 2010. https://iris.who.int/handle/10665/44261. (Accessed 18 December 2024).

[22] L. Rouhana, J.A. Weiss, D.J. Forsthoefel, H. Lee, R.S. King, T. Inoue, N. Shibata, K. Agata, P.A. Newmark, RNA interference by feeding in vitro-synthesized double-stranded RNA to planarians: methodology and dynamics, Dev. Dyn. 242 (2013) 718–730, https://doi.org/10.1002/dvdy.23950.

[23] A. Rozanski, H. Moon, H. Brandl, J.M. Martín-Durán, M.A. Grohme, K. Hüttner, K. Bartscherer, I. Henry, J.C. Rink, PlanMine 3.0-improvements to a mineable resource of flatworm biology and biodiversity, Nucleic Acids Res. 47 (2019) D812–D820, https://doi.org/10.1093/nar/gky1070.

[24] T. Horn, M. Boutros, E-RNAi: a web application for the multi-species design of RNAi reagents—2010 update, Nucleic Acids Res. 38 (2010) W332–W339, https://doi.org/10.1093/nar/gkq317.

[25] P. Rompolas, J. Azimzadeh, W.F. Marshall, S.M. King, Analysis of ciliary assembly and function in planaria, Methods Enzymol. 525 (2013) 245–264, https://doi.org/10.1016/B978-0-12-397944-5.00012-2.

[26] L. Behan, B.D. Dimitrov, C.E. Kuehni, C. Hogg, M. Carroll, H.J. Evans, M. Goutaki, A. Harris, S. Packham, W.T. Walker, J.S. Lucas, PICADAR: a diagnostic predictive tool for primary ciliary dyskinesia, Eur. Respir. J. 47 (2016) 1103–1112, https://doi.org/10.1183/13993003.01551-2015.

[27] N. Beydon, P. Kouis, J.K. Marthin, P. Latzin, M. Colas, S.D. Davis, E. Haarman, A. L. Harris, C. Hogg, E. Kilbride, C.E. Kuehni, D. Marangu, K.G. Nielsen, C. Pendergrast, P. Robinson, N. Rumman, M. Rutter, W.T. Walker, T. Ferkol, J. S. Lucas, Nasal nitric oxide measurement in children for the diagnosis of primary ciliary dyskinesia: European Respiratory Society technical standard, Eur. Respir. J. 61 (2023) 2202031, https://doi.org/10.1183/13993003.02031-2022.

[28] M.W. Leigh, M.J. Hazucha, K.K. Chawla, B.R. Baker, A.J. Shapiro, D.E. Brown, L. M. LaVange, B.J. Horton, B. Qaqish, J.L. Carson, S.D. Davis, S.D. Dell, T.W. Ferkol, J.J. Atkinson, K.N. Olivier, S.D. Sagel, M. Rosenfeld, C. Milla, H.-S. Lee, J. Krischer, M.A. Zariwala, M.R. Knowles, the G.D. of M.C. Consortium, Standardizing Nasal Nitric Oxide Measurement as a Test for Primary Ciliary Dyskinesia 10, Annals of the American Thoracic Society, 2013, p. 574, https://doi.org/10.1513/AnnalsATS.201305-110OC.

[29] C.G. DiPetrillo, E.F. Smith, Pcdp1 is a central apparatus protein that binds Ca2+-calmodulin and regulates ciliary motility, J. Cell Biol. 189 (2010) 601–612, https://doi.org/10.1083/jcb.200912009.

[30] C.W. McKenzie, L. Lee, Genetic interaction between central pair apparatus genes CFAP221, CFAP54, and SPEF2 in mouse models of primary ciliary dyskinesia, Sci. Rep. 10 (2020) 12337, https://doi.org/10.1038/s41598-020-69359-3.

[31] C. Edelbusch, S. Cindrić, G.W. Dougherty, N.T. Loges, H. Olbrich, J. Rivlin, J. Wallmeier, P. Pennekamp, I. Amirav, H. Omran, Mutation of serine/threonine protein kinase 36 (STK36) causes primary ciliary dyskinesia with a central pair defect, Hum. Mutat. 38 (2017) 964–969, https://doi.org/10.1002/humu.23261.

[32] L. Lee, D.R. Campagna, J.L. Pinkus, H. Mulhern, T.A. Wyatt, J.H. Sisson, J. A. Pavlik, G.S. Pinkus, M.D. Fleming, Primary ciliary dyskinesia in mice lacking the novel ciliary protein Pcdp1, Mol. Cell. Biol. 28 (2008) 949–957, https://doi.org/10.1128/MCB.00354-07.

[33] M. Ito, K. Morimoto, M. Ohasi, K. Wakabayashi, A. Miyabayashi, H. Yamada, M. Hijikata, N. Keicho, Primary ciliary dyskinesia due to compound heterozygous variants in CFAP221 with obstructive azoospermia: young's syndrome may be a phenotype of primary ciliary dyskinesia, Intern. Med. (2024), https://doi.org/10.2169/internalmedicine.3978-24.

[34] K. Wohlgemuth, N. Hoersting, J. Koenig, N.T. Loges, J. Raidt, S. George, S. Cindrić, A. Schramm, L. Biebach, S. Lay, G.W. Dougherty, H. Olbrich, P. Pennekamp, B. Dworniczak, H. Omran, Pathogenic variants in CFAP46, CFAP54, CFAP74 and CFAP221 cause primary ciliary dyskinesia with a defective C1d projection of the central apparatus, Eur. Respir. J. 64 (2024) 2400790, https://doi.org/10.1183/13993003.00790-2024.

Supplementary Materials

A novel pathogenic variant of *CFAP221* is a cause of a mild form of primary ciliary dyskinesia

Alicja Rabiasz[1*], Zuzanna Bukowy-Bieryłło[1], Patrycja Kaźmierczak[1#], Hanna Przystałowska-Macioła[1#], Marcin Mikoś[2,3], Irena Wojsyk-Banaszak[2], Ewa Ziętkiewicz[1*]

1 Institute of Human Genetics, Polish Academy of Sciences, Poznań, Poland

2 Department of Pneumonology, Paediatric Allergy and Clinical Immunology, Poznan University of Medical Sciences, Poznań, Poland

3 Vilda Clinic, Poznań, Poland

*Correspondence: Alicja Rabiasz alicja.rabiasz@igcz.poznan.pl, phone: +48 616579253;

Ewa Ziętkiewicz ewa.zietkiewicz@igcz.poznan.pl, phone: +48 616579203

#Equal Contribution

1. Additional clinical description of the proband

Proband's neonatal and early childhood history: pregnancy II, vaginal delivery at 38 weeks of pregnancy, Apgars 9/6/8, mass 4150g. History of neonatal respiratory distress, respiratory support (nCPAP), hospitalized for 19 days in the neonatal unit, infection was ruled out, 2nd degree intraventricular hemorrhage, heart arrhythmia and congenital heart defect (IAS aneurysm, ASD II) were confirmed. Suspected laryngomalacia was ruled out in directoscopy (normal larynx and epiglottis). Since infancy, history of recurrent respiratory tract infections, frequent antibiotic treatment, hospitalized 4 times for pneumonia. The patient presented chronic, productive cough, intermittent abnormal breath sound on auscultation (coarse rales), chronic nasal congestion, recurrent otitis media and sinusitis. Chronic nasosinusitis (CT scan), history of glue ear and chronic, conductive hearing loss. Immune deficiency and cystic fibrosis were ruled out (IgA/M/G, IgG subclasses, flow cytometry normal, sweat chloride non-elevated). The patient receive salbutamol, nebulized hypertonic saline, nasal topical steroid, and performs regular chest physiotherapy. Follow up studies at 18 years ruled out bronchiectasis on chest CT-scan and showed preserved, normal lung function, which suggests clinically mild manifestation of PCD, with predominant ENT symptoms, presence of non-severe congenital heart defect and no laterality defect. Nasal NO (nNO) concentration (tidal breathing; FeNO+PFS; sample flow rate 250 ml/min): patient 18 yo: 174 ppb (44 nl/min); control male 40 years old: 957 ppb (239 nl/min).

Chest imaging: chest X-ray at 14 years of age revealed lung fields with no focal lesions in the parenchyma. Pleural cavities were free. Heart silhouette was within normal limits. Chest CT at 17 years of age revealed irregular outline of the intermediate and lower right bronchus, no evidence of thickening of the bronchial wall, with the structure of both lungs appearing normal. No bronchiectasis was observed. Residual thymus measuring 18mm in width and 16mm in midline thickness had normal structure. No enlarged mediastinal or hilar lymph nodes were seen. Pleural cavities appeared normal. A slight right-sided scoliosis was noted.

Microbiology: sputum cultures - at 3 years of age a massive growth of *Streptococcus pneumoniae*; at 16 years of age: *Streptococcus pyogenes*. Multiple other studies identified normal airway microbiota, with no pathogenic bacterial growth. Bronchoscopy: at 12 years of age - Storz bronchoscope was introduced into the trachea. A large amount of mucous secretions was aspirated. The mucous membrane of the trachea and bronchi was inflamed. Pulmonary function tests; last follow up at 17 years old: LCI MBW (Multiple breath washout): LCI 2,5% -1,71 Z-Score (decreased, non-elevated - no signs of inhomogeneous ventilation). Spirometry: FEV1/FVC 79% = -1.05 Z-Score (normal), FEV1 104% predicted = +0.31 Z-Score (normal), FVC 112% predicted = +1.05 Z-Score (normal). Normal spirometry, no signs of obstructive disease. Body Plethysmography: TLC 108% predicted = +1.4 Z-Score (normal), RV%TLC 137% predicted = +1.01 Z-Score (normal) - no signs of reduced TLC, no signs of hyperinflation.

Ear-Nose-Throat history: chronic nasosinusitis (CT scan), history of glue ear and chronic, conductive hearing loss. ENT surgery: 9 years of age: bilateral tube tympanostomy, signs of bilateral glue ear. Drainage. Implantation of tympanostomy tubes; 10 years of age: glue ear drainage, tube tympanostomy. Adenotomy; 12 years of age: Endoscopic sinus surgery, maxillary antrostomy; 13 years of age: Endoscopic sinus surgery, maxillary antrostomy. Re-adenotomy; 16 years of age: Endoscopic sinus surgery, bilateral nasalization; 17 year of age: Septoplasty.

Echocardiography: interatrial septum / IAS aneurysm (0.6cm) with two micro ASD II (atrial septal defects), 0.1 and 0.2 cm with L-R flow. Slightly flaccid mitral valve flaps and widened aortic bulbus (3.6 cm).

2. Supplementary Tables

Supplementary Table 1. List of primers used for patients samples analysis.

Primer name	Primer sequence
Primers for PCR and Sanger sequencing	
LRRC6_5A_F	atcaacctggggctgattc
LRRC6_5B_R	tgcaaacaacttggaaagagaa
CFAP221_16_F	acacacccacccactaattg
CFAP221_16_R	atgatcatgtccactccccg
Primers for cDNA analysis	
CFAP221_e3F	tggcataatacattttggaggct
CFAP221_e4R	ggggtaaaatatgaacacgtgtg
CFAP221_e8F	cgcagttcaactctcaacca
CFAP221_e9R	ctggcggtcggtgaaaattt
CFAP221_e14F	taacacttggctcagcaggt
CFAP221_e15R	tcgattgttttgcttggcca
CFAP221_e15F	tggccaagcaaaacaatcga
CFAP221_e17R	accagtccaaggccatcag
CFAP221_e18F	gccattctctgtccacaagtc
CFAP221_e19R	aaggcctcaggtggtttcat
CFAP221_e23F	gactccagaaatgatcaaagtgg
CFAP221_e24R	atctcctcgagcagcttctc
GAPDH_e4_F	acgggaagcttgtcatcaat
GAPDH_e8_R	gggccatccacagtcttct

Supplementary Table 2. List of antibodies used in IF and WB analyses

Antibody	Manufacturer	Host and clonality	Concentration	Catalog and lot number
Immunofluorescence				
GAS8	Atlas Antibodies	rabbit, polyclonal	1:600	HPA041311 (000034380)
DNAI2	Abnova	mouse, monoclonal	1:550	H00064446-M01 (J4291-1C8)
RSPH9	Atlas Antibodies	rabbit, polyclonal	1:400	HPA031703 (000004506)
SPEF2	Atlas Antibodies	rabbit, polyclonal	1:300	HPA039606 (000027916)
STK36	Atlas Antibodies	rabbit, polyclonal	1:200	HPA027453 (A117096)
Ac-α-tubulin	Sigma Aldrich	mouse, monoclonal	1:10 000	T6793 (042M4761)
IgG-594 secondary	Molecular Probes, Thermo Fisher Scientific	goat anti-rabbit, Alexa Fluor™ 594, polyclonal, highly cross-adsorbed	1:2 500	A11037 (2005936)

IgG-488 secondary	Molecular Probes, Thermo Fisher Scientific	goat anti-mouse, Alexa Fluor™ 488, polyclonal, highly cross-adsorbed	1:2 500	A11029 (1942237)
Western blot				
CFAP221	Invitrogen	rabbit, polyclonal	1:500	PA5-23823 (ZF4370654)
GAPDH	Abcam	rabbit, polyclonal	1:20 000	ab9485 (1064471-1)
IgG-HRP secondary	Abcam	goat anti-rabbit, polyclonal, HRP-conjugated,	1:40 000	ab97051 (GR3231028-8)

Lot numbers are marked in brackets

Supplementary Table 3. List of primers used for dsRNA synthesis and RT-qPCR in planarians

Primers name	**Primer sequence**
Primers for dsRNA synthesis	
dsRNA_Smed_cfap221_F	TAATACGACTCACTATAGGGagaagtgcattttgctggct
dsRNA_Smed_cfap221_R	TAATACGACTCACTATAGGGtcagttggcagaaagctcaa
dsRNA_eGFP_F	TAATACGACTCACTATAGGGcacatgaagcagcacgactt
dsRNA_eGFP_R	TAATACGACTCACTATAGGGagttcaccttgatgccgttc
Primers for qRT-PCR	
RTPCR_Smed_gapdh_F	atcaaggccgctattaagca
RTPCR_Smed_gapdh_R	cagatcgattacacggcaac
RTPCR_Smed_sfap221_F	attactgccgattcaaccgc
RTPCR_Smed_cfap221_R	acttccgtgtctgtcgaaga

Upper case letters indicate the sequence recognized by T7 RNA polymerase

Supplementary Table 4. Variants identified in the proband

Gene (alias); affected exon	**Pathogenic variant description: HGVS; gnomAD v4.1.0; dbSNP**	**gnomAD v4.1.0 frequency***	**Evidence of pathogenicity**	**ACMG/AMP category**
LRRC6 (*DNAAF11*); exon 5	NM_012472.6:c.436G>C (p.Asp146His); 8-132632957-C-G (GRCh38); rs200321595	0.0001863 170/1179741 alleles	Strong	PS4 prevalence in affected exceeds that in controls
CFAP221 (*PCDP1*); exon 16	NM_001271049.2:c.1641dup (p.Asn548GlnfsTer6); 2-119627775-T-TC (GRCh38); rs779457532	0.0001441 170/1179741 alleles	Very strong	PVS1 null variant - frameshift

* In non-Finnish Europeans; in European Finnish 0.0003125 (20/64004 alleles)

Supplementary Table 5 Semen analysis results

Semen parameters	Proband's semen	Lower reference limit (WHO)
Volume	5 ml	1.5 ml
pH	8	7.2
Sperm concentration (spermatozoa/ml)	4.5 mln/ml	15 mln/ml
Sperm concentration (total per ejaculate)	22.5 ml	39 mln
Progressive motility	35%	32%
Total motility	43%	40%
Viability	63%	58%
Normal morphology	4%	4%

3. Supplementary Figures

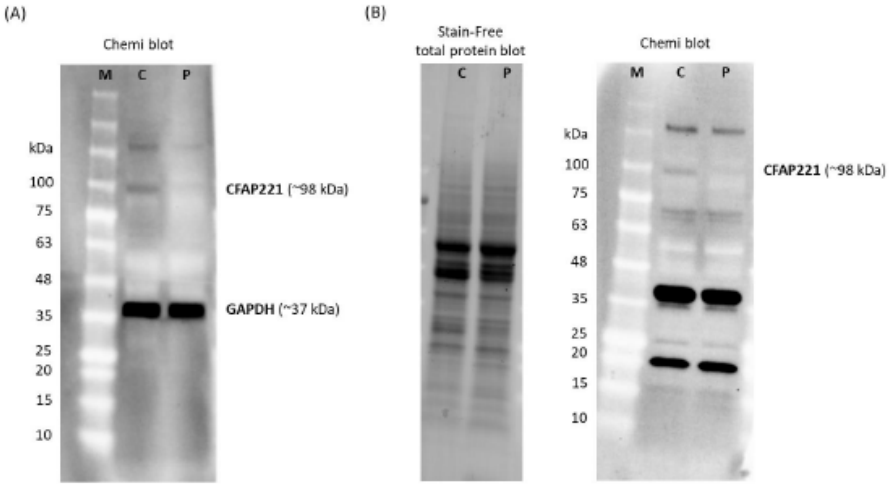

Supplementary Figure 1. Analysis of the expression of *CFAP221* at protein level in NE cells (ALI culture) (A) Chemiluminescent blot for Western Blot of CFAP221 in reference to GAPDH . (B) Left: Whole total protein membrane (in Bio-Rad Stain-free technology, before incubation with primary

antibody, anti-CFAP221); Right: Chemiluminescent blot for Western Blot of CFAP221 in reference to the total protein. M- Protein Molecular Weight Marker C - non-PCD control, P - proband,

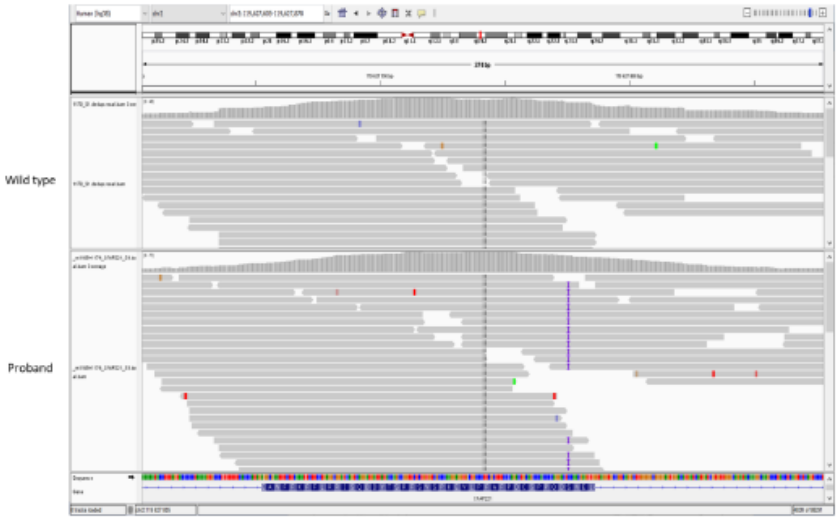

Supplementary Figure 2. A snapshot of *CFAP221* exon 16 with the single nucleotide insertion detected by WES.

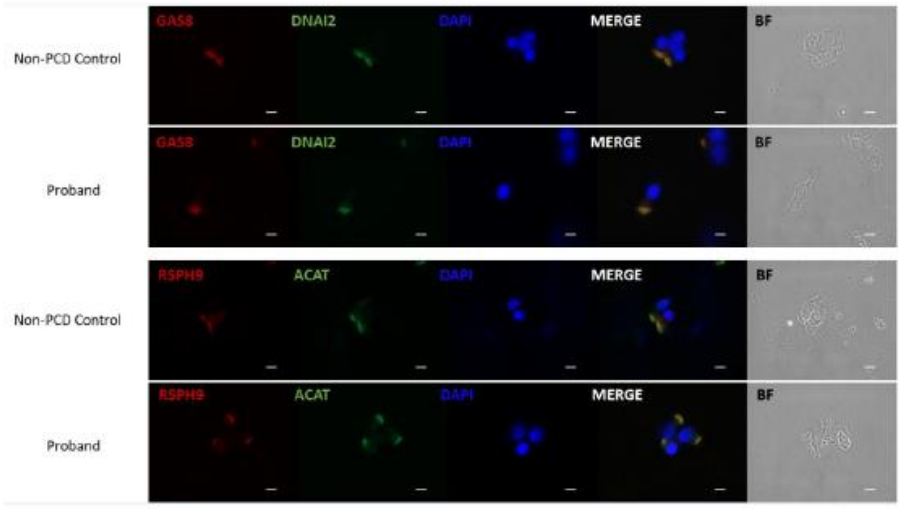

Supplementary Figure 3. IF staining of NE cells using antibodies targeting elements of motile cilia: dynein arms, N-DRC, radial spokes. Scale bar 10 µm; BF- Bright Field; ACAT- Acetylated-α-tubulin

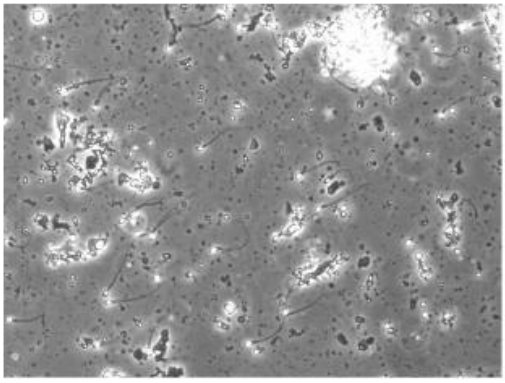

Supplementary Figure 4. Representative picture of sperm cells from proband (10x magnification).

Artykuł 4

The lack of homozygotes with a large deletion encompassing *SPAG1* and *POLR2K* in primary ciliary dyskinesia patients suggests the lethal effect of the loss of POLR2K protein

Alicja Rabiasz, Monika Drobna-Śledzińska, Patrycja Kaźmierczak, Michał Witt, Ewa Ziętkiewicz

Genes & Diseases, https://doi.org/10.1016/j.gendis.2025.101535

SPAG1 (*sperm-associated antigen 1*) zlokalizowany w chromosomie 8, jest jednym z genów, którego patogenne warianty prowadzą do wystąpienia PCD na skutek uszkodzenia składania ramion dyneinowych, które stanowią istotny element strukturalny i funkcjonalny rzęsek ruchowych. Pacjenci z patogennymi wariantami *SPAG1* mają typowe pulmonologiczne objawy PCD, u większości obserwowane jest zaburzenia osi symetrii ciała (odwrócenia narządów), a rzęski komórek nabłonka oddechowego pacjentów są nieruchome w związku z brakiem ramion dyneinowych. W grupie prawie 300 pacjentów, u których w toku długoletnich badań prowadzonych w Zakładzie zidentyfikowano genetyczne podłoże PCD, patogenne warianty w *SPAG1* występowały u 60 niespokrewnionych pacjentów, czyniąc ten gen najczęściej zaangażowanym w patogenezę PCD u polskich pacjentów. Dwa najczęściej występujące i wcześniej opublikowane warianty to: nonsensowny wariant w eksonie 16 (NM_003114.5:c.2014C>T; p.Gln672Ter) oraz duża delecja 11 973 bp, [NM_005034.4:c.61+201__NM_003114.5:c.140+1169]del), obejmująca dwa pierwsze eksony *SPAG1* oraz eksony 3-4 genu *POLR2K* (*RNA Polymerase II, I and III Subunit K*), który znajduje się 5’ w stosunku do *SPAG1*. Wariant c.2014C>T był obserwowany u 27 homozygot oraz 31 złożonych heterozygot, z czego u 28 pacjentów drugim patogennym wariantem była duża delecja; delecja 11 973 bp została również zidentyfikowana u 2 innych złożonych heterozygot. Podobnie jak w dwóch wcześniejszych pracach opisujących *SPAG1*, nie zaobserwowano homozygot z delecją obejmującą części genów *SPAG1* i *POLR2K*. Celem pracy było wyjaśnienie przyczyny braku homozygotycznych pacjentów z delecją obejmującą eksony 1-2 genu *SPAG1* oraz eksony 3-4 genu powyżej *SPAG1, POLR2K*.

Zgodnie z prawem Hardy’ego-Weinberga, w grupie 60 pacjentów z patogennymi wariatami w genie *SPAG1* powinny występować 4 homozygoty z delecją 11 973 bp. Aby

zwiększyć istotność prowadzonej analizy, do grupy 60 analizowanych pacjentów, dołączono dane dla wcześniej raportowanych 16 pacjentów (w tym 8 złożonych heterozygot z delecją) oraz 25 niemieckich pacjentów prof. Heymuta Omrana (6 homozygot c.2014C>T i 19 heterozygot zawierających c.2014C>T i dużą delecję; tam również nie zaobserwowano żadnej homozygoty z dużą delecją). Według prawa Hardy'ego-Weinberga w rozszerzonej grupie 103 pacjentów PCD liczba oczekiwanych homozygot powinna wzrosnąć do ośmiu. Na podstawie obserwowanego rozkładu genotypów sformułowano hipotezę, że brak homozygot z delecją obejmującą 1-2 eksony *SPAG1* i 3-4 *POLR2K* wynika ze szkodliwego, potencjalnie letalnego wpływu braku funkcjonalnej formy POLR2K. *POLR2K* jest najmniejszą podjednostką polimerazy II RNA, dzieloną z polimerazą RNA I oraz III; jest zaangażowana w powstawanie każdego rodzaju cząsteczek RNA oraz wpływa na składanie kompleksu preinicjacyjnego polimerazy III RNA.

W celu weryfikacji hipotezy porównano wpływ wyciszenia homologów *SPAG1* i *POLR2K* na poziomie całego organizmu. W tym celu przeprowadzono RNAi dla każdego z genów w modelu *S. mediterranea;* organizm ten jest nie tylko wykorzystywany do badania genów rzęskowych, ale jest również opisywany jako alternatywny model do badania embrionalnie letalnych genów w dorosłym organizmie. Wyciszenie badanych genów przeprowadzono poprzez podawanie dsRNA skierowanych przeciwko *Smed-spag1* lub *Smed-polr2k* (jako kontrolę użyto robaki karmione dsRNA przeciwko *eGFP*), efektywność wyciszenia potwierdzono na poziomie mRNA. RNAi *Smed-spag1* nie wpłynęła na morfologię *S. mediterranea,* ale spowodowała zaburzenie wzoru i prędkości ruchu robaków; planarie przemieszczały się w sposób charakterystyczny dla defektu rzęsek ruchowych, przy pomocy mięśni (*inchworming movement*), a prędkość ich poruszania była około 3 razy mniejsza niż w kontroli (0.354 ± 0.065 mm/s i 1.189 ± 0.371, odpowiednio; $p < 0.001$). W przeciwieństwie do *Smed-spag1,* wyciszenie *Smed-polr2k* nie wpłynęło na lokomocję robaków, ale spowodowało liczne defekty ciała robaków (np. lizę tkanki, regresję głowy), finalnie prowadząc do ich śmierci. Ze względu na ogromne zdolności regeneracyjne *S. mediterranea* zbadano wpływ RNAi *Smed-polr2k* na regenerację robaków (dzień po ostatnim podaniu dsRNA robaki pocięto w celu stymulacji procesu regeneracji). Wyciszenie badanego genu spowodowało zaburzenie regeneracji robaków, co finalnie, podobnie jak w przypadku nieciętych robaków, doprowadziło do ich śmierci. W celu lepszego zrozumienia wpływu wyciszenia *Smed-polr2k* na fenotyp planarii i odniesienia uzyskanych wyników do ludzi, dokonano analizy wyciszenia *POL2RK* na funkcje życiowe komórek linii

HEK293T. Komórki transfekowano oddzielnie przy użyciu dwóch komercyjnie dostępnych siRNA (*POLR2K* siRNA_1 i siRNA_2) celujących w różne miejsca eksonu 3 *POLR2K* (jako kontrole użyto rekomendowane siRNA niecelujące w sekwencje kodujące); efektywność wyciszenia potwierdzono na poziomie mRNA oraz białka. 48h po transfekcji z użyciem *POLR2K* siRNA_1 i siRNA_2 zaobserwowano wzrost liczby komórek apoptotycznych w porównaniu do kontroli negatywnej. Ponadto wyciszenie *POLR2K* z użyciem obu siRNA doprowadziło do znacznego obniżenia proliferacji komórek w porównaniu do komórek transfekowanych kontrolnym siRNA.

Uzyskane wyniki pozwoliły na potwierdzenie hipotezy, że brak homozygotycznych pacjentów z dużą delecją wynika z braku funkcjonalnego białka POLR2K, nie zaś SPAG1 (homozygoty patogennego wariantu w eksonie 16 *SPAG1* występowały w badanej grupie z częstością zgodną z oczekiwaną na podstawie częstości allelu w populacji chorych). Badania z użyciem *S. mediterranea* potwierdziły ewolucyjnie zakonserwowaną rolę *Smed-spag1* w funkcjonowaniu rzęsek ruchowych. Wyciszenie *Smed-polr2k* wykazało, że gen ten jest niezbędny do utrzymania homeostazy organizmu, prawdopodobnie poprzez regulację obiegu komórek, np. poprzez wpływ na proliferację dorosłych komórek macierzystych robaka. Wyciszenie *POLR2K* w ludzkiej linii komórkowej (HEK293T) pozwoliło na potwierdzenie wpływu *POLR2K* na funkcje życiowe komórek, proliferację i apoptozę. Analiza rozkładu genotypów u pacjentów z patogennymi wariantami w genie *SPAG1* oraz uzyskane wyniki sugerują, że w przypadku opracowywania terapii, np. w oparciu o mRNA, leczenie pacjentów PCD, u których jednym z patogennych wariantów jest duża delecja obejmująca część *SPAG1* oraz *POLR2K,* powinno opierać się na przywróceniu funkcji SPAG1.

Mój wkład w powstanie publikacji:

- ustalenie koncepcji i planu badań
- zabezpieczenie środków finansowych
- zaprojektowanie, wykonanie i interpretacja doświadczeń z wykorzystaniem *S. mediterranea*: analiza *in silico,* wyciszenie homologa genu *SPAG1* i *POLR2K* (w tym zaprojektowanie i synteza dsRNA przy użyciu transkrypcji *in vitro*), potwierdzenie efektywności wyciszenia na poziomie mRNA (izolacja RNA, synteza cDNA, qRT-PCR), analiza wpływu wyciszenia obu genów na fenotyp planarii

(w tym na lokomocję robaków), analiza wpływu wyciszenia *POLR2K* na zdolności regeneracyjne *S. mediterranea*

- zaprojektowanie, wykonanie i interpretacja doświadczeń z wykorzystaniem ludzkiej linii komórkowej: wyciszenie *POLR2K* w komórkach HEK293T, potwierdzenie efektywności wyciszenia na poziomie mRNA i białka (izolacja RNA, synteza cDNA, qRT-PCR, izolacja białka, Western-Blot), przeprowadzenie testów funkcjonalnych
- pisanie oryginalnej wersji manuskryptu, przygotowanie tabel i rycin
- przygotowanie ostatecznej wersji manuskryptu
- obowiązki autora korespondencyjnego.

Publikacja oraz informacje dodatkowe (załączniki) są dostępne pod następującym adresem internetowym:
https://doi.org/10.1016/j.gendis.2025.101535

Journal Pre-proof

The lack of homozygotes with a large deletion encompassing *SPAG1* and *POLR2K* in primary ciliary dyskinesia patients suggests the lethal effect of the loss of POLR2K protein

Alicja Rabiasz, Monika Drobna-Śledzińska, Patrycja Kaźmierczak, Michał Witt, Ewa Ziętkiewicz

PII: S2352-3042(25)00024-8

DOI: https://doi.org/10.1016/j.gendis.2025.101535

Reference: GENDIS 101535

To appear in: *Genes & Diseases*

Received Date: 21 August 2024

Revised Date: 4 December 2024

Accepted Date: 18 December 2024

Please cite this article as: Rabiasz A, Drobna-Śledzińska M, Kaźmierczak P, Witt M, Ziętkiewicz E, The lack of homozygotes with a large deletion encompassing *SPAG1* and *POLR2K* in primary ciliary dyskinesia patients suggests the lethal effect of the loss of POLR2K protein, *Genes & Diseases*, https://doi.org/10.1016/j.gendis.2025.101535.

The lack of homozygotes with a large deletion encompassing *SPAG1* and *POLR2K* in primary ciliary dyskinesia patients suggests the lethal effect of the loss of POLR2K protein

SPAG1 (sperm-associated antigen 1) is one of over 50 genes whose pathogenic variants underlie primary ciliary dyskinesia (PCD; OMIM244400), an inherited disorder affecting the function of motile cilia[1], highly conserved organelles protruding from the surface of eukaryotic cells. Pathogenic *SPAG1* variants impair the assembly of dynein arms, essential elements of cilia. In a cohort of almost 300 affected individuals with the genetic bases of PCD explained during our long-term studies, pathogenic variants in *SPAG1* were found in 60 unrelated patients, making it one of the most frequently involved genes in the Polish PCD population. Two predominant, previously reported variants[1,2] were a nonsense mutation c.2014C>T in exon 16, found in both homozygotes and in compound heterozygotes, and a large 11,973 bp deletion encompassing parts of *SPAG1*, and of the upstream *POLR2K* (RNA polymerase II, I and III subunit K). c.2014C>T was found in 27 homozygotes and 31 compound heterozygotes, of whom 28 had the large deletion as the second allele; the large deletion was found in two more compound heterozygotes, accompanied in trans by rare pathogenic variants (Fig. 1A and Table S1, 2). Similar to previous reports[1,2], the large deletion was repetitively found in compound heterozygosity, but no homozygotes were identified.

In our group of 60 *SPAG1*-PCD patients, ~4 homozygotes with the large deletion are expected under Hardy-Weinberg equilibrium; however, none was observed. This difference in the predicted and observed distribution of genotypes was not statistically significant (chi-square, $P = 0.1663$). To achieve the statistical power, we added data for 18 Caucasians reported earlier[1,2] (8 compound heterozygotes carrying the large deletion), and for 25 *SPAG1*-PCD

German patients (6 c.2014C>T homozygotes and 19 heterozygotes for c.2014C>T and the large deletion; Heymut Omran, personal communication). The expected number of the large deletion homozygotes in the joint group of 103 patients raised to eight (Fig. 1B); with none observed, the unbalanced distribution of the genotypes was statistically significant ($P = 0.006$).

The lack of large deletion homozygotes in the combined group of 103 patients suggested a seriously deleterious effect (presumably lethality) of this genotype. Given that the large deletion encompasses the C-terminal part of *POLR2K* in addition to exons 1 and 2 of *SPAG1*, we hypothesized that this was due to the lack of functional POLR2K rather than SPAG1 protein. *POLR2K* represents one of the smallest subunits of RNA polymerase II, shared with two other RNA polymerases; in consequence, *POLR2K* is involved in the RNA processing machinery and improves RNA polymerase III pre-initiation complex assembly[3]. To confirm our hypothesis, we examined the effect of RNA interference-mediated knockdown of *POLR2K* at two levels: the whole organism (ciliated flatworm, *Schmidtea mediterranea*), and cellular (human cell line).

S. mediterranea is used as a model organism to study the functionality of embryonic-lethal genes in the adult body and cilia-related genes (worms' locomotion depends on motile cilia covering the ventral side of their body). To compare the phenotypes caused by the deficiency of *Smed-spag1* and *Smed-polr2k* in *S. mediterranea*, we first performed a Smed-*spag1* knockdown. The effectiveness of gene silencing was confirmed using quantitative reverse transcription PCR (Fig. 1C-left). The worms upon knockdown displayed no morphological defects, but moved three times slower than controls, using characteristic inchworming (Fig. 1C-right; supplementary movies 1 and 2).

In *Smed-polr2k*-knockdown worms, the relative expression level was also significantly reduced (Fig. 1D-left). In contrast to *Smed-spag1*-silencing, the knockdown of *Smed-polr2k* led to severe defects of planarian bodies, including tissue lysis and head regression, which ultimately led to worms' death (Fig. 1D-right). Furthermore, despite the enormous regenerative capacity of planarians, *Smed-polr2k* deficiency resulted in disruption of the regeneration process (the lack of worms' regrowth after cutting) (Fig. S1). On the other hand, until the point of tissue lysis, no worms' motility impairment was observed (supplementary movie 3), indicating the lack of *Smed-polr2k* involvement in motile cilia function.

To better understand the phenotype observed in worms and to relate the obtained results to humans, the effect of *POLR2K* knockdown on the vital cell functions was assessed in the human HEK293T cell line transfected in parallel with two siRNAs targeting different regions of *POLR2K* exon 3. Quantitative reverse transcription PCR and western blotting confirmed the effectiveness of the gene knockdown at both mRNA and protein levels, respectively (Fig. 1E). *POLR2K* knockdown resulted in a gentle but statistically significant increase in the number of apoptotic cells (Fig. 1F-left). The cell proliferation was significantly decreased in the *POLR2K*-silenced cells compared with the control (Fig. 1F-right).

In the presented study, we examined the hypothesis that the discrepancy between the observed and expected distribution of haplotypes in *SPAG1*-PCD patients (the lack of homozygotes with the large deletion encompassing parts of *SPAG1* and *POLR2K*), reflected a highly deleterious, possibly lethal effect of the loss of a functional POLR2K rather than of SPAG1 protein. A similarly unbalanced distribution of genotypes has been described for *PMM2* gene[4] (zero observed versus eight expected p.R141H homozygotes in 54 Caucasian patients with

carbohydrate-deficient glycoprotein syndrome type 1A). The authors concluded that this distribution was probably caused by selection against the homozygous R141H[4]. It should be emphasized that the frequency of homozygous pathogenic variants introducing premature STOP codon located in *SPAG1* exon 16 (c.2014C>T) was even higher than expected under equilibrium, indicating the lack of selection against a homozygous deficiency of the wild-type *SPAG1*.

To provide a molecular context to our observation, we analyzed the impact of *POLR2K* silencing on phenotypes at the whole organism (planarians) and cellular levels. The dsRNA-mediated knockdown of *Smed-spag1* in *S. mediterranea* did not affect the viability of the organisms, but as expected, impaired worms' movement, confirming the evolutionary conserved role of *SPAG1* in the motile cilia function (previously demonstrated using a vertebrate model, zebrafish[1]). In contrast, silencing of *Smed-polr2k* resulted in a much more severe phenotype and suggested that *Smed-polr2k* played an essential role in maintaining body homeostasis by regulating cell turnover, probably through the impact on planarian stem cell proliferation. Our observations are in line with those in other studies where deleterious effects of other essential gene knockdowns on *S. mediterranea* phenotype have been reported. For example, RNA interference-mediated knockdown of *Argonaute RISC catalytic component 2* (*Smed-ago2*)[5] led to regeneration defects or tissue regression in worms, ultimately causing their death, demonstrating that *Smed-ago2* is crucial for tissue homeostasis and regeneration and acts through a regulation of adult stem cell proliferation[5].

Our results of siRNA-mediated *POLR2K* knockdown in the human cell culture shed light on the mechanisms of defects observed in the planarian model. They confirmed the essential role

of *POLR2K* in the regulation of vital cell functions, manifested by decreased cell proliferation and increased apoptosis upon its knockdown.

Despite the repetitive reports suggesting *POLR2K's* importance in many cellular processes (additional discussion), no direct experimental proof of phenotype changes after *POLR2K* knockdown has been published. Our findings confirm that *POLR2K* is necessary for the functioning of living organisms and suggest that its influence on cell turnover is exerted through the regulation of cell proliferation and apoptosis. Moreover, our study provides evidence that the essential role of *POLR2K* in vital cell functions is evolutionarily conserved. Finally, these results, together with the earlier studies regarding *POLR2K* as a hub gene involved in many essential interactions, support our starting hypothesis that the lack of homozygotes of the large deletion involving *SPAG1* and *POLR2K* genes is caused by the lethal impact of the POLR2K deficiency; at the same time, it indicates that *POLR2K* is not directly involved in the PCD pathogenesis. Our findings suggest that potential mRNA-based therapy for *SPAG1*-PCD patients with large deletion should be designed to restore SPAG1, and not POLR2K function.

Ethics declaration

The diagnostics were conducted according to the recommendation of the World Medical Association. Written informed consent was obtained from the participating subjects or their guardians. Procedures representing part of the diagnostic scheme were approved by the institutional committee (the Ethics Committee of the Medical University in Poznań, 960/11, 435/13, and 381/22).

Author contributions

A.R.: conceptualization, data curation, formal analysis, funding acquisition, investigation, methodology, validation, visualization, writing–original draft, and writing–review & editing. M.D.Ś.: formal analysis, investigation, methodology, and writing–review & editing. P.K.: investigation and writing–review & editing. M.W.: supervision and writing–review & editing. E.Z.: conceptualization, data curation, formal analysis, funding acquisition, investigation, supervision, writing–original draft, and writing–review & editing.

Conflict of interests

The authors declare that they have no known competing financial interests or personal relationships that could have appeared to influence the work reported in this paper.

Funding

This research was funded by the National Science Centre, Poland (No. 2018/29/N/NZ5/00810 to A.R.; 2018/31/B/NZ2/03248 to E.Z.) and the Institute of Human Genetics PAS, Minigrant (No. 2021/01 to A.R.).

Acknowledgements

The authors gratefully acknowledge: Professor Heymut Omran for providing information on the genotype distribution among German *SPAG1*-PCD patients; Doctors Andrzej Pogorzelski and Peter Durdik for providing biological material and clinical information concerning Polish-Slovakian *SPAG1*-PCD patients; all PCD families for contributing biological material for this study. The authors thank Katarzyna Voelkel (previously employed at the Institute of Human Genetics of the Polish Academy of Sciences) for many years of technical assistance and help in the genetic screening of PCD patients, and Dr. Patrick Perrigue (NanoBioMedical Centre, Adam Mickiewicz University) for providing *S. mediterranea* and help in developing the

planarian facility. M.D.Ś was supported by the Foundation for Polish Science (FNP) within the START scholarship program.

Data availability

The data that support the findings of this study are available from the corresponding authors upon reasonable request.

References

1. Knowles MR, Ostrowski LE, Loges NT, et al. Mutations in SPAG1 cause primary ciliary dyskinesia associated with defective outer and inner dynein arms. *Am J Hum Genet*. 2013;93(4):711-720.

2. Djakow J, Kramná L, Dušátková L, et al. An effective combination of Sanger and next generation sequencing in diagnostics of primary ciliary dyskinesia. *Pediatr Pulmonol*. 2016;51(5):498-509.

3. Li Q, Xu Z, Fang F, Shen Y, Lei H, Shen X. Identification of key pathways, genes and immune cell infiltration in hypoxia of high-altitude acclimatization via meta-analysis and integrated bioinformatics analysis. *Front Genet*. 2023;14:1055372.

4. Matthijs G, Schollen E, Van Schaftingen E, Cassiman JJ, Jaeken J. Lack of homozygotes for the most frequent disease allele in carbohydrate-deficient glycoprotein syndrome type 1A. *Am J Hum Genet*. 1998;62(3):542-550.

5. Li YQ, Zeng A, Han XS, et al. Argonaute-2 regulates the proliferation of adult stem cells in planarian. *Cell Res*. 2011;21(12):1750-1754.

Alicja Rabiasz[**], Monika Drobna-Śledzińska, Patrycja Kaźmierczak, Michał Witt[#], Ewa Ziętkiewicz[*]

Institute of Human Genetics, Polish Academy of Sciences, Poznań 60-479, Poland

* Corresponding author. Phone: +48 616579203.

** Corresponding author. Phone: +48 616579253.

E-mail addresses: ewa.zietkiewicz@igcz.poznan.pl (E. Ziętkiewicz),

alicja.rabiasz@igcz.poznan.pl (A. Rabiasz).

Affiliation expired.

Figure 1 The elucidation of the role of *POLR2K* in the pathogenesis of primary ciliary dyskinesia (PCD). **(A)** Scheme of the localization of pathogenic variants detected in the analyzed group of 60 *SPAG1*-PCD patients. Two frequent deletion are indicated above the gene scheme: 11,973 bp del: a large 11,973 bp deletion [NM_005034.4:c.61+201_NM_003114.5:c.140+1169]del, encompassing exons 1 and 2 of SPAG1 (sperm-associated antigen 1) and exons 3 and 4 of POLR2K (RNA polymerase II, I and III subunit K) located upstream of SPAG1 in chromosome 8q22.2 (indicated by a bracket); c.2014C>T in exon 16 (NM_003114.5:c.2014C>T; NP_003105.2:p.Gln672*). *SPAG1* exons with pathogenic variants are indicated by numbers. **(B)** Distribution of *SPAG1* genotypes in the combined group of 103 unrelated Caucasian *SPAG1*-PCD patients. Left panel: The count of observed genotypes. Right panel: The expected number of genotypes calculated assuming Hardy-Weinberg equilibrium. The expected number of the deletion homozygotes in the joint group of 103 *SPAG1*-PCD patients raised to eight; with none observed, the difference between observed and expected was statistically significant (P = 0.0066). **(C)** Analysis of the impact of *Smed-spag1* knockdown on *S. mediterranea* movement. Left: Effectiveness of the dsRNA-mediated *Smed-spag1* knockdown. DsRNA-

mediated knockdown reduced the relative expression level of *Smed-spag1* to 27% compared with control worms treated with dsRNA targeting *eGFP* (measured by quantitative reverse transcription PCR one day after the last administration of dsRNA; $n = 4$; $^{***}P < 0.001$). Right: The speed of planarians' locomotion at day 2 after the last administration of dsRNA (1.189 ± 0.371 and 0.354 ± 0.065 mm/s, in controls and *Smed-spag1*-silenced worms, respectively). Plots show the mean value of biological replicates ($n = 10$); error bars indicate standard deviation; $^{***}P < 0.001$. **(D)** Analysis of the impact of *Smed-polr2k* knockdown on *S. mediterranea*'s phenotype. Left: Effectiveness of the dsRNA-mediated *Smed-polr2k* knockdown. Quantitative reverse transcription PCR (measured one day after the last administration of dsRNA) showed a decrease in *Smed-polr2k* expression level to 14% compared with control worms; plots show the mean value of biological replicates ($n = 4$); error bars indicate standard deviation; $^{**}P < 0.01$. Right: Examples of worm's phenotype abnormalities (deformation of body shape, tissue lysis) after *Smed-polr2k* knockdown, compared with a control (upper and lower panel: day 3 and 11 after last dsRNA feeding, respectively); the defects finally lead to worms' death. The first changes in the worm's phenotype were observed 3 days after the last dsRNA feeding and affected 54% of the worms; it gradually affected all *Smed-polr2k*-silenced worms. Scale bar: 1 mm. **(E)** Efficiency of the siRNAs-mediated *POLR2K* knockdown in human cells, 48 h post transfection. Left: Quantitative reverse transcription PCR analysis of *POLR2K* mRNA level. *POLR2K* siRNA_1 and *POLR2K* siRNA_2 reduced the relative expression level of *POLR2K* to ~54% and ~78%, respectively (non-targeting siRNA was used as a negative control). Quantitative reverse transcription PCR plots show the mean value of biological replicates ($n = 5$); error bars indicate standard deviation; $^{**}P < 0.01$, $^{***}P < 0.001$. Right: Western blot analysis of POLR2K; at the protein level, the knockdown efficiency was comparable for both siRNAs; normalized to GAPDH. **(F)** Analysis of the impact of *POLR2K* knockdown on vital functions

in human cells. Left: Apoptosis assay performed using flow cytometry. Percentage of apoptotic cells: 7.2% and 8.3% 48 h after transfection with *POLR2K* siRNA_1 and *POLR2K* siRNA_2, respectively, compared with 3.9% in the negative control. Plots show the mean value of biological replicates ($n = 3$); error bars indicate standard deviation; $^{*}P < 0.05$, $^{***}P < 0.001$. Right: Cell proliferation rate (assessed using colorimetric assay) was calculated as the fold change in OD450 for each examined time point in reference to the starting point (0 h); biological replicates, $n = 3$; $^{***}P < 0.001$.

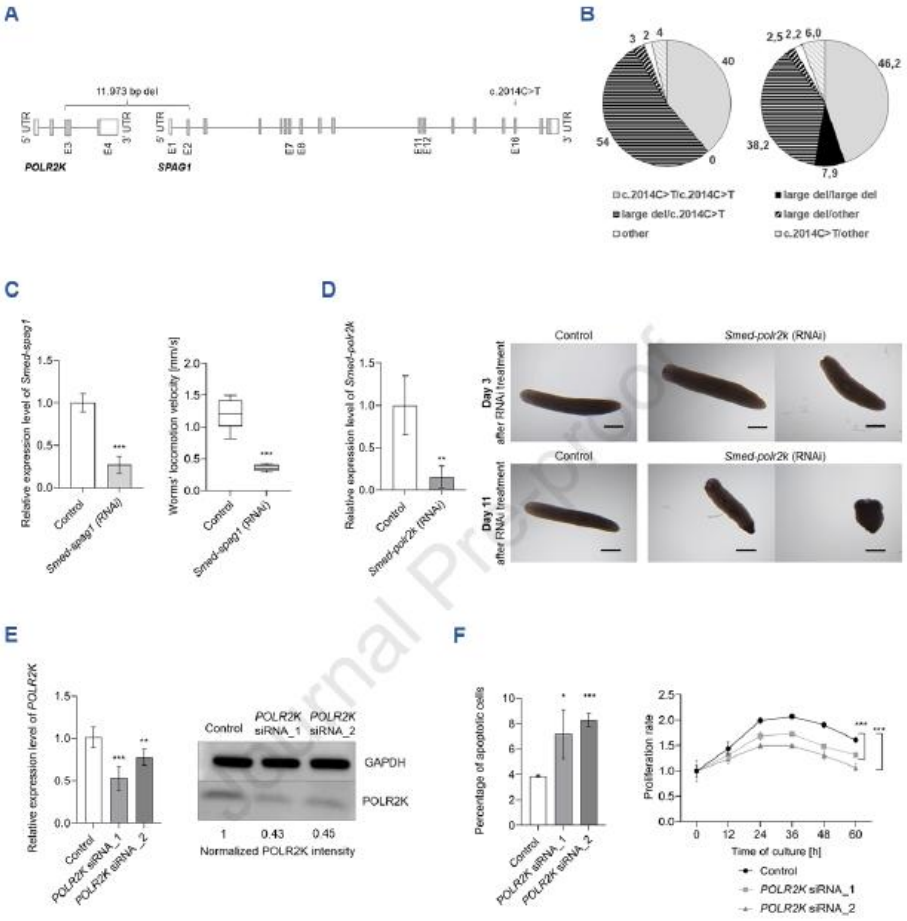

Supplementary Materials

The lack of homozygotes with large deletion encompassing *SPAG1* and *POLR2K* in primary ciliary dyskinesia patients suggests lethal effect of the loss of POLR2K protein

Alicja Rabiasz*, Monika Drobna-Śledzińska, Patrycja Kaźmierczak, Michał Witt#, Ewa Ziętkiewicz*

Institute of Human Genetics, Polish Academy of Sciences, 60-479 Poznań, Poland

*Correspondence: Alicja Rabiasz alicja.rabiasz@igcz.poznan.pl, phone: +48 616579253; Ewa Ziętkiewicz ewa.zietkiewicz@igcz.poznan.pl, phone: +48 616579203

#affiliation expired

1. Additional Background

Cilia and flagella are highly conserved organelles that form protrusions on the surface of many eukaryotic cells. Mutations in genes encoding ciliary structural proteins or proteins involved in cilia biogenesis affect a variety of tissues and organs of the human body and lead to a wide range of diseases and syndromic disorders named ciliopathies [1]. Primary ciliary dyskinesia, PCD (OMIM244400) is a key example of a hereditary ciliopathy caused by the dysfunction of motile cilia. Multiple clinical symptoms of PCD (lower and upper respiratory tract distress, hearing impairment, infertility in men or lower fertility in women, and randomization of the body plan symmetry in 50% of PCD patients) reflect the role of motile cilia in human body [2,3]. The most cited population frequency of PCD is 1:10,000 to 1:20,000 [e.g. [4]], but due to the heterogeneity of clinical symptoms its actual prevalence may be higher; in addition, it differs considerably depending on the population [5,6]. PCD is mainly inherited in an autosomal recessive manner, and is characterized by a high genetic and allelic heterogeneity; until now, more than 50 genes have been identified to underlie the molecular basis of PCD [2,7].

SPAG1 (sperm-associated antigen 1) is one of the genes whose recessively inherited pathogenic variants cause PCD, through impairing assembly of dynein arms, essential elements of the ciliary structure and function [8]. Two most frequent pathogenic variants in *SPAG1*, originally reported in eight of ten [8] and later in eight more [9] unrelated Caucasian PCD patients, are: nonsense mutation in exon 16 (NM_003114.5:c.2014C>T; NP_003105.2:p.Gln672*), and a large 11,973 bp deletion, [NM_005034.4:c.61+201__NM_003114.5:c.140+1169]del, encompassing exons 1 and 2 of *SPAG1* and exons 3 and 4 of another gene, *POLR2K* (RNA Polymerase II, I and III Subunit K) located upstream of *SPAG1* in chromosome 8q22.2. Of these two variants, c.2014C>T has been described in both

homozygotes and in compound heterozygotes, most frequently with the large 11,973 bp deletion as the second allele. However, no homozygotes of the large deletion have been reported. The same was observed in a much larger group of 60 *SPAG1*-PCD patients reported in our study, and in the German group of 25 *SPAG1*-PCD individuals (Heymut Omran, personal communication), prompting us to examine the basis of this unbalanced distribution of the genotypes. We suspected that the lack of homozygous patients with the large deletion reflected lethal effect of the loss of a functional POLR2K rather than of SPAG1 protein. To confirm this hypothesis we examined the effect of RNA interference (RNAi)-mediated knockdown of *POLR2K* at two levels: the whole model organism (ciliated flatworm, *Schmidtea mediterranea),* and the human cell line. *S. mediterranea* is a free-living invertebrate from phylum *Platyhelminthes* (flatworms) and it is well known for its remarkable ability to regenerate after injury or amputation thanks to the presence of numerous adult stem cells (neoblast) [10]. Planarians are used as an alternative model system for studying the functionality of embryonic lethal genes in the adult body [11]. They also provide an attractive model to study cilia-related genes, including PCD genes, because their locomotion (so-called gliding movement) depends on motile cilia covering the ventral site of their body. Knockdown of genes encoding ciliary proteins results in changes in the speed and locomotion pattern of worms (the so-called inchworming movement) [12].

2. Materials and methods

Patient samples collection and genetic screening

Patients were classified as PCD in concordance with European guidelines in PCD. The general clinical evaluation criteria followed the European Respiratory Society recommendations for PCD diagnosis [13]. The majority of the patients had *situs inversus* in addition to pulmonary symptoms [see Supplementary Table 3]. Genetic data referred to in the manuscript were collected over many years as a component of routine hospital diagnostic procedures. DNA isolated form peripheral blood samples collected from affected individuals was subjected to genetic testing as earlier described [14]. Genetic testing was a combination of single-strand conformation polymorphism (SSCP) screening, multiplex ligation-dependent probe amplification (MLPA) analysis and/or whole exome sequencing (WES); detected variants were confirmed by direct dideoxy sequencing [see Supplementary Table 4 and Sequence analysis of the pathogenic variants]. All identified pathogenic variants were examined using a variant validation tool, VariantValidator [15], and were classified according to the recommendation of the American College of Medical Genetics and Genomics (ACMG) and the Association for Molecular Pathology (AMP) [16].

Schmidtea mediterranea

An asexual strain of *S. mediterranea* planarian, originally obtained from Kerstin Bartscherer (Osnabrück University, Germany), was kindly provided by Patrick Perrigue (NanoBioMedical Centre, Adam Mickiewicz University, Poland). Planarians were maintained at 20°C (Binder cooling incubator) in water culture (1 x Montjuïch salts [17]). Before experiments, planarians 3-5 mm in length were starved for at least 7 days.

Human cell line

The HEK293T cell line, a kind gift from Maciej Kurpisz (Institute of Human Genetics, Polish Academy of Sciences, Poland), was used. Cells were maintained in standard conditions in Dulbecco's modified Eagle's medium (Gibco, Thermo Fisher Scientific, Waltham, MA, USA) with 10% fetal bovine serum (Gibco, Thermo Fisher Scientific) and 1% penicillin/streptomycin solution (Sigma Aldrich, St. Louis, MO, USA), and incubated at 37°C and 5% CO_2 in a humidified atmosphere (Binder CO_2 incubator).

RNA interference (RNAi)-mediated knockdown in planarians

Gene knockdown was performed using double-stranded RNA (dsRNA)-feeding method, as described earlier [18]. DsRNAs were designed based on the available transcriptomic and genomic data deposited in Planmine database [19], using the E-RNAi webservice [20] which provides information on the possible off-target effect at the dsRNA design stage. DsRNAs of *Smed-polr2k* (dd_Smed_v6_2720_0_1) and *Smed-spag1* (dd_Smed_v6_2532_0_1), hereafter referred to as *polr2k* and *spag1*, respectively), were synthetized using MEGAscript™ T7 Transcription Kit (Invitrogen). Of note, dd_Smed_v6_2532_0_1 (3145 nt) is annotated as a putative chimeric transcript in Planmine database (accessed on 06 February 2024). To prevent designing dsRNA targeting chimera, homologous transcripts of dd_Smed_v6_2532_0_1 in other *S. mediterranea* transcriptomes deposited in Planmine database were analyzed; following comparison of the homologous transcripts and predicted gene sequences, ka_Smed_v1_GCZZ01056363.1 (2315 nt) was used as a template to design and synthesize dsRNA targeting *spag1*. Transcripts to be used as a template for dsRNAs synthesis were amplified from asexual *S. mediterranea* cDNA using primers tagged with T7 RNA polymerase promotor [see Supplementary Table 5].

DsRNAs targeting *polr2k* or *spag1* were mixed with a homogenized chicken liver and administered to the worms by repetitive feeding (two times per week for 2 weeks); 10 µg dsRNA mixed with 50 µL of liver paste per 10 worms were used. As a control, worms were fed with dsRNA targeting eGFP (enhanced green fluorescence protein) prepared from the pEGFP-C1 plasmid containing eGFP insert. The plasmid was kindly provided by Maciej Śmiałek (Institute of Human Genetics, Polish Academy of Sciences, Poland). One day after the last feeding, a subgroup of worms treated with *polr2k* or *eGFP* dsRNA were cut to stimulate regeneration process.

Effects of *spag1* or *polr2k* genes knockdown on the worms phenotype were analyzed and recorded using a stereoscope (Opta-Tech, SK series) with camera. The locomotion speed of worms after *spag1* knockdown and control worms (fed with eGFP dsRNA) was measured using ImageJ [21] (ten worms were analyzed for each condition). Measurement of the speed of planarian' locomotion was calculated by dividing the actual distance traveled by a worm (distance traveled minus the length of a worm) by the duration of the movie.

Transfection of HEK293T cell line

The HEK293T cells at ~ 50% confluence were separately transfected with three siRNAs (Invitrogen, Carlsbad, CA, USA) at the final concentration of 5 nM; two siRNAs targeting different regions of *POLR2K* exon 3 (Silencer™ Select siRNA, ID 10822 and 10824), and a non-targeting control (Silencer™ Select Negative Control No. 1 siRNA). Cells were transfected using jetPRIME® transfection reagent (Polyplus-transfection SA, Illkirch-Graffenstaden, France) according to the manufacturer's protocol. Transfected cells were used for RT-qPCR, Western blot and cellular assays (cell proliferation, apoptosis).

RNA extraction and qRT-PCR in HEK293T cell line and *S. mediterranea*

Quantitative real-time reverse-transcription PCR (qRT-PCR) was carried out to confirm the effectiveness of *polr2k* and *spag1* knockdown in *S. mediterranea* or *POLR2K* knockdown in the HEK293T cell line. RNA was collected one day after the last feeding of worms or 48h after HEK293T cells transfection. Total RNA was isolated using TRI Reagent (Invitrogen) and purified from DNA contaminants using TURBO DNA-free Kit (Ambion) according to the manufacturer's protocols. 500 ng of RNA was reverse transcribed with RevertAid H Minus First Strand cDNA Synthesis Kit (ThermoScientific), using oligo(dT) primer to process messenger RNA only. The resulting cDNA was used as a template in qRT-PCR performed using 7900HT Fast Real-Time PCR System with 96-well block module (Applied Biosystems), with HOT FIREPol® EvaGreen® qPCR Mix Plus (Solis BioDyne) and primers designed to target specific mRNAs [see Supplementary Table 5]. The level of house-keeping transcripts, Smed-*gapdh* (for worms) or ACTB (for HEK293T), was used as an endogenous control. The relative quantification of the studied genes' expression level was performed using a comparative CT (ΔΔ CT) method. All qRT-PCR reactions were performed in three technical replicates for each biological replicate (four replicates for worms and five replicates for the cell line).

Protein analysis

48 h after transfection, cells were collected and lysed using RIPA buffer with protease inhibitor cocktail and EDTA (ThermoScientific). Protein concentration was determined using Pierce BCA Protein Assay Kit (ThermoScientific). Proteins were denatured and separated on 4-20% Mini-PROTEAN TGX Stain-

free Gel (Bio Rad). After electrophoresis, proteins were transferred onto 0.45 µm PVDF Low Fluorescence membrane (Bio Rad). Membranes were blocked using 5% non-fat milk and incubated with 1:1500 anti-POLR2K (Gene-Tex, GTX132871) or 1:20000 anti-GAPDH (Abcam, ab9485). After washing, membranes were incubated with 1:40000 anti-Rabbit (Abcam, ab97051) secondary antibody. Immunoreactive protein bands were detected with Clarity Western ECL Substrate (Bio-Rad) on Chemidoc Imaging System (Bio Rad). The abundance of POLR2K was assessed in reference to GAPDH using Image Lab 6.0.1 software (Bio Rad). Each experiment was conducted in three biological replicates. Whole uncropped membrane is shown in Supplementary Figure 2.

Proliferation assay

Cells were seeded on 96-well plate (40,000 cells per well) in culture medium and were transfected 24h after seeding. The CCK8 test (Cell Counting Kit 8, Sigma Aldrich) was conducted in a time-dependent manner from 0 to 60 h after transfection. Cells were incubated with 10 µL of CCK8 reagent for 4 h at 37◦C. Absorbance was measured using GloMax-Multi+ Detection System (Promega). Each experiment was conducted in four technical and three biological replicates.

Apoptosis assay

Cells were seeded on 12-well plate (200,000 cells per well) in culture medium and were transfected 24h after seeding. 48 h after transfection, cells were collected and stained with Annexin V-FITC (BD Biosciences, San Jose, CA, USA). Populations of apoptotic and non-apoptotic cells were detected with a CytoFlex S cytometer (Beckman Coulter, Brea, CA, USA). Results were analyzed using CytExpert Software (Beckman Coulter). Each experiment was conducted in three biological replicates. Representative plots for apoptosis assay are shown in Supplementary Figure 3.

Statistical analysis

The statistical significance of differences between the proportion of genotypes observed and expected under Hardy-Weinberg equilibrium was calculated using chi-square test.

In the analysis of the relative gene expression level, apoptosis or planarians' locomotion speed, where two independent means were compared, data were first analyzed for the normality with Shapiro–Wilk test, and statistical significance of the difference was calculated using unpaired two-tailed t-test.

In proliferation assays, the statistical significance of the differences between control and *POLR2K* siRNAs-treated cells was calculated with a two-way ANOVA using the Tukey post-hoc test. The statistical significance of the results was evaluated and visualized using the GraphPad Prism version 9 (GraphPad Software).

3. Additional Discussion

The lack of homozygotes of the large deletion encompassing parts of *SPAG1* and the upstream *POLR2K* has been observed in the earlier studies [8,9], but was not as obvious due to the smaller number of reported unrelated Caucasian PCD patients with pathogenic *SPAG1* variants (n=18). In 60 unrelated Polish-Slovakian patients with two *SPAG1* mutations, as well as in the German group of 25 patients, the lack of homozygotes with the large deletion was striking. The expected number of homozygotes under Hardy-Weinberg equilibrium in the combined group of 103 Caucasian SPAG1-PCD patients was eight, while none was observed; this discrepancy between the observed and expected distribution of haplotypes was highly significant (p=0.0066). A similar distribution of genotypes, with the significant lack of homozygotes of one of the alleles, has been described in *PMM2* gene. In the cohort of 54 Caucasian patients suffering with carbohydrate-deficient–glycoprotein syndrome type 1 with a PMM deficiency, 43 were heterozygous for R141H variant, but no homozygotes were observed in contrast to 8 expected under Hardy-Weinberg equilibrium; the authors concluded that this distribution was probably caused by selection against the homozygous R141H [22] .

It should be emphasized that the frequency of homozygous mutations introducing premature STOP codon located in *SPAG1* exon 16 (c.2014C>T) was even higher than expected under equilibrium, indicating the lack of selection against a homozygous deficiency of the wild-type *SPAG1*. The possibility that homozygous truncation at exon 16 was less deleterious than the lack of the full-length protein can be rejected based on the observation that the compound heterozygote, in whom the large deletion was combined with the pathogenic variant in exon 2 (c.1A>G, expected to abrogate the start codon and thus to prevent translation of the whole protein), had a typical PCD phenotype. We hypothesized that the lack of homozygotes with the large deletion, encompassing exons 1-2 of *SPAG1* and exons 3-4 of *POLR2K*, reflected a highly deleterious, possibly lethal effect of the loss of a functional POLR2K rather than of SPAG1 protein.

To provide a molecular context to this observation, we analyzed the impact of *POLR2K* silencing on phenotypes at the whole organism (planarians) and cellular (human cell line) levels. The dsRNA-mediated knockdown of *spag1* in the *S. mediterranea* model did not affect viability of the organisms, but – as expected – impaired worms movement, confirming the evolutionary conserved role of *SPAG1* in the motile cilia function, which was also previously demonstrated using a vertebrate model, zebrafish [8]. In contrast, silencing of *polr2k* in the same model resulted in a much more severe phenotype, and suggested that *polr2k* plays an essential role in maintaining body homeostasis by regulating cell turnover, probably through the impact on planarian stem cells proliferation. Our observations in the planarian model are in line with those in other studies where the deleterious/lethal

effects of the knockdown of other essential genes on *S. mediterranea* phenotype have been reported [e.g. [11,23–27]]. For example, RNAi-mediated knockdown of the essential gene, *Argonaute RISC Catalytic Component 2* (*Smed-ago2*), led to regeneration defects or tissue regression in worms, ultimately causing their death, demonstrating that *Smed-ago2* is crucial for tissue homeostasis and regeneration and acts through a regulation of adult stem cells proliferation [24].

Our results obtained in the human cell culture with siRNA-mediated knockdown of *POLR2K* shed light on the mechanisms of defects observed in the planarian model, confirming essential role of *POLR2K* in the regulation of vital cell functions, manifested by decreased cell proliferation and increased apoptosis upon its knockdown.

The essential role of *POLR2K* is supported by many studies. *POLR2K* represents one of the smallest subunits of RNA polymerase II, shared with two other RNA polymerases; in consequence, *POLR2K* is involved in the RNA processing machinery and improves RNA polymerase III pre-initiation complex assembly [28]. There are reports about the association of this gene with cancer development [29,30], lethal prostate cancer [31], and predicted breast cancer immunotherapy [32]. Other studies indicate protective role of *POLR2K* against liver injury [33] and its participation in lymphocyte innateness [34]. In a few reports *POLR2K* has been mentioned among hub genes responsible for diverse gene interaction networks: in chronic kidney disease [35], polycystic ovary syndrome [36], cancer [37], high-altitude hypoxia [28]. In the study, which demonstrated that the high mortality of bovine embryos derived from somatic cell nuclear transfer is related to the absence of three regulatory networks in the early embryonic stage, *POLR2K* has been mentioned in the core of one of these networks [38].

In spite of the repetitive reports suggesting the importance of *POLR2K* in many cellular processes, which is expected given the role of POLR2K in RNA processing machinery, the direct observation of phenotype changes after RNAi-mediated *POLR2K* knockdown in a model organism or a human cell line has not been published so far. Our findings confirm that *POLR2K* is necessary for functioning of living organisms and suggest that its influence on cell turnover is exerted through a regulation of cell proliferation and protection from cell apoptosis. Moreover, our study provides evidence that the essential role of *POLR2K* in vital cell functions is evolutionary conserved. Finally, these results, together with the aforementioned studies regarding *POLR2K* as a hub gene involved in many essential interactions, support our starting hypothesis that the lack of homozygotes of the large deletion involving *SPAG1* and *POLR2K* genes is caused by the lethal impact of the POLR2K deficiency.

In view of the fundamental role of *POLR2K* in the normal functioning of the cell, it is tempting to hypothesize that its absence is lethal. Similar to earlier suggestions concerning the missing variant in the *PMM2* gene[22], it would be interesting to look for the association of the homozygous large deletion

variant encompassing *POLR2K* and *SPAG1* with idiopathic miscarriages; however, the expected frequency of families, in which both parents are carriers of the large deletion, is very low. Alternatively, analyzing progeny of a transgenic animal model (e.g. mouse or fish) carrying the heterogenic large deletion may be the way to confirm a possible lethality of the homozygous deficiency of *POLR2K*.

4. Supplementary Tables

Supplementary Table 1. Description of pathogenic variants.

Affected *SPAG1* exons	**Pathogenic variants** (genome build: GRCh38)	Evidence of pathogenicity	ACMG/AMP category
1_2	large (11,973bp) deletion, encompassing: chr8(GRCh38):g.100151617_100163589del nsv3873246, corresponding to [NM_005034.4:c.61+201 (*POLR2K* intron 2)_ NM_003114.5:c.140+1169 (*SPAG1* intron 2)]del	very strong	PVS1 null variant - multiexonic deletion
2	NM_003114.5:c.1A>G; NP_003105.2:p.Met1 loss of start or splice region variant novel	very strong	PVS1 null variant - initiation codon
7	NM_003114.5:c.600_603del; NP_003105.2:p.T201Rfs*28 novel; rs1258068273	very strong	PVS1 null variant - frameshift
8	NM_003114.5:c.762_763insAAAA NP_003105.2:p.L255Kfs*7 novel	very strong	PVS1 null variant - frameshift
11	NM_003114.5:c.1395del; p.G466Afs*21 novel	very strong	PVS1 null variant - frameshift
12	NM_003114.5:c.1436G>A; NP_003105.2:p.G479E; acceptor splice site region novel; rs1817848640	strong	PS3 acceptor splice site region – experiment confirmed damaging effect on the gene product[1]
16	NM_003114.5:c.2014C>T; NP_003105.2:p.Q672* rs201740530	very strong	PVS1 null variant - nonsense

Available rs numbers are indicated in superscript; "novel" superscript indicates pathogenic *SPAG1* variants not reported before in the context of PCD; [1]the disruption of acceptor splice site was confirmed at the mRNA level [Supplementary Figure 4].

Supplementary Table 2. Distribution of patients' genotypes in the analyzed group of 60 *SPAG1*-PCD patients.

Observed genotypes (affected *SPAG1* exons)	Number of unrelated individuals with a particular genotype
1_2/16	28 (including 1 Slovak)
16/16	27 (including 6 Slovaks)
16/8	1
16/11	1
16/12	1
1_2/7	1
1_2/2	1

Supplementary Table 3. Number of patients with and without *situs inversus*.

Observed genotypes (affected *SPAG1* exons)	Number of patients with the presence/absence of situs inversus (SI)
1_2/16	20 with SI; 5 without SI; 3 N/A
16/16	16 with SI; 10 without SI; 1 N/A
16/8	1 without SI
16/11	1 without SI
16/12	1 without SI
1_2/7	1 with SI
1_2/2	1 without SI

N/A- not applicable; no information about SI in medical information.

Supplementary Table 4. List of primers used for patients samples analysis.

Primers name	Primer sequence	Expected product size [bp]
POLR2K_i2_F	tagacctgggttcgtccttg	in sample with deletion:
SPAG1_i2_R	tttttatttatccgtccttgacc	311
SPAG1_2_F	tggttaccactatccaaattgag	321
SPAG1_2_R	catgcatgggcaaaaaca	
SPAG1_7_F	cctaagcttggggaacctttt	281
SPAG1_7_R	aaaccccaacaaacatctgc	
SPAG1_8_F	accttaggcttgcttgttgc	229
SPAG1_8_R	tggtctttattaatggatcctgc	
SPAG1_11B_F2	ctgaagagccagggcaac	201
SPAG1_11B_R2	gcgcctgtcattcagga	
SPAG1_12_F	ggccgtcttgtaattctggt	247
SPAG1_12_R	ggatcttggatattgcattcac	
SPAG1_16_F	acagatagccaatctttacctttca	277
SPAG1_16_R	cctcaatcccatcccaagat	
Primers for cDNA analysis		
SPAG1_e11_F	CAAGTACTCGGCGGCAAT	180
SPAG1_e13_R	CGCCTCAGAAGAGGTTTCAT	
GAPDH_e4_F	ACGGGAAGCTTGTCATCAAT	382
GAPDH_e8_R	GGGCCATCCACAGTCTTCT	

Lower case – primers in introns; upper case – primers in exons

Supplementary Table 5. List of primers used for dsRNA synthesis and in RT-qPCR

Primers name	Primer sequence
Primers for dsRNA synthesis	
dsRNA_Smed_POLR2K_R	TAATACGACTCACTATAGGGcaacacttcaacgaccttcaaa
dsRNA_Smed_POLR2K_F	TAATACGACTCACTATAGGGttcgtctgaagcaaaacaagt
dsRNA_Smed_SPAG1_R	TAATACGACTCACTATAGGGttctttttctaacacggcagc
dsRNA_Smed_SPAG1_F	TAATACGACTCACTATAGGGaattgccgacgaacttgaga
dsRNA_eGFP_R	TAATACGACTCACTATAGGGagttcaccttgatgccgttc
dsRNA_eGFP_F	TAATACGACTCACTATAGGGcacatgaagcagcacgactt
Primers for RT-qPCR of worms (Smed) and human (Hs) samples	
RTPCR_Smed_POLR2K_R	ataatgtctttaggcttcatttcg
RTPCR_Smed_POLR2K _F	tgaataattcgtctgaagcaaaac
RTPCR_Smed_SPAG1_R	tccccatttcccgatagcat
RTPCR_Smed_SPAG1_F	cgattgcaaaagttgtcgcc
RTPCR_Smed_GAPDH_R	cagatcgattacacggcaac
RTPCR_Smed_GAPDH_F	atcaaggccgctattaagca
RTPCR_Hs_POLR2K_R	cccagcattcatcgagcatc
RTPCR_Hs_POLR2K_F	cctccaaagcagcaaccaat
RTPCR_Hs_ACTB_R	atcttgatcttcattgtgctg
RTPCR_Hs_ACTB_F	cttcctgggcatggagtcc

The uppercase letters describe the sequence recognized by the T7 RNA polymerase.

5. Supplementary Figures

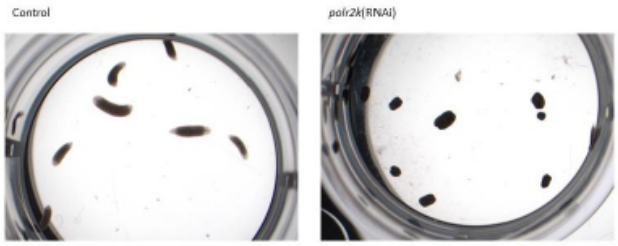

Supplementary Figure 1. Analysis of the effect of dsRNA-mediated *polr2k* knockdown on the regeneration capacity of *S. mediterranea;* an example of *polr2k*(RNAi) worms regenerated from the middle part of worm in comparison to a control group at the same time point (7 days post amputation, dpa); the presented defects of the regeneration process ultimately lead to the death of *polr2k*-silenced worms.

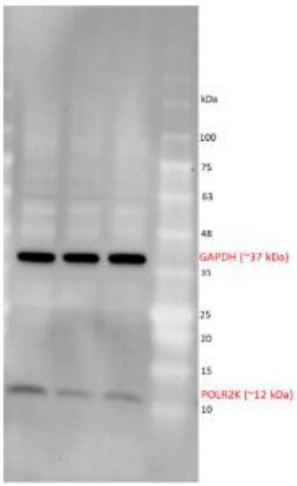

Supplementary Figure 2. Chemiluminescent blot for Western Blot of POLR2K and GAPDH proteins in HEK293T cell line after *POLR2K* gene silencing.

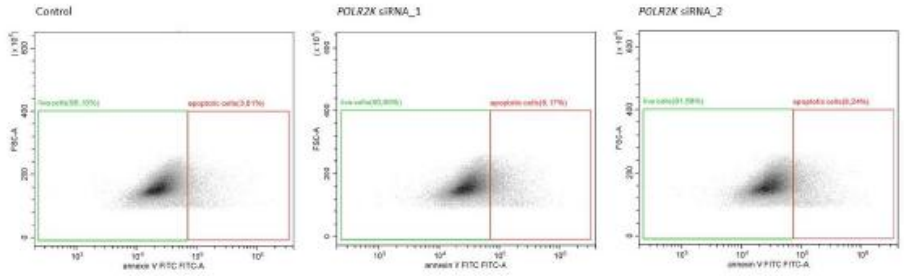

Supplementary Figure 3 Representative plots for apoptosis assay of HEK293T cells after *POLR2K* siRNA-mediated knockdown.

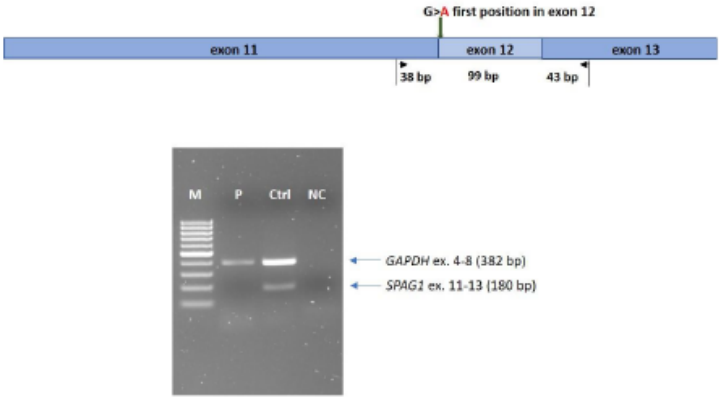

Supplementary Figure 4. Analysis of the effect of a substitution at the first position of exon 12 of *SPAG1*. The G>A substitution at the first position of exon 12 (theoretically causing a missense mutation, p.G479E) from patient's cDNA disrupted acceptor splicing site, resulting in the lack of a product amplified with primers located in exons 11 and 13. Legend: M- marker DNA Molecular Weight Marker, 100bp Ladder (Thermofisher), P- patient, Ctrl- healthy control (non-PCD individual), NC- negative control (water).

6. Sequence analysis of the pathogenic variants

***POLR2K* exons 3_4 - *SPAG1* exons 1_2**

Only sequence of the allele with the large deletion was analyzable using Sanger sequencing

chr8(GRCh38):g.100151617_100163589del; breakpoint: in *POLR2K* intron 2 (c.61+201) and *SPAG1* intron 2 (c.140+1169);

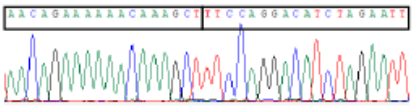

large deletion

POLR2K intron 2…*SPAG1* intron2

AACAGAAAAAAACAAAGCTcgttgagatttcattctctctcctgga…cacttgtggagcatgaactgctttgctTTCCAGGACATCTAGAATT

Uppercase: the sequence in the individual with the large deletion.

***SPAG1* exon 2**

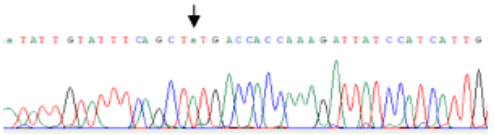

wt

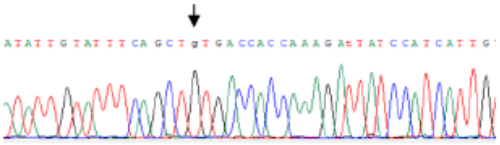

NM_003114.5:c.1A>G

hemizygote

***SPAG1* exon 7**

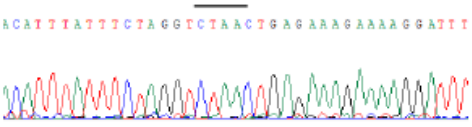

wt

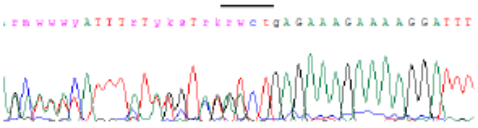

NM_003114.5:c.600_603delCTAA

heterozygote

***SPAG1* exon 8**

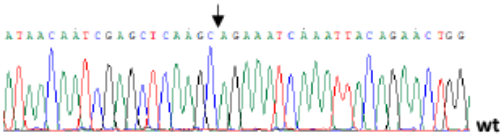

wt

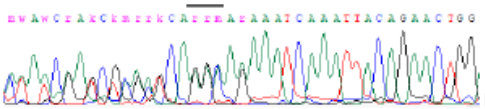

NM_003114.5:c.762_763insAAAA

heterozygote

***SPAG1* exon 11**

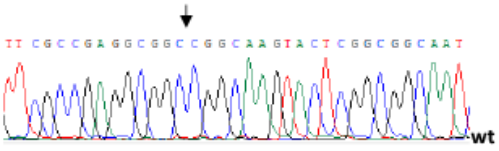

wt

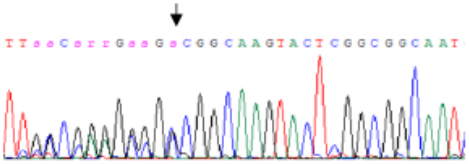

NM_003114.5:c.1395delC

heterozygote

***SPAG1* exon 12**

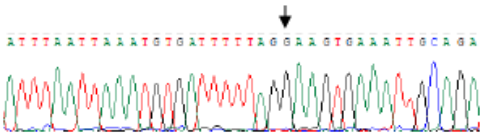

wt

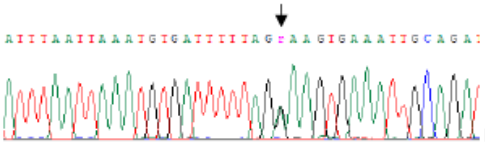

NM_003114.5:c.1436G>A

heterozygote

***SPAG1* exon 16**

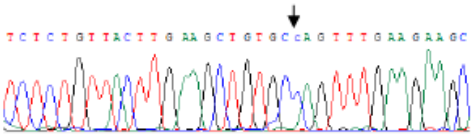

wt

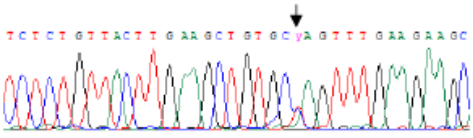

NM_003114.5:c.2014C>T

heterozygote

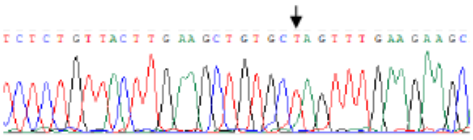

NM_003114.5:c.2014C>T homozygote

Supplementary References

1. Wirschell M, Yamamoto R, Alford L, Gokhale A, Gaillard A, Sale WS. Regulation of ciliary motility: conserved protein kinases and phosphatases are targeted and anchored in the ciliary axoneme. *Arch Biochem Biophys*. 2011;510(2):93-100. doi:10.1016/j.abb.2011.04.003

2. Goutaki M, Shoemark A. Diagnosis of Primary Ciliary Dyskinesia. *Clin Chest Med*. 2022;43(1):127-140. doi:10.1016/j.ccm.2021.11.008

3. Wallmeier J, Nielsen KG, Kuehni CE, et al. Motile ciliopathies. *Nat Rev Dis Primers*. 2020;6(1):77. doi:10.1038/s41572-020-0209-6

4. Wee WB, Gatt D, Seidl E, Santyr G, To T, Dell SD. Estimates of primary ciliary dyskinesia prevalence: a scoping review. *ERJ Open Res*. 2024;10(4):00989-02023. doi:10.1183/23120541.00989-2023

5. Ardura-Garcia C, Goutaki M, Carr SB, et al. Registries and collaborative studies for primary ciliary dyskinesia in Europe. *ERJ Open Res*. 2020;6(2):00005-02020. doi:10.1183/23120541.00005-2020

6. Hannah WB, Seifert BA, Truty R, et al. The global prevalence and ethnic heterogeneity of primary ciliary dyskinesia gene variants: a genetic database analysis. *Lancet Respir Med*. 2022;10(5):459-468. doi:10.1016/S2213-2600(21)00453-7

7. Legendre M, Zaragosi LE, Mitchison HM. Motile cilia and airway disease. *Semin Cell Dev Biol*. 2021;110:19-33. doi:10.1016/j.semcdb.2020.11.007

8. Knowles MR, Ostrowski LE, Loges NT, et al. Mutations in SPAG1 cause primary ciliary dyskinesia associated with defective outer and inner dynein arms. *Am J Hum Genet*. 2013;93(4):711-720. doi:10.1016/j.ajhg.2013.07.025

9. Djakow J, Kramná L, Dušátková L, et al. An effective combination of sanger and next generation sequencing in diagnostics of primary ciliary dyskinesia. *Pediatr Pulmonol*. 2016;51(5):498-509. doi:10.1002/ppul.23261

10. Reddien PW. The Cellular and Molecular Basis for Planarian Regeneration. *Cell*. 2018;175(2):327-345. doi:10.1016/j.cell.2018.09.021

11. Ziman B, Barghouth PG, Maciel EI, Oviedo NJ. TRAF-like Proteins Regulate Cellular Survival in the Planarian Schmidtea mediterranea. *iScience*. 2020;23(11):101665. doi:10.1016/j.isci.2020.101665

12. Rabiasz A, Ziętkiewicz E. Schmidtea mediterranea as a Model Organism to Study the Molecular Background of Human Motile Ciliopathies. *Int J Mol Sci*. 2023;24(5):4472. doi:10.3390/ijms24054472

13. Lucas JS, Barbato A, Collins SA, et al. European Respiratory Society guidelines for the diagnosis of primary ciliary dyskinesia. *Eur Respir J*. 2017;49(1):1601090. doi:10.1183/13993003.01090-2016

14. Zietkiewicz E, Bukowy-Bieryllo Z, Rabiasz A, et al. CFAP300: Mutations in Slavic Patients with Primary Ciliary Dyskinesia and a Role in Ciliary Dynein Arms Trafficking. *Am J Respir Cell Mol Biol*. 2019;61(4):440-449. doi:10.1165/rcmb.2018-0260OC

15. Freeman PJ, Hart RK, Gretton LJ, Brookes AJ, Dalgleish R. VariantValidator: Accurate validation, mapping, and formatting of sequence variation descriptions. *Hum Mutat*. 2018;39(1):61-68. doi:10.1002/humu.23348

16. Richards S, Aziz N, Bale S, et al. Standards and guidelines for the interpretation of sequence variants: a joint consensus recommendation of the American College of Medical Genetics and Genomics and the Association for Molecular Pathology. *Genet Med*. 2015;17(5):405-424. doi:10.1038/gim.2015.30

17. Cebrià F, Newmark PA. Planarian homologs of netrin and netrin receptor are required for proper regeneration of the central nervous system and the maintenance of nervous system architecture. *Development*. 2005;132(16):3691-3703. doi:10.1242/dev.01941

18. Rouhana L, Weiss JA, Forsthoefel DJ, et al. RNA interference by feeding in vitro-synthesized double-stranded RNA to planarians: methodology and dynamics. *Dev Dyn*. 2013;242(6):718-730. doi:10.1002/dvdy.23950

19. Rozanski A, Moon H, Brandl H, et al. PlanMine 3.0-improvements to a mineable resource of flatworm biology and biodiversity. *Nucleic Acids Res*. 2019;47(D1):D812-D820. doi:10.1093/nar/gky1070

20. Horn T, Boutros M. E-RNAi: a web application for the multi-species design of RNAi reagents—2010 update. *Nucleic Acids Res*. 2010;38(Web Server issue):W332-W339. doi:10.1093/nar/gkq317

21. Rompolas P, Azimzadeh J, Marshall WF, King SM. Analysis of ciliary assembly and function in planaria. *Methods Enzymol*. 2013;525:245-264. doi:10.1016/B978-0-12-397944-5.00012-2

22. Matthijs G, Schollen E, Van Schaftingen E, Cassiman JJ, Jaeken J. Lack of homozygotes for the most frequent disease allele in carbohydrate-deficient glycoprotein syndrome type 1A. *Am J Hum Genet*. 1998;62(3):542-550.

23. Palakodeti D, Smielewska M, Lu YC, Yeo GW, Graveley BR. The PIWI proteins SMEDWI-2 and SMEDWI-3 are required for stem cell function and piRNA expression in planarians. *RNA*. 2008;14(6):1174-1186. doi:10.1261/rna.1085008

24. Li YQ, Zeng A, Han XS, et al. Argonaute-2 regulates the proliferation of adult stem cells in planarian. *Cell Res*. 2011;21(12):1750-1754. doi:10.1038/cr.2011.151

25. Thiruvalluvan M, Barghouth PG, Tsur A, Broday L, Oviedo NJ. SUMOylation controls stem cell proliferation and regional cell death through Hedgehog signaling in planarians. *Cell Mol Life Sci*. 2018;75(7):1285-1301. doi:10.1007/s00018-017-2697-4

26. Pryszlak M, Wiggans M, Chen X, et al. The DEAD-box helicase DDX56 is a conserved stemness regulator in normal and cancer stem cells. *Cell Rep*. 2021;34(13):108903. doi:10.1016/j.celrep.2021.108903

27. Allen JM, Balagtas M, Barajas E, et al. RNAi Screen of RING/U-Box Domain Ubiquitin Ligases Identifies Critical Regulators of Tissue Regeneration in Planarians. *Frontiers in Cell and Developmental Biology*. 2022;9. Accessed February 25, 2024. https://www.frontiersin.org/articles/10.3389/fcell.2021.803419

28. Li Q, Xu Z, Fang F, Shen Y, Lei H, Shen X. Identification of key pathways, genes and immune cell infiltration in hypoxia of high-altitude acclimatization via meta-analysis and integrated bioinformatics analysis. *Front Genet*. 2023;14:1055372. doi:10.3389/fgene.2023.1055372

29. Heidenblad M, Lindgren D, Jonson T, et al. Tiling resolution array CGH and high density expression profiling of urothelial carcinomas delineate genomic amplicons and candidate target genes specific for advanced tumors. *BMC Med Genomics*. 2008;1:3. doi:10.1186/1755-8794-1-3

30. Lin Y, Li Z, Ozsolak F, et al. An in-depth map of polyadenylation sites in cancer. *Nucleic Acids Res*. 2012;40(17):8460-8471. doi:10.1093/nar/gks637

31. Kelly RS, Sinnott JA, Rider JR, et al. The role of tumor metabolism as a driver of prostate cancer progression and lethal disease: results from a nested case-control study. *Cancer Metab*. 2016;4:22. doi:10.1186/s40170-016-0161-9

32. López-Cortés A, Cabrera-Andrade A, Vázquez-Naya JM, et al. Prediction of breast cancer proteins involved in immunotherapy, metastasis, and RNA-binding using molecular descriptors and artificial neural networks. *Sci Rep*. 2020;10(1):8515. doi:10.1038/s41598-020-65584-y

33. Pang C, Sheng Y chen, Jiang P, Wei H, Ji L li. Chlorogenic acid prevents acetaminophen-induced liver injury: the involvement of CYP450 metabolic enzymes and some antioxidant signals. *J Zhejiang Univ Sci B*. 2015;16(7):602-610. doi:10.1631/jzus.B1400346

34. Gutierrez-Arcelus M, Teslovich N, Mola AR, et al. Lymphocyte innateness defined by transcriptional states reflects a balance between proliferation and effector functions. *Nat Commun*. 2019;10(1):687. doi:10.1038/s41467-019-08604-4

35. Xia J, Hou Y, Cai A, et al. An integrated co-expression network analysis reveals novel genetic biomarkers for immune cell infiltration in chronic kidney disease. *Front Immunol*. 2023;14:1129524. doi:10.3389/fimmu.2023.1129524

36. Devarbhavi P, Telang L, Vastrad B, Tengli A, Vastrad C, Kottursheti I. Identification of key pathways and genes in polycystic ovary syndrome via integrated bioinformatics analysis and prediction of small therapeutic molecules. *Reprod Biol Endocrinol*. 2021;19(1):31. doi:10.1186/s12958-021-00706-3

37. Zhang WJ, Yue KL, Wang JZ, Zhang Y. Association between heat shock factor protein 4 methylation and colorectal cancer risk and potential molecular mechanisms: A bioinformatics study. *World J Gastrointest Oncol*. 2023;15(12):2150-2168. doi:10.4251/wjgo.v15.i12.2150

38. Zhao L, Long C, Zhao G, et al. Reprogramming barriers in bovine cells nuclear transfer revealed by single-cell RNA-seq analysis. *J Cell Mol Med*. 2022;26(18):4792-4804. doi:10.1111/jcmm.17505

Wnioski

Poszukiwanie nowych wariantów i genów potencjalnie zaangażowanych w patogenezę PCD, w połączeniu z potwierdzeniem ich roli w funkcjonowaniu rzęsek ruchowych, stanowi wciąż aktualne wyzwanie badawcze. W niniejszej pracy do przeprowadzenia analizy funkcjonalnej wybranych genów o nieznanej, niedostatecznie poznanej i znanej roli w PCD, opracowano i zastosowano organizm modelowy *Schmidtea mediterranea*.

W wyniku przeprowadzonych analiz opisanych w niniejszej rozprawie sformułowano następujące wnioski:

- *Schmidtea mediterranea* stanowi obiecujący, ale dotychczas mało wykorzystany model do przeprowadzenia przesiewowej analizy funkcjonalnej zakonserwowanych ewolucyjnie genów potencjalnie związanych z patogenezą PCD.
- Badanie wpływu wyciszenia genów na funkcjonowanie rzęsek ruchowych jest bardziej skuteczne przy wykorzystaniu całych, niecietych robaków niż robaków pociętych.
- Rola genów *Smed-cfap300, Smed-cfap221* oraz *Smed-spag1* w funkcjonowaniu rzęsek ruchowych jest ewolucyjnie zakonserwowana.
- Wyciszenie homologów genów *CFAP300* i *CFAP221* w modelu *S. mediterranea* wskazało na ich istotną rolę w funkcjonowaniu rzęsek ruchowych, tym samym potwierdzono udział badanych genów w patogenezie PCD.
- Badania z użyciem *S. mediterranea* (uzupełnione o badania na ludzkiej linii komórkowej) potwierdziły hipotezę, że brak homozygotycznych pacjentów z dużą delecją obejmującą eksony 1-2 genu *SPAG1* oraz eksony 3-4 genu *POLR2K* wynika z braku funkcjonalnej formy POLR2K; tym samym wykluczono rolę *POLR2K* w patogenezie PCD.
- Obserwowany wpływ wyciszenia badanych genów na funkcjonowanie rzęsek ruchowych planarii był podobny do wpływu patogennych wariantów na funkcję nabłonka oddechowego u chorych na PCD (silny wpływ wyciszenia *Smed-cfap300* i *Smed-spag1* na lokomocję robaków był spójny ze znacznymi zmianami funkcji rzęsek nabłonka oddechowego u pacjentów; subtelne zmiany w lokomocji i ruchu rzęsek robaków z wyciszonym *Smed-cfap221* były spójne z łagodnym fenotypem obserwowanym u pacjenta).

Streszczenie

Rzęski ruchowe są ewolucyjnie zakonserwowanymi organellami komórkowymi, które tworzą wypustki na powierzchni wielu komórek eukariotycznych. Patogenne warianty w genach kodujących białka strukturalne rzęsek lub białka zaangażowane w ich biogenezę, prowadzą do rozwoju chorób genetycznych zwanych ciliopatiami. Sztandarowym przykładem ciliopatii związanej z dysfunkcją rzęsek ruchowych jest pierwotna dyskineza rzęsek (*primary ciliary dyskinesia*, PCD; OMIM244400). PCD jest rzadką chorobą dziedziczoną głównie autosomalnie w sposób recesywny, którą charakteryzuje duża heterogenność genetyczna i kliniczna. Objawy PCD obejmują m.in. na nawracające infekcje dróg oddechowych, ucha i zatok oraz ograniczoną płodność lub bezpłodność; ponadto u około 50% pacjentów z PCD obserwuje się odwrócenie narządów ciała.

Chociaż znanych jest aktualnie ponad 50 genów zaangażowanych w patogenezę tej choroby, u około 30% pacjentów genetyczne podłoże PCD pozostaje nieznane. Poszukiwanie nowych wariantów i genów odpowiadających za wystąpienie tej choroby, w połączeniu z potwierdzeniem ich roli w funkcjonowaniu rzęsek ruchowych, stanowi wciąż aktualne wyzwanie badawcze. Celem niniejszej rozprawy doktorskiej było zoptymalizowanie i praktyczne zastosowanie *Schmidtea mediterranea* jako organizmu modelowego do potwierdzenia związku wybranych genów z zaburzeniami funkcji rzęsek ruchowych i patogenezą PCD. Ruch *S. mediterranea* zależy od komórek wielorzęskowych nabłonka pokrywającego brzuszną stronę ich ciała; wyciszenie genów związanych z rzęskami objawia się zaburzeniem ruchu robaków. Chociaż *S. mediterranea* jest opisywana jako model do badania rzęsek ruchowych, niewiele jest doniesień naukowych opisujących użycie tego organizmu jako modelu *in vivo* do potwierdzenia roli badanych genów w patogenezie PCD.

Niniejsza rozprawa doktorska stanowi zbiór czterech prac, w których zweryfikowano możliwość użycia płazińca (planarii), *S. mediterranea*, do badania genów zaangażowanych w patogenezę PCD. Pierwsza publikacja (praca przeglądowa) opisuje aktualny stan wiedzy na temat możliwości wykorzystania planarii do badania rzęsek ruchowych oraz ciliopatii związanych z dysfunkcją tych organelli. Pozostałe publikacje to prace oryginalne, których celem było potwierdzenie roli zidentyfikowanych patogennych wariantów w genach *CFAP221* i *CFAP300* oraz genu *POLR2K* (którego fragment ulega delecji razem z częścią znanego genu PCD, *SPAG1),* w patogenezie PCD.

W celu potwierdzenia roli badanych genów w funkcjonowaniu rzęsek ruchowych i patogenezie PCD, przeprowadzono ich wyciszenie przy użyciu metody interferencji RNA (*RNA interference*, RNAi) w modelu płazińca. Uzyskane wyniki pozwoliły na potwierdzenie roli *CFAP221* i *CFAP300* w patogenezie badanej choroby oraz wskazały na brak zaangażowania genu *POLR2K* w PCD. Badania z wykorzystaniem *S. mediterranea* udowodniły ewolucyjne zakonserwowanie roli *CFAP300, CFAP221* i *SPAG1* w funkcjonowaniu rzęsek ruchowych. Planarie z wyciszonym *CFAP300, SPAG1* poruszały się kilka razy wolniej od kontroli, czemu towarzyszyła zmiana wzorca ruchu; efekt wyciszenia był podobny do silnego wpływu obecności patogennych wariantów na funkcję komórek nabłonka oddechowego pacjentów. Wpływ wyciszenia *CFAP221* na funkcjonowanie rzęsek ruchowych u robaków był subtelniejszy, zgodny z fenotypem obserwowanym u pacjenta. Uzyskane wyniki pozwoliły na potwierdzenie, że *Schmidtea mediterranea* stanowi prosty, tani i łatwo dostępny model do badania genów potencjalnie zaangażowanych w patogenezę PCD.

Abstract

Motile cilia are evolutionary conserved organelles that form protrusions on the surface of many eukaryotic cells. Pathogenic variants in genes encoding structural proteins or proteins involved in the biogenesis of cilia lead to a range of genetic disorders collectively called ciliopathies. A key example of ciliopathy caused by dysfunction of motile cilia is primary ciliary dyskinesia (PCD; OMIM244400). PCD is a rare disease inherited mainly in an autosomal recessive manner and is characterized by a great genetic and clinical heterogeneity. Symptoms of PCD include recurrent respiratory, ear and sinus infections and reduced fertility or infertility; in addition, in about 50% of PCD patients, *situs inversus* is observed.

Although more than 50 genes are known to be involved in the pathogenesis of PCD, in about 30% of patients the genetic basis of PCD remains unknown. Therefore, the search for new pathogenic variants and genes responsible for the occurrence of this disease, combined with confirmation of their role in the functioning of motile cilia, is still a current research challenge. The aim of this doctoral dissertation was to optimize and practically apply *Schmidtea mediterranea* as a model organism to confirm the role of genes associated with dysfunction of motile cilia and the PCD pathogenesis. *S. mediterranea'* movement depends on multiciliated cells covering the ventral site of the planarian body; knockdown of cilia-related genes is manifested by changes in worm locomotion. Although planarians are described as an animal model for studying motile cilia, there is insufficient information in the literature on the use *S. mediterranea* as an *in vivo* model to confirm the role of studied genes in the pathogenesis of PCD.

This dissertation is a collection of four publications that verify the possibility of using *S. mediterranea* to study genes involved in the pathogenesis of PCD. The first publication (a review article) describes the current state of knowledge on the possibility of using planarians to study motile cilia and ciliopathies associated with dysfunction of these organelles. The remaining publications are original papers, the aim of which was to confirm the role of identified pathogenic variants in the *CFAP221* and *CFAP300* genes, and the *POLR2K* gene (a part of which is deleted, together with part of the known PCD gene, *SPAG1*). In order to confirm the role of selected genes in the functioning of motile cilia and the PCD pathogenesis, their silencing was carried out using the RNA interference (RNAi) method in the planarian model. The obtained results allowed to confirm the role of *CFAP221* and *CFAP300* in the pathogenesis of studied disorder and indicated the lack on involvement

of *POLR2K* in PCD. Studies using *S. mediterranea* have demonstrated the evolutionary conserved role of *CFAP221*, *CFAP300* and *SPAG1* in the functioning of motile cilia. *S. mediterranea* after *SPAG1* and *CFAP300* silencing moved several times slower than controls, which was accompanied by a change in the movement pattern; the effect of silencing was similar to the significant impact of the presence of pathogenic variants on the function of respiratory epithelial cells of the PCD patients. The influence of *CFAP221* silencing on the function of motile cilia in worms was more subtle, consistent with mild phenotype observed in patient. The obtained results confirmed that *Schmidtea mediterranea* is a simple, cheap and easily accessible model for studying genes potentially involved in the pathogenesis of PCD.

Bibliografia

1. Kurkowiak M, Ziętkiewicz E, Witt M. Recent advances in primary ciliary dyskinesia genetics. *J Med Genet*. 2015;52(1):1-9. doi:10.1136/jmedgenet-2014-102755

2. Takeda S, Narita K. Structure and function of vertebrate cilia, towards a new taxonomy. *Differentiation*. 2012;83(2):S4-11. doi:10.1016/j.diff.2011.11.002

3. Kempeneers C, Chilvers MA. To beat, or not to beat, that is question! The spectrum of ciliopathies. *Pediatr Pulmonol*. 2018;53(8):1122-1129. doi:10.1002/ppul.24078

4. Hyland RM, Brody SL. Impact of Motile Ciliopathies on Human Development and Clinical Consequences in the Newborn. *Cells*. 2021;11(1):125. doi:10.3390/cells11010125

5. Ibañez-Tallon I, Heintz N, Omran H. To beat or not to beat: roles of cilia in development and disease. *Hum Mol Genet*. 2003;12 Spec No 1:R27-35. doi:10.1093/hmg/ddg061

6. Brooks ER, Wallingford JB. Multiciliated cells. *Curr Biol*. 2014;24(19):R973-982. doi:10.1016/j.cub.2014.08.047

7. Wallmeier J, Nielsen KG, Kuehni CE, et al. Motile ciliopathies. *Nat Rev Dis Primers*. 2020;6(1):77. doi:10.1038/s41572-020-0209-6

8. Shah AS, Ben-Shahar Y, Moninger TO, Kline JN, Welsh MJ. Motile cilia of human airway epithelia are chemosensory. *Science*. 2009;325(5944):1131-1134. doi:10.1126/science.1173869

9. Carvalho-Santos Z, Azimzadeh J, Pereira-Leal JB, Bettencourt-Dias M. Evolution: Tracing the origins of centrioles, cilia, and flagella. *J Cell Biol*. 2011;194(2):165-175. doi:10.1083/jcb.201011152

10. Anvarian Z, Mykytyn K, Mukhopadhyay S, Pedersen LB, Christensen ST. Cellular signalling by primary cilia in development, organ function and disease. *Nat Rev Nephrol*. 2019;15(4):199-219. doi:10.1038/s41581-019-0116-9

11. Christensen ST, Pedersen LB, Schneider L, Satir P. Sensory cilia and integration of signal transduction in human health and disease. *Traffic*. 2007;8(2):97-109. doi:10.1111/j.1600-0854.2006.00516.x

12. Waters AM, Beales PL. Ciliopathies: an expanding disease spectrum. *Pediatr Nephrol*. 2011;26(7):1039-1056. doi:10.1007/s00467-010-1731-7

13. Cardenas-Rodriguez M, Badano JL. Ciliary biology: understanding the cellular and genetic basis of human ciliopathies. *Am J Med Genet C Semin Med Genet*. 2009;151C(4):263-280. doi:10.1002/ajmg.c.30227

14. Smith EF, Yang P. The Radial Spokes and Central Apparatus: Mechano-Chemical Transducers That Regulate Flagellar Motility. *Cell Motil Cytoskeleton*. 2004;57(1):8-17. doi:10.1002/cm.10155

15. Lin J, Nicastro D. Asymmetric distribution and spatial switching of dynein activity generates ciliary motility. *Science*. 2018;360(6387):eaar1968. doi:10.1126/science.aar1968

16. Roberts AJ, Kon T, Knight PJ, Sutoh K, Burgess SA. Functions and mechanics of dynein motor proteins. *Nat Rev Mol Cell Biol*. 2013;14(11):713-726. doi:10.1038/nrm3667

17. Satir P, Heuser T, Sale WS. A Structural Basis for How Motile Cilia Beat. *Bioscience*. 2014;64(12):1073-1083. doi:10.1093/biosci/biu180

18. Meng X, Xu C, Li J, et al. Multi-scale structures of the mammalian radial spoke and divergence of axonemal complexes in ependymal cilia. *Nat Commun*. 2024;15(1):362. doi:10.1038/s41467-023-44577-1

19. Lechtreck KF. IFT-Cargo Interactions and Protein Transport in Cilia. *Trends Biochem Sci*. 2015;40(12):765-778. doi:10.1016/j.tibs.2015.09.003

20. Ishikawa H, Marshall WF. Intraflagellar Transport and Ciliary Dynamics. *Cold Spring Harb Perspect Biol*. 2017;9(3):a021998. doi:10.1101/cshperspect.a021998

21. Pazour GJ, Agrin N, Leszyk J, Witman GB. Proteomic analysis of a eukaryotic cilium. *J Cell Biol*. 2005;170(1):103-113. doi:10.1083/jcb.200504008

22. Quigley IK, Kintner C. Rfx2 Stabilizes Foxj1 Binding at Chromatin Loops to Enable Multiciliated Cell Gene Expression. *PLoS Genet*. 2017;13(1):e1006538. doi:10.1371/journal.pgen.1006538

23. van Dam TJP, Kennedy J, van der Lee R, et al. CiliaCarta: An integrated and validated compendium of ciliary genes. *PLoS One*. 2019;14(5):e0216705. doi:10.1371/journal.pone.0216705

24. Horani A, Ferkol TW, Dutcher SK, Brody SL. Genetics and biology of primary ciliary dyskinesia. *Paediatr Respir Rev*. 2016;18:18-24. doi:10.1016/j.prrv.2015.09.001

25. Ardura-Garcia C, Goutaki M, Carr SB, et al. Registries and collaborative studies for primary ciliary dyskinesia in Europe. *ERJ Open Res*. 2020;6(2):00005-02020. doi:10.1183/23120541.00005-2020

26. Lucas JS, Davis SD, Omran H, Shoemark A. Primary ciliary dyskinesia in the genomics age. *Lancet Respir Med*. 2020;8(2):202-216. doi:10.1016/S2213-2600(19)30374-1

27. Frija-Masson J, Bassinet L, Honoré I, et al. Clinical characteristics, functional respiratory decline and follow-up in adult patients with primary ciliary dyskinesia. *Thorax*. 2017;72(2):154-160. doi:10.1136/thoraxjnl-2015-207891

28. Bukowy-Bieryllo Z, Witt M, Zietkiewicz E. Perspectives for Primary Ciliary Dyskinesia. *Int J Mol Sci*. 2022;23(8):4122. doi:10.3390/ijms23084122

29. Shapiro AJ, Davis SD, Polineni D, et al. Diagnosis of Primary Ciliary Dyskinesia. An Official American Thoracic Society Clinical Practice Guideline. *American Journal of Respiratory and Critical Care Medicine*. 2018;197(12):e24. doi:10.1164/rccm.201805-0819ST

30. Wee WB, Gatt D, Seidl E, Santyr G, To T, Dell SD. Estimates of primary ciliary dyskinesia prevalence: a scoping review. *ERJ Open Res*. 2024;10(4):00989-02023. doi:10.1183/23120541.00989-2023

31. Goutaki M, Maurer E, Halbeisen FS, et al. The international primary ciliary dyskinesia cohort (iPCD Cohort): methods and first results. *Eur Respir J*. 2017;49(1):1601181. doi:10.1183/13993003.01181-2016

32. Raidt J, Riepenhausen S, Pennekamp P, et al. Analyses of 1236 genotyped primary ciliary dyskinesia individuals identify regional clusters of distinct DNA variants and significant genotype-phenotype correlations. *Eur Respir J*. 2024;64(2):2301769. doi:10.1183/13993003.01769-2023

33. Shapiro AJ, Leigh MW. Value of transmission electron microscopy for primary ciliary dyskinesia diagnosis in the era of molecular medicine: Genetic defects with normal and non-diagnostic ciliary ultrastructure. *Ultrastruct Pathol*. 2017;41(6):373-385. doi:10.1080/01913123.2017.1362088

34. Goutaki M, Shoemark A. Diagnosis of Primary Ciliary Dyskinesia. *Clin Chest Med*. 2022;43(1):127-140. doi:10.1016/j.ccm.2021.11.008

35. Raidt J, Loges NT, Olbrich H, Wallmeier J, Pennekamp P, Omran H. Primary ciliary dyskinesia. *La Presse Médicale*. 2023;52(3):104171. doi:10.1016/j.lpm.2023.104171

36. Mirra V, Werner C, Santamaria F. Primary Ciliary Dyskinesia: An Update on Clinical Aspects, Genetics, Diagnosis, and Future Treatment Strategies. *Front Pediatr*. 2017;5:135. doi:10.3389/fped.2017.00135

37. Horani A, Ferkol TW. Understanding Primary Ciliary Dyskinesia and Other Ciliopathies. *J Pediatr*. 2021;230:15-22.e1. doi:10.1016/j.jpeds.2020.11.040

38. Wallmeier J, Boon M, Mutairi DA, et al. Mutations in CCNO and MCIDAS lead to a mucociliary clearance disorder due to reduced generation of multiple motile cilia. *Mol Cell Pediatr*. 2015;2(Suppl 1):A15. doi:10.1186/2194-7791-2-S1-A15

39. Loges NT, Antony D, Maver A, et al. Recessive DNAH9 Loss-of-Function Mutations Cause Laterality Defects and Subtle Respiratory Ciliary-Beating Defects. *Am J Hum Genet*. 2018;103(6):995-1008. doi:10.1016/j.ajhg.2018.10.020

40. Biebach L, Cindrić S, Koenig J, et al. Recessive Mutations in CFAP74 Cause Primary Ciliary Dyskinesia with Normal Ciliary Ultrastructure. *Am J Respir Cell Mol Biol*. 2022;67(3):409-413. doi:10.1165/rcmb.2022-0032LE

41. Legendre M, Zaragosi LE, Mitchison HM. Motile cilia and airway disease. *Semin Cell Dev Biol*. 2021;110:19-33. doi:10.1016/j.semcdb.2020.11.007

42. Bukowy-Bieryłło Z. Long-term differentiating primary human airway epithelial cell cultures: how far are we? *Cell Commun Signal*. 2021;19(1):63. doi:10.1186/s12964-021-00740-z

43. Bukowy Z, Ziętkiewicz E, Witt M. In vitro culturing of ciliary respiratory cells—a model for studies of genetic diseases. *J Appl Genet*. 2011;52(1):39-51. doi:10.1007/s13353-010-0005-1

44. Fulcher ML, Randell SH. Human nasal and tracheo-bronchial respiratory epithelial cell culture. *Methods Mol Biol*. 2013;945:109-121. doi:10.1007/978-1-62703-125-7_8

45. Thomas L, Bouhouche K, Whitfield M, et al. TTC12 Loss-of-Function Mutations Cause Primary Ciliary Dyskinesia and Unveil Distinct Dynein Assembly Mechanisms in Motile Cilia Versus Flagella. *Am J Hum Genet*. 2020;106(2):153-169. doi:10.1016/j.ajhg.2019.12.010

46. Pazour GJ, Witman GB. The *Chlamydomonas* Flagellum as a Model for Human Ciliary Disease. In: Harris EH, Stern DB, Witman GB, eds. *The Chlamydomonas Sourcebook (Second Edition)*. Academic Press; 2009:445-478. doi:10.1016/B978-0-12-370873-1.00052-6

47. Kong JN, Hardin K, Dinkins M, et al. Regulation of Chlamydomonas flagella and ependymal cell motile cilia by ceramide-mediated translocation of GSK3. *Mol Biol Cell*. 2015;26(24):4451-4465. doi:10.1091/mbc.E15-06-0371

48. Pennarun G, Escudier E, Chapelin C, et al. Loss-of-function mutations in a human gene related to Chlamydomonas reinhardtii dynein IC78 result in primary ciliary dyskinesia. *Am J Hum Genet*. 1999;65(6):1508-1519. doi:10.1086/302683

49. Fassad MR, Shoemark A, Legendre M, et al. Mutations in Outer Dynein Arm Heavy Chain DNAH9 Cause Motile Cilia Defects and Situs Inversus. *Am J Hum Genet*. 2018;103(6):984-994. doi:10.1016/j.ajhg.2018.10.016

50. Broadhead R, Dawe HR, Farr H, et al. Flagellar motility is required for the viability of the bloodstream trypanosome. *Nature*. 2006;440(7081):224-227. doi:10.1038/nature04541

51. Kavlie RG, Kernan MJ, Eberl DF. Hearing in Drosophila requires TilB, a conserved protein associated with ciliary motility. *Genetics*. 2010;185(1):177-188. doi:10.1534/genetics.110.114009

52. Lesko SL, Rouhana L. Dynein assembly factor with WD repeat domains 1 (DAW1) is required for the function of motile cilia in the planarian Schmidtea mediterranea. *Dev Growth Differ*. 2020;62(6):423-437. doi:10.1111/dgd.12669

53. Wallmeier J, Al-Mutairi DA, Chen CT, et al. Mutations in CCNO result in congenital mucociliary clearance disorder with reduced generation of multiple motile cilia. *Nat Genet*. 2014;46(6):646-651. doi:10.1038/ng.2961

54. Austin-Tse C, Halbritter J, Zariwala MA, et al. Zebrafish Ciliopathy Screen Plus Human Mutational Analysis Identifies C21orf59 and CCDC65 Defects as Causing Primary Ciliary Dyskinesia. *Am J Hum Genet*. 2013;93(4):672-686. doi:10.1016/j.ajhg.2013.08.015

55. Yoke H, Ueno H, Narita A, et al. Rsph4a is essential for the triplet radial spoke head assembly of the mouse motile cilia. *PLoS Genet*. 2020;16(3):e1008664. doi:10.1371/journal.pgen.1008664

56. Merveille AC, Battaille G, Billen F, et al. Clinical findings and prevalence of the mutation associated with primary ciliary dyskinesia in Old English Sheepdogs. *J Vet Intern Med*. 2014;28(3):771-778. doi:10.1111/jvim.12336

57. Newmark PA, Sánchez Alvarado A. Not your father's planarian: a classic model enters the era of functional genomics. *Nat Rev Genet*. 2002;3(3):210-219. doi:10.1038/nrg759

58. Wagner DE, Wang IE, Reddien PW. Clonogenic neoblasts are pluripotent adult stem cells that underlie planarian regeneration. *Science*. 2011;332(6031):811-816. doi:10.1126/science.1203983

59. De Sousa N, Adell T. Maintenance of Schmidtea mediterranea in the Laboratory. *Bio Protoc*. 2018;8(19):e3040. doi:10.21769/BioProtoc.3040

60. Park C, Owusu-Boaitey KE, Valdes GM, Reddien PW. Fate specification is spatially intermingled across planarian stem cells. *Nat Commun*. 2023;14(1):7422. doi:10.1038/s41467-023-43267-2

61. Rozanski A, Moon H, Brandl H, et al. PlanMine 3.0-improvements to a mineable resource of flatworm biology and biodiversity. *Nucleic Acids Res*. 2019;47(D1):D812-D820. doi:10.1093/nar/gky1070

62. Fincher CT, Wurtzel O, de Hoog T, Kravarik KM, Reddien PW. Cell type transcriptome atlas for the planarian Schmidtea mediterranea. *Science*. 2018;360(6391):eaaq1736. doi:10.1126/science.aaq1736

63. Rouhana L, Weiss JA, Forsthoefel DJ, et al. RNA interference by feeding in vitro-synthesized double-stranded RNA to planarians: methodology and dynamics. *Dev Dyn*. 2013;242(6):718-730. doi:10.1002/dvdy.23950

64. Merryman MS, Alvarado AS, Jenkin JC. Culturing Planarians in the Laboratory. *Methods Mol Biol*. 2018;1774:241-258. doi:10.1007/978-1-4939-7802-1_5

65. Basquin C, Orfila AM, Azimzadeh J. The planarian Schmidtea mediterranea as a model for studying motile cilia and multiciliated cells. *Methods Cell Biol*. 2015;127:243-262. doi:10.1016/bs.mcb.2015.01.009

Oświadczenia współautorów publikacji

Oświadczenia współautorów Artykułu 1

50 LAT
INSTYTUT
GENETYKI CZŁOWIEKA
POLSKIEJ AKADEMII NAUK

ul. Strzeszyńska 32
60-479 Poznań

tel. +48/61/657 91 00
fax +48/61/823 32 35
e-mail: igcz@man.poznan.pl

www.igcz.poznan.pl

Poznań, 24.02.2025

mgr Alicja Rabiasz

OŚWIADCZENIE

Niniejszym oświadczam, że mój wkład w powstanie manuskryptu pt. „*Schmidtea mediterranea* as a Model Organism to Study the Molecular Background of Human Motile Ciliopathies"
Int J Mol Sci. 2023 Feb 24;24(5):4472
Alicja Rabiasz, Ewa Ziętkiewicz
był następujący:

- ustalenie koncepcji i planu pracy
- przegląd i wybór prac omówionych w publikacji
- pisanie oryginalnej wersji publikacji
- opracowanie rycin i tabel

Z wyrazami szacunku

50 LAT
INSTYTUT
GENETYKI CZŁOWIEKA
POLSKIEJ AKADEMII NAUK

ul. Strzeszyńska 32
60-479 Poznań

tel. +48/61/657 91 00
fax +48/61/823 32 35
e-mail: igcz@man.poznan.pl

www.igcz.poznan.pl

Poznań, 24.02.2025

prof. dr hab. Ewa Ziętkiewicz

OŚWIADCZENIE

Niniejszym oświadczam, że mój wkład w powstanie manuskryptu pt. „*Schmidtea mediterranea* as a Model Organism to Study the Molecular Background of Human Motile Ciliopathies"
Int J Mol Sci. 2023 Feb 24;24(5):4472
Alicja Rabiasz, **Ewa Ziętkiewicz**
był następujący:

- ustalenie koncepcji pracy
- udział w pisaniu oryginalnej wersji publikacji i zaplanowaniu rycin
- korekta ostatecznej wersji manuskryptu
- obowiązki autora korespondencyjnego

Z wyrazami szacunku

Oświadczenia współautorów Artykułu 2

50 LAT
INSTYTUT
GENETYKI CZŁOWIEKA
POLSKIEJ AKADEMII NAUK

ul. Strzeszyńska 32
60-479 Poznań

tel. +48/61/657 91 00
fax +48/61/823 32 35
e-mail: igcz@man.poznan.pl

www.igcz.poznan.pl

Poznań, 24.02.2025

prof. dr hab. Ewa Ziętkiewicz

OŚWIADCZENIE

Niniejszym oświadczam, że mój wkład w powstanie manuskryptu pt. „*CFAP300*: Mutations in Slavic Patients with Primary Ciliary Dyskinesia and a Role in Ciliary Dynein Arms Trafficking"
Am J Respir Cell Mol Biol. 2019 Oct;61(4):440-449
Ewa Ziętkiewicz, Zuzanna Bukowy-Bieryłło, Alicja Rabiasz, Patrycja Daca-Roszak, Alina Wojda, Katarzyna Voelkel, Ewa Rutkiewicz, Andrzej Pogorzelski, Margarida Rasteiro, Michał Witt
był następujący:

- ustalenie koncepcji i planu pracy
- zabezpieczenie środków finansowych i opieka nad właściwą realizacją projektu
- wytypowanie próbek DNA pacjentów o nieznanym podłożu PCD oraz analiza danych z SSCP i WES; analiza archiwalnych zdjęć przekroju rzęsek z transmisyjnego mikroskopu elektronowego
- analiza haplotypu tła patogennego wariantu genu *CFAP300*
- interpretacja wyników analizy profilu ekspresji wybranych genów rzęskowych w trakcie różnicowania komórek nabłonka oddechowego
- pisanie oryginalnej wersji manuskryptu i korekta ostatecznej wersji manuskryptu
- obowiązki autora korespondencyjnego

Z wyrazami szacunku

50 LAT
INSTYTUT
GENETYKI CZŁOWIEKA
POLSKIEJ AKADEMII NAUK

ul. Strzeszyńska 32
60-479 Poznań

tel. +48/61/657 91 00
fax +48/61/823 32 35
e-mail: igcz@man.poznan.pl

www.igcz.poznan.pl

Poznań, 24.02.2025

dr hab. Zuzanna Bukowy-Bieryłło, prof. IGC PAN

OŚWIADCZENIE

Niniejszym oświadczam, że mój wkład w powstanie manuskryptu pt. „*CFAP300*: Mutations in Slavic Patients with Primary Ciliary Dyskinesia and a Role in Ciliary Dynein Arms Trafficking"
Am J Respir Cell Mol Biol. 2019 Oct;61(4):440-449
Ewa Ziętkiewicz, **Zuzanna Bukowy-Bieryłło**, Alicja Rabiasz, Patrycja Daca-Roszak, Alina Wojda, Katarzyna Voelkel, Ewa Rutkiewicz, Andrzej Pogorzelski, Margarida Rasteiro, Michał Witt
był następujący:

- udział w koncepcji i planowaniu badań
- zabezpieczenie środków finansowych
- analiza ruchu rzęsek komórek nabłonka oddechowego
- hodowla i różnicowanie komórek nabłonka oddechowego w kierunku ciliogenezy, izolacja RNA z komórek w wybranych punktach czasowych, synteza cDNA
- interpretacja wyników analizy profilu ekspresji wybranych genów rzęskowych w trakcie różnicowania komórek nabłonka oddechowego
- udział w przygotowaniu tabel i figur
- udział w pisaniu oryginalnej wersji manuskryptu i krytyczny przegląd ostatecznej wersji manuskryptu

Z wyrazami szacunku

ZBukowy-Bieryłło

50 LAT
INSTYTUT
GENETYKI CZŁOWIEKA
POLSKIEJ AKADEMII NAUK

ul. Strzeszyńska 32
60-479 Poznań

tel. +48/61/657 91 00
fax +48/61/823 32 35
e-mail: igcz@man.poznan.pl

www.igcz.poznan.pl

Poznań, 24.02.2025

mgr Alicja Rabiasz

OŚWIADCZENIE

Niniejszym oświadczam, że mój wkład w powstanie manuskryptu pt. „*CFAP300*: Mutations in Slavic Patients with Primary Ciliary Dyskinesia and a Role in Ciliary Dynein Arms Trafficking"
Am J Respir Cell Mol Biol. 2019 Oct;61(4):440-449
Ewa Ziętkiewicz, Zuzanna Bukowy-Bieryłło, **Alicja Rabiasz**, Patrycja Daca-Roszak, Alina Wojda, Katarzyna Voelkel, Ewa Rutkiewicz, Andrzej Pogorzelski, Margarida Rasteiro, Michał Witt
był następujący:

- udział w koncepcji i ustaleniu metodologii badań
- analiza wpływu obecności patogennego wariantu na poziom ekspresji wybranych genów (RT-PCR na archiwalnym materiale pacjenta)
- udział w hodowli komórek nabłonka oddechowego
- analiza *in silico* ewolucyjnego zakonserwowania *CFAP300* między organizmami
- zaprojektowanie, wykonanie i interpretacja doświadczeń z wykorzystaniem *S. mediterranea*: wyciszenie homologa genu *CFAP300* (w tym zaprojektowanie i synteza dsRNA przy użyciu transkrypcji *in vitro*), potwierdzenie efektywności wyciszenia na poziomie mRNA (izolacja RNA, synteza cDNA, qRT-PCR), analiza wpływu wyciszenia na funkcjonowanie rzęsek ruchowych planarii (analiza lokomocji robaków i ruchu rzęsek)
- udział w przygotowaniu figur i tabel
- udział w pisaniu oryginalnej wersji manuskryptu i krytyczny przegląd ostatecznej wersji manuskryptu

Z wyrazami szacunku

50 LAT
INSTYTUT
GENETYKI CZŁOWIEKA
POLSKIEJ AKADEMII NAUK

ul. Strzeszyńska 32
60-479 Poznań

tel. +48/61/657 91 00
fax +48/61/823 32 35
e-mail: igcz@man.poznan.pl

www.igcz.poznan.pl

Poznań, 24.02.2025

dr Patrycja Daca-Roszak

OŚWIADCZENIE

Niniejszym oświadczam, że mój wkład w powstanie manuskryptu pt. „*CFAP300*: Mutations in Slavic Patients with Primary Ciliary Dyskinesia and a Role in Ciliary Dynein Arms Trafficking"
Am J Respir Cell Mol Biol. 2019 Oct;61(4):440-449
Ewa Ziętkiewicz, Zuzanna Bukowy-Bieryłło, Alicja Rabiasz, **Patrycja Daca-Roszak**, Alina Wojda, Katarzyna Voelkel, Ewa Rutkiewicz, Andrzej Pogorzelski, Margarida Rasteiro, Michał Witt
był następujący:

- zaprojektowanie i wykonanie analizy profilu ekspresji wybranych genów rzęskowych w trakcie ciliogenezy (metoda TLDA)
- udział w pisaniu oryginalnej wersji manuskryptu i krytyczny przegląd ostatecznej wersji manuskryptu

Z wyrazami szacunku

Daca-Roszak

Poznań, 24.02.2025

mgr Katarzyna Voelkel

OŚWIADCZENIE

Niniejszym oświadczam, że mój wkład w powstanie manuskryptu pt. „*CFAP300*: Mutations in Slavic Patients with Primary Ciliary Dyskinesia and a Role in Ciliary Dynein Arms Trafficking"
Am J Respir Cell Mol Biol. 2019 Oct;61(4):440-449
Ewa Ziętkiewicz, Zuzanna Bukowy-Bieryłło, Alicja Rabiasz, Patrycja Daca-Roszak, Alina Wojda, **Katarzyna Voelkel**, Ewa Rutkiewicz, Andrzej Pogorzelski, Margarida Rasteiro, Michał Witt
był następujący:

- przygotowanie próbek DNA do analizy WES
- analiza DNA pacjentów i wybranych rodzin metodą SSCP i sekwencjonowania Sangera

Z wyrazami szacunku

Katarzyna Voelkel

50 LAT
INSTYTUT
GENETYKI CZŁOWIEKA
POLSKIEJ AKADEMII NAUK

ul. Strzeszyńska 32
60-479 Poznań

tel. +48/61/657 91 00
fax +48/61/823 32 35
e-mail: igcz@man.poznan.pl

www.igcz.poznan.pl

Poznań, 24.02.2025

Ewa Rutkiewicz

OŚWIADCZENIE

Niniejszym oświadczam, że mój wkład w powstanie manuskryptu pt. „*CFAP300*: Mutations in Slavic Patients with Primary Ciliary Dyskinesia and a Role in Ciliary Dynein Arms Trafficking"
Am J Respir Cell Mol Biol. 2019 Oct;61(4):440-449
Ewa Ziętkiewicz, Zuzanna Bukowy-Bieryłło, Alicja Rabiasz, Patrycja Daca-Roszak, Alina Wojda, Katarzyna Voelkel, **Ewa Rutkiewicz**, Andrzej Pogorzelski, Margarida Rasteiro, Michał Witt
był następujący:

- przygotowaniu materiału do badań (izolacja DNA z krwi obwodowej)

Z wyrazami szacunku

Ewa Rutkiewicz

Poznań, 24.02.2025

dr n. med. Andrzej Pogorzelski

Instytut Gruźlicy i Chorób Płuc
Oddział Terenowy im. Jana i Ireny Rudników
w Rabce-Zdrój

OŚWIADCZENIE

Niniejszym oświadczam, że mój wkład w powstanie manuskryptu pt. „*CFAP300*: Mutations in Slavic Patients with Primary Ciliary Dyskinesia and a Role in Ciliary Dynein Arms Trafficking"
Am J Respir Cell Mol Biol. 2019 Oct;61(4):440-449
Ewa Ziętkiewicz, Zuzanna Bukowy-Bieryłło, Alicja Rabiasz, Patrycja Daca-Roszak, Alina Wojda, Katarzyna Voelkel, Ewa Rutkiewicz, **Andrzej Pogorzelski**, Margarida Rasteiro, Michał Witt
był następujący:

- zbieranie i opracowanie danych klinicznych pacjentów
- zabezpieczenie materiału do badań
- krytyczny przegląd ostatecznej wersji manuskryptu

Z wyrazami szacunku

Elektronicznie podpisany przez:
Andrzej Kazimierz Pogorzelski
Data:
2025-2-24 14:18:32

Poznań, 24.02.2025

prof. dr hab. Michał Witt

OŚWIADCZENIE

Niniejszym oświadczam, że mój wkład w powstanie manuskryptu pt. „*CFAP300*: Mutations in Slavic Patients with Primary Ciliary Dyskinesia and a Role in Ciliary Dynein Arms Trafficking"
Am J Respir Cell Mol Biol. 2019 Oct;61(4):440-449
Ewa Ziętkiewicz, Zuzanna Bukowy-Bieryłło, Alicja Rabiasz, Patrycja Daca-Roszak, Alina Wojda, Katarzyna Voelkel, Ewa Rutkiewicz, Andrzej Pogorzelski, Margarida Rasteiro, **Michał Witt**
był następujący:

- zatwierdzenie koncepcji pracy
- krytyczny przegląd ostatecznej wersji manuskryptu

Z wyrazami szacunku

Oświadczenia współautorów Artykułu 3

50 LAT
INSTYTUT
GENETYKI CZŁOWIEKA
POLSKIEJ AKADEMII NAUK

ul. Strzeszyńska 32
60-479 Poznań

tel. +48/61/657 91 00
fax +48/61/823 32 35
e-mail: igcz@man.poznan.pl

www.igcz.poznan.pl

Poznań, 24.02.2025

mgr Alicja Rabiasz

OŚWIADCZENIE

Niniejszym oświadczam, że mój wkład w powstanie manuskryptu pt. „A novel pathogenic variant of *CFAP221* is a cause of a mild form of primary ciliary dyskinesia"
Alicja Rabiasz, Zuzanna Bukowy-Bieryłło, Patrycja Kaźmierczak*, Hanna Przystałowska-Macioła*, Marcin Mikoś, Irena Wojsyk-Banaszak, Ewa Ziętkiewicz
*równorzędny wkład
był następujący:

- udział w ustaleniu koncepcji; przygotowanie planu badań
- zabezpieczenie środków finansowych
- analiza wpływu obecności patogennego wariantu na poziom ekspresji mRNA i białka u pacjenta (w tym izolacja białka i RNA, synteza cDNA, qRT-PCR, Western-Blot)
- udział w analizie nasienia pacjenta
- zaprojektowanie, wykonanie i interpretacja doświadczeń z wykorzystaniem S. mediterranea: analiza *in silico*, wyciszenie homologa genu *CFAP221* (w tym zaprojektowanie i synteza dsRNA przy użyciu transkrypcji *in vitro*), potwierdzenie efektywności wyciszenia na poziomie mRNA (izolacja RNA, synteza cDNA, qRT-PCR), analiza wpływu wyciszenia na funkcjonowanie rzęsek ruchowych planarii (analiza lokomocji robaków i ruchu rzęsek)
- pisanie oryginalnej wersji manuskryptu, przygotowanie tabel i większości figur
- przygotowanie ostatecznej wersji manuskryptu
- obowiązki autora korespondencyjnego

Z wyrazami szacunku

Alicja Rabiasz

50 LAT
INSTYTUT
GENETYKI CZŁOWIEKA
POLSKIEJ AKADEMII NAUK

ul. Strzeszyńska 32
60-479 Poznań

tel. +48/61/657 91 00
fax +48/61/823 32 35
e-mail: igcz@man.poznan.pl

www.igcz.poznan.pl

Poznań, 24.02.2025

dr hab. Zuzanna Bukowy-Bieryłło, prof. IGC PAN

OŚWIADCZENIE

Niniejszym oświadczam, że mój wkład w powstanie manuskryptu pt. „A novel pathogenic variant of *CFAP221* is a cause of a mild form of primary ciliary dyskinesia"
Alicja Rabiasz, **Zuzanna Bukowy-Bieryłło**, Patrycja Kaźmierczak*, Hanna Przystałowska-Macioła*, Marcin Mikoś, Irena Wojsyk-Banaszak, Ewa Ziętkiewicz
*równorzędny wkład
był następujący:

- analiza ruchu rzęsek komórek nabłonka oddechowego z wymazu oraz hodowli komórkowej
- hodowla i różnicowanie komórek nabłonka oddechowego w kierunku ciliogenezy
- zaprojektowanie, wykonanie i interpretacja analizy transportu śluzowo-rzęskowego dla hodowli komórek nabłonka oddechowego
- udział w pisaniu oryginalnej wersji manuskryptu, krytyczny przegląd i edycja manuskryptu

Z wyrazami szacunku

Z. Bukowy-Bieryłło

50 LAT
INSTYTUT
GENETYKI CZŁOWIEKA
POLSKIEJ AKADEMII NAUK

ul. Strzeszyńska 32
60-479 Poznań

tel. +48/61/657 91 00
fax +48/61/823 32 35
e-mail: igcz@man.poznan.pl

www.igcz.poznan.pl

Poznań, 24.02.2025

mgr Patrycja Kaźmierczak

OŚWIADCZENIE

Niniejszym oświadczam, że mój wkład w powstanie manuskryptu pt. „A novel pathogenic variant of *CFAP221* is a cause of a mild form of primary ciliary dyskinesia"
Alicja Rabiasz, Zuzanna Bukowy-Bieryłło, **Patrycja Kaźmierczak***, Hanna Przystałowska-Macioła*, Marcin Mikoś, Irena Wojsyk-Banaszak, Ewa Ziętkiewicz
*równorzędny wkład
był następujący:

- przygotowania materiału do badań (izolacja DNA pacjenta i rodziny z krwi obwodowej)
- analiza DNA metodą PCR i sekwencjonowania Sangera
- udział w przygotowaniu figur, krytyczny przegląd i edycja manuskryptu

Z wyrazami szacunku

Kaźmierczak

50 LAT
INSTYTUT
GENETYKI CZŁOWIEKA
POLSKIEJ AKADEMII NAUK

ul. Strzeszyńska 32
60-479 Poznań

tel. +48/61/657 91 00
fax +48/61/823 32 35
e-mail: igcz@man.poznan.pl

www.igcz.poznan.pl

Poznań, 25.02.2025

dr Hanna Przystałowska-Macioła

OŚWIADCZENIE

Niniejszym oświadczam, że mój wkład w powstanie manuskryptu pt. „A novel pathogenic variant of *CFAP221* is a cause of a mild form of primary ciliary dyskinesia"
Alicja Rabiasz, Zuzanna Bukowy-Bieryłło, Patrycja Kaźmierczak*, **Hanna Przystałowska-Macioła***, Marcin Mikoś, Irena Wojsyk-Banaszak, Ewa Ziętkiewicz
*równorzędny wkład
był następujący:

- wykonanie i analiza barwień immunofluorescencyjnych komórek nabłonka oddechowego
- udział w przygotowaniu figur, krytyczny przegląd i edycja manuskryptu

Z wyrazami szacunku

Poznań, 24.02.2025

dr n. med. Marcin Mikoś

Klinika Pneumonologii, Alergologii Dziecięcej
i Immunologii Klinicznej
Uniwersytet Medyczny im. K. Marcinkowskiego
w Poznaniu

Poradnia Pulmonologiczna dla Dzieci, Vilda Clinic, Poznań

OŚWIADCZENIE

Niniejszym oświadczam, że mój wkład w powstanie manuskryptu pt. „A novel pathogenic variant of *CFAP221* is a cause of a mild form of primary ciliary dyskinesia"
Alicja Rabiasz, Zuzanna Bukowy-Bieryłło, Patrycja Kaźmierczak*, Hanna Przystałowska-Macioła*, **Marcin Mikoś**, Irena Wojsyk-Banaszak, Ewa Ziętkiewicz
*równorzędny wkład
był następujący:

- zbieranie i opracowanie danych klinicznych pacjenta
- zabezpieczenie materiału do badań
- krytyczny przegląd ostatecznej wersji manuskryptu

Z wyrazami szacunku

dr n. med. Marcin Mikoś
lekarz specjalista pediatrii
i chorób płuc dzieci
2507235

Poznań, 24.02.2025

dr hab. med. Irena Wojsyk-Banaszak

Klinika Pneumonologii, Alergologii Dziecięcej
i Immunologii Klinicznej
Uniwersytet Medyczny im. K. Marcinkowskiego
w Poznaniu

OŚWIADCZENIE

Niniejszym oświadczam, że mój wkład w powstanie manuskryptu pt. „A novel pathogenic variant of *CFAP221* is a cause of a mild form of primary ciliary dyskinesia"
Alicja Rabiasz, Zuzanna Bukowy-Bieryłło, Patrycja Kaźmierczak*, Hanna Przystałowska-Macioła*, Marcin Mikoś, **Irena Wojsyk-Banaszak**, Ewa Ziętkiewicz
*równorzędny wkład
był następujący:

- udział w zbieraniu i opracowaniu danych klinicznych pacjenta
- krytyczny przegląd ostatecznej wersji manuskryptu

Z wyrazami szacunku

dr hab. n. med. Irena Wojsyk-Banaszak
Specjalista pediatrii, chorób płuc,
chorób płuc dzieci i alergologii
6390183

50 LAT
INSTYTUT
GENETYKI CZŁOWIEKA
POLSKIEJ AKADEMII NAUK

ul. Strzeszyńska 32
60-479 Poznań

tel. +48/61/657 91 00
fax +48/61/823 32 35
e-mail: igcz@man.poznan.pl

www.igcz.poznan.pl

Poznań, 24.02.2025

prof. dr hab. Ewa Ziętkiewicz

OŚWIADCZENIE

Niniejszym oświadczam, że mój wkład w powstanie manuskryptu pt. „A novel pathogenic variant of *CFAP221* is a cause of a mild form of primary ciliary dyskinesia"
Alicja Rabiasz, Zuzanna Bukowy-Bieryłło, Patrycja Kaźmierczak*, Hanna Przystałowska-Macioła*, Marcin Mikoś, Irena Wojsyk-Banaszak, **Ewa Ziętkiewicz**
*równorzędny wkład
był następujący:

- ustalenie koncepcji badań
- zabezpieczenie środków finansowych i opieka nad właściwą realizacją projektu
- udział w interpretacji wyników badań
- udział w pisaniu oryginalnej wersji manuskryptu, redagowanie i korekta ostatecznej wersji manuskryptu
- obowiązki autora korespondencyjnego

Z wyrazami szacunku

Oświadczenia współautorów Artykułu 4

50 LAT
INSTYTUT
GENETYKI CZŁOWIEKA
POLSKIEJ AKADEMII NAUK

ul. Strzeszyńska 32
60-479 Poznań

tel. +48/61/657 91 00
fax +48/61/823 32 35
e-mail: igcz@man.poznan.pl

www.igcz.poznan.pl

Poznań, 24.02.2025

mgr Alicja Rabiasz

OŚWIADCZENIE

Niniejszym oświadczam, że mój udział w powstaniu manuskryptu pt. „The lack of homozygotes with a large deletion encompassing *SPAG1* and *POLR2K* in primary ciliary dyskinesia patients suggests the lethal effect of the loss of POLR2K protein"
Genes & Diseases, https://doi.org/10.1016/j.gendis.2025.101535
Alicja Rabiasz, Monika Drobna-Śledzińska, Patrycja Kaźmierczak, Michał Witt, Ewa Ziętkiewicz
był następujący:

- ustalenie koncepcji i planu badań
- zabezpieczenie środków finansowych
- zaprojektowanie, wykonanie i interpretacja doświadczeń z wykorzystaniem *S. mediterranea*: analiza *in silico*, wyciszenie homologa genu *SPAG1* i *POLR2K* (w tym zaprojektowanie i synteza dsRNA przy użyciu transkrypcji *in vitro*), potwierdzenie efektywności wyciszenia na poziomie mRNA (izolacja RNA, synteza cDNA, qRT-PCR), analiza wpływu wyciszenia obu genów na fenotyp planarii (w tym na lokomocję robaków), analiza wpływu wyciszenia *POLR2K* na zdolności regeneracyjne *S. mediterranea*
- zaprojektowanie, wykonanie i interpretacja doświadczeń z wykorzystaniem ludzkiej linii komórkowej: wyciszenie *POLR2K* w komórkach HEK293T, potwierdzenie efektywności wyciszenia na poziomie mRNA i białka (izolacja RNA, synteza cDNA, qRT-PCR, izolacja białka, Western-Blot), przeprowadzenie testów funkcjonalnych
- pisanie oryginalnej wersji manuskryptu, przygotowanie tabel i figur
- przygotowanie ostatecznej wersji manuskryptu
- obowiązki autora korespondencyjnego

Z wyrazami szacunku

Alicja Rabiasz

50 LAT
INSTYTUT
GENETYKI CZŁOWIEKA
POLSKIEJ AKADEMII NAUK

ul. Strzeszyńska 32
60-479 Poznań

tel. +48/61/657 91 00
fax +48/61/823 32 35
e-mail: igcz@man.poznan.pl

www.igcz.poznan.pl

Poznań, 24.02.2025

dr Monika Drobna-Śledzińska

OŚWIADCZENIE

Niniejszym oświadczam, że mój udział w powstaniu manuskryptu pt. „The lack of homozygotes with a large deletion encompassing *SPAG1* and *POLR2K* in primary ciliary dyskinesia patients suggests the lethal effect of the loss of POLR2K protein"
Genes & Diseases, https://doi.org/10.1016/j.gendis.2025.101535
Alicja Rabiasz, **Monika Drobna-Śledzińska**, Patrycja Kaźmierczak, Michał Witt, Ewa Ziętkiewicz
był następujący:

- udział w przeprowadzeniu i analizie wyników funkcjonalnych testów komórkowych, udział w potwierdzeniu efektywności wyciszenia na poziomie białka (Western Blot)
- krytyczny przegląd i edycja manuskryptu

Z wyrazami szacunku

Monika Drobna-Śledzińska

50 LAT
INSTYTUT
GENETYKI CZŁOWIEKA
POLSKIEJ AKADEMII NAUK

ul. Strzeszyńska 32
60-479 Poznań

tel. +48/61/657 91 00
fax +48/61/823 32 35
e-mail: igcz@man.poznan.pl

www.igcz.poznan.pl

Poznań, 24.02.2025

mgr Patrycja Kaźmierczak

OŚWIADCZENIE

Niniejszym oświadczam, że mój udział w powstaniu manuskryptu pt. „The lack of homozygotes with a large deletion encompassing *SPAG1* and *POLR2K* in primary ciliary dyskinesia patients suggests the lethal effect of the loss of POLR2K protein"
Genes & Diseases, https://doi.org/10.1016/j.gendis.2025.101535
Alicja Rabiasz, Monika Drobna-Śledzińska, **Patrycja Kaźmierczak**, Michał Witt, Ewa Ziętkiewicz
był następujący:

- udział w przygotowaniu materiału do badań (izolacja DNA) i w genotypowaniu pacjentów
- analiza wpływu obecności patogennego wariantu na poziom ekspresji mRNA (RT-PCR na archiwalnym materiale pacjenta)
- krytyczny przegląd ostatecznej wersji manuskryptu

Z wyrazami szacunku

Poznań, 24.02.2025

prof. dr hab. Michał Witt

OŚWIADCZENIE

Niniejszym oświadczam, że mój udział w powstaniu manuskryptu pt. „The lack of homozygotes with a large deletion encompassing *SPAG1* and *POLR2K* in primary ciliary dyskinesia patients suggests the lethal effect of the loss of POLR2K protein"
Genes & Diseases, https://doi.org/10.1016/j.gendis.2025.101535
Alicja Rabiasz, Monika Drobna-Śledzińska, Patrycja Kaźmierczak, **Michał Witt**, Ewa Ziętkiewicz
był następujący:

- udział w nadzorowaniu realizacji projektu
- krytyczny przegląd ostatecznej wersji manuskryptu

Z wyrazami szacunku

50 LAT
INSTYTUT
GENETYKI CZŁOWIEKA
POLSKIEJ AKADEMII NAUK

ul. Strzeszyńska 32
60-479 Poznań

tel. +48/61/657 91 00
fax +48/61/823 32 35
e-mail: igcz@man.poznan.pl

www.igcz.poznan.pl

Poznań, 24.02.2025

prof. dr hab. Ewa Ziętkiewicz

OŚWIADCZENIE

Niniejszym oświadczam, że mój udział w powstaniu manuskryptu pt. „The lack of homozygotes with a large deletion encompassing *SPAG1* and *POLR2K* in primary ciliary dyskinesia patients suggests the lethal effect of the loss of POLR2K protein"
Genes & Diseases, https://doi.org/10.1016/j.gendis.2025.101535
Alicja Rabiasz, Monika Drobna-Śledzińska, Patrycja Kaźmierczak, Michał Witt, **Ewa Ziętkiewicz**
był następujący:

- ustalenie koncepcji i planu badań
- zabezpieczenie środków finansowych i opieka nad właściwą realizacją projektu
- analiza rozkładu genotypów u pacjentów
- udział w interpretacji wyników badań
- udział w pisaniu oryginalnej wersji manuskryptu, korekta ostatecznej wersji manuskryptu
- obowiązki autora korespondencyjnego

Z wyrazami szacunku